UNIVERSITY OF LIVERPOOL

DEVELOPING NOVEL PYRETHROID ACTIVITY BASED PROBES TO IDENTIFY CYTOCHROME P450S ASSOCIATED WITH PYRETHROID RESISTANCE IN DISEASE VECTORS

Thesis submitted in accordance with the requirements of the University of Liverpool for the degree of Doctor of Philosophy

by

Hanafy Mahmoud Ismail Mohamed

MSc. (University of Alexandria)

April 2011

DECLARATION

I declare that the work presented in this thesis is all my work and that has not been submitted for any other degree.

The research work was carried out in the Liverpool School of Tropical medicine, university of Liverpool, United Kingdom.

Hanafy Mahmoud Ismail Mohamed (2011)

DEDICATION

To my parents Mahmoud Ismail Mohamed and Madeha Awad Soliman, my loving wife Asmaa El-Saied Hamed Gomaa and my daughters Shahd and Shaza

Thank you for all your support.

ACKNOWLEDGMENTS

I am ever grateful to almighty Allah, the creator, and to him I owe my very existence. I also owe him great thanks for providing me this opportunity and granting me the capability to proceed successfully.

I owe my thanks to my supervisors Dr. Mark J. I. Paine and Professor. Janet Hemingway for guiding me into my PhD project, their doors have always been open for young scientists. I would like to thank Dr. Mark for giving me this opportunity to work in the group and for being constant source of encouragement and support through the land of P450s, also for his proof reading and corrections of my thesis.

My sincere thanks to Professor Paul M.O' Neil, Chemistry Department, Liverpool University, for his valuable advices and accepting me in his laboratory to perform the chemistry part of this project. I would like also to thank Dr. David Hong and Dr. Ian Hall for their incredible support during my stay in Paul O' Neil Laboratory.

My sincere thanks to Dr. Hilary Ranson for her willingness to provide me with valuable comments during my project progress and finding additional funding during my project. I would like also to thank Billy Dean for his great help in finding additional funding during my project. I also wish to thank the LSTM for providing additional funding during this project.

I am very grateful to innovative vector control consortium (IVCC) project and the IVCC people for main funding. Special thank to Dr. Johan G. Vontas, University of Athens, Greece for being source of engorgement and support.

My sincere thanks to Professor Stephen Ward, Parasitology department, Liverpool school of tropical Medicine, for reading my thesis and being a source of encouragement and support.

I am very grateful to Professor Benjamin Cravatt and his colleagues Dr. Aaron Wright and Dr. Anna Speers, Cravatt's laboratory, Scripps Research Institute, USA for their kind supply with general generic P450 probe and rhodamine biotin trifunctional azide. Also, thanks to Professor Roland Wolf, Biomedical Research Institute, University of Dundee (UK) for providing male mouse liver microsomes samples.

Thanks to Dr. Alison Shone, Molecular Biochemical Parasitology Group, Liverpool School of Tropical Medicine, Liverpool, (UK), for providing rat liver microsomes.

Thanks to Dr. Jaclyn Bibby and Professor Michael J. Sutcliffe, Manchester Interdisciplinary Biocentre, School of Chemical Engineering and Analytical Science, University of Manchester, Manchester, (UK), for their help in inhibitor and probe molecular modelling calculations.

I would like say a massive thank you to everyone in the vector group who have helped throughout this project especially my fellow PhD students. Thanks to Dr. Gareth

Lycett, Dr. Bradley Stevenson, Dr. Andrew Dwood, Dr. Evangelia Mouro, Andy Steven who were always happy to answer the numerous questions I ever had.

My parents, my wife Asmaa, my daughters, brothers and sister deserve the warmest thanks for their love, patience and support during my study period.

This project received financial support from IVCC project and Leverhulm trust.

ABSTRACT

The use of insecticide treated materials is a major preventive tool in the global fight against malaria and other diseases. Synthetic pyrethroids are the only class of insecticides suitable for insecticide treated materials, thus resistance threatens to undermine disease control. Detoxification by cytochrome P450-mediated insecticide metabolism is a major cause of pyrethroid resistance. However, given the large numbers of P450s in insects (>100) there is no easy way of rapidly identifying which are involved in insecticide metabolism, which is critical information for vector control. This thesis describes the development of novel activity based protein probes (ABPP) that are based on a pyrethroid scaffold and can be used to selectively label and identify P450s that metabolise pyrethroids.

Activity based protein probes require two functional groups; a 'warhead' reactive functional group that is able to be covalently attached to the active site of the target enzyme, and a reporter tag for probe-protein adduct formation for visualization or isolation for quantification and identification. Acetylene is a common functional group. A wide variety of acetylated molecules were therefore screened against rat liver microsomes and individual mosquito recombinant pyrethroid metabolizing P450s (CYP6P3 and CYP6M2) to identify suitable mechanism based inhibitor molecules. The final probe design and positioning of functional groups was aided by *in silico* analysis of active-site interactions of probes with CYP6P3 models.

Six pyrethroid ABPPs belong to the type II class were synthesized (P3R, P4S, P5R, P6S, P7RS and P8RS) with the functional acetylene 'warhead' positioned on the phenoxybenzyl group in the 2' or 4' position, and the acetylene tag positioned either at the opposite acidic end of the molecule or in the middle replacing the alpha cyano-group. One other probe representing a type I pyrethroid (P2) was synthesized. The characterisation of these probes against individual *Anopheles gambiae* P450s and rodent and mosquito microsomes is described.

Finally, P7RS, which closely resembles deltamethrin, was used to screen and selectively pull-down deltamethrin metabolizing P450s from rat liver and whole mosquito microsomes. Viable quantities of enzyme for LC-MS/MS identification were only obtained from rat pull-downs, reflecting the high P450 content in mammalian liver. The majority (84%) of proteins pulled-down were P450s, while the rest were phase II drug metabolizing enzymes *i.e.* uridine 5'-diphospho-glucuronosyltransferase, Flavin containing monooxygenase 3, epoxide hydrolase and aldehyde dehydrogenase, suggesting a potential role in deltamethrin clearance in *vivo*. The most abundant protein, CYP2C11 (46% of total protein), was a P450 that metabolized deltamethrin, while the next hit (19% of total protein) was an orthlogues of a human pyrethroid metabolizing P450, CYP2C19. This striking result demonstrates the development of a powerful new diagnostic tool for the direct identification of enzymes that are capable of pyrethroid metabolism, and therefore associated with metabolic resistance.

PUBLICATIONS AND POSTER PRESENTATIONS

1. Publications

- **Hanafy M. Ismail**, David W. Hong, Paul M. O'Neill, Steve A Ward, Janet Hemingway and Mark J. Paine. Developing Novel Pyrethroid Activity Based Probes to Selectively pull-out P450s that metabolise pyrethroids in disease vectors. ***Manuscript in preparation.***

- **Ismail HM**, Dowd A J, Steven A, Morou E, Coleman M, Morgan J, Das P, Hemingway J, Vontas J and Paine MJI (2010). A Simple Test for the Determination of DDT on Sprayed Surfaces, PLOS Neglected Tropical Diseases ***(Submitted)***

- Dowd A J, Morou E, Steven A, **Ismail HM**, Labrou N, Hemingway J, Paine MJI and Vontas J (2010).Development of a colourimetric pH assay for the quantification of pyrethroids based on glutathione-S-transferase. *Intern. J. Environ. Anal. Chem.* Volume 90, Issue 12, 2010, Pages 922 - 933

- Morou E, **Ismail HM***, Dowd AJ, Hemingway J, Labrou N, Paine MIJ and Vontas J. (2008). A dehydrochlorinase-based pH change assay for determination of DDT in sprayed surfaces. *Analytical Biochemistry* 378: 60-64. (***Co-first author**).

2. Presentations

- **Hanafy M. Ismail**, David W. Hong, Paul M. O'Neill, Steve A Ward, Janet Hemingway and Mark J. Paine. Hitting insecticide resistance hard: developing activity based probes to selectively pull-out P450s that metabolise pyrethroids in disease vectors. **17th International Conference on Cytochrome P450, Biochemistry, Biophysics and Structure, 26-30 June 2011, Manchester, UK**

- **Hanafy M. Ismail**, David W. Hong, Paul M. O'Neill, Janet Hemingway and Mark J. Paine. Developing Novel Chemical Probes to Identify Cytochrome P450s Associated with Pyrethroid Resistance in Malaria Vectors. *Poster Presentation*, **Spring Meeting 2010 30th March - 1st April 2010, Cardiff, UK (Awarded BioMed Central, Parasites and Vectors Prize for best poster presentation)**

- John Vontas, Andrew Dowd, Evangelia Morou, **Hanafy Ismail**, Andrew Stevens, Janet Hemingway and Mark Paine. Simple tests for measuring insecticides in treated/sprayed surfaces. *Poster presentation,* **5th MIM Pan-African Malaria Conference 2-6 November 2009, Narobi, Kenya**

CONTENTS

LIST OF FIGURES

.

LIST OF SCHEMES

LIST OF TABLES

ABBREVIATIOS

ABPP	Activity-Based Protein Profiling
Ach	Acetylcholine
Alpha-cypermethrin	A racemate comprising (S)-alpha-cyano-3-phenoxybenzyl (1R)-cis-3-(2,2-dichloro-vinyl)-2,2-dimethylcyclopropane carboxylate and(R)-alpha-cyano-3-phenoxybenzyl (1S)-cis-3-(2,2-dichlorovinyl)-2,2-dimethylcyclopropane carboxylate.
b5	Cytochrome *b5*
Bifenthrin	2-Methyl-3-phenylphenyl)methyl(1*S*,3*S*)-3-[(*Z*)-2-chloro-3,3,3-trifluoroprop-1-enyl]-2,2-dimethylcyclopropane-1-carboxylate
br	Broad Peaks
BROD	7-benzoylresorufin-O-depenzylation
°C	Celsius degree
C1	(4'-ethynyl-2-methyl-[1,1'-biphenyl]-3-yl)methyl 3-(2,2-dibromovinyl)-2,2-dimethylcyclopropanecarboxylate
C18 column	Carbon 18 column
C2	(Z)-(4'-ethynyl-2-methyl-[1,1'-biphenyl]-3-yl)methyl 3-(2-chloro-3,3,3-trifluoroprop-1-en-1-yl)-2,2-dimethylcyclopropanecarboxylate
C3	cyano(3-(prop-2-yn-1-yloxy)phenyl)methyl 3-(2,2-dibromovinyl)-2,2-dimethylcyclopropanecarboxylate
C4	(Z)-cyano(3-(prop-2-yn-1-yloxy)phenyl)methyl 3-(2-chloro-3,3,3-trifluoroprop-1-en-1-yl)-2,2-dimethylcyclopropanecarboxylate
CC	Click Chemistry
CC-ABPP	Click Chemistry Compatible Activity Based Protein Profiling
CE	Capillary Electrophoresis
ChAT	Choline Acetyl-Transferase,
CI	Chemical Ionisation
cm	Centimetre
CO	Carbon Monoxide
Conc.	Concentration
CPR	Cytochrome P450 oxidoreductase
Cu	Copper
Cyfluthrin	[(R)-cyano-[4-fluoro-3-(phenoxy)phenyl]methyl] (1R,3R)-3-(2,2-dichloroethenyl)-2,2-dimethylcyclopropane-1-carboxylate
CYP	Cytochrome P450 enzyme
d	Doublet
DCM	Dichloromethane
dd	Doublets of doublets
DDT	Dichlorodiphenyltrichloroethane

Deltamethrin	[cyano-(3-phenoxyphenyl)-methyl]3-(2,2-dibromoethenyl)-2,2-dimethyl-cyclopropane-1-carboxylate
DIFO	Difluorinated Cyclooctyne
DIGE	Differential Gel Electrophoresis
DMF	Dimethylformamide
DMSO	Dimethylsulfoxide
dt	Doublets of triplets
EI	Electron Ionisation
em	Emission
eq.	Equivalent
EROD	7-Ethoxyresorufin-O-deethylation
ES	Electron Spray
Et_2O	Diethyl ether
Et_3N	Triethylamine
EtOAc	Ethyl acetate
Etofenprox	1-ethoxy-4-[2-methyl-1-([3-(phenoxy)phenyl]methoxy)propan-2-yl]benzene
ex	Excitation
G6PDH	Glucose-6-phosphate dehydrogenase
GSTs	Glutathione S-transferases
HCl	Hydrochloric acid
HPLC	High performance liquid chromatography
hr	Hour
hrs	Hours
ICAT	Isotope Coded Affinity Tags
IRS	Indoor Residual Spraying
ITNs	Insecticide Treated Nets
J	Coupling value in Hz
K_d	Apparent dissociation constant
kdr	Knock-down resistance.
Lambda-cyhalothrin	3-(2-chloro-3,3,3-trifluoro-1-propenyl)-2,2-dimethyl-cyano(3-phenoxyphenyl)methyl cyclopropanecarboxylate
LC-MS/MS	Liquid Chromatography coupled with two dimension mass spectrometer
$LiAlH_4$	Lithium Aluminium Hydride
LIF	Laser-Induced Fluorescence
Li-TMSA	Lithium trimethyl silylacetylene
LLINs	Long-Lasting Insecticide Treated Nets
LSTM	Liverpool School of Tropical Medicine
M	Molar
m	Multiplets
MACE	Modified Acetylcholinesterase,
MBI	Mechanism Base Inhibition

Me_2SO	Dimethyl sulfoxide
mg	Milligram
$MgCl_2$	Magnesium chloride
$MgSO_4$	Magnesium sulphate
MHz	Mega hertz
min.	Minutes
ml	Millilitre
mM	Mille molar
MROD	7-methoxyresorufin-O-demethylation
MudPIT	Multidimensional Protein Identification Technology
$Na_2S_2O_4$	Sodium hydrosulphite
Na_2SO_4	Sodium Sulphate
NADP+	Nicotinamide adenine dinucleotide phosphate
NADPH	Reduced form of nicotinamide adenine dinucleotide phosphate
NH_4Cl	Ammonium chloride
nm	Nanometre
nmol/well	Nano mole per well
NMR	Nuclear magnetic resonance
P1	N-((6-ethynylnaphthalen-2-yl)methyl)hept-6-ynamide
P2	(1R,3R)-(6-ethynylnaphthalen-2-yl)methyl3-ethynyl-2,2-dimethylcyclopropane-carboxylate
P3R	(1R, 3R)-(R)-cyano(3-(4-ethynylphenoxy)phenyl)methyl 3-ethynyl-2,2-dimethyl cyclopropanecarboxylate
P450	Cytochrome P450 enzymes
P4S	(1R,3R)-(S)-cyano(3-(4-ethynylphenoxy) phenyl)methyl 3-ethynyl-2,2-dimethylcyclopropanecarboxylate
P5R	(1R,3R)-(R)-cyano(3-(2-ethynylphenoxy)phenyl)methyl 3-ethynyl-2,2-dimethy lcyclopropanecarboxylate
P6S	(1R,3R)-(S)-cyano(3-(2-ethynylphenoxy) phenyl) methyl 3-ethynyl-2,2-dimethylcyclopropanecarboxylate
P7RS	(1R, 3R)-1-(3-(4-ethynylphenoxy) phenyl)prop-2-yn-1-yl 3-(2,2-dibromovinyl)-2,2 –dimethylcyclopropanecarboxylate
P8RS	(1R,3R)-1-(3-(2-ethynylphenoxy) phenyl) prop-2-yn-1-yl 3-(2,2-dibromovinyl)-2,2 -dimethylcyclopropanecarboxylate
$Pd(PPh_3)_2Cl_2$	Palladium catalyst
Permethrin	3-Phenoxybenzyl(1RS)-cis,trans-3-(2,2-dichlorovinyl)-2,2-dimethylcyclopropanecarboxylate
pmol	Pico mole
ppm	Parts per million
PROD	7-resorufin-O-depentylation
PS	Phenylsulphonate

PSA	Prostate Specific Antigen
q	Quartets
QTL	Quantitative trait loci
RLM	Rat liver microsomes
RLU	Relative Luminescence Unit
RT	Room Temperature
s	Singlet
SDS-PAGE	One dimensional polyacrylamide gel
t	Triplets
TBAF	Tetra-*n*-butyl ammonium fluoride
THF	Tetrahydrofuran
TLC	Thin Layer Chromatography
TMSCN	Trimethylsilyl cyanide
U	Unit
UV	Ultra violet
vg-Na+ channel	Voltage-gated sodium channel,
Vis	Visible light
vs.	Versus
WHOPES	World Health Pesticide Evaluation Scheme
ε	Extinction Coefficient
λmax	Wave length maximum
λmin	Wave length minimum
µl	Microliter
µM	Micro molar
WHO	World Health Organization
^{13}C	Carbon 13 NMR
1EPh	1-ethynyl-4-phenoxybenzene
^{1}HNMR	Hydrogen NMR
2D-GE	Two-Dimensional Gel Electrophoresis
2EMe	2-ethynyl-6-methoxynaphthalene
2-EN	2-ethynyl naphthalene
2EN-ABP	2 ethynyl naphthalene activity based probe
2POX	(prop-2-yn-1-yloxy) benzene
2x	Two fold
4EBi	4-ethynylbiphenyl
4EDF	4-ethynyl-1,2-difluorobenzene

Chapter 1

1. Introduction and Literature Review

1.1. The medical importance of mosquitoes

Insects represent more than half of all known living organisms on earth and inhabit nearly all environments. In general, insect vectors are responsible for almost 20% of all infectious diseases affecting humanity in developing countries (WHO, 2004), with mosquitoes amongst the most common human and animal disease carrier for parasites, bacteria or viruses infectious to man (Brandling-Bennett and Penheiro, 1996; Briseno-Garcia *et al.*, 1996; Gubler and Clark, 1995; Krogstad, 1996; Meslin, 1997; Roberts *et al.*, 1997a; Sanders *et al.*, 1996; Thompson *et al.*, 1996). Of these, malaria is considered to be the most important infectious disease of mankind. It is most common in tropical and subtropical regions of the world but it is also established in some temperate climates as well (WHO, 2005) (Figure 1.1).

Malaria infection remains a devastating global problem, with an estimated 300–500 million cases occurring annually. Forty-one percent of the world's population lives in areas where malaria is transmitted. Up to 2.7 million people die of malaria each year, 75% of them are African children (WHO, 2005), and those that survive severe malaria are prone to learning difficulties or may suffer brain damage. Furthermore, malaria is a major cause of infant death due to infection of pregnant women, while low birth weight and maternal anaemia may occur upon malaria infection of pregnant women (Luxemburger *et al.*, 2001; UNICEF, 2004).

Malaria in humans is caused by infection with one or more of five species of single cell *Plasmodium* parasites (i.e., *P. falciparum, P. vivax, P. ovale, P. malariae* and *P. knowlesi*) (Cox-Singh *et al.*, 2010; Cox-Singh and Singh, 2008).

The infection is transmitted from person to person by the bite of an infected female mosquito of the *Anopheles* species, such as *Anopheles gambiae* and *An. funestus*. The female mosquitoes transmit malaria because they need the blood meal as a protein source to develop their eggs (Olayemi, 2011).

1.2. Vector control methods

Parasites are becoming increasingly resistant to anti-malarial drugs, which are also expensive (Djimde *et al.*, 2001; Price and Nosten, 2001; Wellems and Plowe, 2001). Vaccines are still not available (Plassmeyer *et al.*, 2009). Vector control using insecticides thus continues to be the major preventive tool in the global fight against vector borne diseases. Indeed selective vector control is an integral part of the integrated management of malaria disease for the global strategy adopted by the World Health Organization (WHO) (Beier *et al.*, 2008). Selective vector control is defined as the application of site-specific targeted use of different and cost-effective vector control methods alone or in combination to reduce human-vector contact (WHO, 1995). This includes the use of insecticide treated materials. Significant advances have been achieved with the development of new formulations to produce long-lasting insecticide treated nets (LLINs), which are ready primed with insecticide which is wash resistant (up to 20 washes) (Atieli *et al.*, 2010).

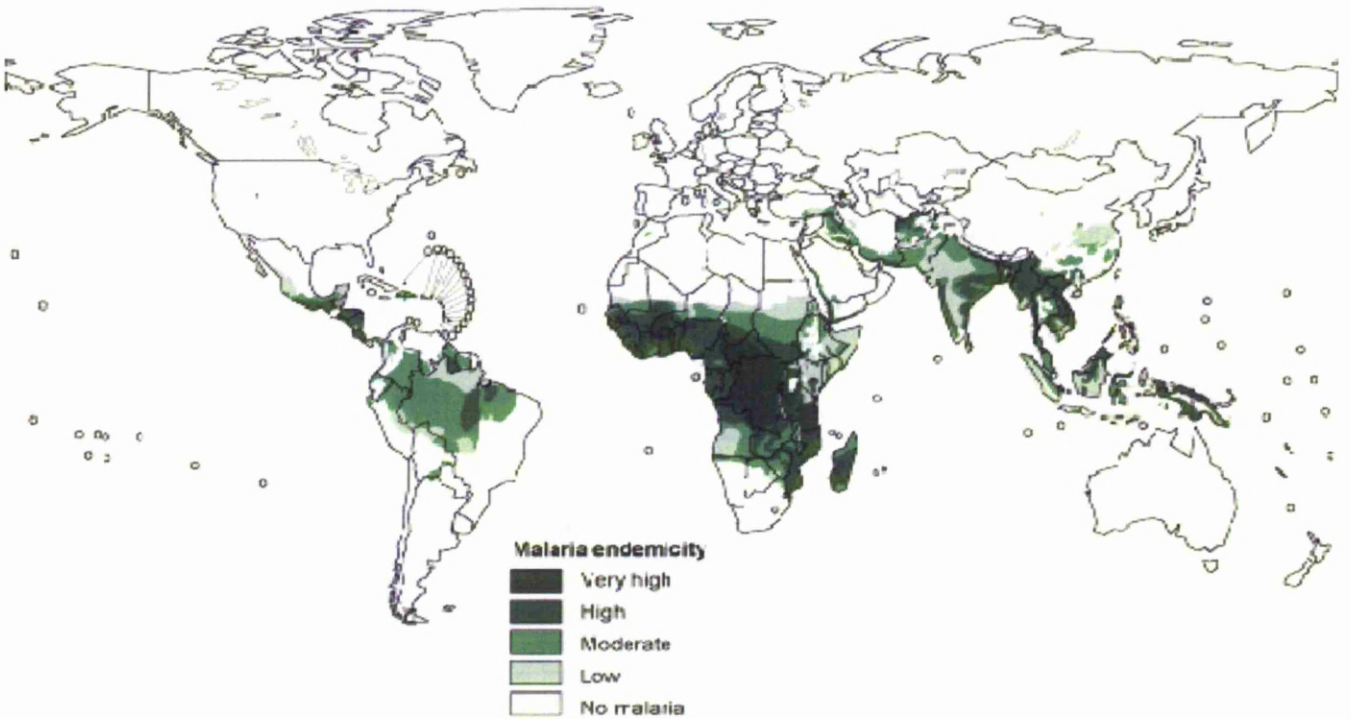

Figure 1.1. Worldwide malaria endemicity (WHO, 2005).

Indoor residual spraying (IRS) is also recommended strongly by WHO, while larval breeding site control in some circumstances may be used as a complementary tool to the LLINs and IRS as a core intervention method (WHO, 2010).

1.2.1. Insecticide treated nets

Insecticide treated nets (ITNs) are used as a physical barrier against vector mosquitoes such as *An. gambiae* and *An. funestus*, which generally bite at night (Nauen, 2007; WHO, 1995; WHO, 2010). Successful use of ITNs has occurred in Saudi Arabia, the Middle East, India, Thailand, Afghanistan, Malaysia, the Philippine Islands and Myanmar in Asia (Das *et al.*, 1993; Dolan *et al.*, 1993; Jamjoom *et al.*, 1994; Leake and Hii, 1994; Rowland *et al.*, 1996; Torres *et al.*, 1997). The WHO has given its approval to the use of pyrethroids for the treatment of bed nets. In Africa pyrethroid-treated bed nets have shown promise in reducing malaria morbidity and mortality (Gatei *et al.*, 2010; Nahlen *et al.*, 2003). Between 2008 and 2010 more than 254 million ITNs have been delivered to malaria endemic countries in Africa (WHO, 2010). However, with exposure to only a single class of insecticide there is growing concern that the evolution of pyrethroid resistance in mosquitoes will reduce the sustainability of ITNs technology for vector control (Hemingway *et al.*, 2006). Recently a strong knockdown resistance to permethrin and DDT was found in *An. gambiae* populations from southern Benin, where LLINs and IRS have been planned to scale up for malaria prevention in this country (Yadouleton *et al.*, 2010). Additionally, metabolism based pyrethroid resistance found in *An. funestus* collected from Tororo, Uganda where the involvement of P450 enzymes has been observed (Morgan *et al.*, 2010).

1.2.2. Indoor residual spraying

Four different insecticides groups can be used for IRS including the chlorinated hydrocarbons (*i.e.* dichlorodiphenyltrichloroethane (DDT)), pyrethroid, carbamates and organophosphates (OPs). With more choice of active ingredient, albeit limited, IRS is gaining more attention in vector control interventions for reducing and interrupting malaria transmission (WHO, 2006; WHO, 2010) (Figure 1.2). The use of IRS has been very successful in malaria control where the number of people protected by application of IRS in Africa has increased from 13 million in 2005 to 75 million in 2009 accounting for 10% of the population at risk (WHO, 2010).

1.3.Pyrethroid insecticides

The chemical characterization of the insecticidal components of pyrethrum flower extract (*Chrysanthemum cinerariaefolium*) has led to the development of the pyrethroid family of insecticides. Synthetic pyrethroids are based on the structure of a natural pyrethrin. They were developed with the aim of improving the stability of natural pyrethrins to light and biodegradation as well as enhancement of insecticidal activity. These include allethrin (Yamamoto *et al.*, 1971) the first synthetic pyrethroid molecule, and permethrin, deltamethrin and cypermethrin. Of these deltamethrin is most widely used as it is one of the most highly potent pyrethroid insecticides (Elliott *et al.*, 1973; Katsuda, 1999).

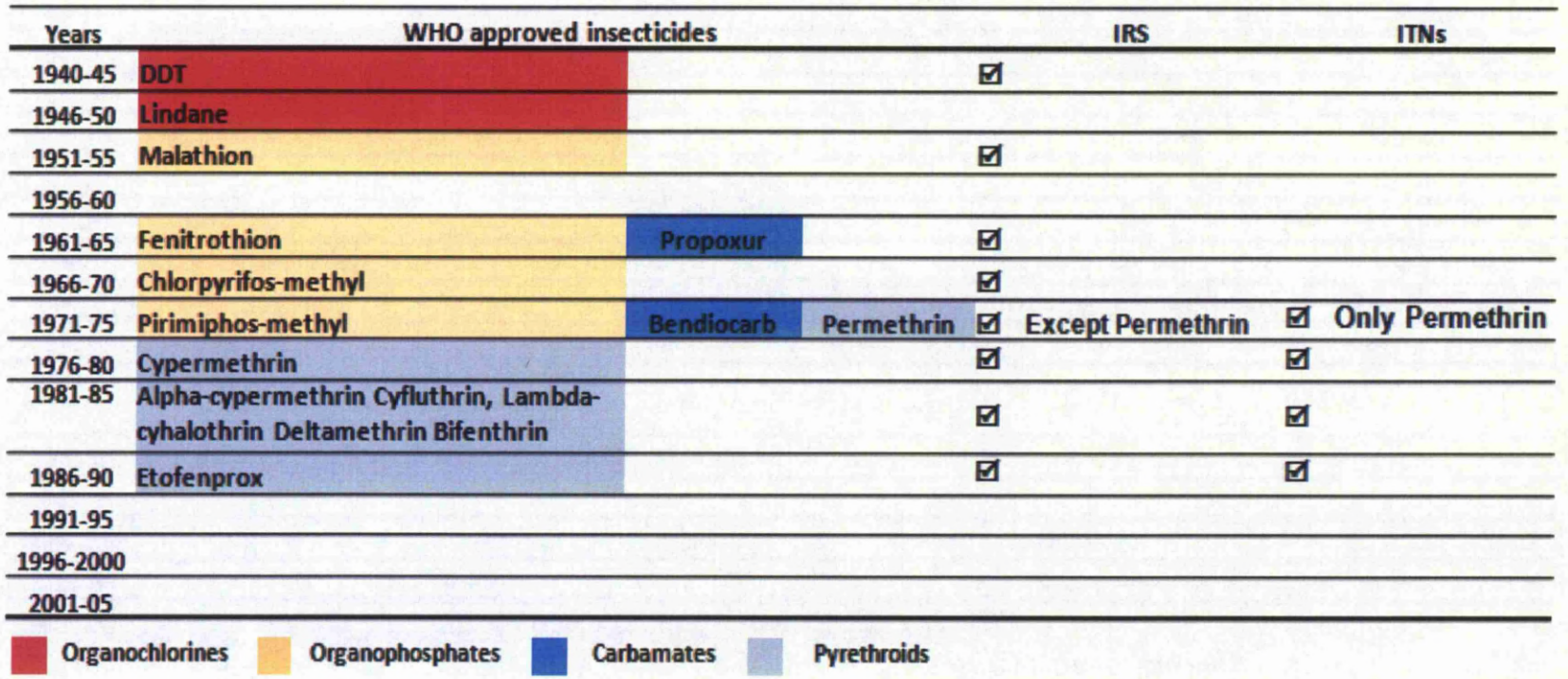

Figure 1.2. History of WHO-approved insecticides for adult malaria mosquito control adapted from (Nauen, 2007).

The majority of pyrethroid molecules are esters, with an alcohol and an acid moiety. An example is deltamethrin shown in figure 1.3 and figure 1.4. The acid moiety usually contains a dimethylcyclopropane ring with variable substituent. Most of the synthetic pyrethroids contain an aromatic alcohol moiety. All pyrethroids are chiral; usually with more than one chiral centre and, therefore, existing as several enantiomers. Only a few of the many chiral pyrethroid insecticides are formulated as single- or enriched enantiomer products (Garrison, 2006). Pyrethroids such as permethrin that lacks an alpha cyano group are classified as type I pyrethroids, while those such as deltamethrin that contain an alpha cyano group are classified as type II pyrethroids. Pyrethroids display high affinity to Na+- channels where they exert their toxic effects by keeping the Na+-channels open, causing complete depolarisation of the nervous membrane (Figure 1.3) (Narahashi, 1996; Narahashi *et al.*, 1995) .

1.4.Operational problems

The fact that only four insecticide classes are available, and there has been no new malaria insecticides approved by WHO in the last 15 years (Figure 1.2), has greatly increased concern that insecticide resistance will threaten the sustainability of these few chemicals for vector control. Pyrethroid insecticides are particularly vulnerable since they are the only group recommended for ITN treatment (Hemingway *et al.*, 2006; Hougard *et al.*, 2003). This is due to their rapid knock-down effect and low toxicity in mammals. Seven pyrethroid compounds are currently considered suitable for impregnation of mosquito nets (Figure 1.4) including type I etofenprox, permethrin and bifenthrin and type II pyrethroids alpha-cypermethrin, cyfluthrin, deltamethrin and lambda-cyhalothrin (Hougard *et al.*, 2003).

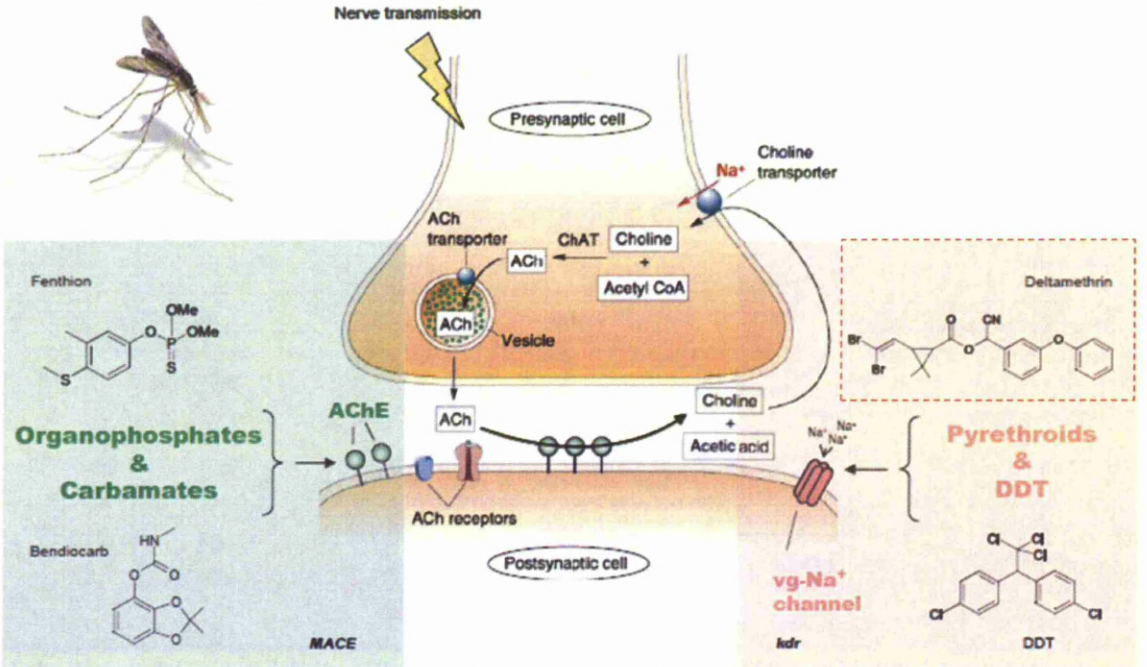

Abbreviations: AChE = Acetylcholinesterase Ach = Acetylcholine, ChAT = Choline Acetyl-Transferase, MACE = Modified Acetylcholinesterase, vg-Na+ channel = voltage-gated sodium channel, kdr = knock-down resistance.

Figure1.3. Biochemical target sites of synthetic insecticides. Organophosphates and carbamates insecticides are inducing phosphorylation and carbamylation toxicity by inhibiting the acetylcholine enzyme which a crucial importance in terminates nerve pulses. Synthetic pyrethroid and DDT exerts their toxic effect by blocking voltage-gated sodium channels producing fast knock-down properties (Source Bayer Environmental Science Journal No.18 November 2006).

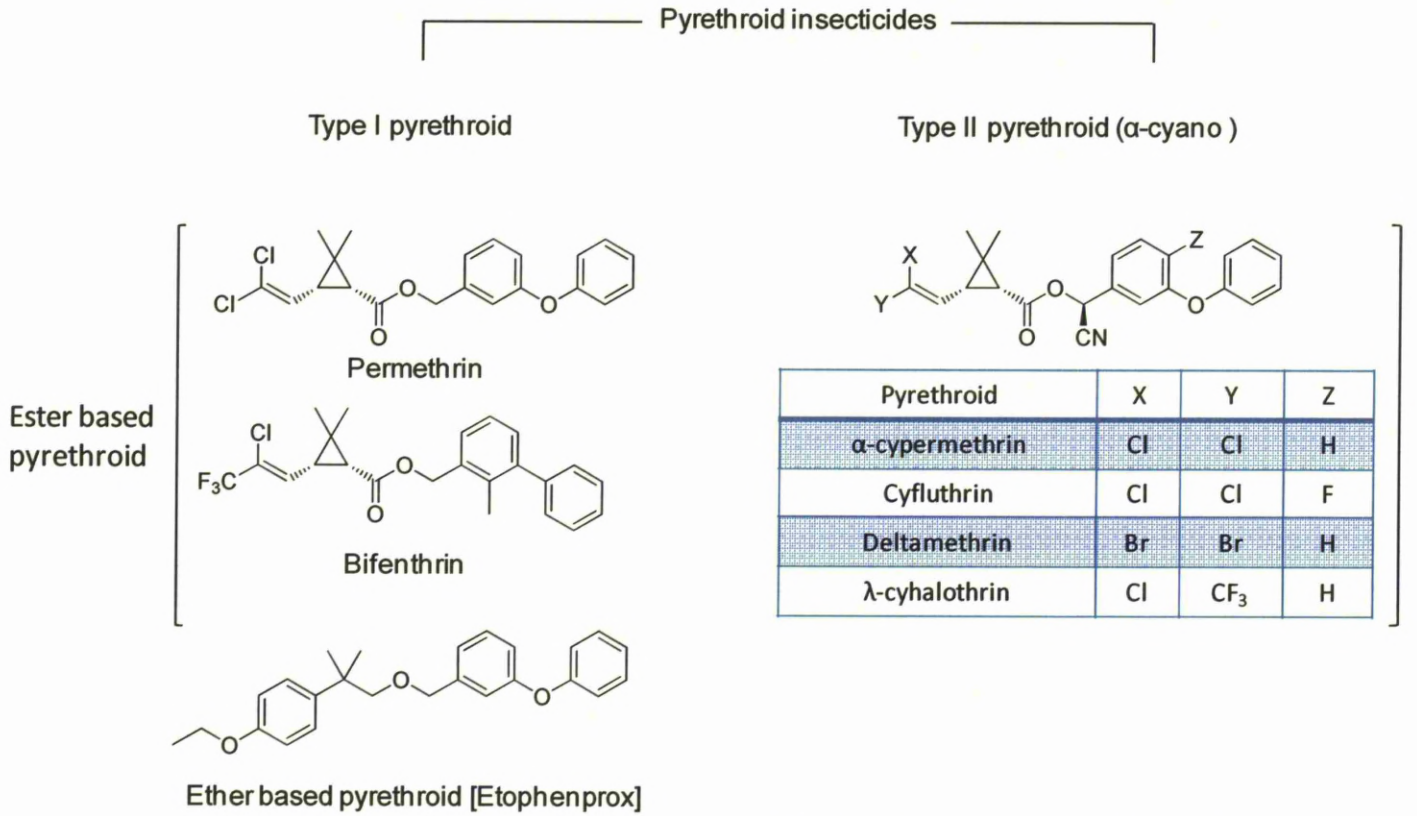

Pyrethroid	X	Y	Z
α-cypermethrin	Cl	Cl	H
Cyfluthrin	Cl	Cl	F
Deltamethrin	Br	Br	H
λ-cyhalothrin	Cl	CF_3	H

Figure 1.4. Chemical structure of pyrethroid insecticides evaluated by the WHO pesticide evaluation scheme (WHOPES) (Hougard *et al.*, 2003).

1.5.Pyrethroid resistance

Mosquitoes can develop resistance to pyrethroid insecticides by changing the insecticide target i.e. target site resistance, or by overproduction of detoxification enzymes i.e. metabolic resistance. Reduced neuronal sensitivity named knock down resistance (Kdr) was first recognized for DDT in the 1950's in housefly (*Musca domestica* L.) (Busvine, 1951). Since DDT attacks the same target as pyrethroids (Na-channel) based Kdr resistance has been known for a long time that this can also lead to cross resistance for pyrethroids (Fine, 1961). Thus the characterization of Kdr resistance to pyrethroid is well documented. For example different Kdr mutations have been reported in pyrethroid resistant *An. gambiae* s.s. from West and East Africa (Chandre *et al.*, 2000; Martinez-Torres *et al.*, 1998; Ranson *et al.*, 2000).

A leucine to phenylalanine substitution in the S6 segment of domain II of the *para*-type sodium channel (L1014F) was reported in West Africa (Martinez-Torres *et al.*, 1998), while leucine to serine in this position (L1014S) is found mainly in malaria vectors from East Africa (Ranson *et al.*, 2000). The West Africa Kdr allele (L1014F allele) has now been reported in four other major malaria vectors from South Lampung, Indonesia including *An. sundaicus*, *An. aconitus*, *An. subpictus* and *An. Vagus* (Syafruddin *et al.*, 2010).

In addition to Kdr based resistance, metabolic resistance to pyrethroids is possible as results of elevated levels of activity of P450s, esterases and glutathione S-transferases (GSTs) (Hemingway and Ranson, 2000). Of these, elevated levels of P450 expression (transcriptional and/or enzyme activity) are most consistently associated with

resistance to pyrethroid from African malaria vectors (Brooke *et al.*, 2001; Etang *et al.*, 2004; Vulule *et al.*, 1999). For instance the two P450s CYP6M2 and CYP6P3 are found over-expressed in permethrin resistant populations of *An. gambiae* in Odumassy and Dodowa in southern Ghana (Müller et al., 2008; Muller et al., 2007), Akron and Gdedjromede in south-eastern Benin (Djouaka *et al.*, 2008), and Ojoo in south west Nigeria (Djouaka *et al.*, 2008). Although little is known about esterase and GST mediated pyrethroid metabolic resistance, ester hydrolysis of pyrethroid leading to detoxification is believed to act as a cause of metabolic resistance in some instances. For example pyrethroid esterase based resistance has been reported in *An. gambiae* in Africa (Vulule *et al.*, 1999). Additionally, the use of fluorescent surrogate substrates selectively designed based on pyrethroid scaffold to measure esterase activity proved carboxylesterases mediated pyrethroid resistance in *Culex pipiens pipiens* collected from California (McAbee *et al.*, 2004).

1.6.Cytochrome P450 monooxygenase-based resistance

Cytochrome P450s are a complex family of enzymes commonly found in the majority of living organisms, including insects. These enzymes are critical for xenobiotics degradation and metabolism of endogenous chemicals like hormones, and may have played a key role in the adaptation of insects to toxic chemicals in their host plants (Feyereisen, 1999). P450s bind molecular oxygen and receive electrons from NADPH via NADPH cytochrome P450 oxidoreductase (CPR) to introduce an oxygen molecule into the substrate, thus rendering a normally hydrophobic substrate into a more hydrophilic and excretable molecule (Figure 1.5). In most cases, oxidative metabolism by P450s inactivates insecticides (Kaneko, 2011; Scott, 1999; Scott *et al.*, 1998), although occasionally the insecticidal activity depends on metabolic activation

by P450s (Croom *et al.*, 2010; Murray and Butler, 2004; Scott, 1999; Scott *et al.*, 1998) as in the case of paraoxon. Rapid inactivation will prevent the insecticide reaching its target to exert its pharmacological effect. Therefore, P450 mediated detoxification leading to insecticide resistance is a major concern (Stevenson *et al.*, 2011). Cytochrome P450-mediated resistance is probably the most frequent type of metabolic based pyrethroid resistance (Scott, 1999).

Due to the large number of P450 genes present in the major malaria vector *An. gambiae,* 111 genes (Nikou D, (2003); Ranson et al., 2002) and large substrate diversity it is difficult to identify which P450 is responsible for the metabolism of a specific insecticide using available biochemical assays. For instance, *An. gambiae* microarray, the detox-chip, was developed to identify up-regulated detoxification genes associated with insecticide resistance (David *et al.*, 2005b). This has identified several P450s in *An. gambiae* associated with pyrethroid resistance, including CYP6Z1, CYP6Z2, CYP6M2, CYP6P3 and CYP325A3 (David et al., 2005a; Müller et al., 2008; Muller et al., 1994; Muller et al., 2007; Nikou et al., 2003). CYP6Z1 has been shown to metabolize DDT (Chiu *et al.*, 2008), CYP6P3 and CYP6M2 metabolize permethrin and deltamethrin (Müller *et al.*, 2008; Stevenson *et al.*, 2011), while CYP6Z2 binds but does not metabolize pyrethroids (McLaughlin *et al.*, 2008). Among those enzymes, the role of CYP6M2 in deltamethrin metabolism that generates multiple metabolites in *vitro* has been characterised using mass spectrometry and nuclear magnetic resonance (NMR) spectroscopic analysis (Figure 1.5) (Stevenson *et al.*, 2011). Interestingly, 4`-hydroxy deltamethrin (M4) was the major metabolites observed in addition to the other metabolites (*i.e.* M1, M2 and M3), representing complexity of pyrethroid metabolism by P450 pyrethroid metaboliser.

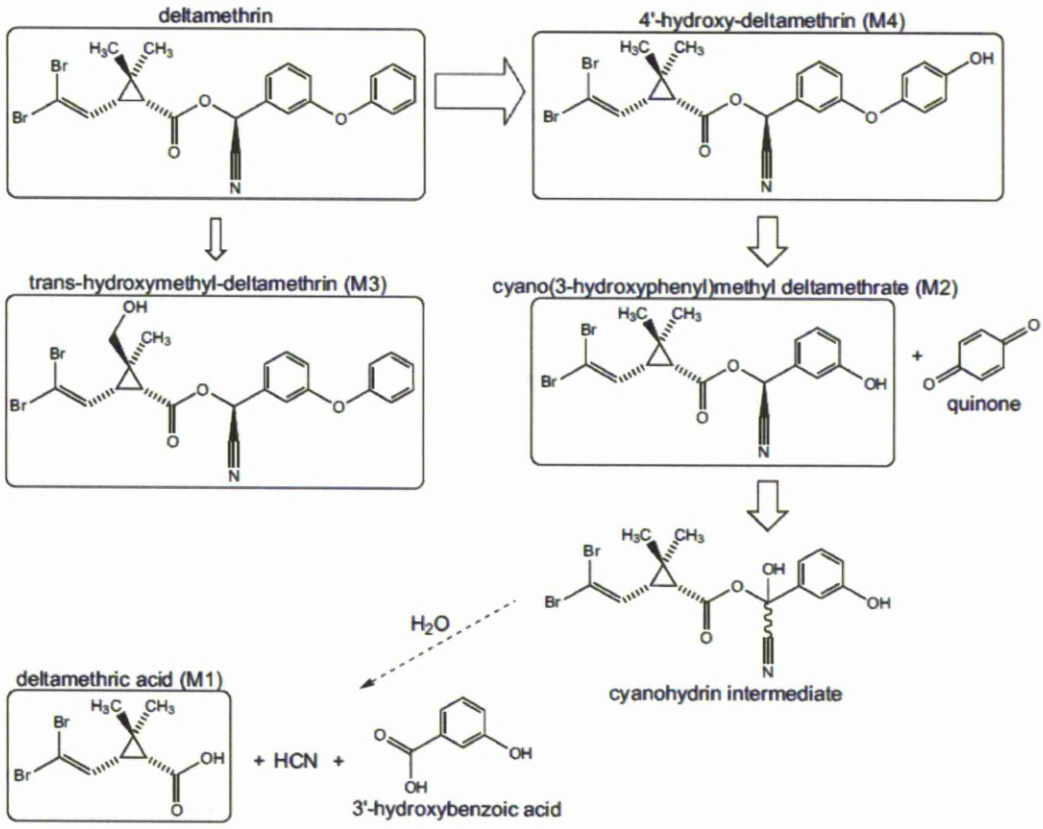

Figure 1.5. Deltamethrin metabolism by CYP6M2. Boxed compounds were experimentally verified. The predominant path for metabolism is indicated by the larger arrow and the non-enzymatic degradation of the cyanohydrin intermediate is indicated by a dotted arrow (Stevenson *et al.*, 2011).

The P450 activities are regulated and affected by many factors in *vivo,* including post translational mechanisms (Aguiar *et al.*, 2005), endogenous inhibitors, allosterically control and protein-protein interactions (Figure 1.6). Also, alteration of P450 enzymes including NADPH-P450 reductases and cytochrome *b5* and endogenous concentrations of the cofactor NADPH may produce dramatic changes in the P450 activity (Berge *et al.*, 1998).

Additionally, because eukaryotic P450s are a membrane associated proteins, the membrane composition and localization of protein binding partners would be expected to have a great influence on P450 activity. Overall these factors may hinder the prediction of key P450 isozyme in insecticide metabolism and resistance using the current available genomic (microarrays), biochemical assays and proteomic methods.

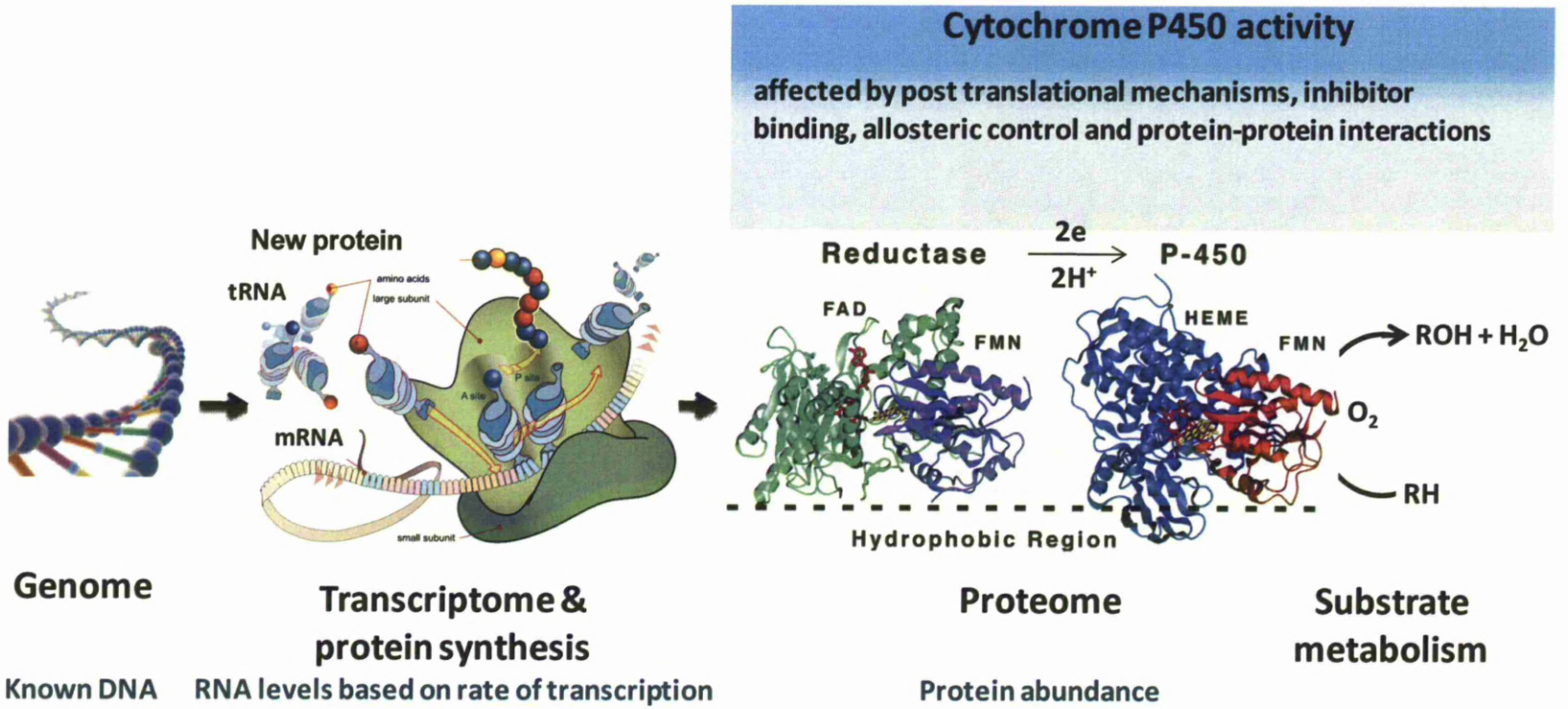

Figure 1.6. Factors affecting cytochrome P450 levels and activity in native proteome (Possible orientation of redox transfer complexes 'reductase/P450' on the membrane surface is obtained from (Bayburt and Sligar, 2002)).

1.7.Identification of genes responsible for insecticide resistance

Early detection of the resistance problem may leads to effective resistance management strategy in medical, veterinary, and agriculture insect pest. The availability of the complete *An. gambiae* genome sequence has allowed the use of new research themes that may leads to development of new effective malaria control tools (Hemingway *et al.*, 2002). For instance, quantitative trait loci (QTL), a positional cloning approach, has identified a polytene chromosome region encoding two genes expressing CYP6P9 and CYP6P4 from pyrethroid resistance strain of malaria vector *An. funestus* (Wondji *et al.*, 2009). Other available genomic technologies including ``transcriptional profiling`` to study metabolic-based insecticide resistance in malaria vectors (David *et al.*, 2005b) and structural analysis (Muller *et al.*, 2008; Stevenson *et al.*, 2011) have provided insights into identification of insecticides resistance mechanisms.

However, currently available genomics and structural analysis tools are usually utilised to indirectly measure the enzymes active in xenobiotics metabolism (in *vitro*) which in fact can be varied in native proteome environment. Although, biochemical assays that measure changes in enzymes activity in proteome's specimens are available (Inceoglu *et al.*, 2009; McAbee *et al.*, 2004; Morou *et al.*, 2010; Shan and Hammock, 2001), these measure global levels of enzyme activity, not individual isozymes. Therefore, it is essential to find more direct methods to assess the activity and functional state of the proteins essential in xenobiotic metabolism and resistance in its native proteomic samples. Proteomic methods such as immunobloting assays (Western blot) (Morou *et al.*, 2010; Scharf *et al.*, 1998; Zhou *et al.*, 2005) and the

methods rely on chromatographic separation including two-dimensional gel electrophoresis (2D-GE) and differential gel electrophoresis (DIGE) (Djegbe *et al.*, 2011; Jin *et al.*, 2010; Jurat-Fuentes and Adang, 2007; Pedra *et al.*, 2005), isotope coded affinity tags (ICAT) (Gygi *et al.*, 1999) and multidimensional protein identification technology (MudPIT) (Chen *et al.*, 2006; Florens *et al.*, 2002) tandem with LC-MS/MS has been introduced for the global analysis of protein identity and quantity. However, these methods do not give a direct estimation of enzymes active in the whole proteome in which would not be used in monitoring insecticide resistance.

1.8.Activity based protein profiling (ABPP), novel approach for protein activity measurements

Activity-based protein profiling (ABPP) is a novel emerging chemical proteomic technology that relies on the design of probes to target the active site of a specific subset of enzymes by covalent linkage. This provides the basis for a quantitative readout of the functional state of individual enzymes in whole proteomes (Patricelli, 2002). Based on the chemical design of ABPP the selectivity of these probes may be tuned to have a low specificity in order to target a wide spectrum of enzymes, or to have a narrow specificity to target a few specific proteins (Cravatt *et al.*, 2008). The ABPP approach has been applied to profiling protein activities in a wide range of diseases including cancer (Jessani *et al.*, 2002), obesity (Birner-Gruenberger and Hermetter, 2007), and parasite invasiveness (Greenbaum *et al.*, 2002a; Greenbaum *et al.*, 2002b). It is therefore feasible that this ABPP can be adapted to target the enzymes involved with insecticide metabolism *in vivo* and to examine their functional state in relation to resistance.

1.8.1. General description and design strategies for ABPP

The classic version of ABPP usually utilized probes that contained a warhead (reactive group) linker and a reporter tag (typically flurophor or biotin) to profile enzyme activities in proteomic samples (Figure 1.7) (Jeffery and Bogyo, 2003; Kidd *et al.*, 2001; Liu *et al.*, 1999; Saghatelian and Cravatt, 2005). The warhead should be a reactive functional group that is able to be covalently attached to the active site of specific enzyme, while the reporter tag allows a probe-protein adduct to be visualized or isolated for quantification and identification. The chemical architecture of the linker ought to connect these two elements, providing selective binding interactions, and preventing steric hindrance of the tag onto the probe's reactive side. For functional activity, probe-labelled proteins can be resolved using straightforward one dimensional polyacrylamide gel (SDS-PAGE) and visualized by in-gel fluorescence scanning (for flurophor based probes) or streptavidin blotting (for biotin probes).

1.8.2. Classification of ABPP

1.8.2.1. Directed vs. non-directed ABPP

Based on the chemical structure of the warhead the ABPP strategy can be classified as directed or non-directed. Directed ABPP is designed to target specific classes of enzymes, such as serine hydrolases and cysteine proteases (Bogyo *et al.*, 2000; Liu *et al.*, 1999; Patricelli *et al.*, 2001), whereas the non-directed approach is used for targeting multiple enzymes simultaneously. For example Cravatt and colleagues synthesized a library of biotinylated sulfonate esters and applied its members to complex proteomes.

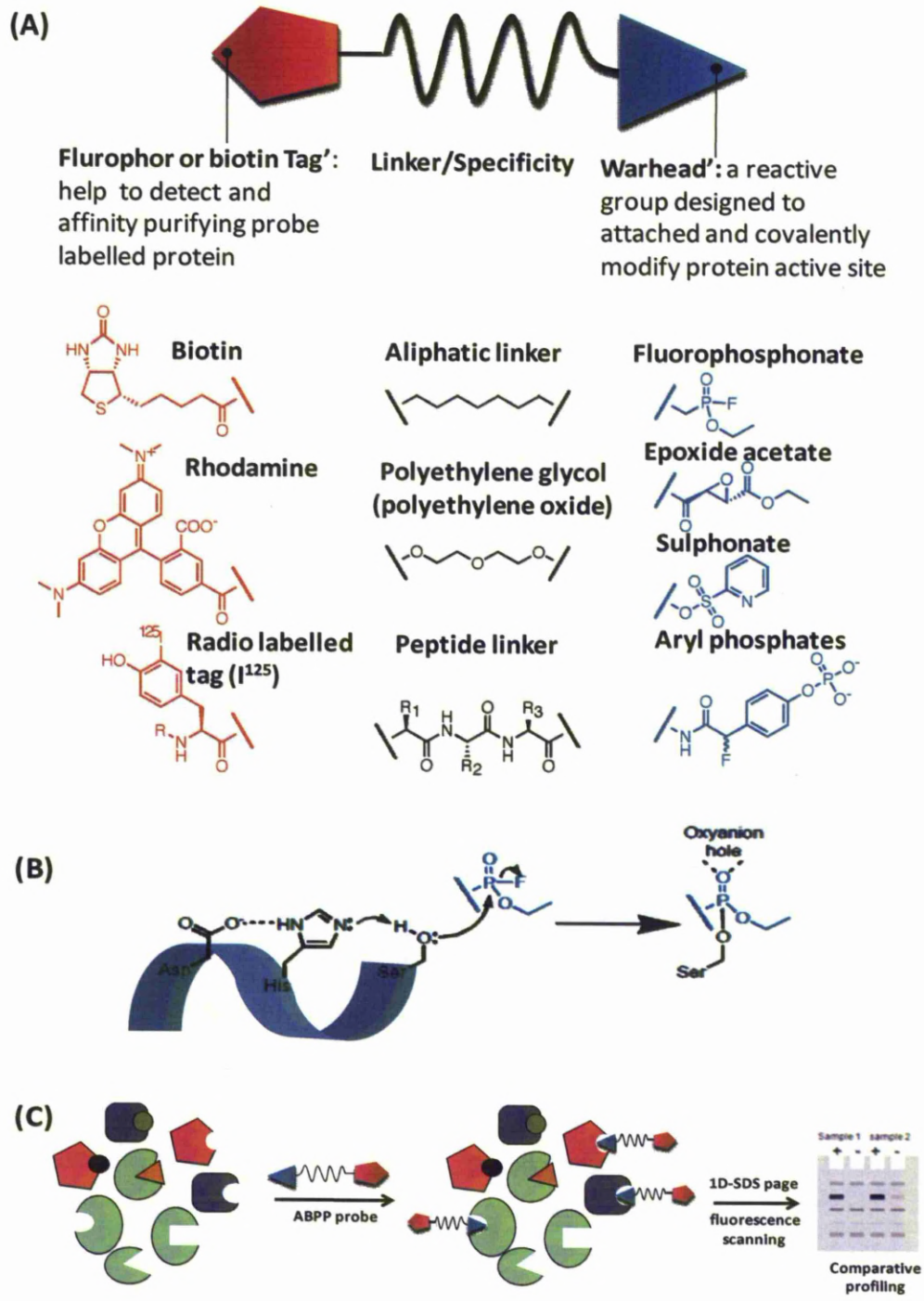

Figure 1.7. Classical ABPP probes design. (A) General components of ABPP probe design with examples of electrophile warhead that targeting different enzymes. (B) Mechanism based inactivation of fluorophosphonate warhead targeting serine hydrolase adapted from (Bogyo *et al.*, 2000). (C) Overview of gel based comparative profiling using ABPP probe.The individual sulfonates exhibited unique profiles of proteome reactivity where labeled protein was identified as a class I aldehyde dehydrogenase (Adam *et al.*, 2001).

1.8.2.2. Mechanism vs. affinity based ABPP

Based on the nature of covalent linkage of the probe within the active site, the mechanism of ABPP can be classified as either mechanism based or affinity based ABPP (Figure 1.8) (Jeffery and Bogyo, 2003; Uttamchandani *et al.*, 2008). In mechanism based ABPP, the reactive species is generated from the probe by direct catalytic activation. For instance, following activation the reactive species can bind covalently with catalytic amino acid residue(s) within the enzyme active site, producing stoichiometric (1:1) labeling. Mechanism-based probes have been reported for many different enzyme classes including serine protease (Bock, 1992a; Bock, 1992b; Grabarek and Darzynkiewicz, 2002; Kam *et al.*, 1993; Williams *et al.*, 1989), cysteine proteases (Nicholson *et al.*, 1995; Thornberry *et al.*, 1994), threonine proteases (Bogyo *et al.*, 1997; Wang *et al.*, 2003), metalloprotease (Saghatelian *et al.*, 2004), tyrosine phosphatises (Kalesh *et al.*, 2010; Kumar *et al.*, 2004; Lo *et al.*, 2002), lipases (Deussen *et al.*, 2000; Schmidinger *et al.*, 2005) and PAF-acetylhydrolases (Deigner *et al.*, 1999) and glycosidases (Tsai *et al.*, 2002; Vocadlo and Bertozzi, 2004). In contrast, the affinity-based probes first bind selectively and tightly, following which they are induced or activated into forming covalent adducts. Thus endogenous target enzyme activity is not required for probe-protein covalent linkage.

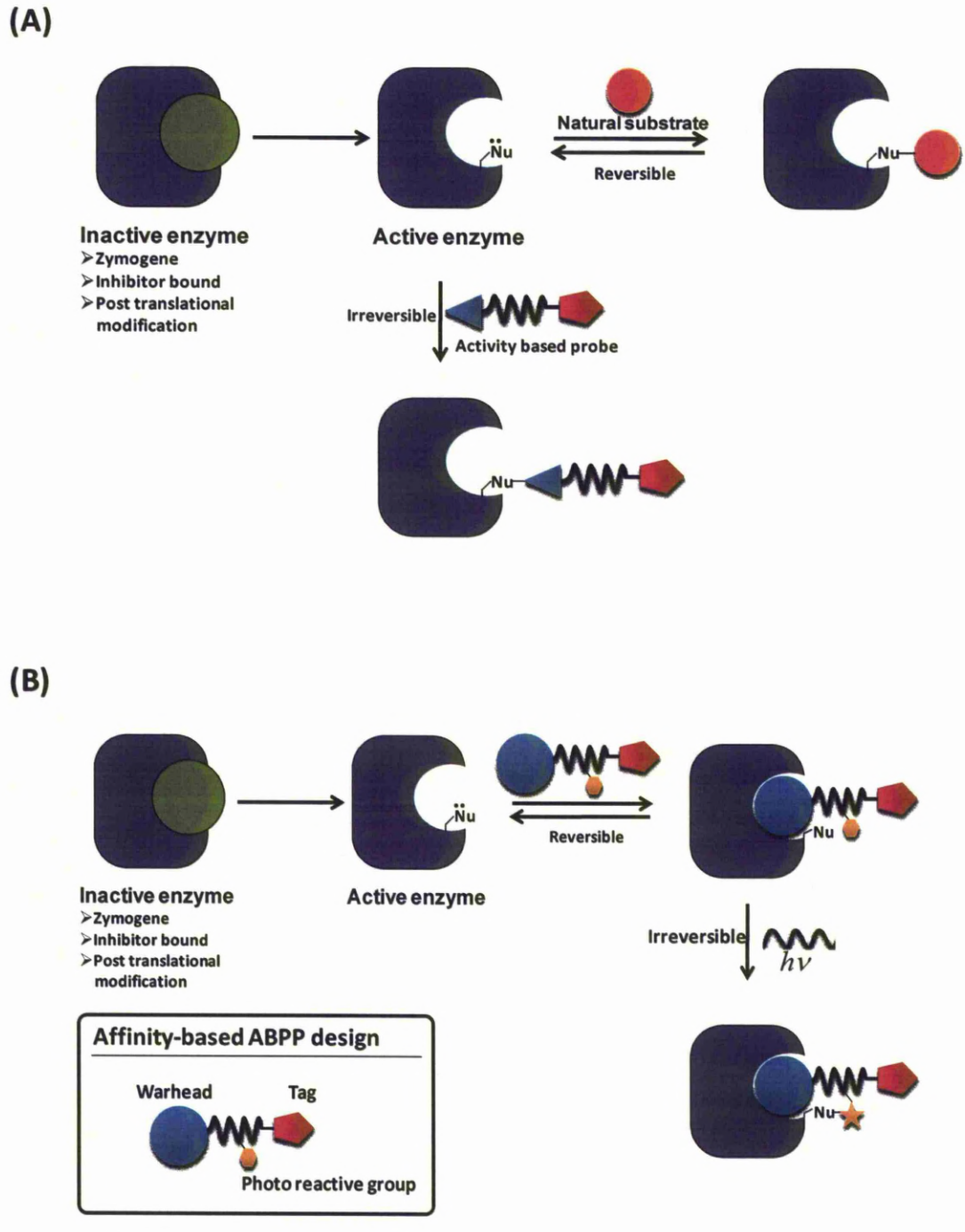

Figure 1.8. General description of ABPP strategies classified based on the mechanism of covalent adduct with protein target. (A) Activity based –ABPP, (B) Affinity-based ABPP (photo reactive probe).

An elegant example of affinity-based probes are those that contain alkylating electrophile or nuclophile that are designed to covalently label amino acid residues in their vicinity to the protein active site. Photoreactive probes with photocross-linking groups that produce covalent adducts upon light treatment are another example (Figure 1.8).

1.8.3. Click chemistry-activity based protein profiling probes (CC-ABPP)

1.8.3.1. Copper based CC-ABPP

The major problem with classic version of ABPPs is the presence of the bulky ``reporter tag``, usually a flurophor group (Rhodamine reporter) or biotin group (Greenbaum *et al.*, 2002a; Liu *et al.*, 1999) which can detrimentally effect probe function and application (Figure 1.8). The large size of the reporter tags can adversely affect probe cell permeability, bioavailability, and protein target interactions. This severely limits the usefulness of ABPP, particularly for in *vivo* monitoring of native enzyme activity. The development of click chemistry (CC) has helped to overcome this problem.

The click reaction which is now widely applied to biological applications is based on the Huisgen-1,3-dipolar cycloaddition of alkynes to azides forming 1,4-disubsituted-1,2,3-triazoles (Rostovtsev *et al.*, 2002) (Scheme 1.1). This reaction is catalyzed by reduced copper salt 'Cu (I)' which is benign (do not degrade proteins) in aqueous solution at ambient temperature and doesn't require protecting groups, or post label purification. Furthermore, the triazole is resistant to oxidation or reduction and is not susceptible to cleavage, while azide and alkyne functional groups have low reactivity

i.e. ''are nearly inert'' towards biological molecules in aqueous environments. These characteristics of the click chemistry reaction inspired Cravatt and co-workers to design and synthesise click chemistry-compatible activity based protein profiling probes (CC-ABPP) to assess enzyme function in aggressive diseases like cancer (Speers *et al.*, 2003; Speers and Cravatt, 2004a; Speers and Cravatt, 2004b).

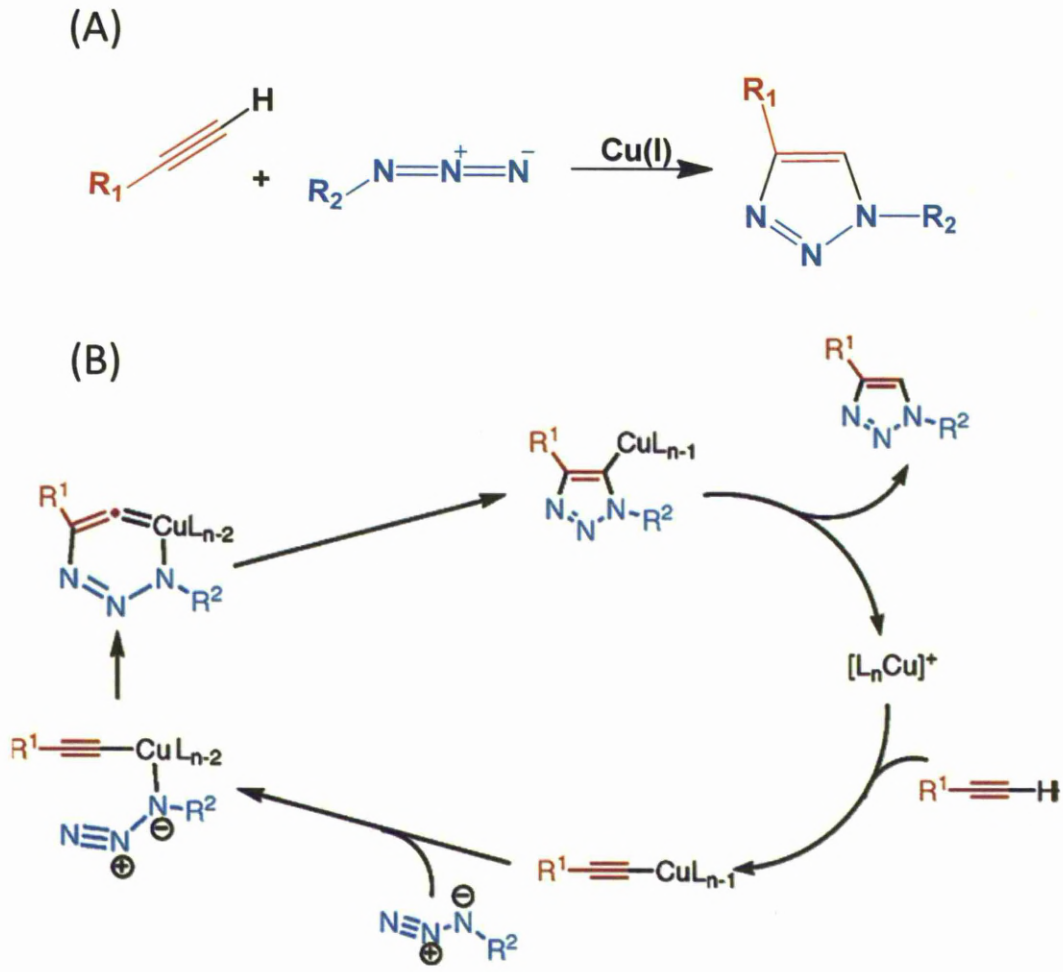

Scheme 1.1.Huisgen-1,3-dipolar cycloaddition of alkynes to azides forming 1,4-disubsituted-1,2,3-triazoles known as click reaction (A) Copper catalyzed click reaction (B) Proposed copper catalyzed click reaction mechanism (Rostovtsev *et al.*, 2002).

This technology integrates click chemistry with ABPP probes to produce tag free-ABPP (Figure 1.9), thus overcoming the problems associated with bulky tagged probes.

The CC-ABPP can be made by adding a click handle (either alkyne or azide group) to replace the reporter ``tag``: the tag is instead incorporated via CC following probe-protein labeling. Speer and Cravat initially reported the conversion of the classic ABPP, phenylsulphonate (PS) ester-rhodamine probe to a CC analogue ``PS-azide``. The labeling pattern of the CC-ABPP probe to GSTs was comparable with the labeling pattern of the PS-rhodamine (Speers *et al.*, 2003). However-ABPP produced much stronger fluorescent signals in protein targets in crude tissue and cell extracts, suggesting that elimination of rhodamine tag from traditional ABPP could accelerate the rate of the reaction between probe and GSTs.

The placement of the alkyne or azide on either the ABPPs probe or reporter did, however, affect the selectivity, binding kinetics and signal-to-noise (background binding) (Speers *et al.*, 2003; Speers and Cravatt, 2004a; Speers and Cravatt, 2004b). For example, high background has been reported for PS-azide compared to those run with rhodamine-tagged probes. This background problem has been eliminated by switching the CC partners of the reporter and tag (i.e., from PS-azide and rhodamine-alkyne to PS-alkyne and rhodamine azide) where high levels of activity-based labeling was maintained.

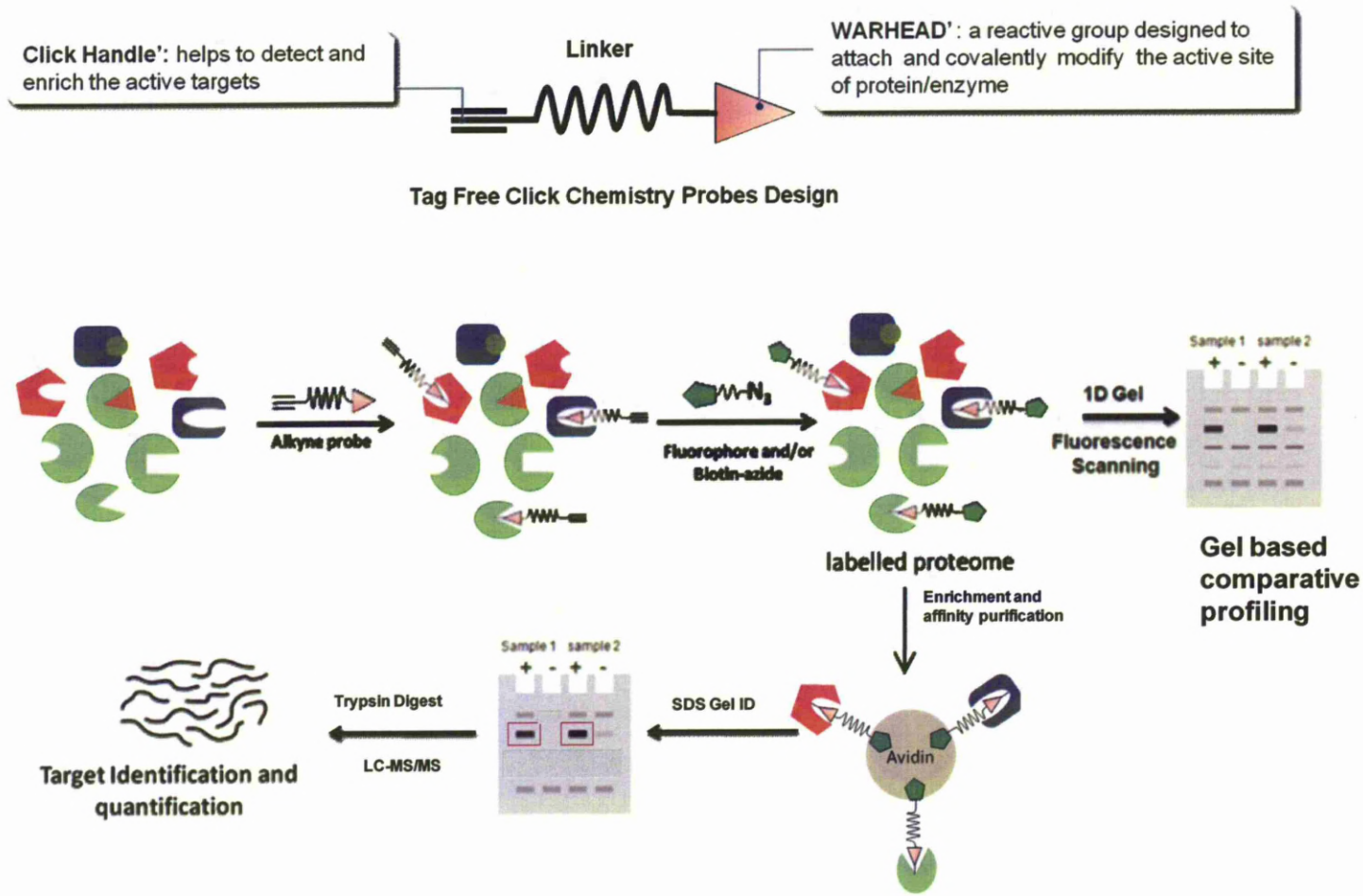

Figure 1.9. Overview of CC-ABPP approach. ABPP enables quantitative and high-sensitivity characterization a myriad of proteins activities in their native settings in a single measurement.

Like the standard ABPP method, CC-ABPP may utilize a fluorophore *e.g.* a rhodamine or biotin group that is linked to a complementary click handle for the identification of the probe/protein binding event via a click reaction. Trifunctional tags containing the complementary click handle 'azide group' as well as rhodamine fluorophore and biotin groups have also been used for simultaneous visualization and purification of the enzymes of interest, enhancing the utility of these probes (Speers and Cravatt, 2004b). For example, Wright and Cravatt successfully used this trifunctional reporter for simultaneous visualization and affinity enrichment of mechanistically labelled P450 enzymes with novel 2-EN-ABP probe (Wright and Cravatt, 2007). The 2-EN-ABP was developed by chemical modification of the generic mechanism-based P450 inhibitor (Foroozesh *et al.*, 1997; Kent *et al.*, 2001; Roberts *et al.*, 1997b) 2-ethynyl naphthalene (2-EN) (Figure 1.10).

The 2-EN-ABP probe has proved to have a relatively broad specificity both in *vitro* and in *vivo* as shown by labeling of mouse CYP1A2, CYP3A11, CYP2C29, and CYP2D9/ CYP2D10, thus allowing alterations in liver P450 activities triggered by P450 inhibitors and inducers to be followed (Wright and Cravatt, 2007). Additionally the 2-EN-ABP probe has proved capable of labeling a large set of human P450s (Wright *et al.*, 2009). More recently a suite of P450-directed CC-ABPPs have been produced, which have been designed against a variety of well known chemical architectures that are MBIs of the P450 enzyme family (Figure 1.11). Thus there is an expanding suite of CC-ABPPs available for the functional profiling of P450, which can be used for understanding P450-drug interactions.

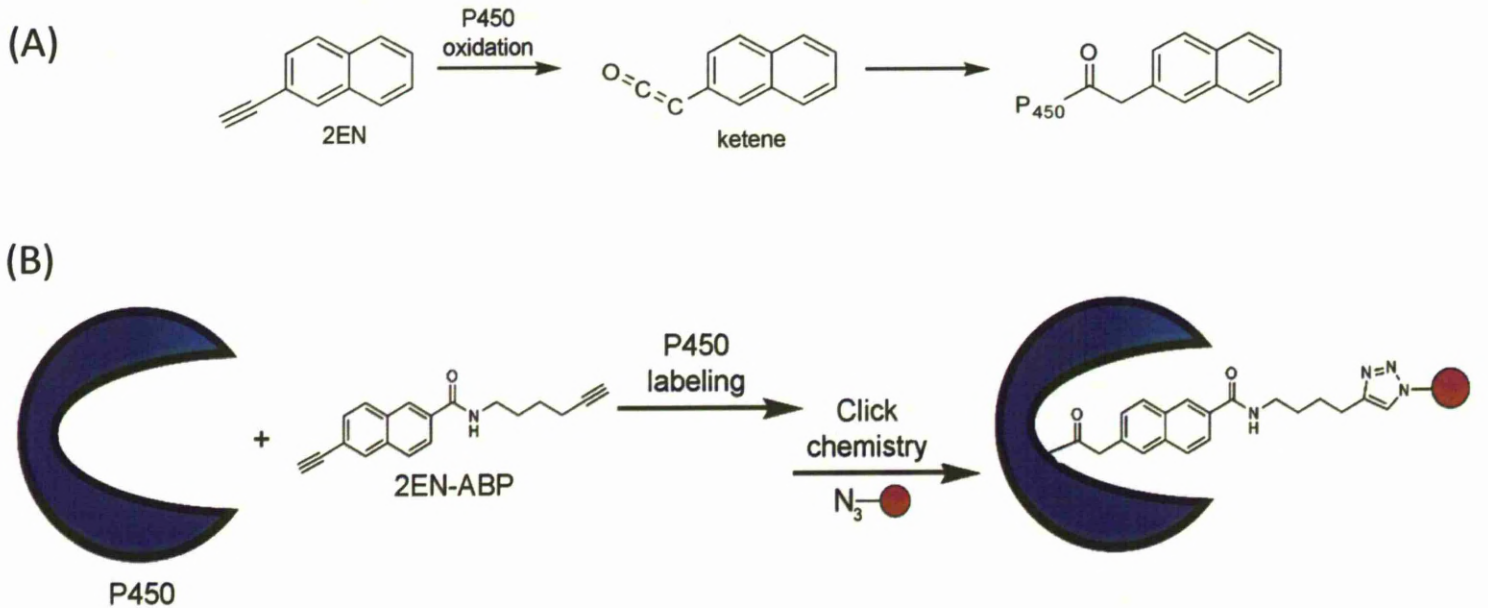

Figure 1.10. Conversion of 2-ethenyl naphthalene into a general activity based probe for P450 enzymes. (A) Mechanism of inhibition of P450 enzymes by 2EN, where the aryl alkyne group of 2EN is first metabolized to an electrophilic ketene that then reacts with amino acid residues in the P450 active site.(B)Addition of an alkyl (unconjugated) acetylene group to 2EN provides a handle for click chemistry (CC) conjugation to azide-modified rhodamine and/or biotin reporter groups (red ball) adapted from Wright and Cravatt 2007 (Wright and Cravatt, 2007).

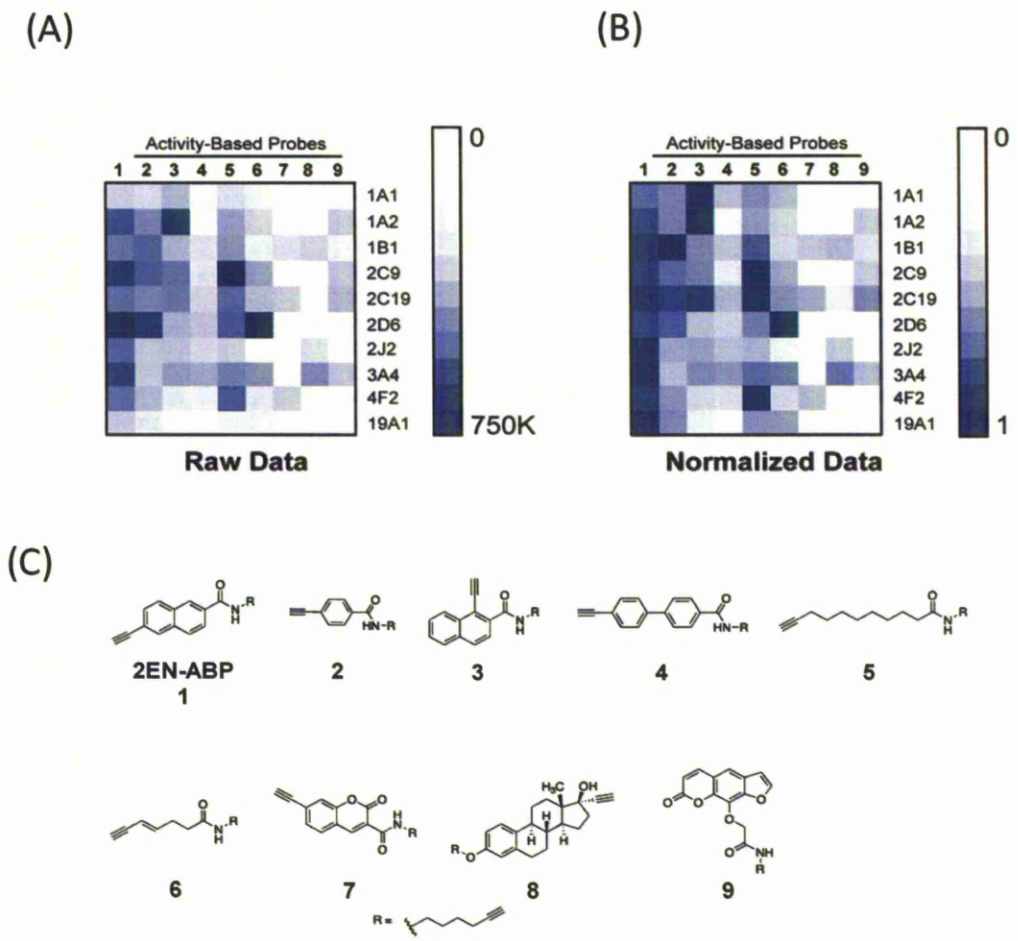

Figure 1.11. Heat maps illustrating probe labeling profiles for individual human P450 enzymes. (A) Absolute fluorescence signals of probe labeling events. (B) Normalized fluorescence signals of probe labeling events, where data for each P450 enzyme is shown as a ratio of the strongest labeling signal for that enzyme. A '1' as being the strongest binding event for an individual P450. Negative values in both the raw data and normalized data (reflecting less labeling in the presence versus absence of NADPH) have been assigned '0.' Fluorescence intensity values are in arbitrary units and represent the mean of three independent experiments per P450. (C) Chemical structure of CC-ABPP probes directed against CYP enzymes (Wright *et al.*, 2009).

1.8.3.2. Copper free CC-ABPP

Although copper catalyzed CC-ABPP has proved its utility to profile the functional state of many enzymes in *vivo* and in *vitro*, this technology is only applicable for living cell imaging when copper cell toxicity is irrelevant. The bio-orthogonal click reaction named Staudinger ligation (variants) which form an amide bond between the azide and an ester-derivatized phosphine can be applied for living cell imaging. However, the limitations of the Staudinger ligation such as slow reaction kinetics and competing oxidation of the phosphine reagents have restricted the wider use of Staudinger ligation for dynamic cell imaging. These require faster reaction kinetics and low cell toxicity. A strain promoted [3+2] azide-alkyne cycloaddition, a bio-orthogonal Cu-free variant of click chemistry that can label biomolecules rapidly and selectively in living systems has been introduced by Bertozzi and co-workers (Agard *et al.*, 2004) to afford faster kinetics and overcome the intrinsic toxicity of the traditional copper catalyzed click reaction (Figure 1.12).

This work has opened the way for labeling and visualizing biomolecules in *vivo*, which was difficult to characterize by traditional genetic manipulation. Subsequently, a difluorinated cyclooctyne (DIFO) was developed that exhibited greatly (Codelli *et al.*, 2008) enhanced reactivity and was effective for bio-orthogonal imaging of azide-tagged sugars in living organisms (Baskin *et al.*, 2007).

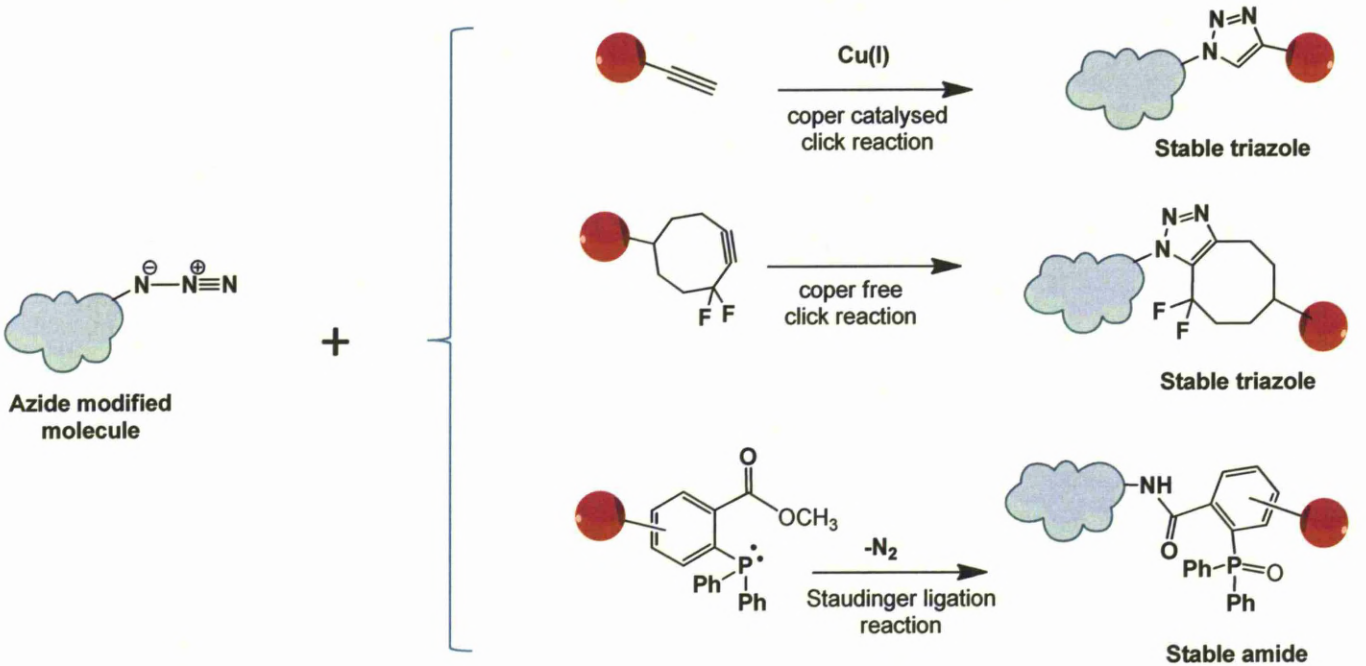

Figure 1.12. Bioorthogonal reactions for labeling of biological molecules, red ball refer to flurophor group.

1.8.4. Enzyme families addressable by ABPPs

ABPP methods have proved a useful approach for the functional annotation of enzymes activities that are myriad and difficult to identify. The application of ABPP is increasingly attracting the attention of drug development for drug target for curing many diseases. Some of the enzyme families that have been successfully annotated are illustrated in Figure 1.13.

1.8.5. Analytical platform for high-throughput, high-resolution ABPP

While SDS PAGE gel is normally utilized for resolving complex proteins labelled with ABPP's probe, quick and direct measurement of gel imaging with a fluorescence imager has been exploited using fluorophore labelled proteins (Adam *et al.*, 2002a) for comparative profiling of different proteomic samples. Moreover, the liquid chromatography-tandem mass spectrometry (LC-MS/MS) based approach has been introduced for further identification of proteins targeted by ABPPs. Gel-based analysis platforms such as 1D-SDS-PAGE in tandem with LC-MS/MS are routinely used for this purpose (Adam *et al.*, 2002c). The limited resolving power and sensitivity of gel based methods, coupled with their inability to directly assign molecular identities to probe targets, have inspired the advancement of gel-free technologies for evaluating probe–proteome reactions. The combination of chemical proteomic methods with the multidimensional protein identification technology (MudPIT) has been exploited to further afford and increase the statistical confidence of protein assignments and get insight in quantifying the relative levels of these proteins in comparative proteomic experiments (Jessani *et al.*, 2005).

Serine proteases

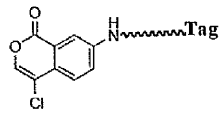

Coumarin scaffold modified to target serine proteases (Kam *et al.*, 1993).

Serine hydrolase

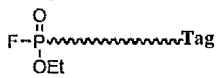

Fluorophosphonate utilised to target serine hydrolase (Liu *et al.*, 1999).

Cysteine proteases

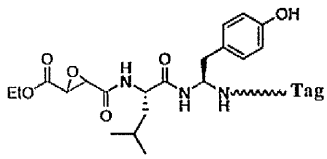

Epoxide group targeting cysteine proteases (Bogyo *et al.*, 2000).

Metalloproteases

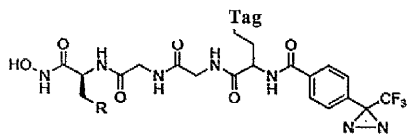

N-Hydroxylamide functionality targeting metalloprotease with a photo affinity reactive group (Saghatelian *et al.*, 2004).

Protein tyrosine phosphatases

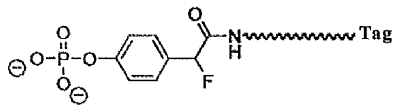

The phosphatase reaction leads to fluoride elimination and formation of a highly reactive quinine method that reacts with the proteine.

Cytochrome P450

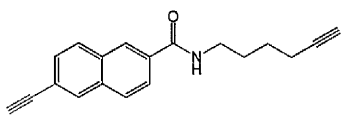

Cytochrome P450 oxidise alkyne group providing reactive species (ketene) that attacks nuclophile residue within enzyme active site and form a covalent adduct with P450s (Wright and Cravatt, 2007).

Glycosidases

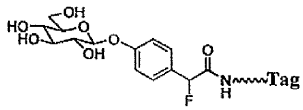

The glycosidase reaction leads to fluoride elimination and formation of a highly reactive quinone methide that reacts with the protein (Tsai *et al.*, 2002).

Kinases

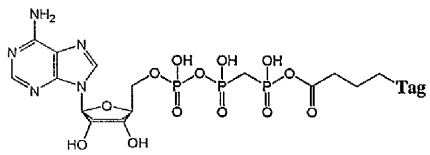

An acyl phosphate ATP probe prepared from a biotin derivative and ATP or ADP , directed activity-based protein profiling probes of Kinases (Patricelli *et al.*, 2007).

Nondirected probe for nucleophilic enzymes

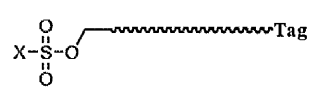

The sulfonate functionality was found to react indiscriminately with thiolase, aldehyde dehydrogenase, NADP-dependent oxidoreductase, Enoyl CoA hydratase andglutathione S-transferase (Adam *et al.*, 2002b).

X= Me, octyl, phenyl, pyridyl, nitropenyl, quinoline, naphtyl, thiophene

Figure 1.13. An example of enzymes families addressable by ABPP methods, chemical structure directed against enzymes classes illustrated where warhead denoted red colour.

The combination between ABPP and MudPIT has been investigated for chemical proteomic strategies including ABPP and CC-ABPP (Jessani *et al.*, 2005; Speers and Cravatt, 2009). This method is unique for drug target identification as it affords a powerful method to enable the discrimination of probes with high selectivity for enzyme active sites from those that show unacceptable levels of non-specific labeling. The ABPP-MudPIT was first applied to primary human breast tumors to enable the identification of enzymes activities of more than 50 probe labelled proteins in a single experiment (Jessani *et al.*, 2005).

The CC-ABPP-MudPIT (Figure 1.14) has provided greater sequence coverage (Jessani, Niessen *et al.* 2005; Speers and Cravatt 2009) of intact probe labelled proteins and circumvents interference from reporter tag compared to traditional ABPP and the active site-peptide profiling method developed by Adam *et al* (Adam *et al.*, 2004). The high sensitivity and high resolution (owing to affinity enrichment of probe-labelled targets and multidimensional separation respectively) are desirable features for ABPP-MudPIT further suggesting the suitability of the system to being used in dissecting the protein function from any complex proteomic sample.

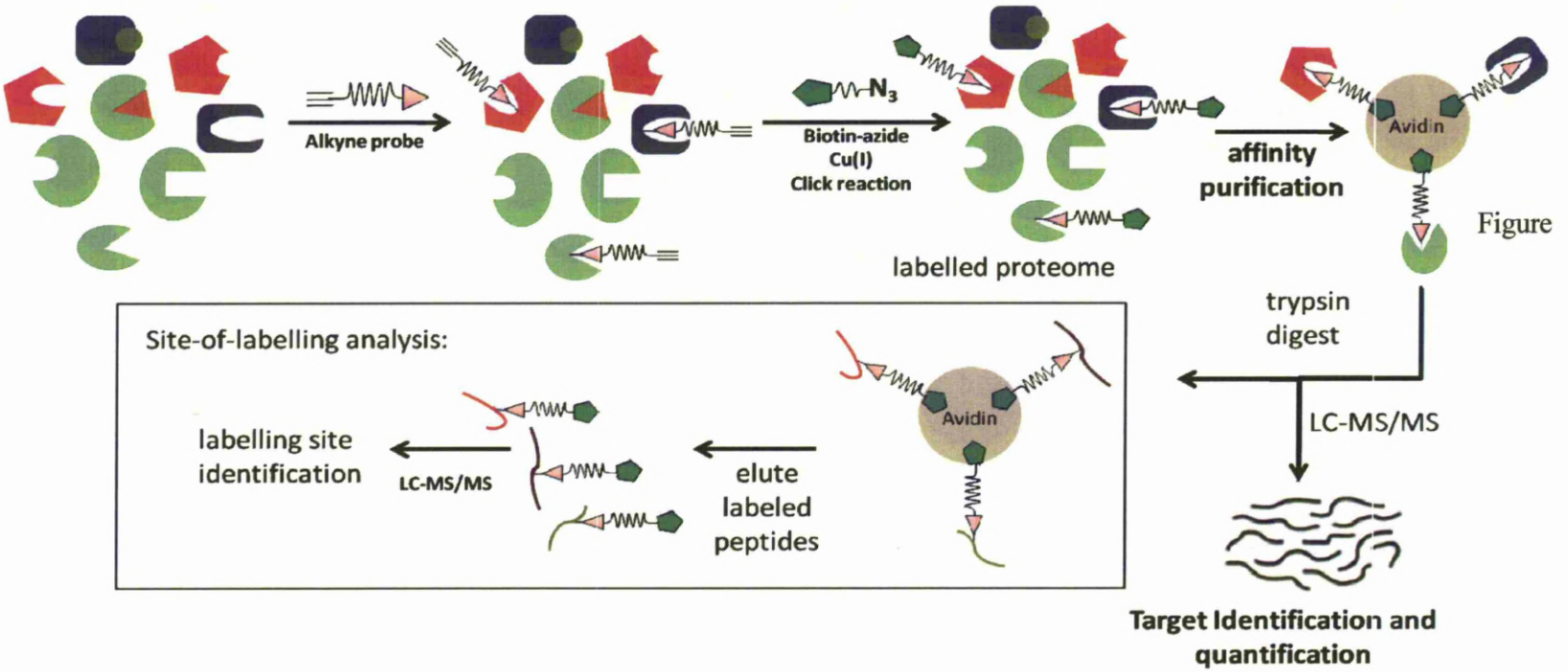

Figure 1.14. Overview of MudPIT-CC-ABPP approach.

Other platforms like capillary electrophoresis (CE) coupled with laser-induced fluorescence (LIF) as separation and detection techniques have also been exploited towards the goal of developing high throughput ABPP platform (Okerberg *et al.*, 2005).

To further extend the application and contribution of ABPP technology in comparative protein profiling experiments with minimum sample requirement, protein microarrays has been exploited. Proteins microarrays provide a novel approach of a miniaturized platform of ABPP that can be consolidated into a single step for the isolation, detection, and identification of probe labelled enzymes (Figure 1.15).

In comparison with gel-based methods, the outstanding feature of ABPP microarrays are that they exhibit much higher sensitivity and resolution. This is illustrated by recent analysis of the clinical prostate cancer biomarker, prostate specific antigen (PSA). The ABPP microarrays produced a 30 fold increase in sensitivity compared to gel-based ABPP and in the range of endogenous serum levels for this serine protease (Sieber *et al.*, 2004). However the major limitation of ABPP microarrays is that this approach requires prior knowledge of the protein targets of probes and availability of high quality antibodies for incorporation into ABPP microarrays.

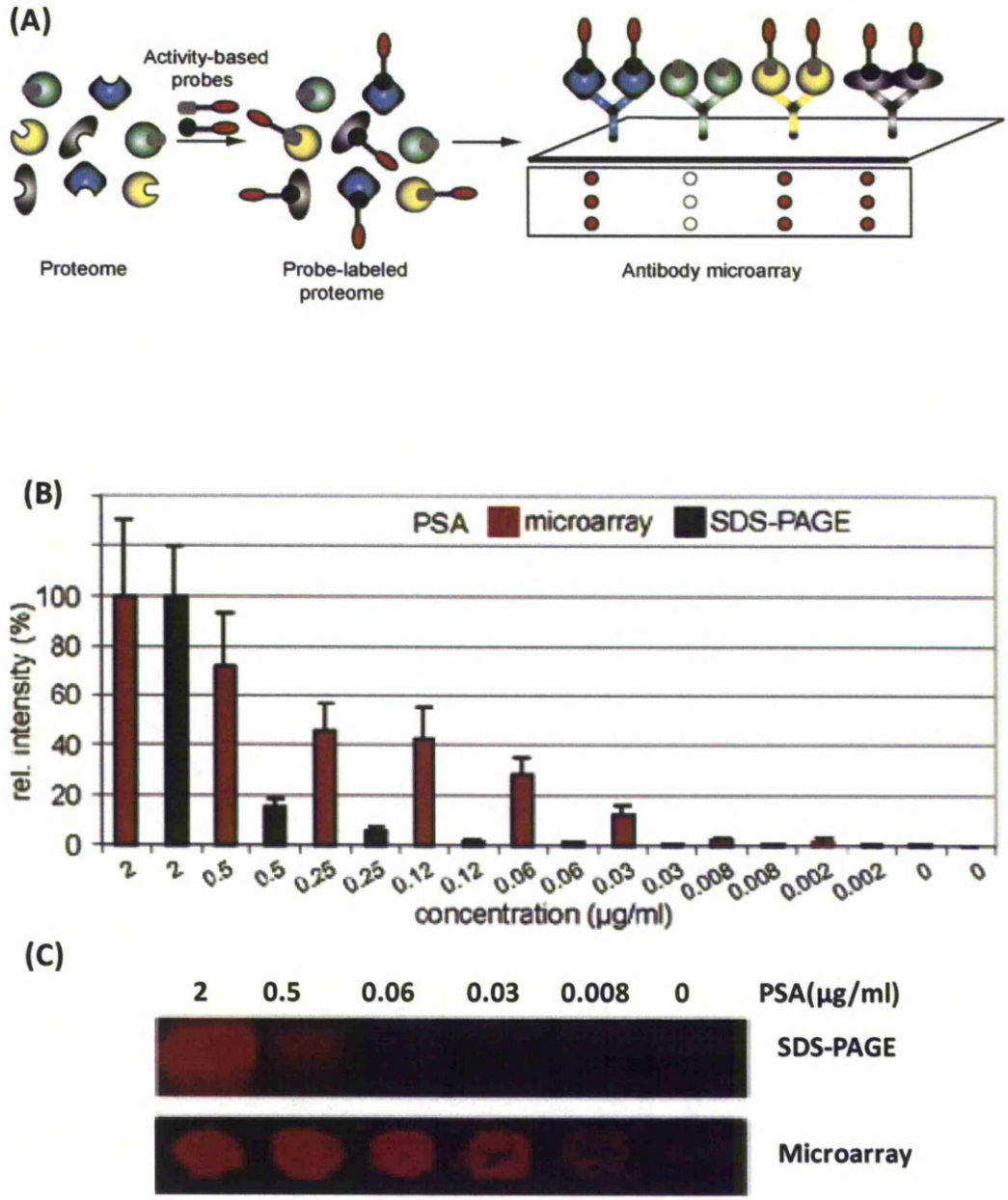

Figure 1.15. Analysis of ABPP experiments by antibody microarrays. (A) Proteomes are treated with flurophor-tagged probes and probe-labelled enzymes captured and visualized on glass slides arrayed with anti-enzyme antibodies. Testing the sensitivity of ABPP microarrays, (B, C) ABPP microarrays exhibit 30-fold greater sensitivity for the detection of PSA activity compared to gel-based ABPP (sensitivity limits: 0.002-0.008 and 0.12-0.25 ng/ml, respectively).

1.9.Research objectives

The main objective of this project is to develop novel pyrethroid ABPP probes for the selective labeling and identification of P450s that can metabolize pyrethroids in the native mosquito proteome (i.e. microsomes). In the context of malaria control, this will allow rapid screening and activity based identification of P450s that are likely to be involved in pyrethroid detoxification and resistance.

To achieve this objective, the following approach, described by Chapter, was taken to produce pyrethroid ABPP probes:

- **Chapter 2**. Assuming the alcohol moiety of the pyrethroids deltamethrin and bifenthrin to be the primary site of P450 attack, validate the MBI potential of a pyrethroid-like alcohol aryl alkyne against rat liver microsomes and the pyrethroid metabolizing *An. gambiae* P450, CYP6P3.
- **Chapter 3**. Examine the mechanism-based properties of a series of larger deltamethrin- and bifenthrin-like arylalkyne analogues for MBI against CYP6P3, and join experimental data with computational docking experiments to aid the final design of pyrethroid ABPPs.
- **Chapter 4**. Synthesise pyrethroid ABPPs
- **Chapter 5**. Validate the pyrethroid ABPPs for their ability to selectively tag, detect, enrich, and identify P450s associated with pyrethroid metabolism in the native proteome state (microsomes).

Chapter 2

2. Constructing pyrethroid ABPPs: investigating mechanism-based inhibition of P450s by arylalkyne components

2.1.Introduction

The major objective of the thesis is to develop novel pyrethroid ABPP probes capable of labelling P450 associated pyrethroid metabolism in an activity based manner. A general activity based probe (2EN-ABP) for P450s (i.e. non-specific ABPP capable of labelling several P450s) was developed by Wright and Cravatt using a click-chemistry approach (Wright and Cravatt, 2007) (see Figure 1.10, Chapter 1). Briefly, 2EN-ABP containing a reactive aryl group is metabolised by P450s, producing covalent attachment. The enzyme is then labelled with an azide fluorescent reporter by click reaction which is detectable by 1D-SDS Gel using fluorescence imager.

A similar approach has been taken here to design a novel set of ABPPs that selectively target and profile P450s with activities associated pyrethroid metabolism. Hence a pyrethroid structure was envisaged containing aryl alcohol moiety (derivatives of 3-phenoxybenzene or biphenyl moiety) which is considered the primary site of oxidation by P450s. Thus introducing a reactive alkyne group at alcohol side should result in mechanism based inactivation to P450s associated pyrethroid metabolism (Figure 2.1).

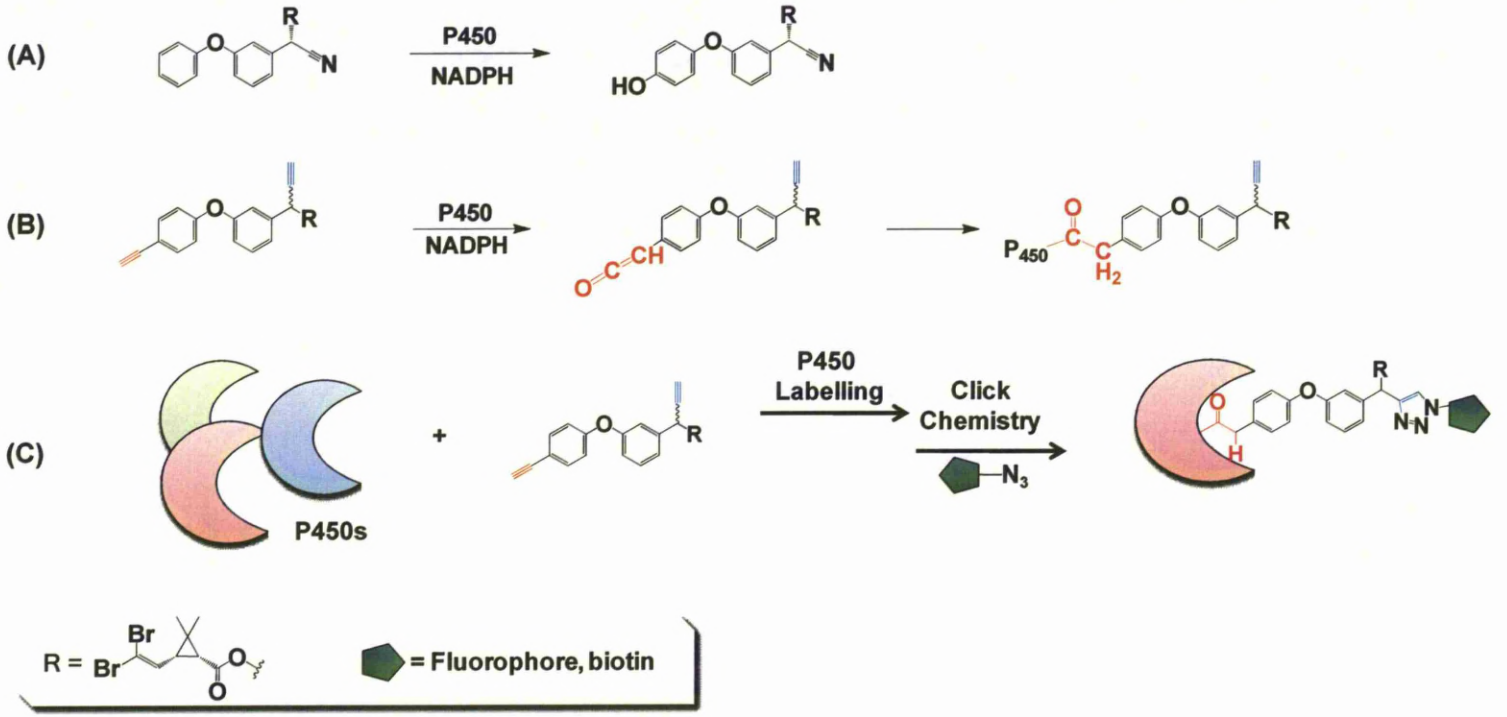

Figure 2.1.Reactivity of deltamethrin and deltamethrin analogue (Pyrethroid ABPP probe) with Cytochrome P450 Enzymes. (A) Typical hydroxylation mechanism of deltamethrin by P450 pyrethroid metabolisers. (B) Deltamethrin is converted to a click chemistry activity based protein profiling probe (ABPP) by including the two basic criteria of probe design - a warhead and a click handle. Addition of 'warhead' acetylene group (coloured red at 4` primary site of oxidation) enables covalent attachment to the active site of P450 enzymes through generation of a reactive ketene group. (C) Replacement of the alpha cyano group with an alkyne (unconjugated) acetylene group (coloured blue) provides a handle for the click chemistry conjugation to azide-modified rhodamine and/or biotin reporter groups.

Aryl-conjugated alkynes (aryl acetylene) are known to promote mechanism-based enzyme inactivation via a highly reactive ketene intermediate (Figure 1.10, Chapter1), which subsequently acylates nucleophilic residues within the P450 active site, leading to enzyme inactivation (Foroozesh *et al.*, 1997; Roberts *et al.*, 1997b; Wright and Cravatt, 2007). A number of criteria are routinely used to assess whether a substrate is a mechanism-based inactivator (Silverman, 1995). They are as follows:

1. The loss of enzyme activity must exhibit time dependence (although it is usually pseudo first order with respect to time that is not absolutely necessary). Thus, a plot of the logarithm of the enzyme activity remaining versus time should give a straight line.
2. The inactivation requires that all of the typical cofactors e.g. NADPH are present and that metabolism is occurring. The addition of the NADPH should be possible to represent metabolism of the inactivator to a reactive intermediate which can lead to enzyme inactivation.
3. The inactivation should be irreversible and activity should not return upon dialysis or gel filtration since the inhibitor should be covalently bound to the apoprotein or the heme prosthetic group.
4. Following inactivation, it should be possible to demonstrate a 1:1 stoichiometry of inactivator to enzyme molecule inactivated. In addition, the presence of exogenous "scavenger" nucleophiles such as glutathione (GSH) should have no effect on the rate of inactivation or the stoichiometry.
5. The inactivation exhibits saturation kinetics with respect to the concentration of the inactivator.

However, at least one or two of these criteria should be satisfied for a mechanism-based inactivator.

The MBI mechanism by a terminally acetylated phenoxybenzyl compound has yet to be demonstrated. Therefore, as a first step in the rational design of pyrethroid ABPPs, the aim of this chapter was to investigate the P450 MBI criteria of 1-ethenyl-4-phenoxybenzene and other arylalkyne compounds (Figure 2.2A). These compounds were chosen for their structural similarity with the alcohol moiety common to pyrethroid compounds normally used for vector control (Figure 2.2B).

2.2. Rationale

Because of the difficulties in purifying large quantities of mosquito microsomes, the ability of aryl alkynes to act as MBIs of P450s was first investigated using rat liver microsomes (RLM), which are enriched with P450s and can be purified in large quantity. Inhibition was measured against resofurin activity, for which there is a broad spectrum of substrate analogues that are used regularly for monitoring general P450 activity (Donato *et al.*, 2004; Foroozesh *et al.*, 1997). To confirm inhibitor reactivity with pyrethroid metabolising P450s, candidates were then screened against known pyrethroid metabolising *An. gambiae* P450s CYP6P3 (Müller *et al.*, 2008).

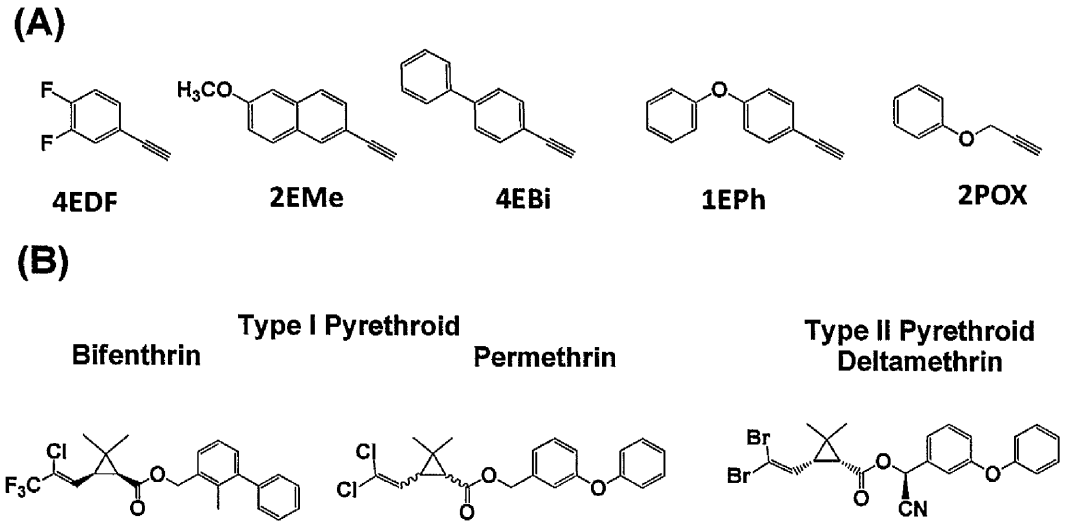

Figure 2.2. Aryl alkynes selected for testing of their MBI potential against CYP enzymes. (A) Chemical structure of different aryl compounds bearing terminal acetylene 4-ethynyl-1, 2-difluorobenzene (4EDF), 2-ethynyl-6-methoxynaphthalene (2EMe), 4-ethynyl-1, 1'-biphenyl (4EBi), 1-ethynyl-4-phenoxybenzene (1EPh) and propargyloxyphenyl (2POX). (B) Chemical structure of the Type I and Type II pyrethroid templates used for the design of pyrethroid mimetic ABPP.

2.3.Results

2.3.1. Dealkylation of 7-alkoxyphenoxazone assay.

In order to determine the best substrate for measuring P450 dealkylation activity in RLM, several 7-alkoxyphenoxazone substrates (synonymously known as alkoxy resorufin) were screened. Dealkylation of 7-alkoxyphenoxazone is catalysed by P450 to generate phenoxazone anion. The dealkylation product has fluorescence emission at *ex* 560 nm and *em* 590nm (which linearly correlates with product concentration). The measurement of the phenoxazone anion production *vs.* time enables catalytic activity to be measured in the presence and absence of xenobiotics (*e.g.* inhibitor). Figure 2.3 represents typical activity of P450s in microsomes measured for methoxyresorufin-O-demethylation (MROD), ethoxyresorufin-O-deethylation (EROD), pentoxyresorufin-O-dependentylation (PROD) and benzyloxyresorufin-O-depenzylation (BROD).

RLM showed highest activity with MROD and EROD, while only slight activity was observed with BROD and none with PROD. Furthermore, kinetic data were estimated for MROD and EROD to calculate the linear range of activity and *K*m value for each substrate. *K*m values were 1.1, 2.3 μM and V_{max} was 0.17 and 0.08 pmoles resorufin/min/pmoles P450 for MROD and EROD respectively.

Therefore, the residual activity (NADPH dependency) of RLM after incubation with inhibitors was measured in the presence of 1 μM methoxy resorufin. Compounds that were stronger inhibitors following pre-incubation with NADPH were classified as MBIs.

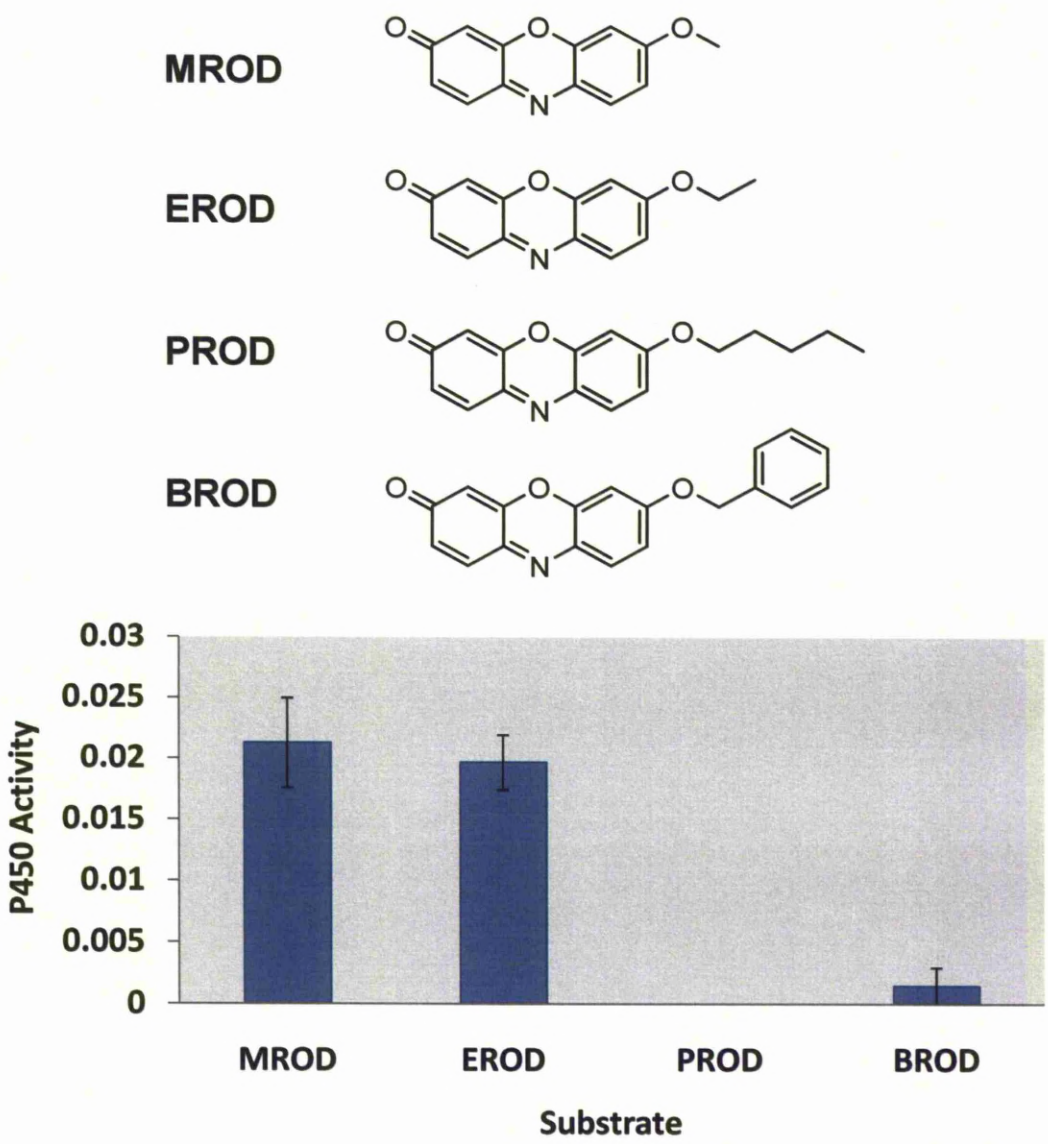

Figure 2.3 Rat liver microsomes activity with flurogenic substrates. P450 activity measured in pmole resorufin/min/pmole P450, error bar refer to standard deviation for three replicates (n=3).

2.3.2. NADPH dependent inhibition of rat liver microsomes

Preliminary screening of, 2EMe, 1EPh, 4EDF, 4EBi and 2POX, was carried out to determine the NADPH dependence of inhibition of MROD activity in RLM. The 4EBi compound is a known MBI (Foroozesh *et al.*, 1997) and included as a positive control. Different concentrations of inhibitor (1.6, 40 and 200 μM) were incubated in the presence and absence of an NADPH generating solution. NADPH dependent inhibition was demonstrated by 2EMe, 1EPh and 4EBi (Figure 2.4). 4EDF showed only minor NADPH dependent inhibition at the higher concentration 200 μM. Therefore, for further investigation of the mechanism based inhibition criteria the selected arylalkynes 2EMe, 1EPh and 4EDF were taken forward for further measurement of kinetic parameters and mode of inhibitor labelling (heme adduct or protein labelling).

2.3.3. Inhibition of P450-dependent methoxyresorufin demethylation activities in rat liver microsomes by 2EMe, 1EPh and 4EDF

Aryl acetylenes 2EMe, 1EPh and 4EDF were investigated for MBI of P450-dependent MROD activity in RLM. Figure 2.5.A represents the pseudo-first-order time-dependent losses of MROD activity in RLM in the presence of different concentrations of 2EMe. The semi log plots of the percent relative activity versus different preincubation intervals (0, 5, 10, 20 and 30 min) and concentrations demonstrated pseudo-first-order linear time-dependent kinetics for losses of enzymatic activity. The decrease of enzyme activity observed rate (k_{obs}) was calculated from the slope of each plot. The Kitz-Wilson plot was obtained by plotting the reciprocals values of k_{obs} vs. reciprocals of the inhibitor concentrations.

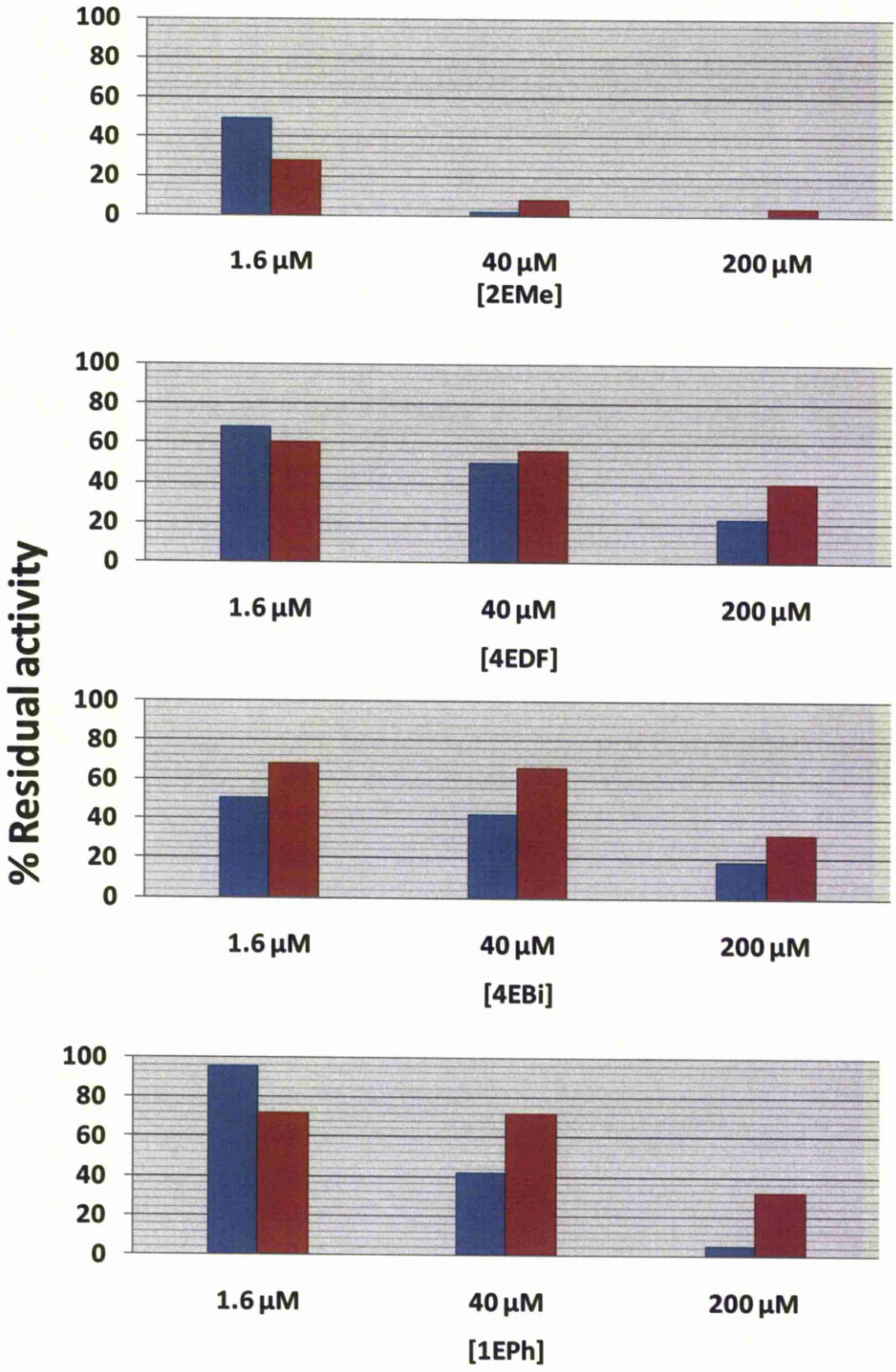

Figure 2.4 MROD remaining activities of P450 in rat liver microsomes after preincubation +■ / -■ NADPH in presence of different aryl acetylene relative to control (absence of inhibitor as mentioned in material and methods section).

The Kitz-Wilson plot of the observed inhibition of MROD activity establishes that 2EMe is a strong suicide inhibitor with a limiting $k_{inactivation}$ of 0.016 +/- 0.00057 min.$^{-1}$ and K_I of 0.018 μM (Figure 2.5.B and Table 2.1). In a similar fashion, 1EPh was found to inactivate MROD activity (Figure 2.6.). The time dependent losses of MROD activity shown in Figure 2.6.A indicate that inhibition, especially at higher inhibitor concentrations, manifest pseudo-first-order time-dependent behaviour. The resulting Kitz-Wilson plot (Figure 2.6.B and Table 2.1), further indicate the suicide inhibition with a K_I of 2.87 μM and $k_{inactivation}$ of 0.029 +/- 0.00446 min^{-1}. In contrast, there is no time-dependent loss of MROD activity for 4EDF (Figure 2.7).

2.3.4. Cytochrome P450 Destruction Assay

For all inhibitors tested the P450 content in RLM was measured after incubation with 10 μM of the potential inhibitor in the presence and absence of NADPH. There was no apparent reduction in P450 content, suggesting that heme adducts are not formed with all inhibitors tested (spectral data shown in Figure A.I.1, A.I.2, A.I.3 and A.I.4, Appendix I). Thus for MBIs 2EMe, 1EPh and 4EBi, inactivation may likely to occur via protein adduct formation.

Mechanism based inhibition parameters from the plots described above for the inhibition of MROD activities in RLM by the different ethynyl aryl compounds are summarised in (Table 2.1).

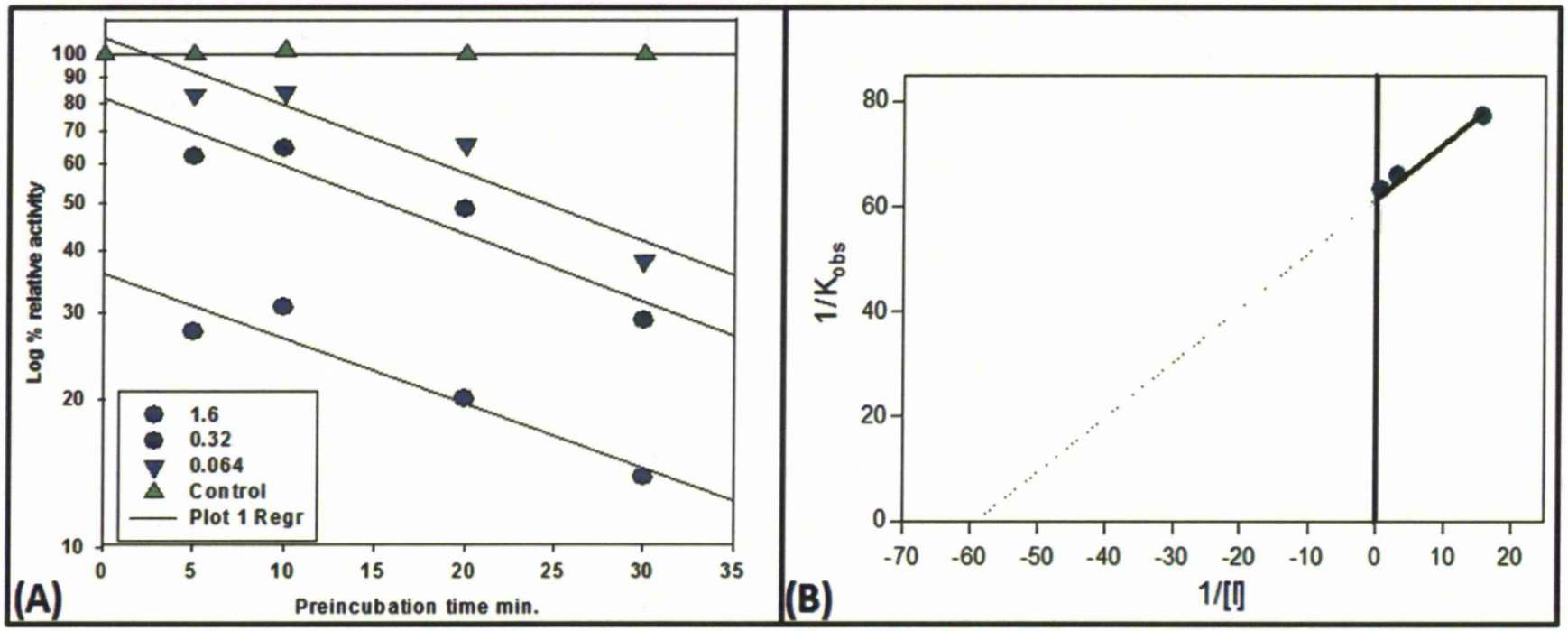

Figure 2.5. Graphical representations relevant to experimental procedure for characterising mechanism based inhibition of 2EMe, (A) time and concentration-dependent inactivation of rat liver microsomes plotted by Log of percent relative activity versus time of the MROD activity in liver microsomes in the absence or in the presence of 2-ethynyl-6-methoxynaphthalene. B) The resulting Kitz-Wilson plot obtained from plotting reciprocal of concentrations 0.064, 0.32 and 1.6 μM *vs.* reciprocal of K_{obs} values; K_I =0.01787μM and $k_{inactivation}$ = 0.016 +/- 0.00057 $min.^{-1}$

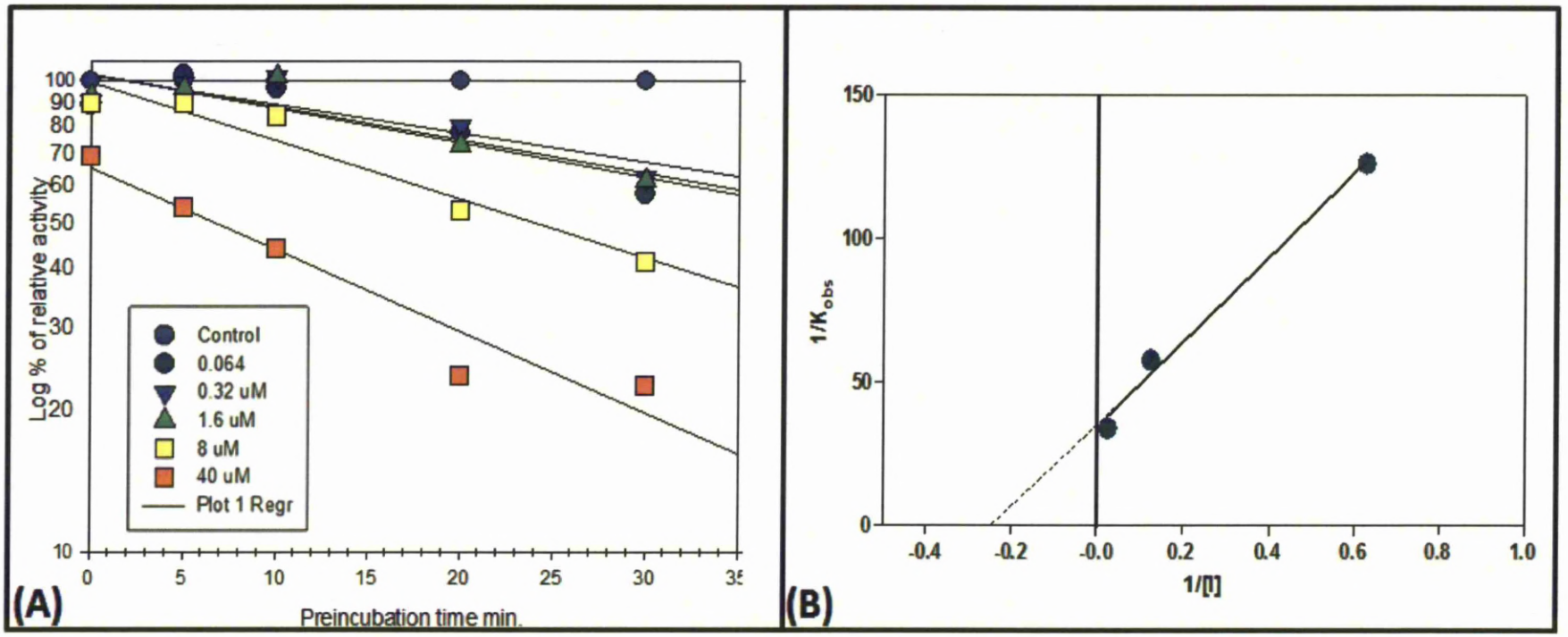

Figure 2.6. Graphical representations relevant to experimental procedure for characterising mechanism based inhibition of 1-EPh, (A) time and concentration-dependent inactivation of rat liver microsomes plotted by Log of percent relative activity versus time of the MROD activity in liver microsomes in the absence or in the presence of 1-ethynyl-4-phenoxybenzene. B) The resulting Kitz-Wilson plot obtained from plotting reciprocal of concentrations 1.6, 8 and 40 μM *vs.* reciprocal of K_{obs} values; $K_I = 2.87\mu M$ and $k_{inactivation} = 0.029 +/- 0.00446\ min^{-1}$.

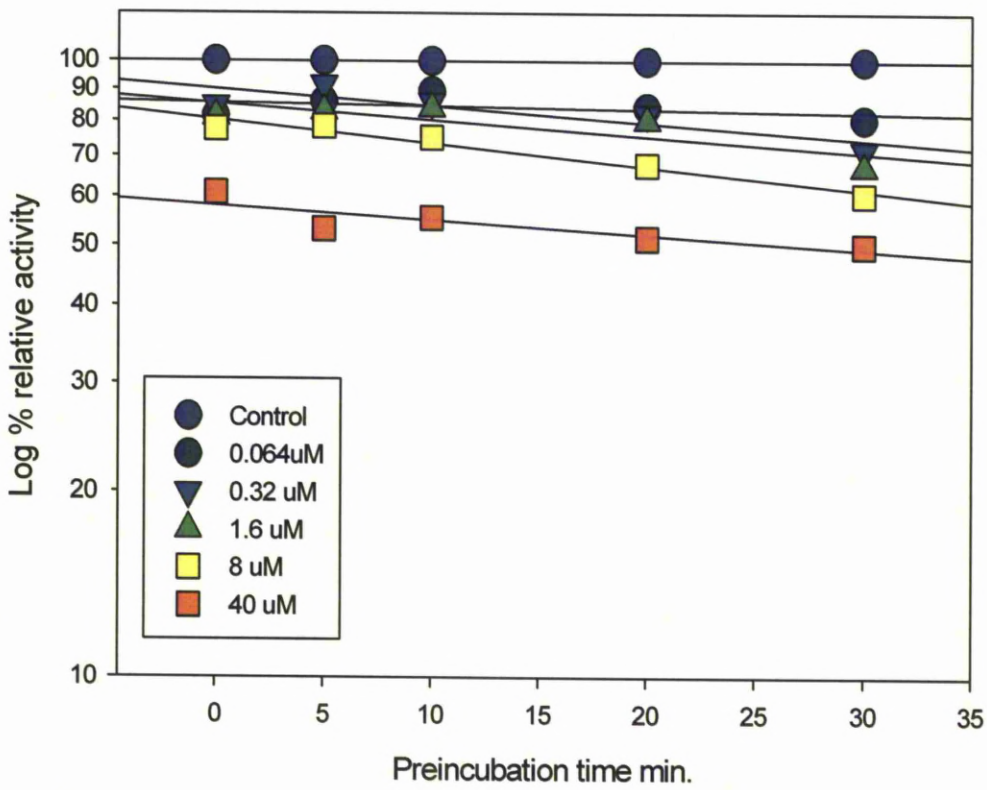

Figure 2.7 Time and concentration-dependent inactivation of rat liver microsomes plotted by log of percent relative activity versus time of the MROD activity in the absence or in the presence of 4EDF.

Table 2.1 Summary of inhibition parameters for aryl acetylene inhibition of 7-methoxyphenoxazone dealkylation in rat liver microsomes

Tested Compound	Mechanism based inactivator	Heme adduct formation	K_I μM	$k_{inactivation}$ min.$^{-1}$	$t_{0.5}$ min*
2EMe	Yes	No	0.018	0.016 +/- 0.00057	43.3
1EPh	Yes	No	2.87	0.029 +/- 0.00446	23
4EDF	No	No	--	--	--

* half- life for inactivation at infinite concentration of inactivator $t_{0.5}=0.693/k_{inactivation}$

2.3.5. Luciferin based substrate assay for measuring recombinant CYP6P3, CYP6M2 and CYP6Z2 activities.

The P450-Glo assays were used to measure the inhibition of recombinant CYP6P3 after preincubation with selected inhibitors. A comparative activity profiling study was carried out to define the optimum substrate for measuring of the P450 activities and to give a prediction about the amenability and selectivity of P450 active site for substrate recognition. Figure 2.8 represents the results of the comparative profiling of CYP6P3, CYP6M2 (both pyrethroid metabolisers) and CYP6Z2 (a pyrethroid non-metaboliser) against luciferin based substrates. Out of six luciferin substrates tested four were active with the recombinant P450s, although rates of activity were quite variable. In general, the larger substrates showed greatest activity. Interestingly, luciferin-PPXE activity was only observed with the pyrethroid metabolisers CYP6P3 and CYP6M2, whereas no activity was recorded for the non-metaboliser CYP6Z2. This might be a reflection of structural similarities between luciferin-PPXE and pyrethroids.

In addition, luciferin-BE activities were observed with all enzymes while no activity was observed for luciferin-PFBE. Luciferin PPXE was further titrated against CYP6P3 to define the linear range of activity (Figure 2.9). Based on this, a concentration of 25 μM luciferin-PPXE was used to measure NADPH dependent inhibition.

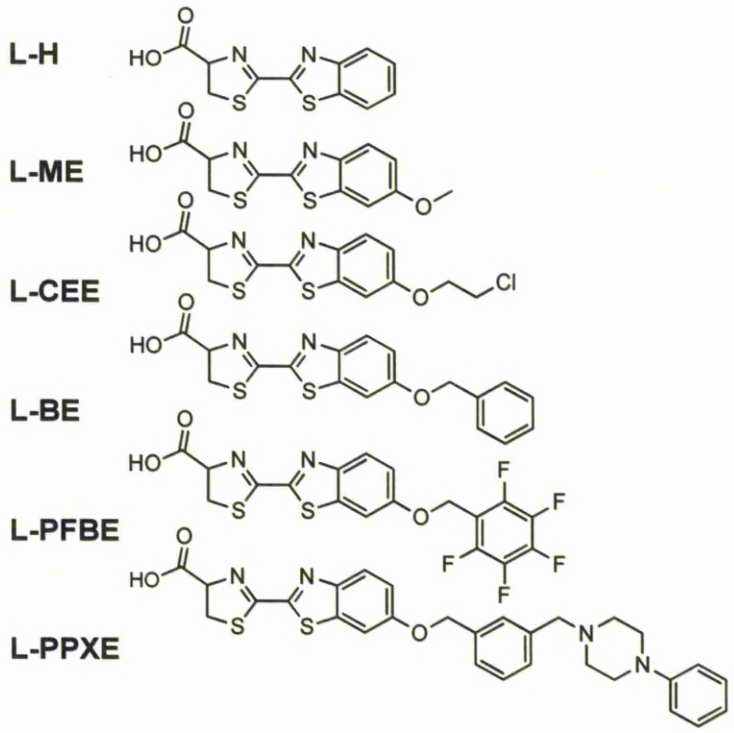

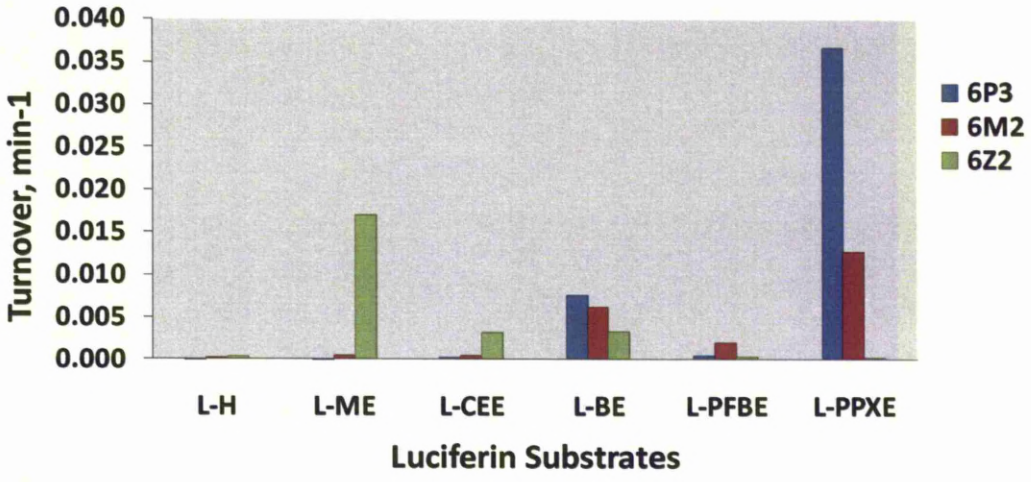

Figure 2.8 Selectivity of the P450-Glo™ substrates for recombinant *An. gambiae* P450s. Recombinant P450s were assayed for 30 minutes. All CYPs were co-expressed with AgCPR. Control reactions used recombinant enzyme without NADPH. Luciferin-PPXE activity observed with only pyrethroid metaboliser CYP6P3 and CYP6M2. L-BE activities were observed with all enzymes while no activity was observed for L-PFBE.

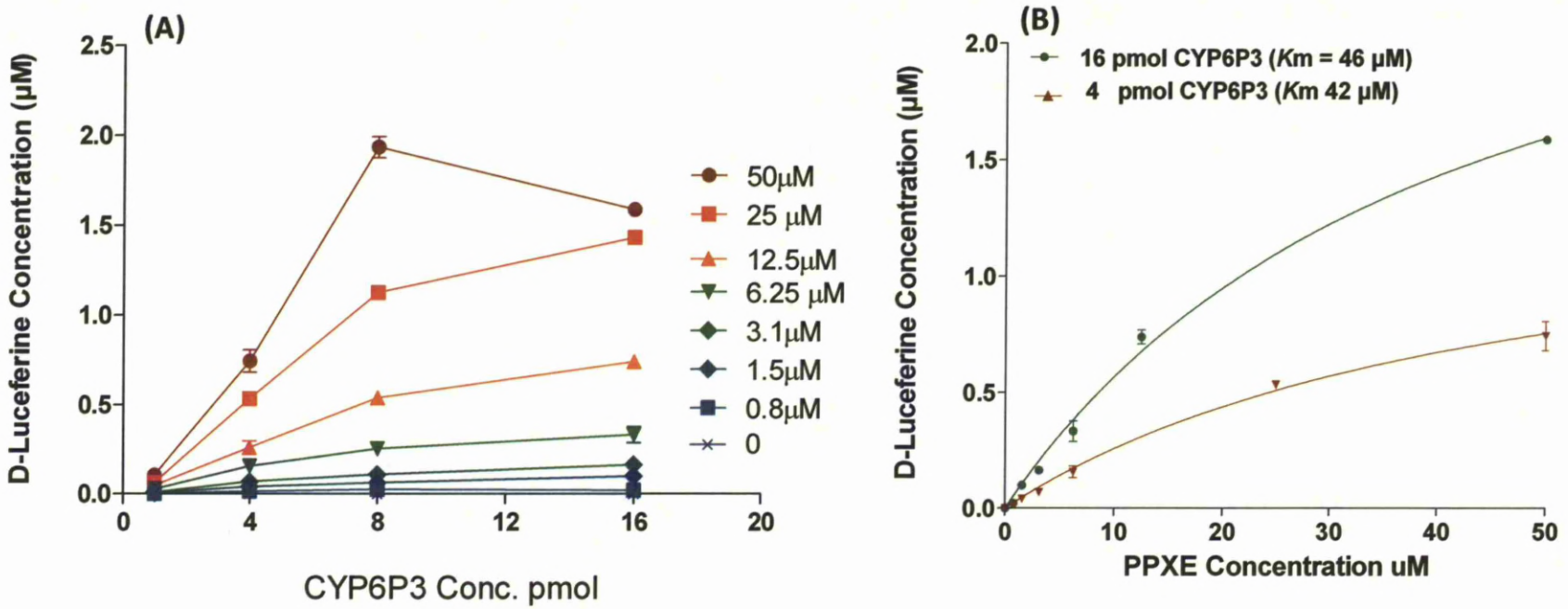

Figure 2.9.Luciferin-PPXE (P450-Glo substrate) titrations against different concentrations of CYP6P3. (A) Titration of CYP6P3 vs. different concentrations of Luciferin-PPXE substrate. (B) Michalis mention kinetics of CYP6P3 to calculate Km of Luciferin-PPXE.

2.3.6. CYP6P3-NADPH dependent inhibitions

Table 2.2 shows the residual activity of CYP6P3 after preincubation with different aryl acetylenes (10 and 100 μM) in the presence and absence of NADPH. To minimize the interference from inhibitor concentration in the second reaction with the PPXE substrate, the initial (PPXE free) reaction was diluted 10 fold into the second PPXE reaction. The selected inhibitors 2EMe, 1EPh, and 2POX showed increased NADPH dependent inhibition at 100 μM with (3, 11 and 4 fold increases over –NADPH control respectively).With 10 μM NADPH the values were 3, 1 and 1. In contrast, no NADPH dependent inhibition was observed for 4EDF and 4EBi at booth concentration tested.

Table 2.2 Remaining activity of CYP6P3 after preincubation -/+NADPH with chemical compounds

Compounds	Chemical Structure	Conc. µM	% Remaining activity [a]		-NADPH[b] / +NADPH
			-NADPH	+NADPH	
2EMe	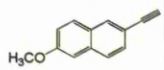	100	70	22	3
		10	147	56	3
1EPh	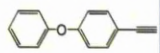	100	64	6	11
		10	66	69	1
4EDF	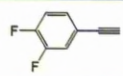	100	104	114	1
		10	109	120	1
4EBi	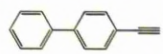	100	84	92	1
		10	88	101	1
2POX	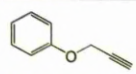	100	85	21	4
		10	102	126	1
No Inhibitor		0	100	100	1

(a) The remaining activity after 30 min preincubation was calculated by dividing P450 activity in the presence of test compound by the activity in the absence of test compound.

(b) Represents the fold increase in inhibition following preincubation of inhibitor reaction with NADPH. Reactions where there has been either no change or an increase in activity are scored as 1. 2EMe, 1EPh and 2POX, which scores >1, are considered to be MBIs.

2.4.Discussion

As the first step in the rational design of selective active site-directed "click" chemistry (CC) ABPP probes for functional analysis of P450s that mediate pyrethroid metabolism, 1EPh, 4EBi, 2EMe, and 4EDF were investigated for their potential MBI against RLM. These small molecules were selected for their structure similarity with the alcohol moieties of bifenthrin and deltamethrin structures, representative pyrethroid scaffolds for commonly used pyrethroid insecticides recommended by the World Health Pesticide Evaluation Scheme (WHOPES) (Hougard *et al.*, 2003). Although, planar structures such as 2-EN, 2-POX and 4-EBi were known suicide inhibitors of P450s (Foroozesh *et al.*, 1997) there is no literature on 1EPh, which is a more flexible derivative of the phenoxybenzyl moiety commonly found in pyrethroids. The determination of the potential MBI by this type of molecule was thus key to final ABPP design.

Here, the MBI by 1EPh and other aryl acetylene are described against MROD activity in RLM, which was found to be the best substrate for P450 measurements in RLM (Figure 2.3). Although PROD activities in rat liver microsomes have been observed to be highly selective measures of P450 2B1/2B2 activities in RLM (Foroozesh *et al.*, 1997) no activity was measured in this microsomes preparation. This might be attributed to the lack of CYP2B1/2B2 induction in the RLM used in the current investigation.

Preliminary screening of RLM with MROD demonstrated the strongest NADPH dependent inhibition by 2EMe, 1EPh and 4EBi and weak inhibitions by 4EDF. This finding may be attributed to the small size of 4EDF and the higher polarity relative to

the other compound tested which might adversely affect enzyme-inhibitor potency. Further investigation carried out using 2EMe, 1EPh and 4EDF indicates significant MBI inhibition for MROD activities in RLM for 2EMe and 1EPh (Table 2.1). The inhibition parameters calculated for MBI inhibition of 2EMe and 1EPh involved both a kinetic term ($k_{inactivation}$ and $t_{0.5}$) and a concentration term (K_I). Although, 2EMe showed high potency with RLM with a K_I value of 18 nM comparing to 1EPh with K_I value 2.8 μM, the inactivation rate of 1EPh was ~2 fold faster than 2EMe ($t_{0.5}$ 43.3 vs. 23 min for 2EMe and 1EPh respectively). Since 2EMe contains two terminal functional groups (methoxy and acetylene) the notably slow rate of inactivation may be explained by the possibility of O-demethylation which might negatively affect the inactivation rate. This argument is supported by the fact that the analogous structure 2-EN, which lacks a methoxy group, gives rapid inactivation and high potency (Foroozesh *et al.*, 1997). In addition, the P450 destruction assay indicated that the labelling of P450s may be linked to protein adduct formation rather than heme ligation in the active site as there is no loss of P450 content in the presence of any of the inhibitors (Appendix I). This result is in agreement with previous studies (Foroozesh *et al.*, 1997).

An early study was carried out to test the inhibitory effect of 33 compounds, comprising five different structural groups (alkynylpyrenes, alkynylphenanthrenes, methylenedioxyarenes, flavones, and miscellaneous), for house fly CYP6D1 (Scott *et al.*, 2000). This enzyme has been reported to mediate pyrethroid resistance in the Learn-PyR (LPR) strain of house fly (Korytko and Scott, 1998; Liu and Scott, 1996; Zhang and Scott, 1996). Interestingly it was found that in general alkynylpyrenes were the most potent group of inhibitors, with maximum effectiveness noted when the

substituent was in the 4 position (the 4`position of the phenoxy moiety in pyrethroids is the major site of P450 oxidation).

Since *An. gambiae* CYP6P3 is a known metaboliser of deltamethrin and permethrin (Muller *et al.*, 2008), NADPH dependent inhibition screening was carried out to further interpret the MBI of selected potential inhibitors against a P450 pyrethroid metaboliser. Because of low activity against resorufin substrates (MROD, EROD, PROD and BROD) (data not shown), an alternative P450-Glo assay was used to measure the residual activity of recombinant CYP6P3 with inhibitors. The comparative profiling screening for six luciferin substrates against CYP6P3 and two other *An. gambiae* P450s, CYP6M2 a pyrethroid metaboliser (Muller *et al.*, 2008; Stevenson *et al.*) and CYP6Z2 a pyrethroid binder but not metaboliser (McLaughlin *et al.*, 2008), was therefore carried out. Interestingly both the pyrethroid metaboliers CYP6P3 and CYP6M2 demonstrated best activity with the high molecular weight luciferin based substrate (L-PPXE). It is possible this may be related to structural similarities of the probe with pyrethroids. Therefore the Luciferin-PPXE substrate was taken forward and used as probe substrate for determination of CYP6P3 residual activity with selected inhibitors.

Although, 4EBi is a known suicide inhibitor of P450 dependent MROD in RLM (Foroozesh *et al.*, 1997) and CYP6D1 (Scott *et al.*, 2000), no NADPH dependent inhibition was indicated for CYP6P3. However, 1EPh and 2POX showed significant NADPH dependent inhibition, particularly at the higher concentration of 100 μM relative to 10 μM (Table 2.2). This data highlights the fact that both the size and shape

of the molecule are important parameters for inactivation of CYP6P3. It is possible the presence of an ether bond in 1EPh and 2POX might play an important role in directing the molecule towards heme binding group in CYP6P3 active site. Accordingly, it was concluded that 1EPh, an analogue of the common phenoxybenzyl moiety in pyrethroid insecticides, can act as a MBI as evident by NADPH dependent inhibition of P450 activity in RLM and the anopheline pyrethroid metaboliser CYP6P3.

The next phase was to assess the ability of 1EPh and other molecules bearing terminal alkyne groups in larger deltamethrin and bifenthrin analogues to fully assess the inhibitory effect in the context of composite pyrethroid molecule. This was examined in the next Chapter along with 3D homology modelling of P450 interactions to predict the inhibitory mechanisms of these inhibitors.

2.5.Materials and methods

2.5.1. Chemicals and reagents

Potential inhibitors 1-ethynyl-4-phenoxybenzene (1EPh), 4-ethynylbiphenyl (4EBi), 2-ethynyl-6-methoxynaphthalene (2EMe), (prop-2-yn-1-yloxy) benzene (2POX) and 4-ethynyl-1, 2-difluorobenzene (4EDF), were purchased from Sigma-Aldrich Chemical Co. (UK). P450s Flurogenic substrates 7-methoxyphenoxazone, 7-ethoxyphenoxazone, 7-pentoxyphenoxazone, and 7-benzyloxyphenoxazone were purchased from Sigma-Aldrich Chemical Co. (UK). DMSO and other solvents were reagent grade (Sigma Aldrich, UK).

2.5.2. Instrumentation

Cytochrome P450 spectral analysis was carried out using Cary 4000 UV-Vis spectrophotometers (VARIAN, UK). Fluorogenic measurement was carried out using Fluoroskan® Ascent microplate fluorometer (Thermo Scientific, UK). Luminescent measurements (P450 Glo assay) were carried out using LUMI star Omega (BMG Laboratories, UK).

2.5.3. Rat liver microsomes preparation

Rat liver microsomes prepared from male Wistar rat which contains 0.52 nmol/mg protein was kindly provided by Dr. Alison Shone, Molecular Biochemical Parasitology group, Liverpool School of Tropical Medicine (LSTM).

2.5.4. Preparation of *E. coli* membranes expressed CYP6P3

The CYP6P3 membrane and its redox partner cytochrome P450 reductase (CPR) expressed in competent *Escherichia coli* DH5α cells were prepared as detailed by Muller *et al.* (Muller *et al.*, 2008), briefly transformant, which was given by Dr. Bradley Stevenson, Vector Group, LSTM, was grown in 0.4 l of Terrific Broth with ampicillin and chloramphenicol selection at 37°C until the optical density at 595 nm reached 0.8 units. The culture was then cooled to 25°C, supplemented with 0.5 mM 5-aminolevulinic acid (Melford, UK) and 1 mM isopropyl β-D-1-thiogalactopyranoside (Melford) before incubation continued at 25°C with orbital shaking at 150 rpm. The cells were harvested and membranes prepared as described previously (McLaughlin *et al.*, 2008). P450 functional expression was quantified by CO-difference spectroscopy (Omura and Sato, 1964a) and CPR activity was estimated by cytochrome c reductase activity (Pritchard *et al.*, 2006). CYP6P3 was expressed at 50–100 nmol of P450 per litre of culture. The isolated bacterial membranes contained 0.428 nmol of CYP6P3 per mg protein and the specific activity of CPR was 10 nmol reduced cytochrome C min^{-1} mg^{-1} proteins. Total protein concentration was determined by Bradford assay, with bovine serum albumin standards according to standard method (Bradford, 1976). CYP6M2 and CYP6Z2 membrane preparation were supplied by Dr. Bradley Stevenson, Vector Group, LSTM.

2.5.5. Assay of 7-Alkoxyphenoxazone dealkylation in rat liver microsomes

To define the optimum substrate for measuring the residual activity of P450s after preincubation with potential inhibitors, the P450 dealkylation activities in RLM were assayed by different flurogenic substrates, 7-methoxyresorufin-O-demethylation (MROD), 7-Ethoxyresorufin-O-deethylation (EROD), 7-resorufin-O-depentylation

(PROD), and 7-benzoylresorufin-O-depenzylation (BROD) according to published method (Foroozesh *et al.*, 1997). Cytochrome P450 enzyme activity was measured as function of phenoxazone anion production, the product anion was monitored every 5 sec by a spectrofluorometer at 560 nm excitation and 590 nm emission. Enzyme activity was calculated based on the difference between phenoxazone production *vs.* time in presence and absence of NADPH. The kinetics data were analysed to calculate the *K*m value for substrates and linear range of enzymatic activity by fitting activity *vs.* substrate concentration to a hyperbolic function using Graph Pad Prism Program Version 5.01.

2.5.6. NADPH dependence of inhibitions in rat liver microsomes

The 7-methoxyphenoxazone demethylation assays were run with the following modifications; the microsomes were preincubated with the inhibitors in 0.2 M tris-HCl buffer containing $MgCl_2$ for 30 min, in the presence or absence of the NADPH-generating solution (1 mM glucose-6-phosphate (Melford), 0.1 mM NADP+ (Melford), 1 unit ml^{-1} glucose-6-phosphate dehydrogenase (G6PDH, Sigma) in a total volume of 50 μl).

The 7-alkoxyphenoxazone substrates and required amount of NADPH-generating solution were then added, and the production of 7-hydroxyphenoxazone was monitored at 590 nm as described above. Control samples were preincubated for 5 min in the presence of the NADPH with 1% of pure DMSO instead of the inhibitors.

2.5.7. Cytochrome P450s residual activity assay estimation

Residual activity of rat liver microsomes after pre-incubation with different concentration of potential inhibitors (2EMe, 1EPh, 4EBi, 4EDF) was carried out on white flat 96 well Microplate. Briefly, in duplicates 50 µl of 0.2 M Tris HCl buffer, pH 7.4 containing a combination of 2x different concentration of potential inhibitor and 6.4 pmol of RLM were incubated for 3 min at 37° C. Thereafter the reaction was initiated by addition of 50 µl of 2x NADPH generating system (1 mM glucose-6-phosphate (Melford), 0.1 mM NADP+ (Melford), 1 unit ml^{-1} glucose-6-phosphate dehydrogenase (G6PDH, Sigma) in a total volume of 50 µl) pre-warmed to 37°C to yield 0 0.064 0.32 1.6, 8, 40 and 200 µM final concentration of inhibitors. Then the microplate was incubated at 37° C for 0, 5, 10, 20 and 30 minutes. After each incubation time, the residual activity of P450s were measured by further addition of 100 µl 1x NADPH generating system containing double the *K*m concentration of methoxy-resofurines substrate (7-methoxyphenoxazone). The production of 7-hydroxyphenoxazone anion was monitored every 5 sec by a spectrofluorometer at 560 nm excitation and 590 nm emission. In the absence of inhibitors the product formation was linear for at least 10 minute. An equation describing product formation with respect to reaction time in seconds was obtained for each inhibitor concentration. Data analysis was performed by plotting the log of the remaining enzymatic activity percent in the presence of inhibitor relative to that in the absence of inhibitor at 0, 5, 10 20 and 30 min intervals by using Sigma-Plot graphics package (Jandel Scientific, San Rafael, CA). For mechanism-based inhibitors, these plots of the change in enzymatic activity versus time manifested pseudo-first-order time-dependent losses of activity (Equation 1).

$$A_t = A_0(e^{-k_{obs}t}) \qquad eq.1$$

Where A_t is the remaining enzyme activity at time t, A_0 is the enzyme activity at $t=0$, k_{obs} is the first-order rate constant for enzyme inactivation determined from the slopes of the initial linear decline in activity.

The hyperbolic relationship between k_{obs} and $[I]$ is fitted by Equation (2) using graphpad prism software to derive estimates of $K_{inactivation}$ and K_I.

$$Kk_{obs} = \frac{(k_{inactivation} \times [I])}{(K_I + [I])} \qquad eq.2$$

Where I, is the initial concentration of the inhibitor, K_I is the apparent dissociation constants of the enzyme-inhibitor complexes leading to enzyme inactivation and $k_{inactivation.}$ is the rate constant that defines the maximal rate of inactive enzyme formation (Silverman, 1995). In addition, the linear regression analysis Kitz–Wilson plot (Kitz and Wilson, 1962), a double reciprocal plot of the observed inactivation rate constant (k_{obs}) as a function of mechanism based inactivator concentration ([I]) were also used to obtain $k_{inactivation.}$ and K_I values. A plot of $1/k_{obs}$ against 1/ [I] generates a trend line, which has a y-intercept of $1/k_{inactivation}$ and an x-intercept of $-1/K_I$.

2.5.8. Cytochrome P450 destruction assay

Cytochrome P450 destruction assay was carried out according to published method (Foroozesh *et al.*, 1997) briefly 1 mg ml^{-1} of microsomal protein was incubated at 37 °C for 3 min in 1.88 ml of 0.2 M Tris-HCl buffer, pH 7.4 containing 0.2 mM ethylenediaminetetraacetic acid, 3.3 mM KCl, and the appropriate concentration of

potential inhibitor (in 10 µl of DMSO), and 0.22 ml of the NADPH-generating system then was added to start the reaction. A 1.0 ml aliquot was removed immediately (zero time) and placed in an iced cuvette. Another 1.0 ml aliquot was removed after 30 additional min of incubation at 37 °C and was placed in a second ice-cooled cuvette. Incubations with 10 µl of DMSO in the absence of the inhibitor were carried out as controls. $Na_2S_2O_4$ (~1 mg) was added to each cuvette and a reference spectrum from 400 to 500 nm recorded. CO was gently bubbled into the solution in the cuvette for 1 min, the cuvette was immediately capped, and the spectrum between 400 and 500 nm was measured. The change in absorbance at 450 nm relative to 490 nm, after subtraction of the dithionite reduced reference spectra, was used to determine the P450 content using 91.000 M^{-1} cm^{-1} as the extinction coefficient (ε).

2.5.9. Luciferin based substrate assay for measuring recombinant CYP6P3, CYP6M2 and CYP6Z2 activities.

Luminescent P450 activity assays were performed in all-white 96-well plates (Thermo Fisher Scientifc, Hudson, NH) using the commercially available P450-Glo (Promega, Madison, WI) substrates against CYP6P3, CYP6M2 and CYP6Z2. Luciferein-H, Luciferin-Me, Luciferin-CEE, Luciferin-Be, Luciferin-PFBE and Luciferin-PPXE substrates were screened in duplicates at 20 µM substrate final concentration and 0.25µM adjusted P450s concentration in final volume of 50 µl. Double final concentration of recombinant P450 substrate combination in 25 µl volume were diluted to 50 µl by addition of 25 µl of an NADPH generating system (1.3 mM $NADP^+$, 3.3 mM glucose-6-phosphate, 0.4 U/ml glucose-6-phosphate dehydrogenase, and 3.3 mM

$MgCl_2$ concentrations; BD Biosciences, San Jose, CA) thereafter the plate was incubated at 37° C for 30 minutes. The P450 reaction was stopped by the addition of 50 µl of luciferin detection reagent (Promega). After the addition of the Luciferin detection reagent, the reactions were incubated at 25° C for an additional 20 min after which luminescence was quantified using an integration time of 1 sec and gain of 450. The average relative luminescence unit (RLU) values from two wells containing all assay components except NADPH were used as a blank. Luminescence readings that were not at least two-fold higher than the blank were considered not detectable. A standard Luciferin curve (0-2000 nmol/well) was generated and used to convert RLU values to nano moles Luciferin produced.

2.5.10. CYP6P3 and luciferin-PPXE substrate titration

Different concentrations (0, 0.781, 1.56, 3.125, 6.25, 12.5, 25 and 50 µM) of Luciferin-PPXE substrate were titrated with different concentration of CYP6P3 (1, 4 8 and 16 pmol) to determine the enzyme and substrate concentration combination that give a linear range of response. CYP6P3 activity was measured as mentioned above; data were fitted by a hyperbolic model using Graphpad prism software to derive the *Km* of PPXE substrate.

2.5.11. CYP6P3-NADPH dependent inhibitions

Recombinant P450 CYP6P3 with CPR, prepared as detailed by Müller *et al.* (Muller *et al.*, 2008), was assayed for residual activity of CYP63 with luciferin-PPXE substrate after preincubation with various concentrations (0, 10 and 100 µM) of Inhibitors (2EMe, 1EPh, 4EDF, 4EBi and 2POX) in a white 96 well plate format at 37 °C. Primary reaction was carried out by incubation of 2x inhibitor concentration in a final

volume of 50 µl contain 20 pmol of recombinant CYP6P3 in the presence of 100 mM potassium phosphate buffer, pH 7.6. Reaction was initiated by addition of 50µl 2x NADPH generating system after a 3 min preincubation. At 30 min of incubation 5 µl aliquots were taken out of the primary incubation mixture and transferred into 45 µl of a secondary incubation mixture (10-fold dilution) containing 100 mM potassium phosphate buffer, pH 7.6, luciferin PPXE (25 µM/per well) as reporter substrate, and NADPH generating system to measure residual activity.

With a 10-fold dilution and saturating concentrations of Luciferin PPXE (25 µM) in the secondary incubation, it was assumed that any further inactivation was minimal. After 30 min of incubation at 37°C the D-Luciferin detected by addition of 50 µl of Luciferin detection reagent as P450 Glo assay protocol recommended (Promega, UK) and the plate incubated at room temperature for 20 min, then the luminescence signal detected by reading the plate at Omega Microplate Readers.

Chapter 3

3. Rational design of pyrethroid ABPP probes

3.1.Introduction

Arylalkynes like propargyloxyphenyl (2POX) and 2-ethynyl naphthalene (2-EN) have been used for decades as synergists for insecticides such as pyrethroid and carbamates (Brown *et al.*, 1996; Fellig *et al.*, 1970; Metcalf *et al.*, 1966; Sacher *et al.*, 1968) (Figure 3.1). The phenoxybenzyl moiety of the conventional pyrethroids (*e.g.* cypermethrin) is considered the major site of oxidative metabolism in resistant insects (Brown *et al.*, 1996; Scott *et al.*, 2000; Shan *et al.*, 1997).

In an earlier study the phenoxybenzyl moiety was replaced to produce new cypermethrin analogues with known P450 monooxygenase blocking groups including pentafluorophenyl, methylenedioxyphenyl, and propargyloxyphenyl groups (Shan *et al.*, 1997). These compounds were tested for their insecticidal and synergistic activity against tobacco budworms that were insecticide-susceptible (LSU) or that expressed metabolic resistance to cypermethrin (Pyr-R). Interestingly it was found that both *trans* and *cis* isomers of α(*S*),1(*R*)-propargyloxyphenyl-containing compounds were insecticidal whereas α(*R*),1(*R*)-*cis*-methylenedioxyphenyl- and -propargyloxyphenyl-containing compounds were nontoxic but significantly enhanced the toxicity of cypermethrin.

In this project, arylalkynes are being used to replace primary or secondary oxidation sites in the alcohol moiety in pyrethroid structures (i.e. deltamethrin and bifenthrin) to produce click chemistry activity based protein profiling probes (Pyrethroid ABPP) to enable direct functional labelling of P450s associated with pyrethroid metabolism,.

In the previous chapter, the arylalkynes 1-ethynyl-4-phenoxybenzene (1EPh) and propargyloxyphenyl (2POX) were demonstrated to be suicide inhibitors of CYP6P3. The aim of this chapter was to understand the structural basis of interactions of composite pyrethroid molecules bearing an arylalkyne group using with CYP6P3 to aid the design and synthesis of novel pyrethroid ABPP probes.

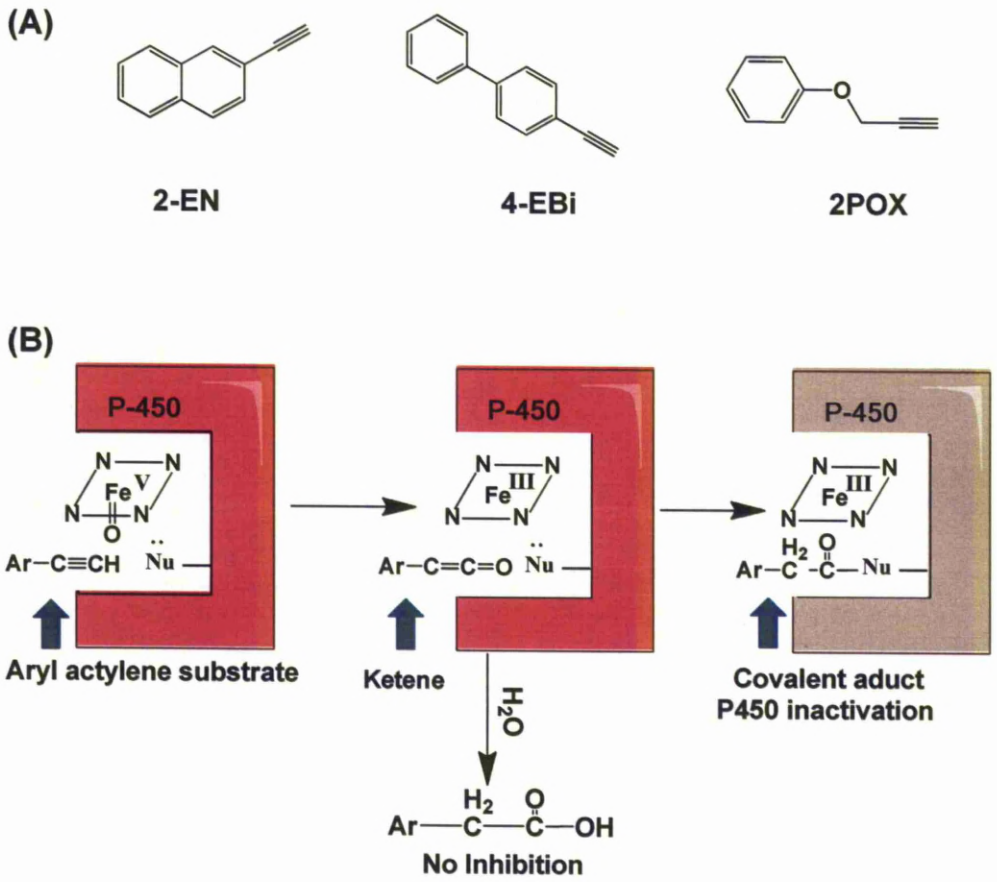

Figure 3.1 Summary of mechanism based inhibition of P450s. (A) Chemical structure of arylalkyne compounds commonly used as P450 inhibitors (Brown *et al.*, 1996; Sacher *et al.*, 1968; Scott *et al.*, 2000) (B) Mechanism based inactivation (MBI) illustrating P450-catalyzed oxidation of the aryl alkyne to produce a highly reactive ketene that subsequently acylates nucleophilic residues within the P450 active site adapted from (Hammons *et al.*, 1989).

3.2.Results and Discussion

3.2.1. CYP6P3 NADPH dependent inhibitions by bifenthrin and deltamethrin analogues

Aryloxypropynes and aryl acetylenes are known to destroy hepatic cytochrome P450 through a suicidal interaction (MBI) (Fellig *et al.*, 1970; Foroozesh *et al.*, 1997). Deltamethrin and bifenthrin analogues containing either propargyloxyphenyl (2POX) or 2-methyl substituted analogue of 4-EBi were further examined for MBI against CYP6P3 (Table 3.1.). The NADPH dependent inhibition was the criterion for irreversible inactivation. In general, deltamethrin and bifenthrin analogues C3 and C4 bearing the 2POX group displayed NADPH-dependent inhibition at 10 μM as demonstrated by 3 and 2 fold lower levels of activity following preincubation with NADPH respectively. In contrast, no inhibition was recorded for C1 and C2 respectively. Although rigid structures like 4-EBi are proven irreversible inhibitors of P450 activity rat liver microsomes (Foroozesh *et al.*, 1997), results in Chapter 2 suggested this molecule was not a MBI for the mosquito CYP6P3. Nevertheless, 4-EBi molecule has been considered here for inclusion in the composite structure of pyrethroid analogues for two reasons. First, a part of this molecule (biphenyl moiety) is commonly found in commercial pyrethroids such as bifenthrin. Second, it was worth testing the effect of the structural rigidity of alcohol moieties containing terminal acetylene on the irreversible inhibition of P450 by a pyrethroid structure. Since both C1 and C2 are derivatives of the planar 4-EBi, which did not show MBI against CYP6P3, this suggest that a flexible aryl ether group such as 2POX or 1EPh in a pyrethroid structure may alter the molecule configuration to allow for better binding and/or metabolism leading to enzyme inactivation.

Table 3.1.Inhibitory effect of deltamethrin and bifenthrin analogues on CYP6P3

Compounds	Chemical Structure	Conc. µM	% Remaining activity [a]		-NADPH[b] / +NADPH
			-NADPH	+NADPH	
C1	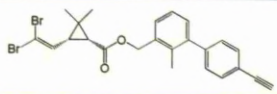	10	78	95	1
C2	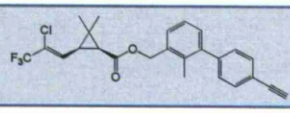	10	88	65	1
C3	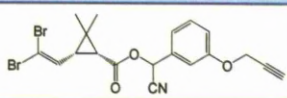	10	50	15	3
C4	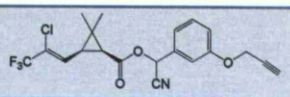	10	21	13	2
Deltamethrin	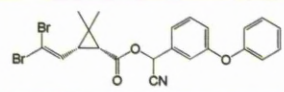	10	110	96	1
No inhibitor		0	100	100	1

(a) The remaining activity after 30 min preincubation was calculated by dividing P450 activity in the presence of test compound by the activity in the absence of test compound. (b) Represents the fold increase in inhibition following preincubation of inhibitor reaction with NADPH.

3.2.2. Binding of deltamethrin and bifenthrin analogues

In P450s at least one of the following three MBI mechanisms usually predominates; (i) N-alkylation of the P450 prosthetic heme moiety; (ii) direct alkylation of the apoprotein at the active site; and (iii) chemical-induced heme modification of the protein at the active site. However, these mechanisms could all also operate concurrently to contribute to some extent to the overall inactivation process (He *et al.*, 1996). To investigate the binding affinity and the irreversible inactivation mechanism of CYP6P3 by C3 and C4, their affinity and binding mode with CYP6P3 was studied. This was determined by measuring changes in the optical difference spectra upon addition of the compounds to *E. coli* membranes expressing CYP6P3 according to McLaughlin et al (McLaughlin *et al.*, 2005). CYP6P3 showed a 'type I' binding spectrum upon C3 and C4 additions with λmax and λmin of ~390 nm and ~420 nm respectively (Figure 3.2.A). This type of spectral change is well known to be associated with a change from a low spin (hexa-coordinated) state to a high spin (penta-coordinated) state of the ferric iron caused by substrate binding.

Spectral differences *vs.* concentration also plotted to calculate the apparent dissociation constant K_d for each compound (Figure 3.2.B). The estimated K_d values for C3 and C4 were 30 and 24 μM respectively, a fairly modest affinity suggestive of substrate interaction with CYP6P3. In general, these observations suggest that these molecules might be substrates for CYP6P3.

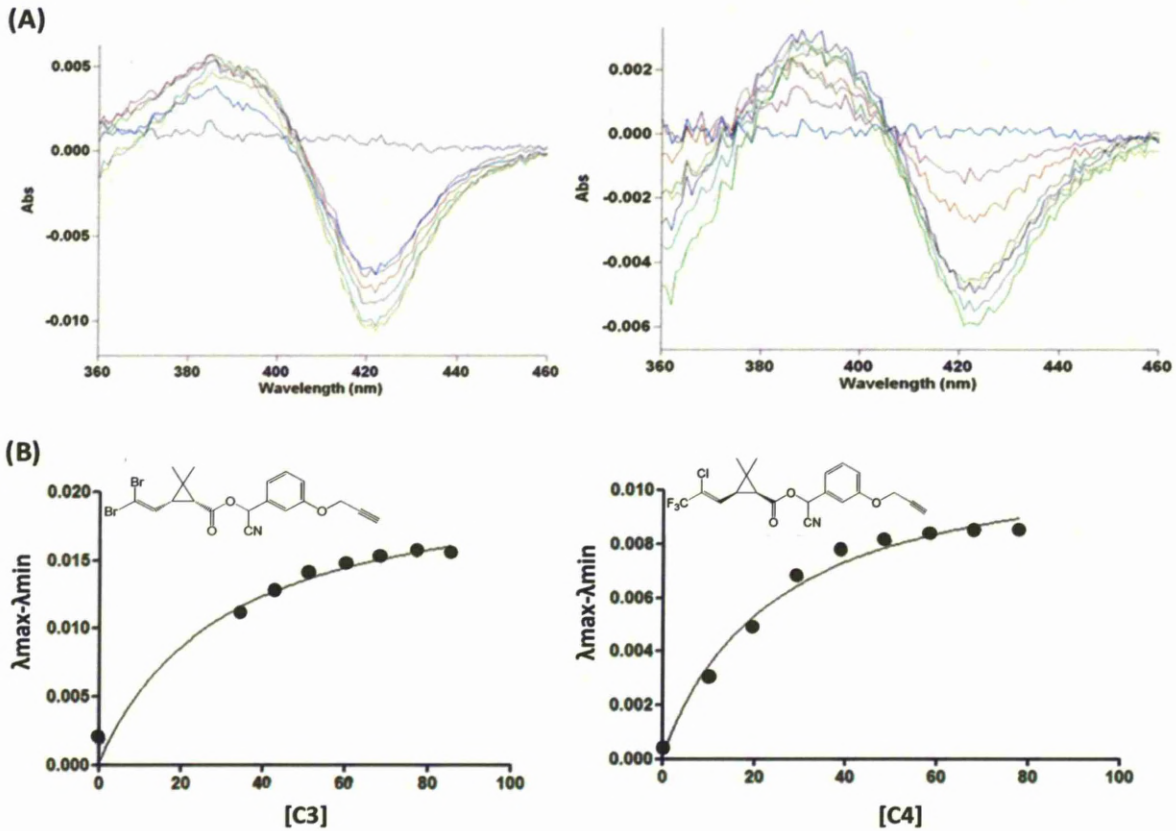

Figure 3.2. Representative optical difference spectra produced by deltamethrin and bifenthrin analogues binding to CYP6P3. (A) Typical type I binding spectra of deltamethrin and bifenthrin analogues. (B) Typical binding curves used to calculate the dissociation constant estimated by spectral difference at different concentration of inhibitors, experiments were performed as described in Materials and Methods section.

3.2.3. HPLC metabolism study

To determine if the deltamethrin and bifenthrin analogues containing the 2POX group were CYP6P3 whither degraded upon enzyme activation or not, they were incubated with CYP6P3 and the products examined by HPLC. Substrate depletion after incubation for 30 minutes +/- NADPH was measured by HPLC using isocratic separation conditions. A decrease in substrate concentration was observed with ~ 65% and 76% elimination of the initial concentrations of C3 and C4 respectively. The metabolites were separated by gradient HPLC. Several metabolite peaks were resolved for C3 and C4. These data demonstrate that both C3 and C4 are metabolised by CYP6P3 (Figure 3.3). Although metabolism at the alkyne group is needed for MBI, P450s often have multiple sites of attack which might affect the efficiency of inhibition.

Summing up, both spectroscopic analysis and the HPLC metabolism profile for C3 and C4 indicated that while they were substrates for CYP6P3, a prerequisite for MBI, there were multiple degradation products, thus the mechanism of inactivation appears complex.

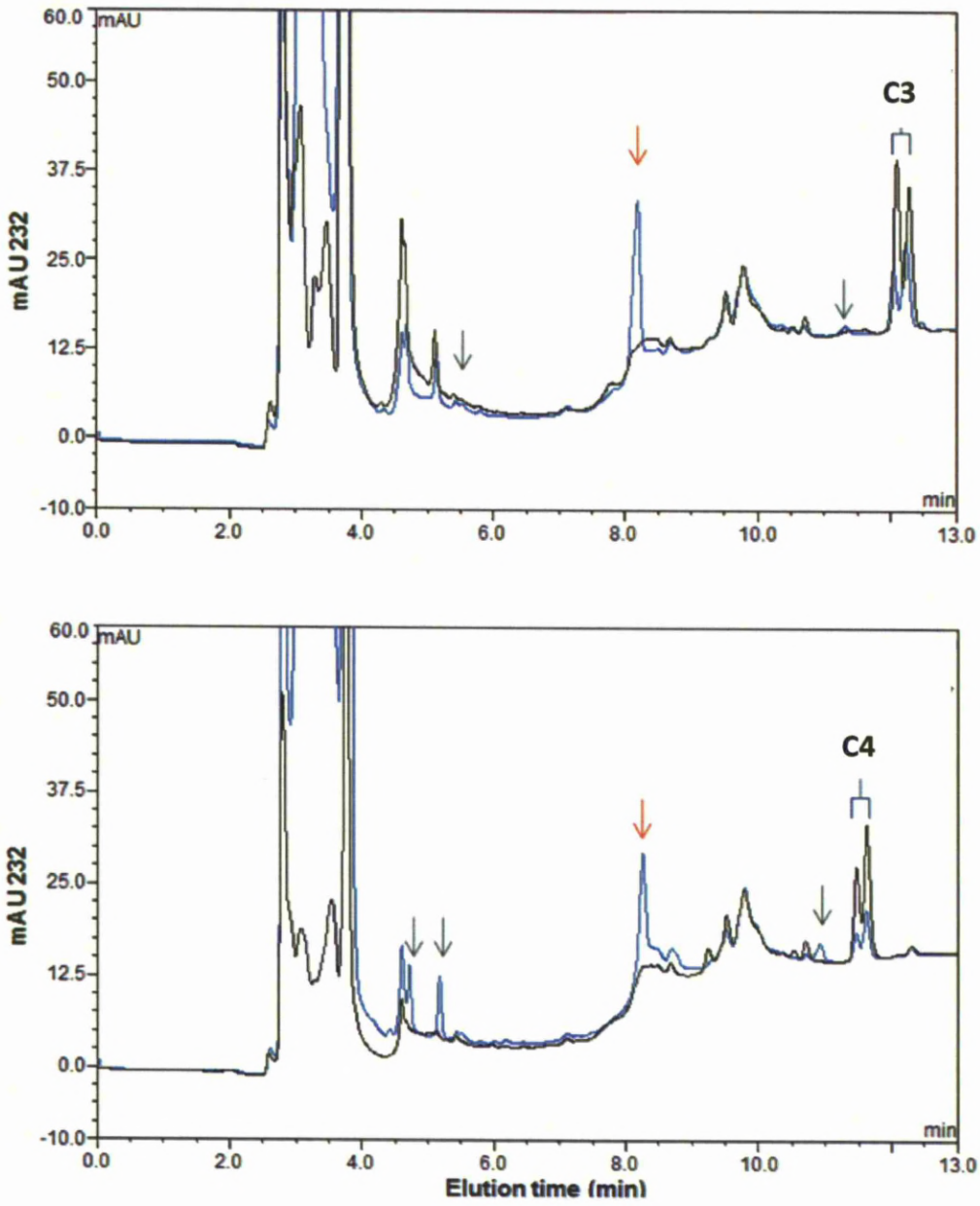

Figure 3.3. HPLC chromatograms of CYP6P3 reactions with C3 and C4. Overlaid reaction traces after 30 min of incubation in absence of NADPH (Black) and presence of NADPH (blue) showing substrate elimination in the presence of NADPH. Putative NADPH-dependant metabolite peaks are indicated by arrows. Red arrows refer to consistent and identical retention time metabolite peak generated from two different substrates (C3 and C4).

3.2.4. Modelling of deltamethrin analogues binding to CYP6P3

To help rationalize the experimental data, computational docking studies were performed using a CYP6P3 model (Stevenson *et al,* 2011). In *silico* modelling studies for C3 with CYP6P3 were used to try predicting the key acetylenic pyrethroid–active site interactions and to inform on how the molecule might be metabolised leading to enzyme inactivation. The most positive binding solution for C3 is shown in (Figure 3.4).

The phenyl propargyl ether group of C3 reduces the length of the molecule so that the molecule may bind in a more favourable position for the metabolism at the ester bond. For example the high ranking binding mode of C3 represented in Figure 3.4 shows the alpha carbon close to the heme with binding free energy -41.1 Kcal. mol^{-1}, suggesting metabolism of the ester bond in C3, this may partly explain the metabolism profile that was experimentally observed for C3 and C4. However, C3 can bind in three poses; it can bind for hydroxylation with binding free energy -38.2. Kcal. mol^{-1}, metabolism on the external carbon of the acetylene group -39.5 Kcal. mol^{-1}; and can bind with the cyano group close to the heme for either coordination or metabolism of the alpha carbon binding free energy -41.1 Kcal. mol^{-1}.

The molecules C3 and C4 are alpha cyano analogues of deltamethrin and bifenthrin, thus it is possible that CYP6P3 can attack these molecules from the alpha carbon site which might lead to ester hydrolysis for both compounds. This would be similar to deltamethrin metabolism by CYP6AA3 (Boonsuepsakul *et al.*, 2008) and CYP6M2 (Stevenson *et al.*, 2011). The lack of the second aromatic ring (ring B) may increase the chance of alpha carbon oxidation by P450 leading to ester hydrolysis. The

metabolic profile of deltamethrin metabolism by CYP6M2 (see figure 1.5, chapter 1) further supports this hypothesis whereby the *ipso* substitution encourages ester hydrolysis of 4` hydroxylated deltamethrin (M4, figure 1.5, chapter 1)primary metabolites (Stevenson *et al.*, 2011). However further characterisation of the metabolites generated by CYP6P3 is needed to validate this hypothesis.

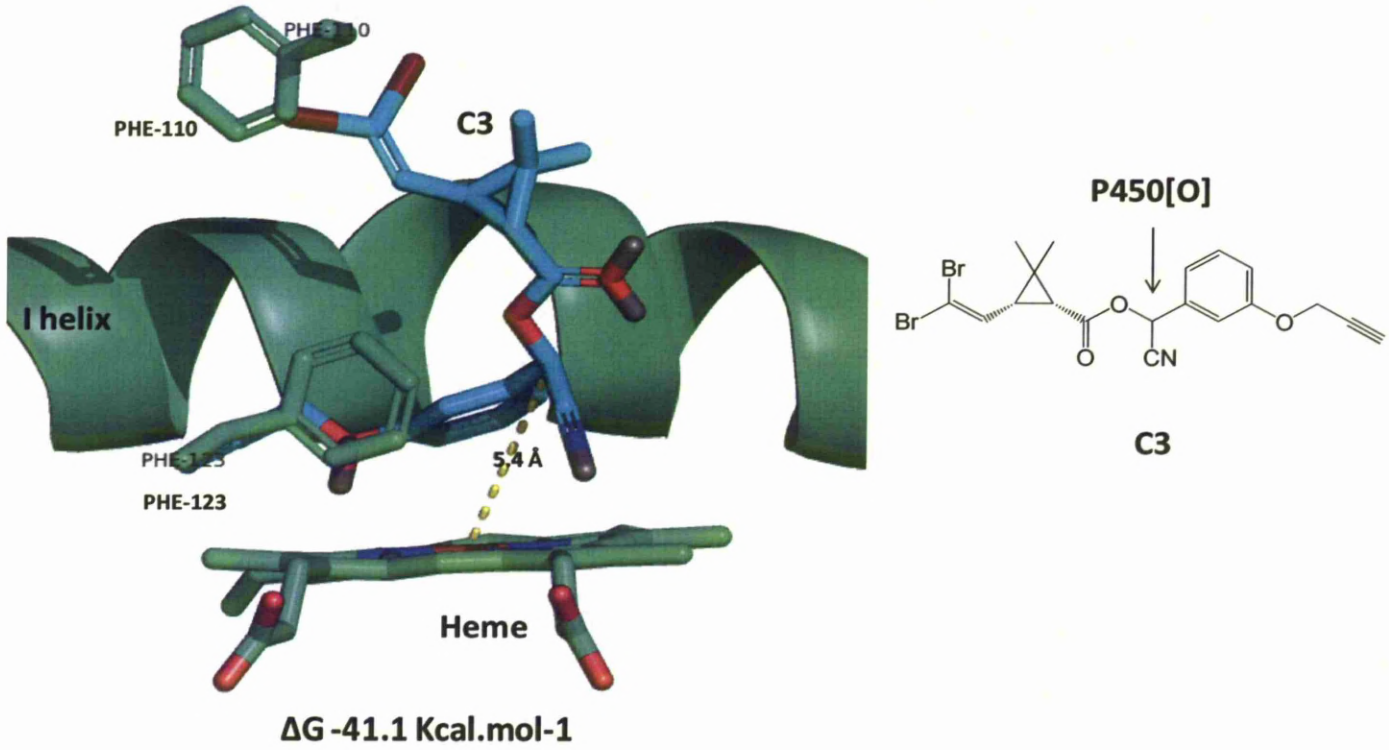

Figure 3.4. Predicted binding modes of C3 (deltamethrin analogue) in CYP6P 3

3.2.5. Rational design of pyrethroid ABPP

The inhibitory effect of arylalkyne ethers including 1EPh, 2POX and biphenyl-alkyne (2EMe) compounds was confirmed by the irreversible inhibition of RLM and CYP6P3 (Chapter II). Furthermore, deltamethrin and bifenthrin analogues containing 2POX alcohol moiety were also proved to be MBIs for CYP6P3, although their mechanism is complex. Therefore, these compounds were used as the basis for the design of pyrethroid mimicking ABPPs. Important design considerations were:

1. The arylalkyne ether group was central to the ABPP design due to its structural similarity to the common 3-phenoxybenzyl alcohol moiety found in commercial cyano pyrethroids (i.e Type 2) such as deltamethrin, cypermethrin and the noncyano pyrethroid (i.e. Type 1) permethrin.
2. What number of benzene rings to use in the aryl ether and what position to substitute the ethynyl group (i.e 2` or 4` position in the B ring, the major sites of P450 attack in pyrethroids).
3. Whether the position for optimal access to the click handle (ethynyl group) should be in the middle of the molecule replacing the alpha-cyano group or in the terminal position in the acid moiety replacing bromine atoms (Figure 3.5).

As a structural model of CYP6P3 was available (Stevenson *et al*, 2011), the probes were subjected to docking experiments to try and predict the optimal compounds and binding modes for successful P450 inactivation or productive binding mode. A binding energy term was used for investigating the potency of these compounds *in silico*. The productive mode was considered to be the binding posture that produced close

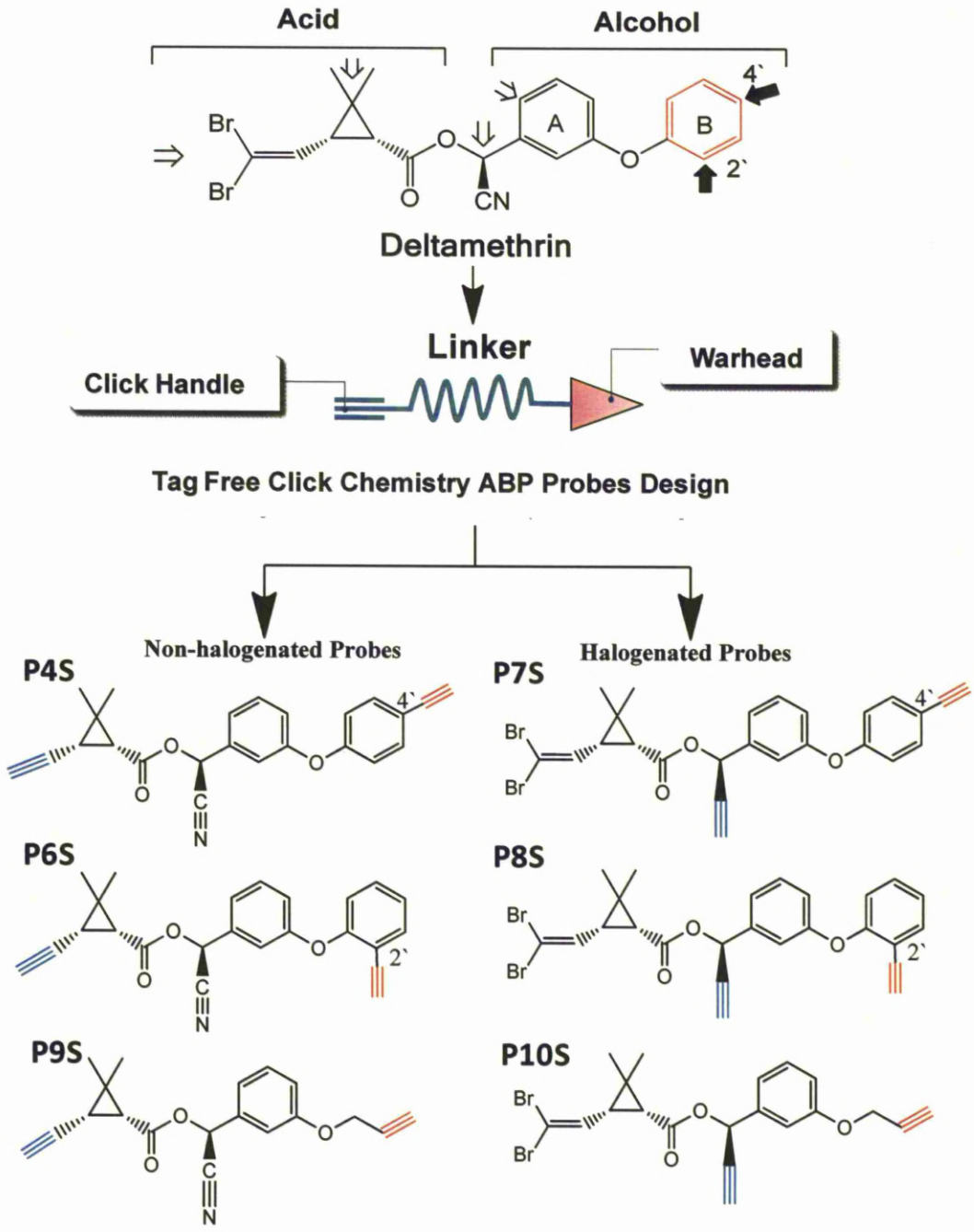

Figure 3.5. Conversion of deltamethrin (pyrethroid Insecticide) structure into an activity based protein pyrethroid (ABPP) probes. The primary sites of deltamethrin oxidation are indicated by black arrows and minor sites by open arrows. Deltamethrin conversion to ABPP requires addition of warhead and click handles. The structures of pyrethroid ABPPs are shown. Red alkyne groups are reactive warheads for P450 inactivation; blue alkyne groups are the click reaction handles for azide reporter fusion and P450 detection. The probes on the left have click handle replacing the bromide atoms, while on the right it replaces the CN group.

proximity of the acetylene terminal carbon to the prosthetic heme-Fe of the enzyme that might lead to P450 activation and mechanistic inactivation. Those productive binding modes with lowest binding energies were taken to represent highest potency and therefore labelling activity against P450s.

3.2.6. Modelling of pyrethroid ABPP probes binding to CYP6P3

The most productive binding modes of pyrethroid ABPPs docked into CYP6P3 model are represented in Figure 3.6 and 3.7. In the bromine click-handle substituted probes, i.e. P4S, P6S and P9S, P4S is predicted to have a binding mode with the lowest binding free energy (ΔG-48.71 Kcal.mol^{-1}) (Figure 3.6). However, while this places the alcohol group above the heme, the external reactive carbon on the acetylene at the 4' position is distant from the reactive Fe centre.

In contrast, the terminal acetylene in the 2` position in P6S points to the Fe atom and is in the best position for oxidation. The modelling also suggests that when the B phenyl ring is replaced by 1-propyne, the binding score for probe 9S drops as this probe has the highest binding free energy -37.94 Kcal mol^{-1}. Additionally the probe P9S represented backward binding mode where the alpha cyano group positioned in close proximity to iron center. This interesting posture might be due to the lack of bromine atoms in the probe structure that seems important for lipophillic interaction with phenylalanine residue. This argue may be justified by the fact that probe P10S stack with phenylalanine residue due to lipophillic interaction with bromine atoms which leads to binding posture for the acetylene close to heme center (Figure 3.7). Interestingly found that this kind of interaction commonly observed for all probes

containing bromine atoms including probes P7S, 8S and 10S, where the click-handle replaces the CN group. However probes P8S (2` warhead substitution) and P7S (4' warhead substitution) have produced a good scoring productive modes i.e. terminal carbon positioned on acetylene in a reactive position relative to Fe (Figure 3.7).

Likewise P9S the replacement of benzene ring B by 1-propyne producing P10S is predicted to reduce the binding energy. Comparisons of the predicted binding energies suggest that the presence of bromine atoms enhances probe binding. Thus probes P7S and P8S were considered to be the best probes for CYP6P3 binding and metabolism. In conclusion to further validate the in *silico* results of the ABPPs probes, the best candidates, i.e. P4S, P6S, P7S and P8S were taken forward for chemical synthesis (see chapter 4).

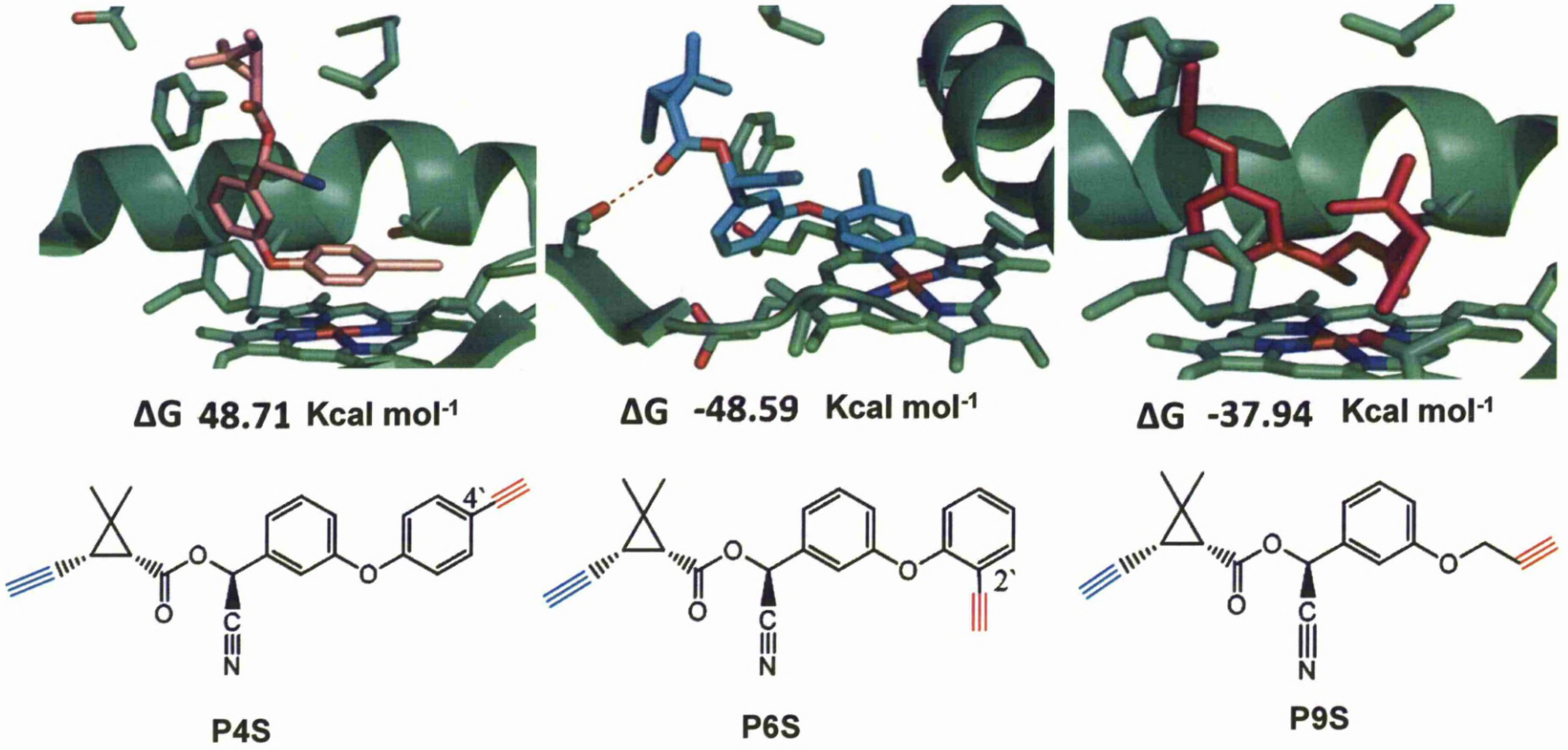

Figure 3.6. Predicted binding modes of pyrethroid ABPPs in CYP6P3. Top the best ranked binding modes of non halogenated pyrethroid ABPP probes 4S, 6S, and 9S in CYP6P3 active site. Bottom chemical structure of the designed probes illustrated the postulated position of enzyme reactive acetylene group red and latent alkyne click handle (acetylene) blue.

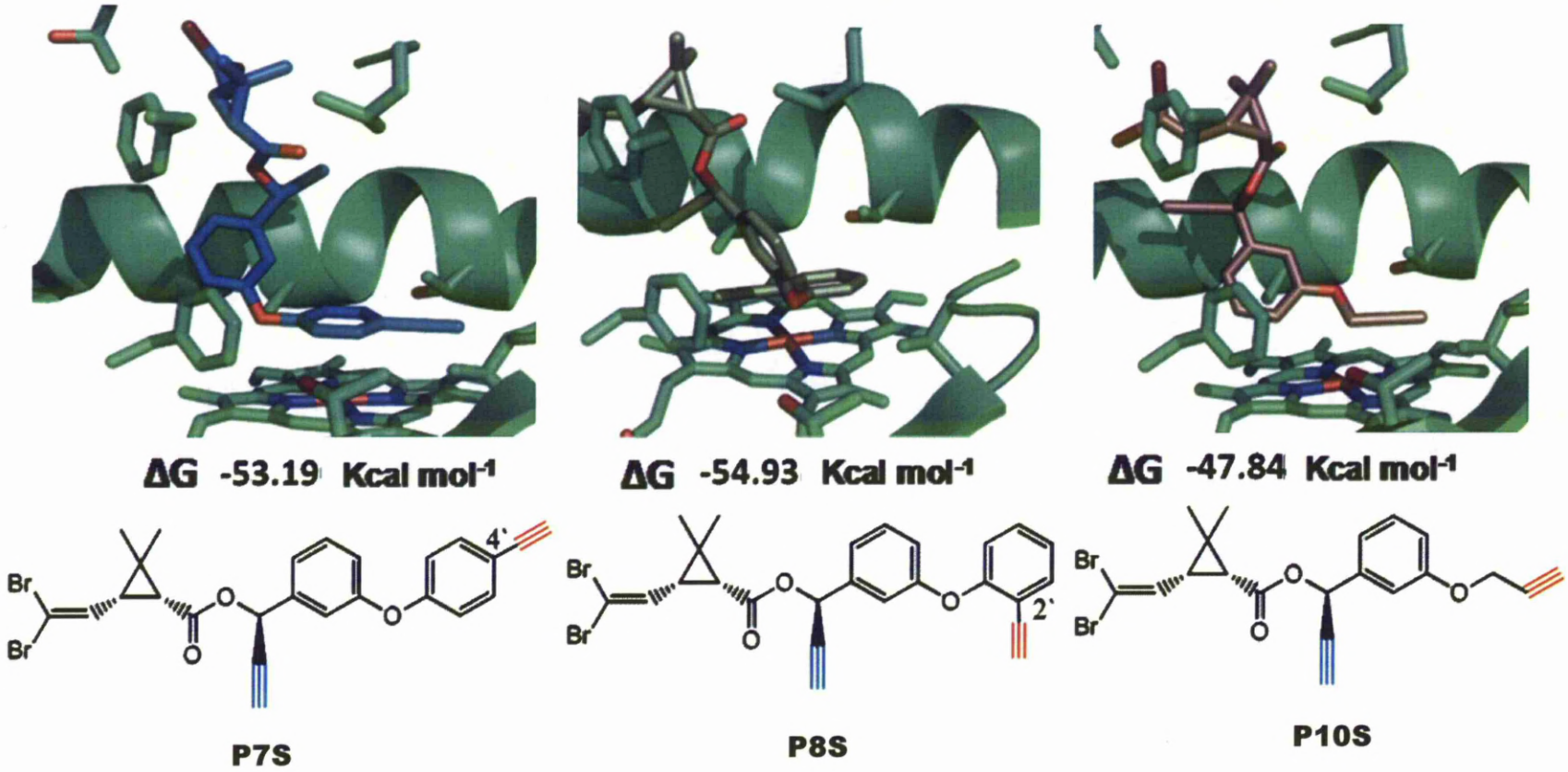

Figure 3.7. Predicted binding modes of pyrethroid ABPPs in CYP6P3. Top the best ranked binding modes of halogenated pyrethroid ABPP probes 7S, 8S, and 10S in CYP6P3 active site. Bottom chemical structure of the designed probes illustrated the postulated position of enzyme reactive acetylene group red and latent alkyne click handle (acetylene) blue.

3.3.Materials and methods

3.3.1. Chemicals and reagents

Pyrethroid analogues were kindly given by Professor Paul O` M Neill, Chemistry Department, Liverpool University. All solvents were HPLC grade solvent from Fisher (UK).

3.3.2. Instrumentation

P450 spectral analysis was carried out using Cary 4000 UV-Vis spectrophotometer (VARIAN, UK). Luminescent measurements (P450 Glo-assay) were carried out using the multiwall plate reader LUMIstar Omega (BMG Laboratories, UK)

3.3.3. Preparation of *E. coli* membranes expressed CYP6P3

CYP6P3/*Ag*CPR membranes and inhibition studies were as described in Chapter 2.

3.3.4. Pyrethroid analogues spectral binding studies

Inhibitors binding was measured by optical difference spectroscopy of CYP6P3 membrane co-expressed with *Ag*CPR, Membranes were diluted in 100 mM potassium phosphate buffer, pH 7.4, to a final concentration of 0.5 μM P450 and split into two matched 0.5.ml black-walled quartz cuvette. After running a base line, 1μl aliquots of C3 and C4 dissolved in acetonitrile were added to the sample cuvette and equal volume of acetonitrile to the reference cuvette.

The samples were left for 2 min between additions to equilibrate, and the difference spectrum was then run between 360-460 nm. The final volume of the inhibitor additions was kept to less than 2.5% of the total volume. Changes in absorbance as a function of inhibitor concentration, at wavelengths selected on the basis of the spectral characteristics of the individual sample, were used to calculate binding constants using non-linear regression analysis (Graph pad Prism). Spectral determinations were performed and found to be reproducible with respect to the spectral profile and the position of *λmax* and *λmin*.

3.3.5. Pyrethroid metabolism assay

The metabolism assays of pyrethroid analogues were carried out with CYP6P3/AgCPR membranes according to the method of Mueller *et al.* 2008, with some modifications. Briefly; a concentration of 20 μM deltamethrin and bifenthrin analogues (C3 and C4) were incubated with 0.25 μM CYP6P3 in 0.2 M Tris. HCl, pH 7.4, 0.25 mM $MgCl_2$ in the presence or absence of an NADPH generating system (1 mM glucose-6-phosphate (Melford), 0.1 mM $NADP^+$ (Melford), 1 unit ml^{-1} glucose-6-phosphate dehydrogenase (G6PDH, Sigma)) in a total volume of 100 μl. Reactions were carried out in triplicate at 30°C with 1,200 rpm shaking. Samples were pre-warmed for 5 min before reactions were initiated by addition of the membrane preparation. Reactions were stopped with 100 μl of acetonitrile and incubated for a further 20 min to ensure that all pyrethroid was dissolved. The quenched reactions were centrifuged at 20,000 g for 10 min before transferring the supernatant to glass HPLC vials. 100 μl of the supernatant was loaded onto a mobile phase with a flow rate of 1 ml min^{-1} and 23°C for separation on a 250 mm C18 column (Acclaim 120,

Dionex). Metabolite separations were achieved with a linear gradient from 0% to 90% methanol in water (v/v) over the first 6 min, 90% methanol was then held for 10 min before returning to 0% with a linear gradient over 2 min followed by equilibration with 100% water for another 4 min. Pyrethroid elution was monitored by absorption at 226/232 nm and quantified by peak integration (Chromeleon, Dionex).

3.3.6. P450 modelling and substrate docking

The molecular model of CYP6P3 was created as described by (Stevenson *et al*, 2011). Figures were prepared using PyMOL (v0.99, DeLano Scientific LLC).

Chapter 4

4. Synthesis of pyrethroid ABPPs

4.1. Introduction

In this project, a pyrethroid scaffold has been utilised for chemical modification to convert it into ABPPs that will enable targeting and identification of P450s that metabolise pyrethroids in proteomic specimens *i.e.* microsomes. To achieve this objective, the alcohol moiety, alpha cyano group and halovinyl groups of a deltamethrin scaffold have been used as the basis for chemical modifications (Figure 4.1).

Initial in *silico* docking experiments of pyrethroid ABPP probes with the pyrethroid metaboliser CYP6P3 predicted that four compounds may have good affinity for CYP6P3 (Chapter 3). To enable further characterisation of the designed probes with P450s, the aim of this chapter was to synthesis the following pyrethroid ABPP structures as illustrated in Figure 4.1; P2, P3R, P4S, P5R,P6S, P7RS and P8RS.

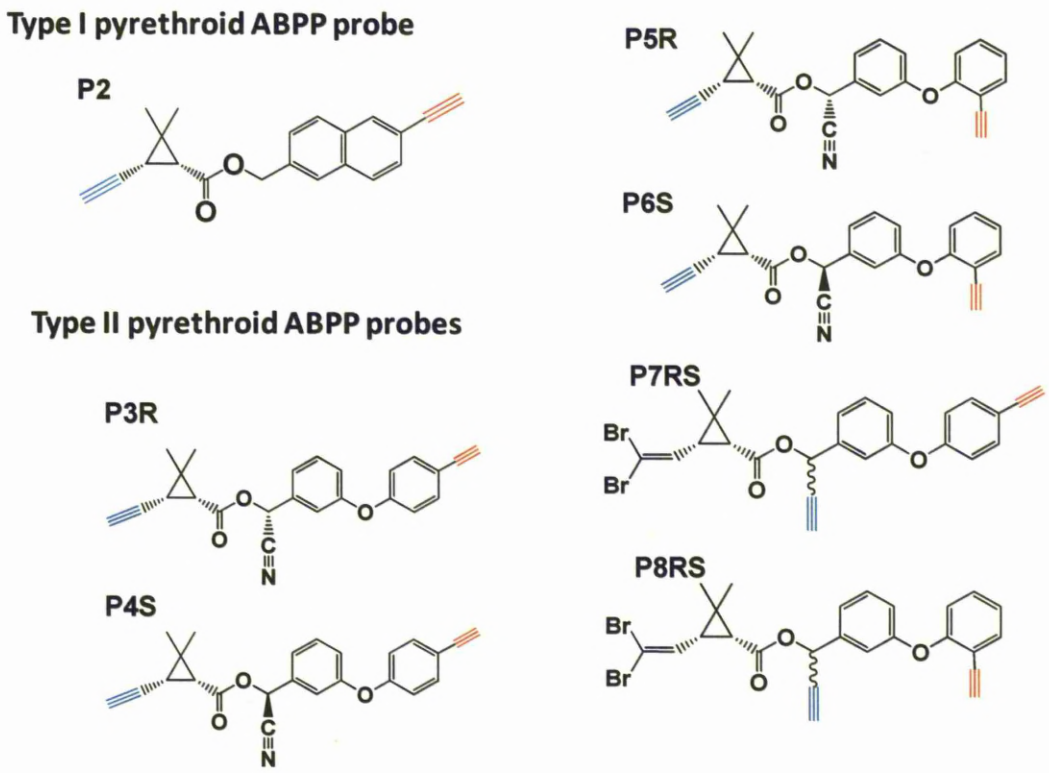

Figure 4.1. Chemical structures of pyrethroid mimetic ABPPs. Pyrethroid ABPP from P2 to P8 were generated by including the a warhead red acetylene at the possible primary site of oxidation and latent click handle blue acetylene group either in the middle replacing the alpha cyano group, or at the terminal end replacing the bromine atoms.

4.2. Results and Discussion

The pyrethroid ABPP should have a reactive group for targeting enzyme active sites, a binding group for directing the probe to a particular enzyme family, and a latent alkyne handle for click chemistry attachment of a reporter group to visualize labelling events (Wright *et al.*, 2009). The substitution position of acetylene in the primary site of oxidation of deltamethrin scaffold either on 2` or 4` in benzene ring B of phenoxybenzyl group was considered in the pyrethroid ABPP design. In addition the locality of latent alkynes "click handle" either terminal (replacing halovinyl) or in middle of the molecule (replacing alpha-cyano group) has been considered in the probe design. In order to append the click handle "alkyne group" in the acid moiety of the pyrethroid mimic probes, dibromoalkene (deltamethric acid) was treated with a lithium base (*n*-BuLi) under the basis of Corey-Fuchs reaction (Gibtner *et al.*, 2002) (Scheme 4.1).

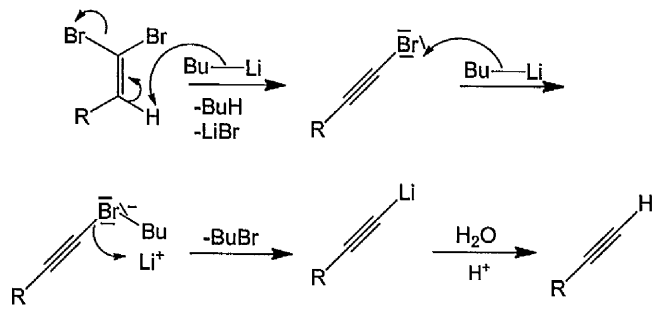

Scheme 4.1. Reaction mechanism of dibromoalkene with *n*-BuLi

This treatment generates a bromoalkyne intermediate via dehydrohalogenation, which undergoes metal-halogen exchange under the reaction conditions and yields a reasonable amount of terminal alkyne (60% product yield). The pure product obtained was further utilised in preparation of P2, P3R, P4S, P5R and P6S by esterification of the acid chloride with aryl alcohol derivatives (Scheme 4.2).

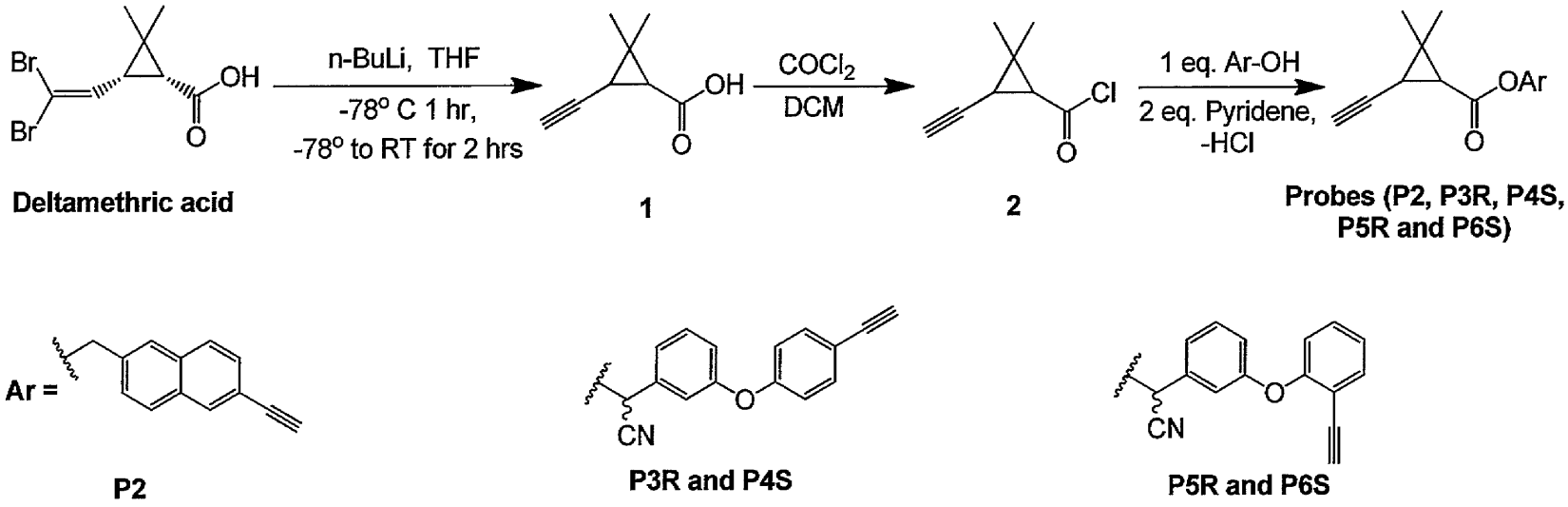

Scheme 4.2. General route for synthesis of pyrethroid ABPPs containing a terminal click handle replacing the halogen atoms.

The ester product was obtained in variable yields between 65-85%. To satisfy aryl alkyne (postulated warhead) in type II pyrethroid mimic probes, substitution of an acetylene group in 2` or 4` position of the phenoxybenzyl moiety (alcohol region) were carried out following two step intermediates synthesis.

Initial thought was given to the use of palladium-catalyzed cross-coupling reaction of the pinacol ester of diboronic acid, with haloarenes as a direct procedure for arylboronic esters (preparation named Miyaura borylation reaction (Ishiyama *et al.*, 1995)). As a next step, the obtained arylboronic esters derivatives can be easily coupled to *meta*-hydroxybenzaldehyde to produce trimethylsilylphenoxy benzaldehyde derivatives (Scheme 4.3). Although the reaction was done under the same conditions reported in the literature (Ishiyama *et al.*, 1995) the reaction was unsuccessful and no product was obtained.

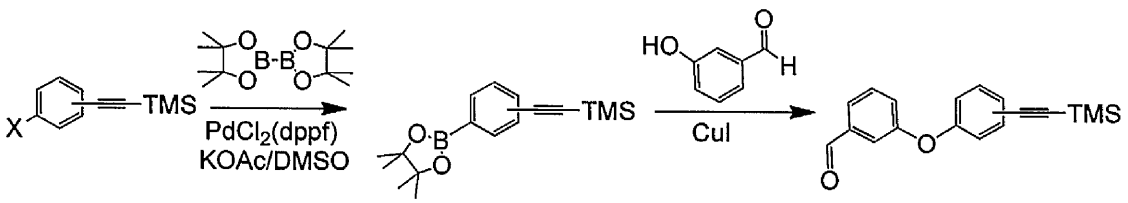

Scheme 4.3. General route of acetylene substituted phenoxybenzaldehyde preparation. Step 1 according Miyaura borylation reaction and Step 2 Ulman reaction

Alternatively, direct ether synthesis catalysed by potassium tert-butoxide and DMF according to the published method (Albericio *et al.*, 1990; Shan *et al.*, 1997) has been followed (Scheme 4.4). However, this was found to give low yield ~5% suggesting

that this reaction may be much more efficient with aliphatic halides rather than the aromatic substituent. Nonetheless, no further improvement has been carried out to this reaction.

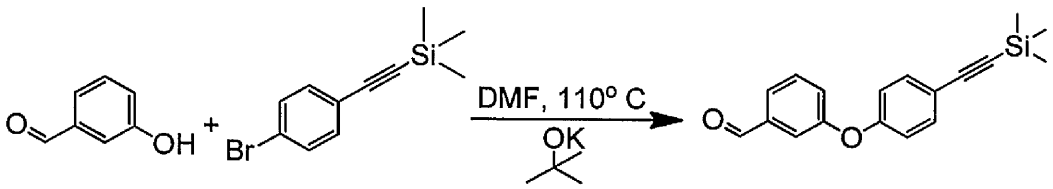

Scheme 4.4. General schematic of General schematic of acetylated phenoxy benzaldehyde preparation

Finally, the trimethylsilyl acetylene substituted phenoxybenzaldehydes were prepared via the synthetic route that was preceded into two steps intermediate synthesis (Scheme 4.5). The first step of this synthetic route is Chan-Lam Coupling reaction (Evans *et al.*, 1998). The arylation of OH containing compounds phenylboronic acids to yield aryl ethers at room temperature is promoted in the presence of cupric acetate and a tertiary amine. Beginning with commercially available 2 or 4-iodophenol, intermediates 3-(2-iodophenoxy) benzaldehyde and 3-(4-iodophenoxy) benzaldehyde were synthesized (Scheme 4.5).

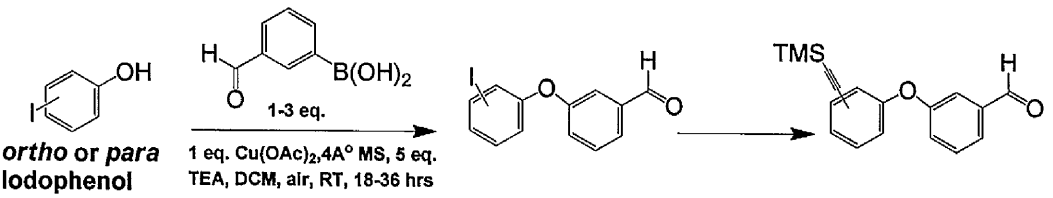

Scheme 4.5. Synthetic route to trimethylsilyl acetylene substituted phenoxybenzaldehyde.

Although the reaction has been reported to be tolerant of a wide range of substituent on both coupling partners (Evans *et al.*, 1998), the yield obtained for our *para* substituted reactant didn't exceed 30%, and for the *ortho* substituted starting material reaction yield did not exceed 25% with extended reaction time and double the amount of phenylboronic acid and catalyst. This finding may be explained by the steric hindrance effect of the *ortho* substituent. No further improvement was made to this reaction as the product yield was sufficient to proceed with the next steps.

Following preparation of 3-iodophenoxybenzaldehyde derivatives, the aryl alkyne moiety was installed via a Sonogashira coupling reaction (Elangovan *et al.*, 2003) producing the trimethylsilyl phenoxybenzaldehyde derivatives (**6** and **7**) with high yield (>95%). This product has been taken forward to prepare compounds **8, 9, 10 and 11** as illustrated in the experimental section. The trimethylsilane protecting group has been removed using mild de protection reagent TBAF (Bu4NF) in THF producing excellent yields of **8** and **9** >95%. To achieve the cyanohydrins of these intermediate, cyanosilylation of aldehydes using trimethylsilyl cyanide and Et_3N has been carried out with excellent yields (>90 %) of **10** and **11**. As a next step trimethylsilyl group has been removed by HCl to produce the corresponding cyanohydrins **12** and **13**. The cyanohydrins were used directly in the esterification reaction with the acid chloride (compound **2**), catalysed by pyridine in DCM to produce a diasterioisomeric mixture of probes P3R/P4S and P5R/P6S in good yields >60%.

Separation of these diasterioisomer has been achieved by normal phase preparative HPLC using gradient of EtOAc in hexane (5-10%) to yield a clear oil of a single

isomer for each probe. However, it was found difficult to crystallise the separated isomers (oil compounds) for identification of their absolute configuration using X-ray crystallography. The direct estimation of R and S configuration of alpha cyano product using HPLC with chiral column and ^{1}H NMR analysis of methine proton (HCCN) are well described in literature (Huang *et al.*, 2005; Jan Gerrits *et al.*, 2001; Tanaka *et al.*, 1990) and may provide useful approach enable defining the absolute configuration of alpha cyano pyrethroids. Here, the same method was adopted to give an approximate estimation for absolute configuration of separated diasterioisomers using comparison between the downfield shift of ^{1}HNMR of hydrogen proton conjugated to alpha carbon (methine) to ester bond and HPLC retention time for separated isomers (Figure 4.2. and Figure 4.3). The S isomer of alpha cyano pyrethroid usually displayed higher polarity comparing to the R isomer which appear at relatively longer retention time (Huang *et al.*, 2005).

Additionally, the diasterioisomer represented different spectroscopic measurements (^{1}H-NMR) for methine hydrogen proton where S configuration usually represented downfield shift comparing to R configuration (Huang *et al.*, 2005). Here in similar manner the hydrogen proton of alpha carbon showed two singlets at δ 6.47 ppm (R, on HPLC) and 6.42 ppm (S, on HPLC) for probe P3R and P4S respectively (Figure 4.2). In similar manner probe P5R and P6S displayed two singlets at δ 6.45 ppm (R) and 6.42 ppm (S) respectively (Figure 4.3).

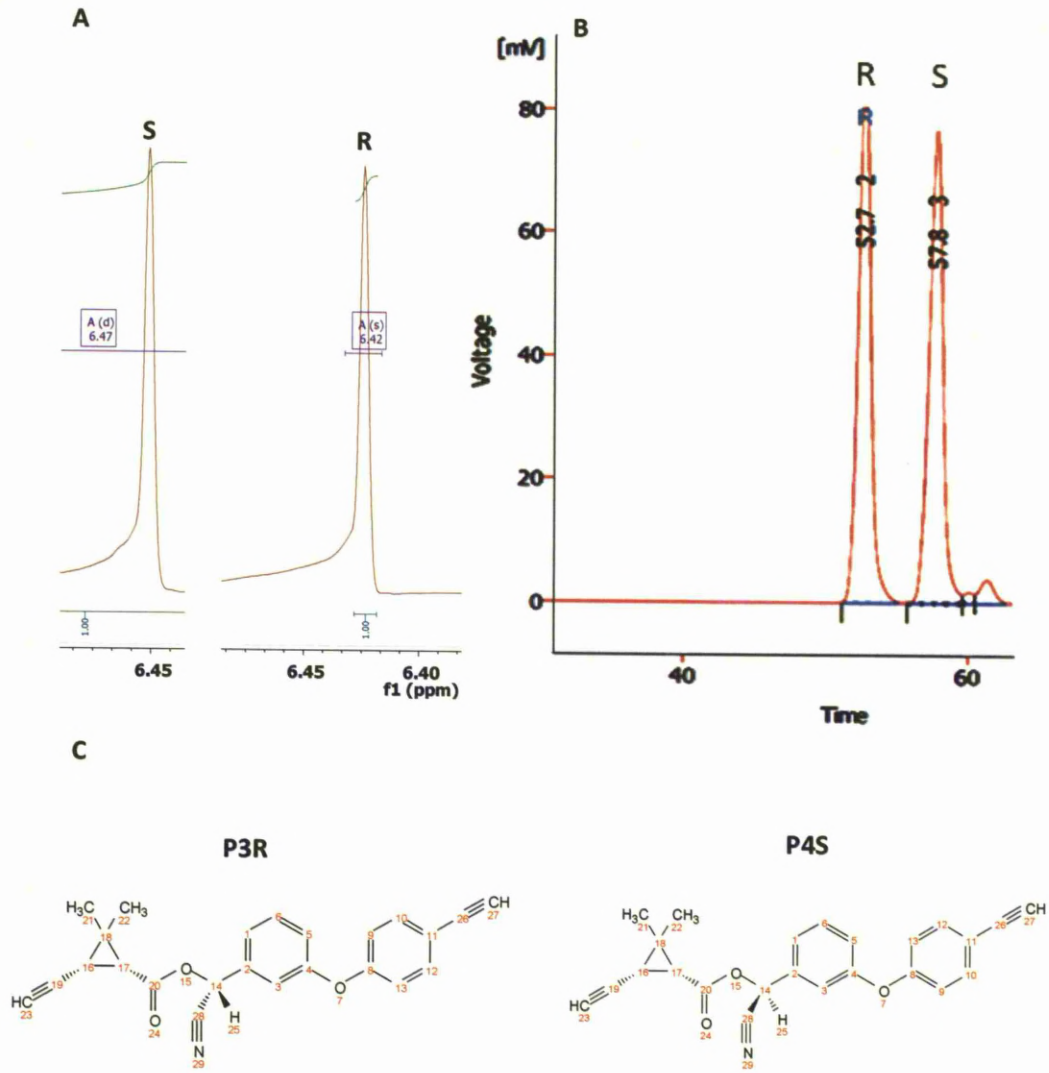

Figure 4.2. Probe 3R and probe P4S α-cyano Alpha cyano isomer separation and confirmation by HPLC and 1HNMR. (A) ^{1}H NMR spectrum (BRUKER 400 Hz) of probes 3R and 4S showing the two peaks of the methine proton of probe 3R [δ 6.42 (S, 1H)] and 4S [δ 6.47 (S, 1H)] (full NMR spectrum are shown in Appendix). (B) HPLC chromatography of probes 3R and 4S with the following conditions normal phase Mobile Phase 5-10% EtoAc in Hexane and separation was carried out at ambient temperature and flow rate 5 ml/min. (C) Chemical structure of probes 3R and 4S.

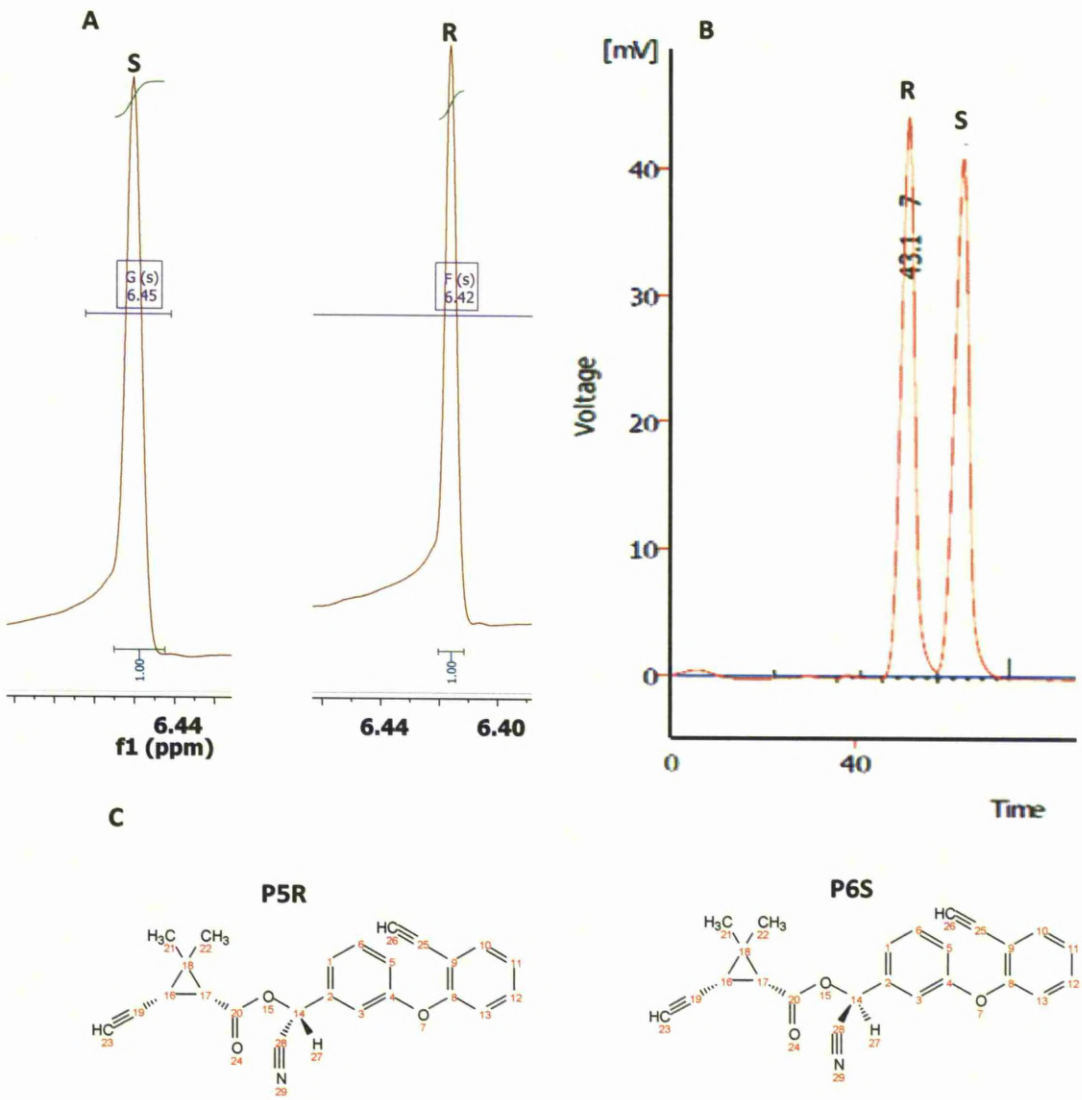

Figure 4.3. Probe 5R and probe P6S α-cyano isomer separation and confirmation by HPLC and 1HNMR. (A) 1H NMR spectrum (BRUKER 400 Hz) of probes 5R and 6S showing the two peaks of the methine proton of probe 5R [δ 6.42 (S, 1H)] and 6S [δ 6.45 (S, 1H)] (full NMR spectrum are shown in Appendix). (B) HPLC chromatography of probes 5R and 6S with the following conditions normal phase Mobile Phase 5-10% EtoAc in Hexane and separation was carried out at ambient temperature and flow rate 5 ml/min. (C) Chemical structure of probes **5R** and **6S**.

The Sonogashira coupling reaction (Elangovan *et al.*, 2003) was also used to install alkyne moiety on methyl 6-bromo-2-naphthoate to prepare probe **(P2)**, producing **18** with excellent yield 90.6%. The product obtained has been reduced to give the corresponding primary alcohol **19** using lithium aluminium hydride (LAH), the most commonly used reagent for the reduction of esters and carboxylic acids to the primary alcohols. Treatment of **19** by TBAF to remove trimethylsilane protecting group produced **20** with excellent yield ~ 95%. This product has been taken forward in the esterification step with the acid chloride compound **2** catalysed by pyridine to produce the desired probe (**P2**) with good yield 85% (figure 4.2). Additionally to append the click handle "alkyne group" in the middle of the pyrethroid molecule to replace the alpha cyano group, trimethylsilyl phenoxybenzaldehyde derivatives were reacted with Lithium TMS acetylene at -78° C to achieve **14** and **15** in good yield >50 %. Subsequently, the two trimethylsilyl groups were removed in a one pot reaction using TBAF which gives **16** and **17** with excellent yield >90%. The probes analogous to deltamethrin were prepared in reasonable yield >60% via esterification reaction for **16** and **17** with acyl chloride of deltamethric acid to gives disterioisomeric mixture of probes **7RS** and **8RS** respectively (Scheme 4.6). Those probes weren't resolved by preparative HPLC even though two different EtOAc gradients at two different concentrations has been utilised, suggesting it is best in future to use reverse phase HPLC or normal phase chiral columns.

In summary, a suite of pyrethroid *ABPPs* was successfully prepared; these probes were taken forward for validation against mosquitoes P450 enzymes and rodent and mosquito microsomes for identification of the P450 enzymes involved in pyrethroid metabolism.

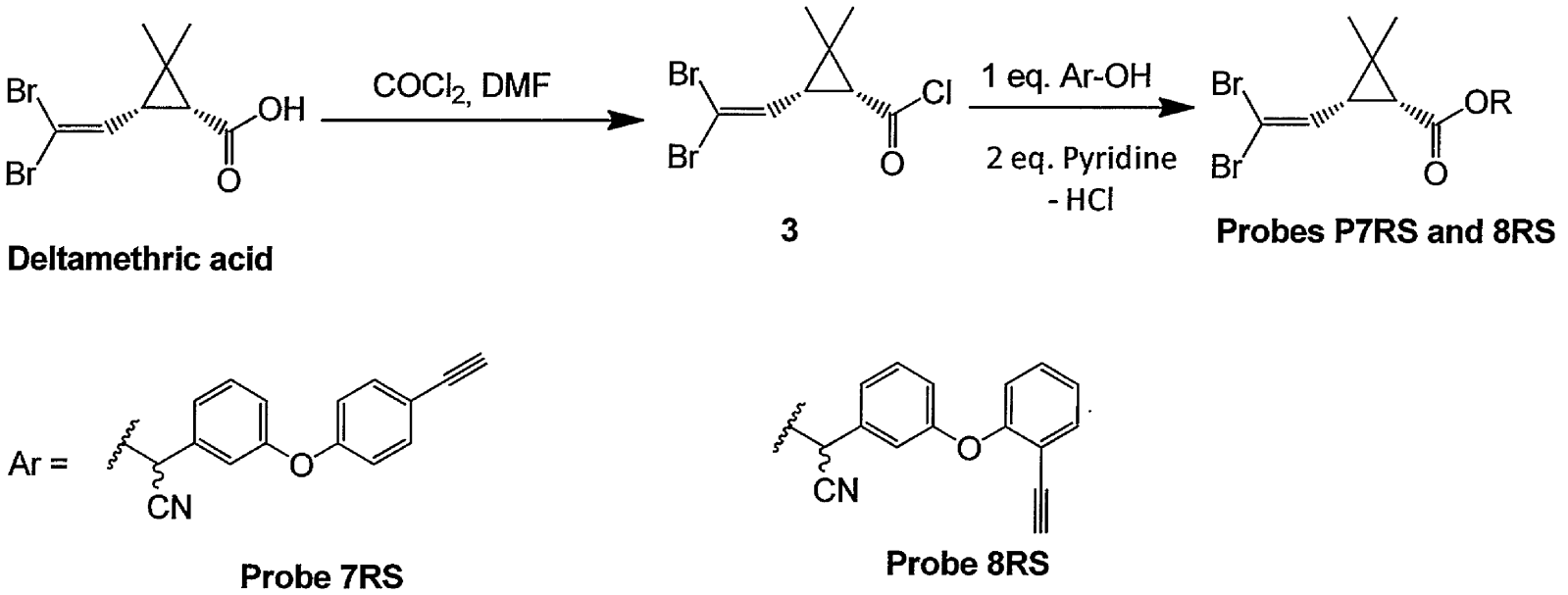

Scheme 4.6. General route for synthesis of pyrethroid *ABPP* contains click handle replacing alpha cyano group.

4.3. Experimental

Air and moisture-sensitive reactions were carried out in oven-dried glassware sealed with rubber septa under positive pressure of dry nitrogen or argon from manifold or balloon. Similarly sensitive liquid and solutions were transferred via syringe, reaction were stirred using Teflon coated magnetic stir bars. Organic solutions were concentrated using Buchi rotary evaporator with a vacuum pump.

4.3.1. Purification of reagents and organic solvents

Anhydrous solvents were either obtained from commercial sources or dried and distilled immediately prior to use under constant flow of dry nitrogen. DCM was distilled from CaH_2. All other reagents were used as received from commercial sources unless otherwise indicated.

4.3.2. Purification of products

Analytical thin layer chromatography was performed with 0.25 mm silica gel 60F plates with 254 nm florescent indicator coated aluminium sheets from Merck. Plates were visualised by ultraviolet light or by treatment with iodine or potassium permanganate followed by gentle heating. Chromatographic purification of products was accomplished by flash column chromatography, as described by Still and co workers (Still *et al.,* 1978). The high performance liquid chromatography (HPLC) (preparative and analytical) was carried out on Gilson HPLC.

4.3.3. Analysis

Nuclear magnetic resonance (NMR) spectra were recorded on a Brucker AMX 400 (^1H, 400MHz; ^{13}C, 100 MHz) spectrometer. Chemical shifts are described in parts per

million (ppm) downfield from an internal standard of trimethylsilane. Multiplicity are recorded as broad peaks (br), singlet (s), doublet (d), triplets (t), quartets (q), doublets of doublets (dd), doublets of triplets (dt) and multiplets (m). Coupling value are in Hz. Mass spectra were recorded on a VG analytical 7070E Machine and Frisons TRIO spectrometers using electron ionisation (EI), chemical ionisation (CI) or electron spray (ES).

4.3.4. General procedure of intermediate synthesis

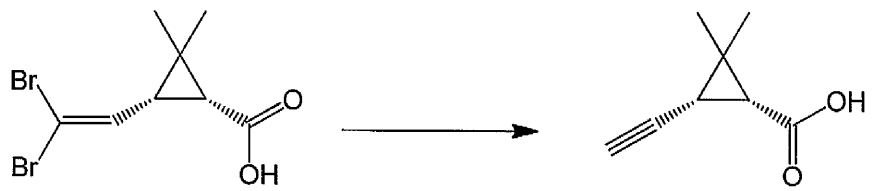

Deltamethric acid **1**

(1R, 3R)-3-ethynyl-2,2-dimethylcyclopropanecarboxylic acid (1) To a stirring solution of deltamethric acid (1.49 g, 5 mmol, Bayer Crop Science . Germany) in 25 ml dry tetrahydrofuran (THF) that has been cooled to -78° C by dry ice acetone bath, a solution of 1.6M (11 ml, 17.5mmol, 3.5 equivalent) normal-butyl lithium (*n*-BuLi) in hexane was slowly added. The mixture was kept stirring at -78 ° C for 1 hr and then the reaction temperature was allowed to rise to room temperature (RT) over next two hours under stirring. Thereafter, the reaction was quenched by addition of 20 ml double distilled-water and the organic layer was separated. The water layer was acidified by 1 M Hydrochloric acid (HCl) to pH 2 and then extracted by dichloromethane (DCM) 25ml three times. The organic layer was combined, washed with brine and dried with anhydrous Na_2SO_4. Thereafter, all organic solvents were removed by vacuum to give the crude product as pale yellow solid which was further

purified by flash column chromatography eluting with 20-50% Ethyl acetate (EtOAc) in hexane to give the product of **1** as a off-white crystal 415 mg (60%).

1: ^{1}H NMR (400 MHz, CDCl3) δ = 7.26 (d, *J*=1.5, 1H), 2.16 (t, *J*=12.4, 1H), 1.82 (dt, *J*=15.8, 7.9, 1H), 1.73 (d, *J*=8.6, 1H), 1.39 (s, 3H), 1.22 (s, 3H).^{13}C NMR (100 MHz, $CDCl_3$) δ 175.26, 79.60, 77.82, 77.74, 77.26 , 71.43, 31.39, 27.83, 22.94, 16.08.

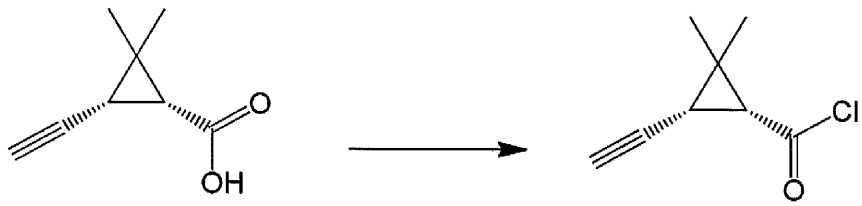

1 **2**

(1R,3R)-3-ethynyl-2,2-dimethylcyclopropanecarbonyl chloride (2) To a solution of compound 1 (100 mg, 0.723 mmol) in DCM (25ml), 2.2 equivalent of $COCl_2$ (157.51 mg, 1.59 mmol) and dimethylformamide (DMF) one tiny drop around 5 µl was added. The mixture was kept stirring for at least 3 hrs at RT. After that DCM and excess $COCl_2$ are removed in *vacuo*. The residue was kept under high vacuum for at least 2 hrs yielding compound **2** as yellow oil residue. The product was used directly without further purification and used in pyridine catalysed esterification reaction with primary or secondary alcohol to produce the desired ABPP probes.

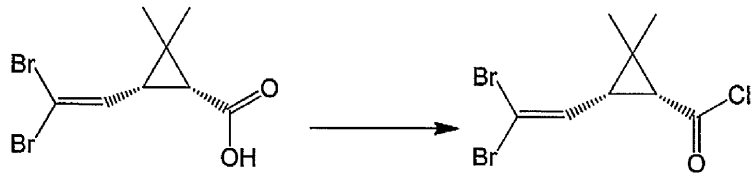

Deltamethric acid **3**

(1R,3R)-3-(2,2-dibromovinyl)-2,2-dimethylcyclopropanecarbonyl chloride (3) Synthesis achieved using general procedure used for preparation of compound **2** to give title compound (**3**) as yellow oil residue. The product was used directly without further purification and used in pyridine catalysed esterification reaction with secondary alcohol to produce the desired ABPP probes.

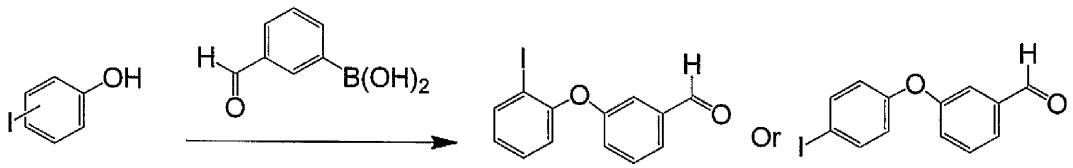

***ortho* or *para* Iodophenol** **4** **5**

3-(2-iodophenoxy) benzaldehyde (4) and 3-(4-iodophenoxy) benzaldehyde (5) A mixture of the substrates 4-iodophenol (881 mg, 4 mmol), (3-formylphenyl)boronic acid (804mg, 5.2 mmol), 1 equivalent of anhydrous $Cu(OAc)_2$ (734 mg, 4 mmol), ~ 1 g of activated molecular sieves (Powdered, 4 Å), and 5 equivalent of triethylamine (Et_3N) (2.79 ml, 20 mmol) in 25 ml DCM was stirred at room temperature for 16 hrs. (in the case of using 2-iodophenol as starting material double the amount of (3-formylphenyl)boronic acid, $Cu(OAc)_2$, activated molecular sieves (Powdered, 4 Å), Et_3N and DCM were doubled and the reaction time is extended to 30 hours). The

progress of the reaction was monitored by thin layer chromatography (TLC). When the reaction reached completion DCM was removed in *vacuo* and the residue re-dissolved in 30 % EtOAc in hexane and filtered through a pad of silica, washed by 30% EtOAc in hexane to give the crude product as pale yellow oil. The crude product was purified by flash column chromatography eluting with 10-20% EtOAc in hexane to give the desired product (**4 and 5**).

4: ^{1}H NMR (400 MHz, $CDCl_3$) δ 9.97 (s, 1H), 7.66 (dd, J = 7.2, 5.2 Hz, 1H), 7.62 (t, J = 6.2 Hz, 1H), 7.51 (dd, J = 14.3, 6.6 Hz, 1H), 7.46 (d, J = 1.9 Hz, 1H), 7.31 – 7.25 (m, 1H), 6.80 (dd, J = 6.9, 5.0 Hz, 1H).^{13}C NMR (100 MHz, $CDCl_3$) δ 191.84, 158.78 – 157.55, 156.93 – 156.18, 139.42, 138.58 – 137.83, 131.02, 125.69, 125.19, 121.87, 118.65, 100.33 – 99.58, 87.61 – 87.55, 79.19 – 75.97.

5: ^{1}H NMR (400 MHz, $CDCl_3$) δ 9.97 (s, 1H), 7.66 (dd, J = 7.2, 5.2 Hz, 1H), 7.62 (t, J = 6.2 Hz, 1H), 7.51 (dd, J = 14.3, 6.6 Hz, 1H), 7.46 (d, J = 1.9 Hz, 1H), 7.31 – 7.25 (m, 1H), 6.80 (dd, J = 6.9, 5.0 Hz, 1H).^{13}C NMR (100 MHz, $CDCl_3$) δ 191.84, 158.78 – 157.55, 156.93 – 156.18, 139.42, 138.58 – 137.83, 131.02, 125.69, 125.19, 121.87, 118.65, 100.33 – 99.58, 87.61 – 87.55, 79.19 – 75.97.

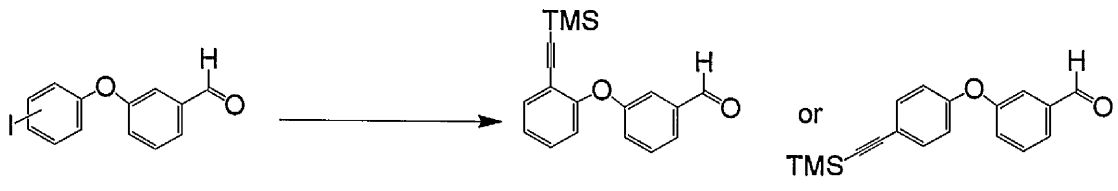

4 or 5 **6** **7**

3-(2-((trimethylsilyl)ethynyl)phenoxy)benzaldehyde (6) and 3-(4-((trimethylsilyl) ethynyl)phenoxy)benzaldehyde (7) To solution of 4 or 5 (150 mg, 0.462 mmol) in 20 ml THF, CuI (1.75 mg, 0.018 mmol, 0.02 eq.), $PdCl_2$ $(PPh_3)_2$, (12.63 mg, 0.04 eq) and 5 ml Et_3N was added and the mixture was degassed. Then 1.3 eq. of trimethylsilylacetylene (TMS acetylene, 59.09 mg, 83 µl) was added to the mixture and the resulting mixture was degassed again and stirred at RT for overnight. Thereafter, all the solvents (THF and Et_3N) was removed in *vacou*, then the residue was dissolved in 20% EtOAc in hexane and filtered through a silica pad, washed by 20% EtOAc in hexane to give the crude products (**6** and **7**). These were purified by flash chromatography 5% EtOAc in hexane to give compound **6** (115 mg, 84.4%) and **7** (120 mg, 88.2%) of yellow oil.

6: ^{1}H NMR (400 MHz, $CDCl_3$) δ 9.90 (s, 1H), 7.53 (d, J = 7.5 Hz, 1H), 7.50 – 7.46 (m, 1H), 7.42 (dd, J = 13.4, 5.7 Hz, 1H), 7.33 – 7.27 (m, 1H), 7.21 (s, 1H), 7.19 (dd, J = 8.1, 2.5 Hz, 1H), 7.12 (t, J = 7.5 Hz, 1H), 7.01 (d, J = 8.1 Hz, 1H), -0.00 (s, 9H).^{13}C NMR (100 MHz, $CDCl_3$) δ 192.52 – 191.46, 159.36 – 158.81, 156.89 – 155.83, 138.49 – 137.85, 135.11 – 134.14, 130.85 – 130.21, 125.31 – 124.76, 124.67 – 124.25, 124.13 – 123.27, 121.29, 117.33, 101.37 – 100.73, 100.51 – 99.88, 78.98 – 75.67, 0.00.

7: ^{1}H NMR (400 MHz, $CDCl_3$) δ 9.92 (s, 1H), 7.85 (dd, J = 7.8, 1.2 Hz, 1H), 7.57 (d, J = 7.5 Hz, 1H), 7.47 (t, J = 7.8 Hz, 1H), 7.35 – 7.32 (m, 1H), 7.32 – 7.28 (m, 1H), 7.24

– 7.19 (m, 2H), 6.94 (s, 1H), 6.92 (dd, J = 4.5, 3.2 Hz, 1H), -0.00 (s, 9H).^{13}C NMR (101 MHz, $CDCl_3$) δ 192.00, 159.23 – 158.10, 140.62, 139.32 – 138.26, 130.97, 130.40, 126.81, 125.43, 124.42, 120.94, 117.70, 100.93 – 99.00, 91.13 – 88.70, 79.52 – 75.41, 1.01 – -0.74.

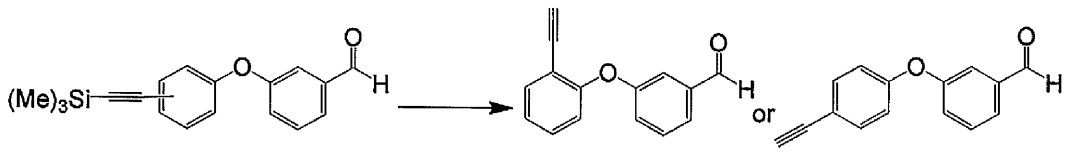

6 or 7 **8** **9**

3-(2-ethynylphenoxy) benzaldehyde (8) and 3-(4-ethynylphenoxy) benzaldehyde (9) To a stirring solution of 6 or 7 (110 mg, 0.373 mmol) in 20 ml of THF that was cooled to -20° C by dry ice/acetone bath (adjusted to -20 ° by frequent addition of dry ice to acetone). Tetra-*n*-butylammonium fluoride (TBAF, Bu_4NF, 1.2 equivalents) was added by syringe. The mixture was kept stirring at -20°C for 30 min and then the reaction is quenched by addition of 20 ml water, and extracted by EtOAc (20x2 ml). The organic layer combined and washed by brine and dried using $MgSO_4$, after all, solvent has been removed in *vacuo* to give the crude product yellow crystal which further purified by flash chromatography eluting with 30% EtOAc in hexane to give product **8** (95%) and **9** (96.35%) of pale yellow oil.

8: ^{1}H NMR (400 MHz, $CDCl_3$) δ 9.98 (s, 2H), 7.64 (t, J = 6.5 Hz, 1H), 7.54 (t, J = 5.9 Hz, 2H), 7.51 (t, J = 2.0 Hz, 2H), 7.50 – 7.47 (m, 2H), 7.30 (dd, J = 8.0, 2.5 Hz, 1H), 7.26 (s, 1H), 6.98 (d, J = 2.6 Hz, 2H), 6.97 – 6.95 (m, 1H), 3.06 (s, 9H).^{13}C NMR (100 MHz, $CDCl_3$) δ 191.82, 158.05 – 157.68, 157.53 – 156.59, 138.99 – 138.11, 134.42,

131.04, 125.78, 125.53, 119.25, 118.63 – 117.29, 84.00 – 82.58, 78.49 – 76.05, 31.44 – 30.10, 30.10 – 28.68.

9: ^{1}H NMR (400 MHz, $CDCl_3$) δ 9.98 (d, J = 2.2 Hz, 1H), 7.64 (t, J = 7.1 Hz, 1H), 7.54 (t, J = 5.7 Hz, 1H), 7.51 (t, J = 2.2 Hz, 1H), 7.50 – 7.48 (m, 1H), 7.30 (dd, J = 8.1, 2.6 Hz, 1H), 7.26 (d, J = 2.0 Hz, 1H), 7.00 – 6.97 (m, 1H), 6.98 – 6.95 (m, 1H), 3.07 (s, 9H).

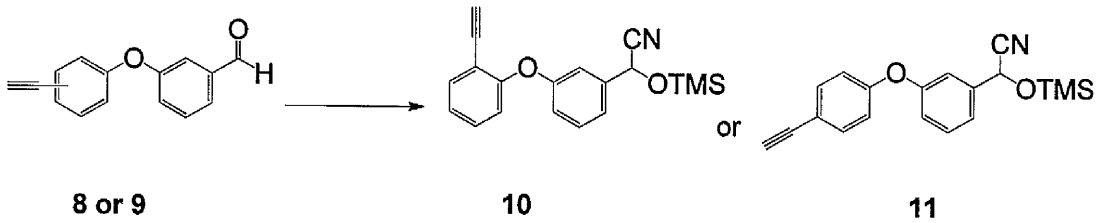

8 or 9 **10** **11**

2-(3-(2-ethynylphenoxy)phenyl)-2-((trimethylsilyl)oxy)acetonitrile (10) and 2-(3-(4-ethynylphenoxy)phenyl)-2-((trimethylsilyl)oxy)acetonitrile (11) To a solution of **8** or **9** (80 mg, 0.359 mmol) in 10 ml DCM, trimethylsilyl cyanide (TMSCN, 10 eq., 0.676 ml) and Et_3N (0.1, 7.5 µl) were added in. The resulting mixture was kept stirring for overnight at RT. After that all of the solvent and the excess TMSCN are removed in *vacuo* to give the product of **10** (110 mg, 78.44%) and **11** (112.2 mg, 80%) as pall yellow oil. These compounds were used in the next step without further purification.

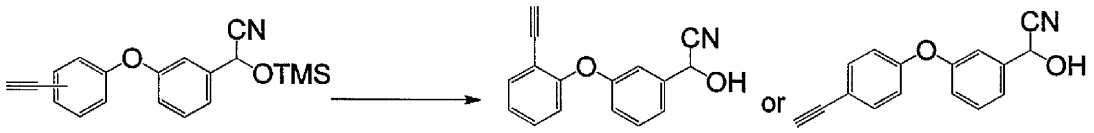

10 or 11 12 13

2-(3-(2-ethynylphenoxy)phenyl)-2-hydroxyacetonitrile (12) and 2-(3-(4-ethynyl-phenoxy)phenyl)-2-hydroxyacetonitrile (13) To a solution of 10 or 11 in 10 ml of THF, 6 ml of HCl (2M) was added and the resulting mixture was kept stirring for at least 4 hrs after that the reaction mixture was diluted with 15 ml of diethyl ether (Et_2O). The organic layer was separated and water layer was extracted with Et_2O (25 mlx2). Then organic layer was combined and washed with brine and dried with Na_2SO_4. All of the organic solvents were removed by *vacuo* to give yellow oil; the product was used in the next step without further purification.

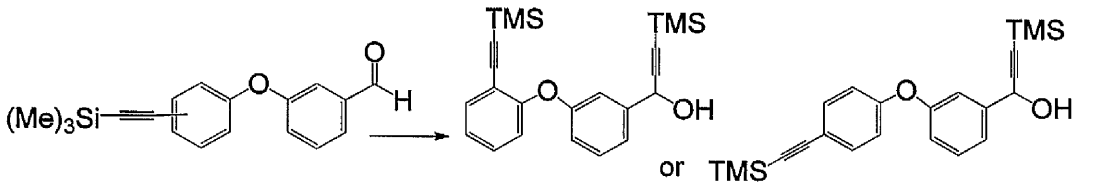

6 or 7 14 15

3-(trimethylsilyl)-1-(3-(2-((trimethylsilyl)ethynyl)phenoxy)phenyl)prop-2-yn-1-ol (14) and 3-(trimethylsilyl)-1-(3-(4-((trimethylsilyl)ethynyl)phenoxy)phenyl)prop-2-yn-1-ol (15) To a solution of 6 or 7 (120 mg, 0.407 mmol) in THF cooled to -78° C in dry ice/acetone bath, a solution of lithium trimethylsilylacetylene (Li-TMSA) in THF 1 ml (0.5 M, 1.2 eq) was added slowly and the mixture stirred for 3hours at -78°

C then the reaction temperature is allowed to raise. When the temperature reaches 0° C the reaction is quenched with saturated solution of ammonium chloride (NH_4Cl), and 15 ml of Et_2O was used to dilute the solution. The organic layer was separated and the water layer was extracted with Et_2O (25 ml×2). The organic layers was combined, washed with brine, and dried with Na_2SO_4. After remove all of the organic solvents in *vacuo* the obtained crude product subsequently was purified by flash column chromatography eluting with 10 % EtOAc in hexane, to give the product 14 (87 mg, 54.4 %) and 15 (80 mg, 50%) as yellow oil.

14: ^{1}H NMR (400 MHz, $CDCl_3$) δ 7.34 (dd, J = 7.7, 1.6 Hz, 1H), 7.18 – 7.11 (m, 1H), 7.09 (d, J = 2.3 Hz, 1H), 7.07 (d, J = 7.7 Hz, 1H), 6.97 (s, 1H), 6.93 (t, J = 7.5 Hz, 1H), 6.82 (d, J = 8.1 Hz, 1H), 6.77 (dd, J = 8.0, 2.2 Hz, 1H), 5.23 (d, J = 6.4 Hz, 1H), 1.88 (s, 1H), -0.00 (s, 9H), -0.07 (s, 9H).^{13}C NMR (100 MHz, $CDCl_3$) δ 158.33, 142.30, 134.53, 133.35, 129.97, 130.07, 123.91, 121.21, 120.59, 117.69, 116.70, 116.03, 77.99, 65.64, 31.15, 0.00.

15: ^{1}H NMR (400 MHz, $CDCl_3$) δ 7.34 (dd, J = 7.7, 1.6 Hz, 1H), 7.16 – 7.10 (m, 1H), 7.09 (d, J = 2.3 Hz, 1H), 7.07 (d, J = 7.7 Hz, 1H), 6.97 (s, 1H), 6.93 (t, J = 7.5 Hz, 1H), 6.82 (d, J = 8.1 Hz, 1H), 6.77 (dd, J = 8.0, 2.2 Hz, 1H), 5.23 (d, J = 6.4 Hz, 1H), 1.88 (s, 1H), -0.00 (s, 9H), -0.07 (s, 9H).^{13}C NMR (100 MHz, $CDCl_3$) δ 158.33 , 141.74, 133.96, 133.35, 129.97, 129.76, 123.91, 120.90, 120.13, 117.69, 116.29, 115.83, 74.45, 64.30, 31.15, 0.00.

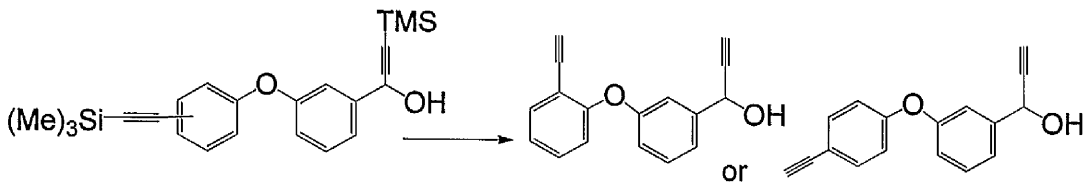

14 or 15 **16** **17**

1-(3-(2-ethynylphenoxy) phenyl) prop-2-yn-1-ol (16) and 1-(3-(4-ethynylphenoxy) phenyl) prop-2-yn-1-ol (17) Synthesis achieved using general procedure used to prepare compounds **8** and **9** with the same scale to give **16 (95%)** and **17 (94%)** as yellow oil residue. There is no further confirmation on the product carried out, but this was taken forward for esterification with the acid chloride.

4.3.5. Synthesis of pyrethroid ABPP contains terminal click handle replacing halogen atoms.

4.3.5.1. Synthesis of Probe 2

Synthesis of probe 2 was achieved using the general route illustrated below (Figure 4.2).

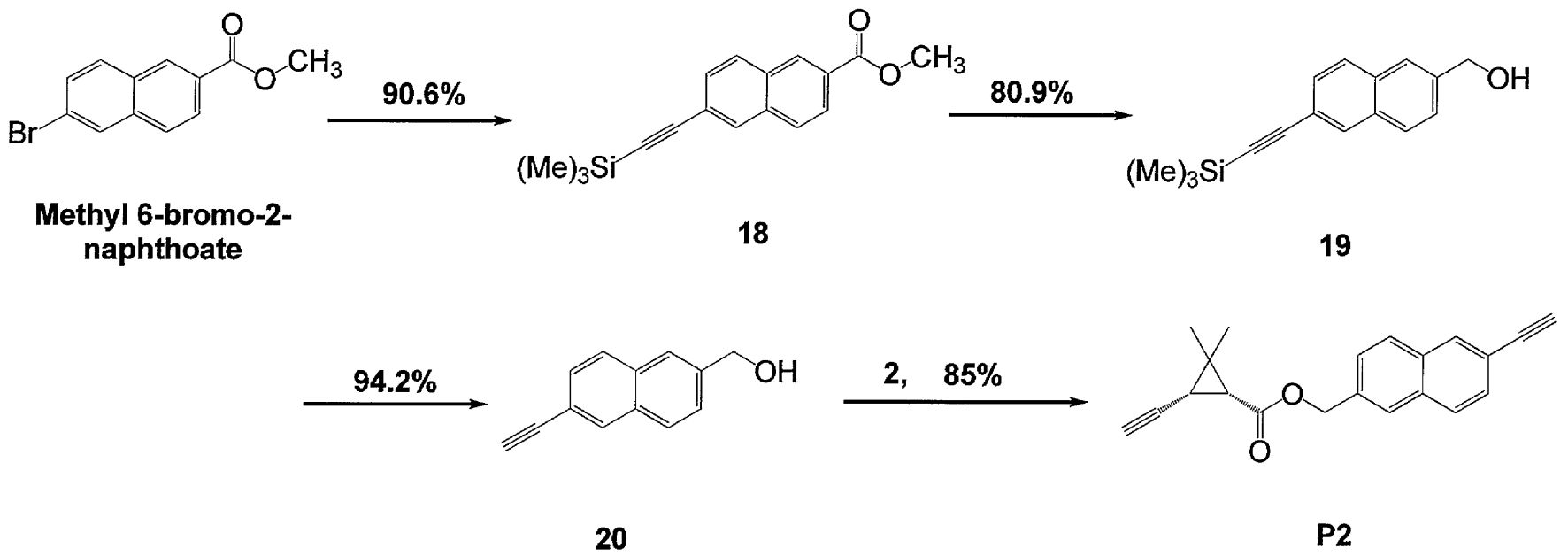

Figure 4.4. General route of P2 synthesis (practical yields are indicated in percentage).

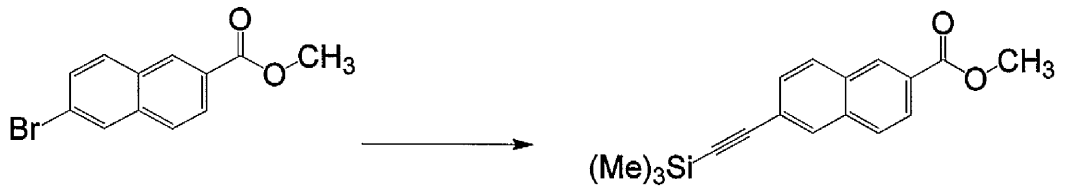

Methyl 6-bromo-2-naphthoate

18

Methyl 6-((trimethylsilyl) ethynyl)-2-naphthoate (18) A mixture of methyl 6-bromo-2-naphthoate (0.541 g, 2 mmol), CuI (7.8 mg, 40 μmol), and the palladium catalyst Pd $(PPh_3)_2Cl_2$ (56 mg, 79.78 μmol) were dissolved in Et_3N (20 ml) in a dry 50 ml flask with a stir bar under N_2 and fitted with a condenser. The solution was dissolved and heated to 90° C for 15 min at which time 1.3 equivalent TMS acetylene (0.37224 ml, 2.6 mmol) was slowly added. The reaction was left on heating at 90 °C for overnight (~14 hrs). The solvents were removed in *vacuo* and the crude residue was redissolved in 25 ml DCM. The organic solution was washed with 25 ml × 2 water, 25 ml 10% citric acid and saturated 25 ml sodium bicarbonate, and brine 10 ml×2. The organic layer was dried with anhydrous sodium sulphate, filtered, and removed in *vacuo*. The product was further purified over silica (hexane: EtOAc (19:1)) yielding 18 (0.512 g, 90.6%) as an off-white solid.

18: ^{1}H NMR (400 MHz, $CDCl_3$) δ 8.56 (s, 1H), 8.23 – 7.99 (m, 1H), 7.99 (d, J = 23.1 Hz, 1H), 7.95 – 7.63 (m, 1H), 7.56 (dd, J = 8.5, 1.4 Hz, 1H), 7.54 – 7.27 (m, 1H), 7.26 (s, 1H), 3.98 (s, 3H), 0.51 – 0.05 (m, 9H).^{13}C NMR (101 MHz, $CDCl_3$) δ 170.30 – 164.24, 135.29 – 134.76, 132.06 – 131.83, 131.72, 130.80, 129.45, 129.30, 128.04, 126.00, 123.14 – 122.38, 108.13 – 102.62, 101.28 – 97.98, 98.53 – 91.61, 79.49 – 74.06, 52.38, 0.00.

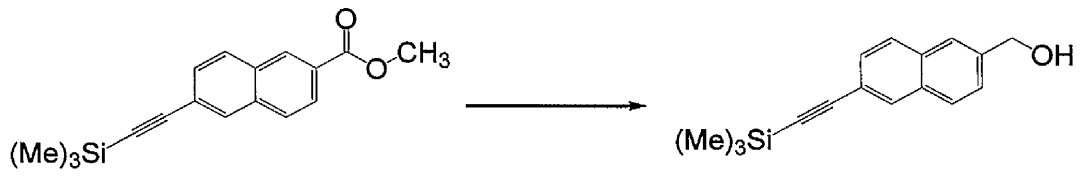

18 **19**

(6-((trimethylsilyl)ethynyl)naphthalen-2-yl)methanol (19) To a stirring solution of **18** (500 mg, 1.77 mmol) in THF which has been cooled to 0° C by an ice water bath, 2 equivalent a solution of lithium aluminium hydride ($LiAlH_4$, 1.013 ml, 3.5M). in THF/toluene was added in slowly. The mixture was then kept stirring at room temperature for 2 hrs. Thereafter, the reaction was quenched by addition of 10 ml dd water and then acidified by HCl (1 M, 10 ml). The mixture was extracted by Et_2O (30 ml×2) and the organic layer is dried by $MgSO_4$. After all organic solvent were removed, the product **19** was given as yellow solid (364 mg, 80.9%) this product were taken forward directly to the next step to prepare **20**.

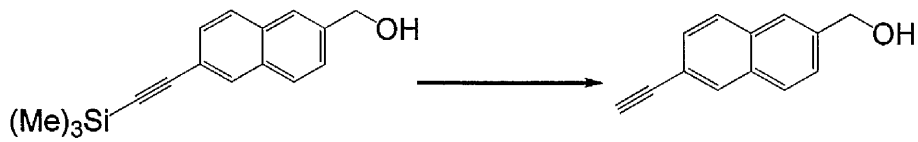

19 **20**

(6-ethynylnaphthalen-2-yl) methanol (20) The solution of **19** in 15 ml of THF (364 mg) which has been cooled to -20° C, 1.1 equivalent of TBAF (1.947 ml) was added in. The mixture was kept stirring at -20°C for 30 min and then the reaction was quenched with water 20 ml. The resulting mixture was extracted by Et_2O (20 ml×2) and the combined organic layer was washed with brine and was dried by $MgSO_4$. All of the solvent was removed in *vacuo* to give the crude product as yellow solid.

crude product was purified by flashy chromatography eluted with 30% EtOAc in hexane to give product **20** (242.9 mg, 94.2%) as pale yellow solid.

20: ^{1}H NMR (400 MHz, $CDCl_3$) δ 8.02 (s, 1H), 7.84 – 7.78 (m, 1H), 7.77 (s, 1H), 7.56 – 7.51 (m, 1H), 7.49 (d, J = 1.1 Hz, 1H), 7.26 (s, 1H), 4.87 (d, J = 5.0 Hz, 1H), 3.15 (s, 2H), 1.57 (s, 1H).^{13}C NMR (101 MHz, $CDCl_3$) δ 200.94 – 197.63, 140.05 – 139.81, 133.48 – 133.28, 132.57 – 132.40, 129.34, 128.62, 128.41, 126.27, 125.60, 101.31 – 98.87, 84.69 – 83.53, 77.55, 65.71.

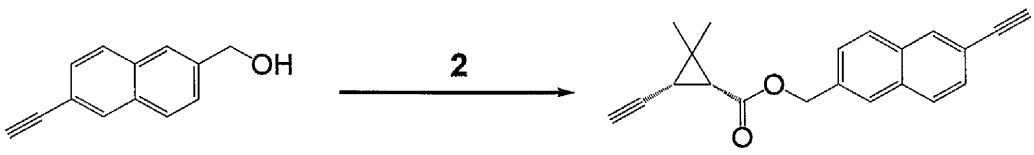

20 **P2**

(1R,3R)-(6-ethynylnaphthalen-2-yl)methyl3-ethynyl-2,2-dimethylcyclopropane-carboxylate (P2) The acid chloride (compound **2,** (384.16μmol)) dissolved in DCM and 2 equivalent of pyridine (30μl) was added in the solution, then reaction proceeds by the addition of the solution of compound **20** (1 eq. 70 mg, 384.16μmol) in DCM. The resulting mixture was kept stirring at RT for overnight, when the reaction finished the solvent and the excess pyridine were removed in *vacou*. The residue was dissolved in Et_2O (50 ml) and was washed by H_2O, $NaHCO_3$ (saturated) and brine. The crude product is purified by flash column chromatography eluting with 5 % -10 % EtOAc in hexane to give the product of 100 mgs (85%) as pale yellow crystal.

P2: ^{1}H NMR (400 MHz, $CDCl_3$) δ 8.01 (s, 1H), 7.80 (s, 1H), 7.79 – 7.75 (m, 1H), 7.52 (dd, J = 8.5, 1.4 Hz, 1H), 7.46 (dd, J = 8.5, 1.4 Hz, 1H), 7.26 (s, 1H), 4.87-4.76 (dd, 2H), (d, J = 11.2 Hz, 1H), 3.49 (s, 1H), 3.15 (s, 1H), 2.14 (q, J = 5.6 Hz, 1H), 1.35 (s, 3H), 1.19 (s, 3H).^{13}C NMR (101 MHz, $CDCl_3$) δ 200.30 – 199.63, 190.19 – 189.33, 174.34 – 173.78, 136.66 – 136.12, 132.66 – 132.11, 129.59 – 129.12, 128.56, 127.20 – 125.79, 121.38 – 118.07, 107.69 – 105.17, 104.07 – 101.63, 85.10 – 83.14, 81.48 – 79.83, 79.04 – 76.05, 65.59 – 63.93, 39.46 – 36.94, 32.11, 27.89 – 25.69, 21.08, 18.77 – 16.56. HRMS (CI); 303.13909 $[M+H]^+$ $C_{21}H_{19}O_2$ requires 392.13850

4.3.5.2. Synthesis of probe 3R and 4S

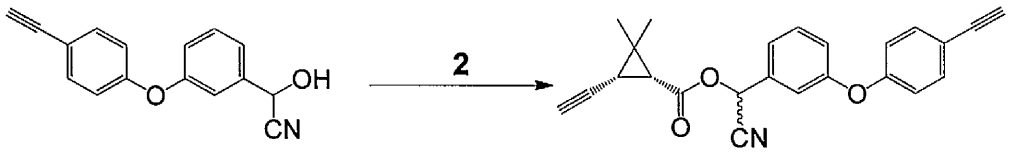

13 **Mixture of P3R and P4S**

(1R, 3R)-(R)-cyano(3-(4-ethynylphenoxy)phenyl)methyl 3-ethynyl-2,2-dimethyl cyclopropanecarboxylate (P3R) and (1R,3R)-(S)-cyano(3-(4-ethynylphenoxy) phenyl)methyl 3-ethynyl-2,2-dimethylcyclopropanecarboxylate (P4S) Synthesis was achieved using the procedure used for preparation of **P2** to give the title compound as a yellow oil residue. The crude product was purified by flash column chromatography eluting with 5 -10 % EtOAc in hexane to give the product of 80 mg (83%) as pale yellow oil of disterioisomers mix of **P3R** and **P4S** that was confirmed by ^{1}HNMR. Separation of these disterioisomeric has been achieved by normal phase preparative HPLC using gradient of as eluent EtOAc in hexane (5-10%) with a flow

rate of 5 ml min-1 to give **P3R** ((1R) retention time 52.7 min, 44 mg) and **P4S** ((1S) retention time 57.8 min 31 mg). The absolute configuration of CHCN was related to deltamethrin.

P3R: ^{1}H NMR (400 MHz, $CDCl_3$) δ 7.50 (s, 1H), 7.48 (s, 1H), 7.43 (t, J = 8.0 Hz, 2H), 7.32 – 7.26 (m, 2H), 7.20 (t, J = 1.9 Hz, 1H), 7.09 (dd, J = 8.1, 2.2 Hz, 1H), 6.97 (s, 1H), 6.95 (s, 1H), 6.42 (s, 1H), 3.06 (s, 1H), 2.11 (d, J = 2.2 Hz, 1H), 1.86 (dt, J = 6.5, 3.3 Hz, 2H), 1.79 (d, J = 8.5 Hz, 1H), 1.41 (s, 3H), 1.24 (s, 3H).^{13}C NMR (101 MHz, $CDCl_3$) δ 167.66 – 167.27, 157.60, 134.30, 131.16, 123.29, 121.18 , 119.15, 118.79, 118.06 – 117.59, 116.62 – 116.16, 83.68 – 83.12, 79.58 – 78.63, 77.40, 71.74, 62.44, 30.84, 28.56, 27.55, 23.36, 16.05. HRMS (ESI); 392.1254 $[M+Na]^+$ $C_{24}H_{19}NO_3$+Na requires 392.1263.

P4S:^{1}H NMR (400 MHz, $CDCl_3$) δ 7.50 (s, 1H), 7.48 (s, 1H), 7.43 (t, J = 7.9 Hz, 1H), 7.33 – 7.26 (m, 1H), 7.20 (d, J = 1.9 Hz, 1H), 7.09 (dd, J = 8.1, 2.3 Hz, 1H), 6.97 (s, 1H), 6.95 (s, 1H), 6.47 (d, J = 19.0 Hz, 1H), 3.06 (s, 1H), 2.15 (d, J = 2.2 Hz, 1H), 1.89 (dt, J = 12.2, 6.1 Hz, 1H), 1.79 (d, J = 8.6 Hz, 1H), 1.34 (s, 3H), 1.20 (s, 3H).^{13}C NMR (101 MHz, $CDCl_3$) δ 167.64 – 167.34, 157.78 – 157.22, 134.37, 131.17, 123.32, 121.15, 119.17, 118.80 , 118.38 – 117.65, 116.56 – 116.14, 83.58 – 83.10, 79.09 – 78.45, 77.41, 71.91, 62.51, 30.86, 28.32, 27.51, 23.41, 16.08.HRMS (ESI); 392.1257 $[M+Na]^+$ $C_{24}H_{19}NO_3$+Na requires 392.1263.

4.3.5.3. Synthesis of probe 5R and 6S

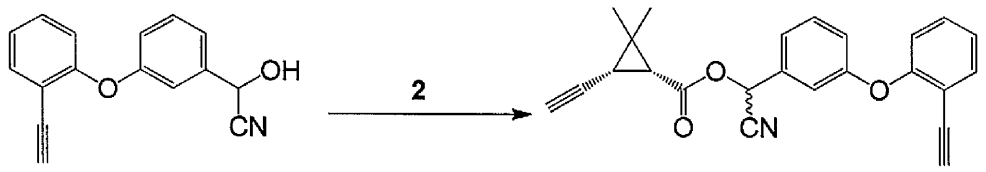

12 Mixture of P5R and P6S

(1R,3R)-(R)-cyano(3-(2-ethynylphenoxy)phenyl)methyl 3-ethynyl-2,2-dimethy lcyclopropanecarboxylate (P5R) and (1R,3R)-(S)-cyano(3-(2-ethynylphenoxy) phenyl) methyl 3-ethynyl-2,2-dimethylcyclopropanecarboxylate (P6S)

Synthesis was achieved using the procedure used for preparation of **P2** to give title compound as yellow oil residue. The crude product was purified by flash column chromatography eluting with 5 -10 % EtOAc in hexane to give the product of 61 mg (63%) as pale yellow oil. The product was further purified by preparative HPLC to give of white clear oil. Separation of these diastermoers has been achieved by normal phase preparative HPLC using eluent gradient of EtOAc in hexane (5-10%) with a flow rate of 5 ml min^{-1} to give **P5R** ((1R) retention time 43.1 min, 32mg) and **P6S** ((1*S*) retention time 46.2 min, 28 mg). The absolute configuration of CHCN was related to deltamethrin.

P5R: ^{1}H NMR (400 MHz, $CDCl_3$) δ 7.57 (dd, *J* = 7.7, 1.6 Hz, 1H), 7.40 (t, *J* = 8.0 Hz, 1H), 7.34 (dt, *J* = 13.1, 2.7 Hz, 1H), 7.26 (t, *J* = 6.3 Hz, 1H), 7.19 (t, *J* = 3.7 Hz, 1H), 7.14 (t, *J* = 7.5 Hz, 1H), 7.05 (dd, *J* = 8.2, 2.3 Hz, 1H), 6.94 (d, *J* = 8.3 Hz, 1H), 6.42 (s, 1H), 3.22 (s, 1H), 2.12 (d, *J* = 2.2 Hz, 1H), 1.86 (dd, *J* = 8.5, 2.2 Hz, 1H), 1.79 (d, *J* = 8.5 Hz, 1H), 1.41 (s, 3H), 1.24 (s, 3H).^{13}C NMR (101 MHz, $CDCl_3$) δ 167.52, 158.15, 157.69, 134.92, 133.95, 130.91, 124.51, 122.82 , 120.35, 119.70, 118.15,

116.46, 115.30, 82.66, 79.23, 78.42 – 76.43, 71.77, 62.51, 30.84, 28.53, 27.55, 23.32, 16.07. HRMS (ESI); 392.1259 $[M+Na]^+$ $C_{24}H_{19}NO_3$+Na requires 392.1263

P6S: ^{1}H NMR (400 MHz, $CDCl_3$) δ 7.57 (dd, J = 7.7, 1.5 Hz, 1H), 7.45 – 7.38 (m, 1H), 7.34 (dt, J = 12.5, 2.4 Hz, 1H), 7.27 (dd, J = 9.0, 6.0 Hz, 1H), 7.18 (d, J = 2.0 Hz, 1H), 7.14 (t, J = 7.5 Hz, 1H), 7.08 – 7.02 (m, 1H), 6.94 (d, J = 8.3 Hz, 1H), 6.45 (s, 1H), 3.21 (s, 1H), 2.16 (d, J = 2.3 Hz, 1H), 1.89 (dd, J = 8.5, 2.2 Hz, 1H), 1.79 (d, J = 8.6 Hz, 1H), 1.34 (s, 3H), 1.20 (s, 3H).^{13}C NMR (101 MHz, $CDCl_3$) δ 167.49, 158.17, 157.65, 134.93, 134.20, 130.92 , 124.56, 122.85, 120.36, 119.74, 118.08, 116.41, 115.32, 100.28 – 99.73, 82.63, 79.35, 78.99, 78.29 – 76.54, 71.91, 62.55, 30.86, 28.33, 27.53, 23.38, 16.09. HRMS (ESI); 392.1246 $[M+Na]^+$ $C_{24}H_{19}NO_3$+ Na requires 392.1263.

4.3.6. Synthesis of pyrethroid ABPP probes containing click handle replacing the alpha cyano group.

4.3.6.1. Synthesis of probe 7RS

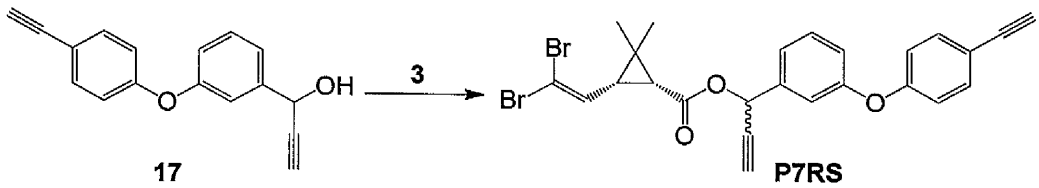

(1R, 3R)-1-(3-(4-ethynylphenoxy) phenyl) prop-2-yn-1-yl 3-(2,2-dibromovinyl)-2,2 –dimethylcyclopropanecarboxylate (7RS) Synthesis achieved using procedure used for preparation of P2 to give title compound as yellow oil residue. The crude product was purified by flash column chromatography eluting with 5 -10 % EtOAc in hexane to give the product of 80 mg (83%) as pall yellow oil. The product is further purified by preparative HPLC to give isomer mix of white clear oil 70 mg **(72%).** ^{1}H NMR (CDCl3) confirmed a mixture of two isomer pairs.

^{1}H NMR (400 MHz, $CDCl_3$) δ 7.47 (dt, J = 6.8, 2.4 Hz, 1H), 7.38 (tt, J = 8.2, 4.1 Hz, 1H), 7.32 – 7.27 (m, 1H), 7.26 (d, J = 3.9 Hz, 1H), 7.22 (dd, J = 10.4, 1.9 Hz, 1H), 7.03 – 6.98 (m, 1H), 6.95 (dt, J = 6.7, 2.4 Hz, 1H), 6.75 (t, J = 8.0 Hz, 1H), 6.40 (dd, J = 12.7, 2.1 Hz, 1H), 4.18 – 4.05 (m, 1H), 3.08 (d, J = 24.9 Hz, 1H), 2.66 (dd, J = 5.7, 2.3 Hz, 1H), 1.96 (ddd, J = 32.4, 17.7, 8.4 Hz, 6H), 1.26 (ddd, J = 22.8, 17.2, 12.2 Hz, 6H). **HRMS** (ESI); 550.9639 $[M+Na]^+$ $C_{25}H_{20}Br_2O_3$+ Na requires 550.9656.

4.3.6.2. Synthesis of probe 8RS

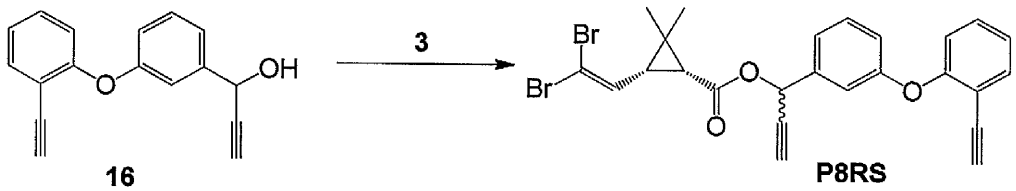

16 P8RS

(1R,3R)-1-(3-(2-ethynylphenoxy) phenyl) prop-2-yn-1-yl 3-(2,2-dibromovinyl)-2,2 -dimethylcyclopropanecarboxylate (P8RS) Synthesis achieved using procedure used for preparation of P2 to give title compound as yellow oil residue. The crude product was purified by flash column chromatography eluting with 5 -10 % EtOAc in hexane to give the product of ~60 mg (62 %) as pall yellow oil. The product is further purified by preparative HPLC to give isomer mix of white clear oil 53 mg (55%). ^{1}H NMR (CDCl3) confirmed a mixture of two isomer pairs.

^{1}H NMR (400 MHz, $CDCl_3$) δ 7.56 (dd, J = 7.7, 1.4 Hz, 1H), 7.39 – 7.33 (m, 1H), 7.30 (d, J = 8.7 Hz, 1H), 7.26 (s, 1H), 7.23 (dd, J = 11.1, 1.9 Hz, 1H), 7.10 (t, J = 7.5 Hz, 1H), 6.99 (d, J = 8.1 Hz, 1H), 6.90 (d, J = 8.0 Hz, 1H), 6.75 (dd, J = 8.3, 5.9 Hz, 1H), 6.40 (dd, J = 13.7, 2.2 Hz, 1H), 4.12 (dd, J = 14.3, 7.1 Hz, 1H), 3.22 (d, J = 1.9 Hz, 1H), 2.65 (dd, J = 5.6, 2.3 Hz, 1H), 2.01 – 1.84 (m, 6H), 1.33 – 1.15 (m, 6H). HRMS (ESI); 550.9634 $[M+Na]^+$ $C_{25}H_{20}Br_2O_3$+Na requires 55

5. Validation of pyrethroid ABPP probes

5.1.Introduction

The development of a novel tool to enable the direct and selective identification of P450's that actually metabolise pyrethroids and represent potential metabolic resistance markers was the principal objective of this PhD project. Having designed and synthesised pyrethroid based clickable activity based protein profiling probes (ABPPs) (Chapters 3 and Chapter 4), the next step was to determine which, if any, were capable of selectively labelling pyrethroid metabolising P450s in microsomes. To do this the specificity and selectivity of the suit of novel pyrethroid ABPPs were tested against *E. coli* membranes expressing individual Anopheline pyrethroid metabolising P450s CYP6P3, CYP6M2 and non pyrethroid metabolising control, CYP6Z2.

Next, the pyrethroids ABPPs were evaluated for their ability to identify relevant pyrethroid metabolisers in microsomes extracted from rodents and mosquitoes. Finally, the identity of proteins selectively pulled down by the probes were examined to determine the power of ABPPs in the selective tagging, detection, enrichment, and identification of the key enzymes involved in pyrethroid metabolism in their native membrane environment.

5.2.Results and Discussion

5.2.1. NADPH dependent inhibition of P450s by ABPP Probe 2 (P2)

To test whether pyrethroid ABPPs can label P450s in an activity-dependent manner, preliminary inhibition testing of P2 against the pyrethroid metabolisers CYP6M2 and CYP6P3 was carried out using P450-Glo assay (Promega, UK). As shown in Figure 5.1. NADPH dependent inhibition was demonstrated for CYP6P3 but not CYP6M2. P2 was taken forward for further characterisation *i.e.* visual detection of P450-probe adducts by click chemistry and azide reporter attachment.

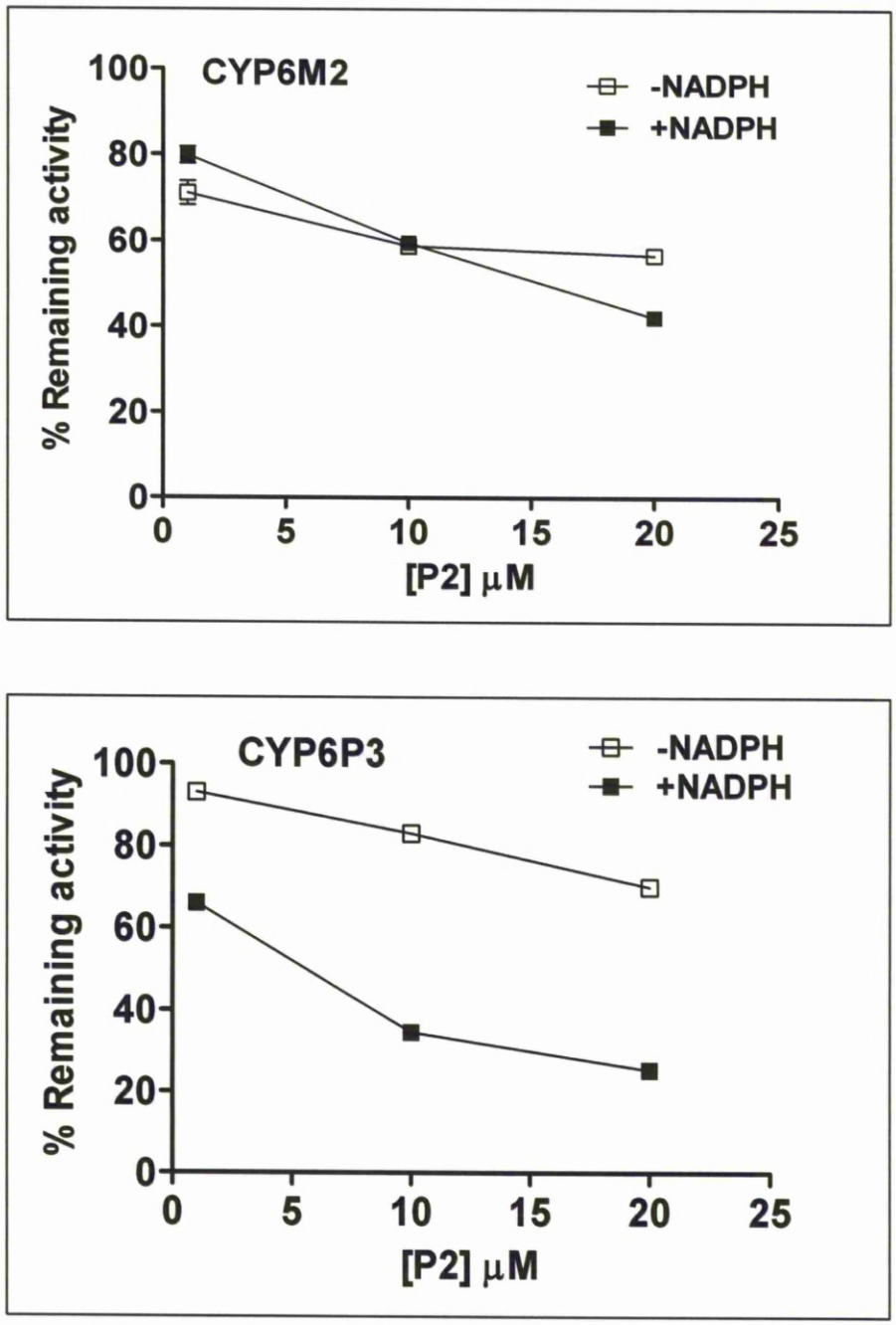

Figure 5.1. Residual activity of CYP6M2 and CYP6P3 after treatment with different concentrations of P2. Different concentrations of P2 (10, 100 and 200 μM) were pre-incubated with 0.2 μM P450 in the presence and absence of 1 mM NADPH before measuring the residual enzyme activity by addition of the probe substrate PPXE. Note, the pre-incubation reaction was diluted 10 fold into the PPXE probe reaction mix to minimize the interference from ABPP carry-over.

5.2.2. Labelling of P450s with P2

5.2.2.1. Western blot detection of activity based P450-P2 adduct formation.

Initial characterisation of CYP6P3 labelling by pyrethroid ABPP probe (P2) was carried out using standard Western blotting and chemiluminescent detection (ECL). It was hoped that the biotin azide labelled P450 would be detected by avidin labelled horseradish peroxidise, resulting in an ECL detectable band. NADPH dependent labelling was observed at the region of 49 and 55 KDa, the size expected for P450s (Figure 5.2), however, labelling was weak with high background even after dilution of avidin horseradish peroxidase to 1:50000, or after precipitation of labelled protein and cold methanol washing to concentrate and remove excess click reagents. The low sensitivity and non specific binding made this system unsuitable for comparative profiling of the reactivity of pyrethroid ABPP probes with P450 enzymes.

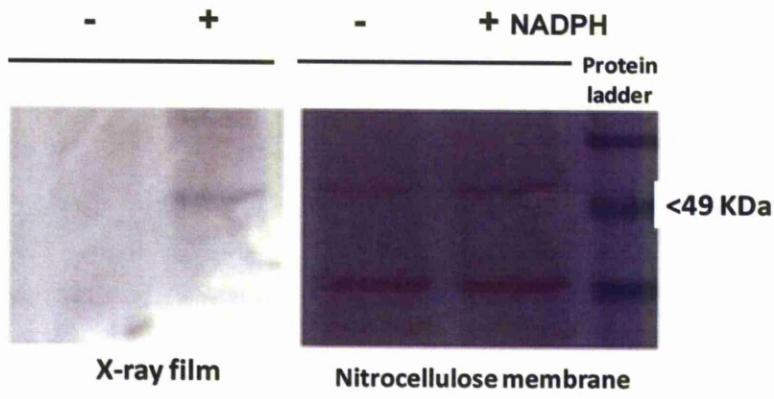

Figure 5.2. Western blots for detection of CYP6P3 labelling by probe 2. The CYP6P3 membrane normalised to 0.2 μM and incubated with probe 2 at 10 μM in presence and absence of NADPH at 37° C. Following 1 h incubation, proteomes were treated with an azide-conjugated biotin tag under CC conditions and resolved by SDS-PAGE. The labelled protein was transferred by electro blotting (semi dried) onto nitrocellulose membranes and detected by blot treatment with an avidin-horseradish peroxidase conjugate, following membrane blocking by 3 % BSA. The super signal chemiluminescence reagents (Thermo, UK), were used to detect the labelling event. The relative amounts of pyrethroid probe-biotin labelling were estimated by film densitometry. The NADPH-dependent probe-labelled proteins were detected at ~ 49KDa, consistent with the molecular masses of P450 enzymes.

5.2.2.2. 1D-Gel fluorescence analysis

To overcome the high background caused by non specific binding of biotin-azide and low sensitivity of the Western blot detection, a 1D-Gel fluorescence scanning technique was used for comparative profiling of pyrethroid ABPPs. An initial experiment with CYP6P3 and CYP6M2 was carried out to investigate the reactivity of P2 with recombinant P450s. This probe was added to P450 membranes co-expressed with AgCPR in the presence or absence of NADPH. Following 1 hr incubation, membranes were treated with an azide conjugated Alexa Fluor® 488 tag under CC conditions and resolved by SDS-PAGE. The green-fluorescent Alexa Fluor® 488 azide was chosen for its azide reactivity with terminal alkynes via a copper-catalyzed click reaction (Speers *et al.*, 2003). In addition to being an exceedingly bright and photostable fluorophore (low photo-bleaching), Alexa Fluor® 488 azide is soluble in water and stable at different pH levels which makes it remarkably adequate to use in different applications and different conditions.

The in-gel fluorescence scanning experiments identified an intensely labelled protein band in the range of 48–55 kDa, which was only observed in the NADPH-treated sample (Figure 5.3). Interestingly, consistent with the lack of MBI against CYP6M2, P2 clearly showed NADPH dependent labelling of CYP6P3 but not CYP6M2.

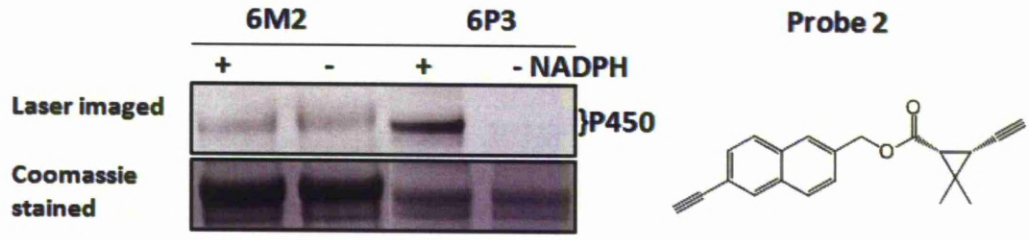

Figure 5.3. Probe reactivity profiles with CYP6M2 and CYP6P3. Selective labeling of P2 by in-gel 1D fluorscence analysis. CYP6M2 and CYP6P3 membranes were incubation of P2 (10 μM) with 0.2 μM P450, Only CYP6P3 was labelled in the presence of NADPH Coomassie staining of the gel confirms equal loading of samples +/- NADPH

5.2.2.3. Optimisation of probe conditions

Titration of P2 with CYP6P3 was carried out to determine the optimum concentration of probe and AlexaFluor® 488 azide reporter. As shown in Figure 5.4, the labelling of CYP6P3 was dependent on probe concentration, and the NADPH dependent labelling intensity increased with increasing concentration of Alexa Fluor® 488 azide from 25 μM to 100 μM. However, the increasing background labelling occurred in the absence of NADPH treatment at high reporter concentrations of the reporter even after fixing and copious washing (gel washed overnight in destaining solution).

The background could be removed by protein precipitation and washing by cold methanol following click reaction to remove the excess click reagents. However, this was found to alter the protein concentration slightly (Figure 5.4.C). This may affect the comparative interpretation of paired samples. Therefore, it was decided to use Alex Fluor 488 azide at low concentration (25μM) in combination with gel destaining to reduce the background.

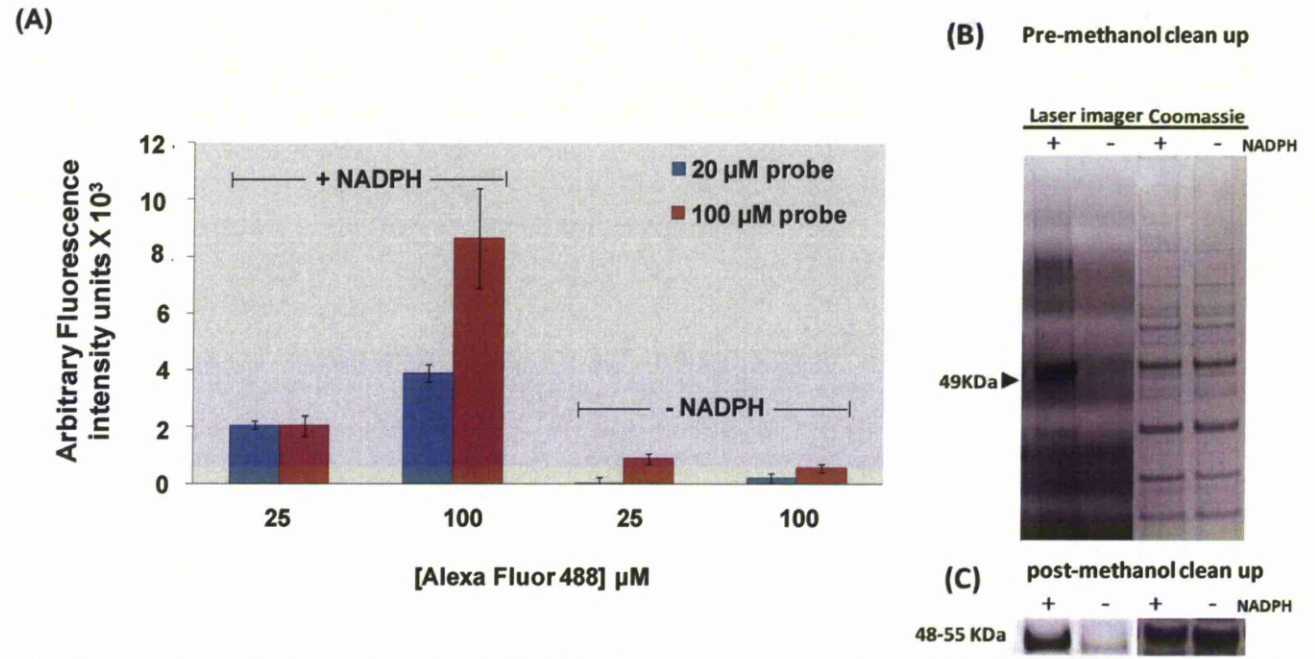

Figure 5.4. Titration of P2 and AlexaFluor azide with CYP6P3. (A). Fluorscence reporter (AlexaFluor 488 azide) titration with different concentrations of P2 bound to P450, error bar refere to standard deviation for three indpendent replicates (n=3) (B) CYP6P3 labeling byP2 at 20 µM pre- methanol clean-up, flourscent P450 bands are visible in the presence of NADPH. The 49KDa marker indficates the expected P450 size./ The adjacent Coomassie stained image confirms equal protein loading (C) Samples in B taken through methanol clean-up (proteine precipitated and washed using using cold methanol to remove excecc click reagents) precipitation shows lower backround i.e. no signal in –NADPH. The adjacent, Coomassie stained gel shows slightly unequal loading.

5.2.3. Pyrethroid ABPP labeling of *An. gambiae* P450s

To determine the selectivity and specificity of ABPPs against pyrethroid metabolising enzymes, the suite of pyrethroid probes were screened against three *An. gambiae* recombinant P450s CYP6M2, CYP6P3 and CYP6Z2. The former two being enzymes that can metabolise deltamethrin and permethrin and are associated with pyrethroid resistance in *An. gambiae* (Müller *et al.*, 2008) while CYP6Z2, although associated with pyrethroid resistance, does not metabolise pyrethroids (McLaughlin *et al.*, 2008). To profile the activity of the P450, the ABPP panel were incubated at a fixed concentration of 20 μM with 0.2 μM P450 at 37°C in the presence and absence of NADPH.

As expected the general substrate control probe, P1, labelled the three P450s. The probe labelling was also clearly NADPH dependent, proving the reaction had worked. In general, the ABPPs show quite widely variable reactivity and selectivity against the three P450s (Figure 5.5). Most of the P450 enzymes were labelled by multiple probes, however strong reactivity was clearly displayed by the probes containing bromine atoms i.e. P7RS and P8RS. This appears consistent with the relatively low binding energies calculated in Chapter 3 for these probes in the CYP6P3 model. This reinforces the role of the bromine atom in binding and further suggests that the deltamethrin like ABPPs are the strongest P450 binders. It was notable that not all reactions were NADPH dependent, with high background particularly evident with CYP6P3 and P7RS (Figure 5.5)

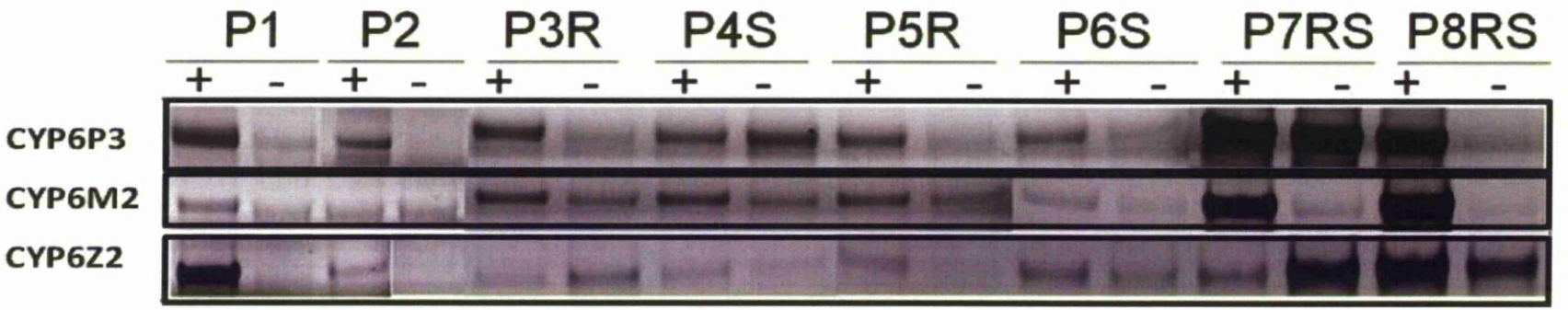

Figure 5.5. Probes suite labelling of three representative members of mosquitoes recombinant P450 panel. Full SDS-PAGE separation was performed, but only the 45-55 kDa region is shown, where NADPH-dependent probe-labelled proteins were detected (consistent with the molecular masses of P450 enzymes).

The differences in P450 reactivity profiles were quantitatively assessed by measuring the intensity of each CYP-probe labelling event using in-gel fluorescence scanning as depicted in Figure 5.6A. To ensure that these measurements reflected activity-based labelling of P450 enzymes, the –NADPH control signals were subtracted and calculated as differences in fluorescent intensity of P450 bands in reactions with or without NADPH according to Wright *et al.*, (Wright *et al.*, 2009). These measurements were used to devise a more complete presentation of labelling profiles for the P450 panel as a heat-map (Figure 5.6B).

The heat map revealed cleaner differences in probe–P450 reactivity profiles allowing the selectivity of the probes to be more clearly assessed. P7RS only recognised CYP6M2, thus selective for the resistance marker. P2 and P3R recognised both the pyrethroid metaboliser, CYP6P3 and CYP6M2, indicating a potential broad preference for pyrethroid metabolising enzymes. Finally, P8RS, and P5R displaying a broad reactivity against all three the enzymes, similar to P1.

Interestingly, the ability to distinguish stereospecific differences was displayed by the optical enantiomer pairs P4S and P3R, where P3R labels CYP6P3 but P4S does not. CYP6P3 was noticeably darkly stained with probe P7RS but did not show NADPH dependent labelling (Figure 5.5). Subtraction of the –NADPH control for the heat map (Figure 5.6) produced a blank value, suggesting non specific probe binding, or perhaps tight binding in absence of NADPH. Similar reasons may be applied to P7RS labelling of CYP6Z2 in the absence of NADPH.

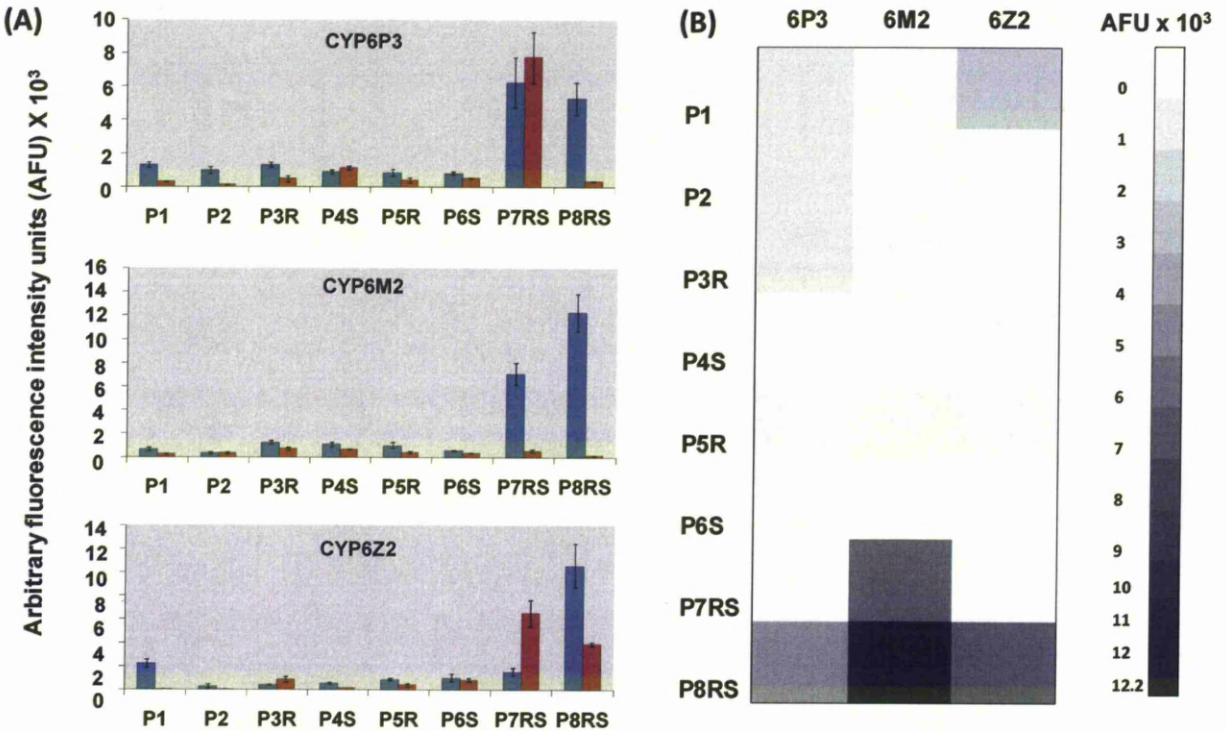

Figure 5.6. Quantitative data from SDS-PAGE gels of probe labelling illustrated in figure 5.5. (A) Bands intensity were measured as arbitrary fluorescence intensity (arbitrary fluorescence units (AFU) are average of four measurements for each band measured by Quantity One V. 4.6.8 BIORAD). (B) Heat maps illustrating probe labelling profiles for individual mosquitoes CYP enzymes devised by abstracting AFU of bands in absence of NADPH from AFU in presence of NADPH (Negative values in reflecting less labelling in the presence versus absence of NADPH have been assigned "0").

5.2.4. Removal of –NADPH background bands

In order to try and overcome the background labelling, affinity purification of CYP6P3 labelled with P7RS was done following the click reactions (presence and absence of NADPH) using a rhodamine-trifunctional biotin azide reporter(Speers and Cravatt, 2004b). This reporter contains a biotin group which enables enrichment of biotin labelled protein using streptavidin agarose beads following click reaction, while rhodamine provides fluorescent detection of labelled proteins resolved by 1D-Gel. As shown in Figure 5.7, the affinity step was successful in cleaning-up the background. Overall, these experiments proved that the ABPPs work and that affinity purification of reaction products can enhance the sensitivity of the technique by removing background binding. The next step was to determine if the probes were capable of identifying pyrethroid metabolising P450s in their native microsomal environment.

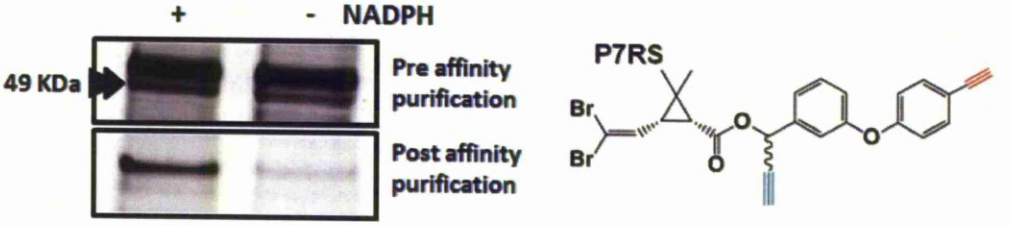

Figure 5.7. Enrichment of NADPH dependent CYP6P3 labelled by probe P7RS.

5.2.5. In *vitro* labelling of P450s from different species

To confirm the suitability of the pyrethroid ABPPs for the detection of pyrethroid metabolising enzymes in a native proteome context, the pyrethroid ABPPs tested against microsomes prepared from different species *i.e.* adult *An. gambiae*, rat and mouse liver.

5.2.5.1. Mouse liver microsomes

For initial profiling, four pyrethroid ABPP probes were tested against mouse liver microsomes. These were P2, the type I pyrethroid mimic probe, P3S, P7RS and P8RS, the type II pyrethroid mimic probes, and P1, the general ABPP control probe known to react with mouse liver microsomes (Wright and Cravatt, 2007; Wright *et al.*, 2009). As shown in Figure 5.8A, a band in the P450 region was detected by all four pyrethroid ABPPs, as well as with the P1 control probe. Thus, NADPH dependent labelling of P450s (*i.e.* activity based) was clearly evident, the halogenated probes including P7RS and P8RS producing strongest signals. These are of particular interest as they mimic deltamethrin, the most widely used pyrethroid insecticide.

5.2.5.2. Rat liver microsomes

These were treated with P7RS, the type 2, deltamethrin mimic probe and the type I non cyano pyrethroid mimic probe, P2. The probes displayed differential reactivity against rat liver microsomes, but again the labelling intensity was much higher with deltamethrin mimic probe P7RS containing bromine atoms (Figure 5.8B).

5.2.5.3. Mosquito microsomes

Microsomes (2 mg/ml) were prepared from *An. gambiae* mosquitoes (2-3 day old adult females) from both a pyrethroid resistant strain collected from Uganda (Tororo strain) (Ramphul *et al.*, 2009) and a laboratory susceptible strain (Kisumu). They were screened with P7RS, chosen because of its structural similarity to deltamethrin and its high reactivity with CYP6M2 and CYP6P3, as well as for its high activity with mouse and rat liver microsomes. Because of the low P450 content in mosquitoes, it was not possible to determine P450 content by the traditional CO-reduced spectral assay (Omura and Sato, 1964b), thus protein concentrations were adjusted to 2 mg/ml to normalise for protein content. After 1 hr labelling incubation samples were treated with Rhodamine-biotin trifunctional azide for click chemistry labelling. Although strong labelling of a P450 sized band was observed in both strains, it was not NADPH dependent regardless of gel scan intensity (Figure 5.8C). A similar observation was seen when using Alexa Fluor® 488 azide. However, when the microsomes were labelled with a trifunctional biotin reporter and affinity purified on streptavaidin agarose beads, NADPH dependent labelling was clearly observed in the region of 48-55KDa after gel fluorescence scanning. Interestingly, labelling was stronger in pyrethroid tolerant Tororo strain (Figure 5.9C, bottom gel). This may indicate higher pyrethroid metabolising activity in the pyrethroid resistance strain, possibly due to higher levels of CYP6P3, CYP6M2 or other P450s, although this still needs to be tested. Attempts were made to identify the labelled bands by mass spectrometry. However, this was unsuccessful due to low quantities of protein. Therefore, rat liver microsomes, which contain high levels of P450, were used to identify proteins reacting with ABPPs (see Section 5.2.6.).

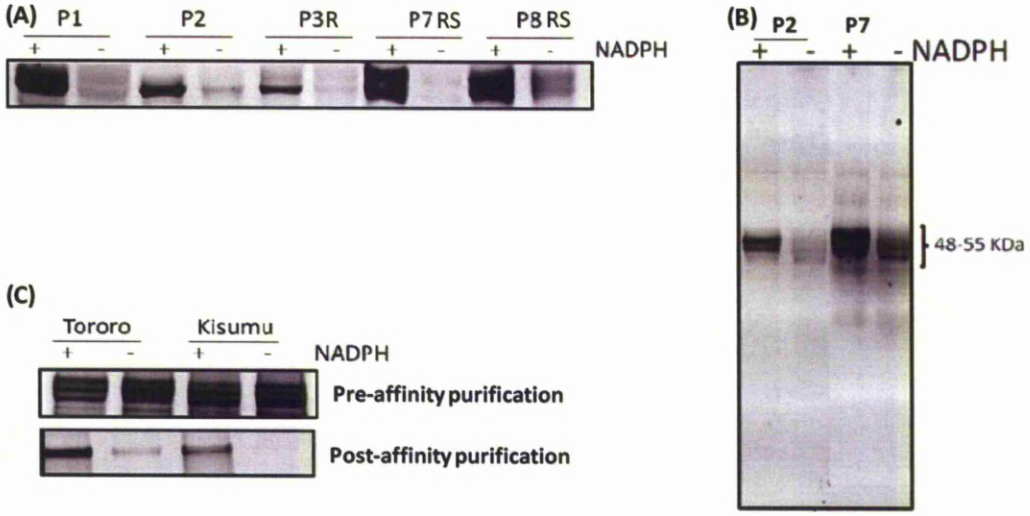

Figure 5.8. In vitro labelling of P450s from different species with Pyrethroid ABPP probes. (A) Treatment of mice liver microsomal proteome (0.2 μM P450s content) with the suite of ABPP probes (20 μM) in the presence or absence of NADPH (1 mM) shows variable probes labelling specificity and strongest labelling events are shown with halogenated probes (P7RS and P8RS). (B) Treatment of rat liver microsomes proteome at 2 mg/ml protein by 20 μM of probes 2 and 7 in presence and absence of (1 mM) NADPH represented NADPH dependent labelling of proteins around 50KDa. Full SDS-PAGE separation of labelled proteins was carried out using 4-12% Tris-Glycine gel. Labelled protein are identified by gel fluorescence scanning after appending AlexaFluor488-azide at 25 μM to labelled proteome via click chemistry (CC) reaction. (C) Treatment of microsomes proteomes extracted from pyrethroid tolerant (Tororo) and susceptible (Kisumu) strains of *Anopheles gambiae* mosquitoes (2-3 day old adult females) by 20 μM P7RS represented variable P450s levels after affinity purification. Labelled proteins were enriched on streptavidin agarose beads after appending Rhodamine-Biotin Trifunctional azide via CC reaction. Full SDS-PAGE separation was performed, but only the 48-55 kDa region is shown, where NADPH-dependent probe-labelled proteins were detected (consistent with the molecular masses of P450s).

5.2.6. The effect of cytochrome P450 reductase and cytochrome *b5* on pyrethroid ABPPs reactivity with P450s

For catalysis P450s require electrons from Cytochrome P450 reductase (CPR) and sometimes *b5* (Paine *et al.*, 2005). In order to show conclusively that the ABPPs are catalytically activated by P450s it was decided to test the probes against membranes lacking CPR or *b5*. Samples of mouse liver microsomes prepared from female transgenic lines containing liver specific gene deletions of CPR and *b5* were obtained from Professor Roland Wolf, University of Dundee (Finn *et al.*, 2008; Pass *et al.*, 2005) and treated with probes P7RS and P8RS. The level of P450s in each sample were normalised and treated in presence and absence of NADPH with 20 μM pyrethroid ABPP. The effect of the conditional deletion of P450 redox partners CPR and *b5* on pyrethroid ABPP probe reactivity is shown in Figure 5.9A. The levels of CPR activity shown in Figure 5.10B confirm the lack of CPR activity in the CPR knockout mice (-CPR/*b5*) versus wild type (CPR/*b5*) and *b5* knockout mice (CPR/-*b5*). There was very little labelling in CPR-null female mice (Figure 5.9A), consistent with lack of CPR activity (Figure 5.9B). This observation demonstrates that probes P7RS and P8RS require enzyme activation to bind and label P450s. More interestingly, there was reduction of P450 labelling in the *b5* knockouts (CPR/-*b5*; Figure 5.9A). This is consistent with the idea that *b5* is not an obligate redox partner, but instead can enhance catalytic activity. Also it is well known that *b5* often enhances insect P450 activity, in particular pyrethroid metabolism (Stevenson *et al.*, 2011; Zhang and Scott, 1996). It was also obvious that P8RS produced a far stronger signal than P7RS in the absence of *b5*. This suggests that some of the P450s involved in P7RS metabolism might be less reliant on *b5* for the oxidation of this pyrethroid.

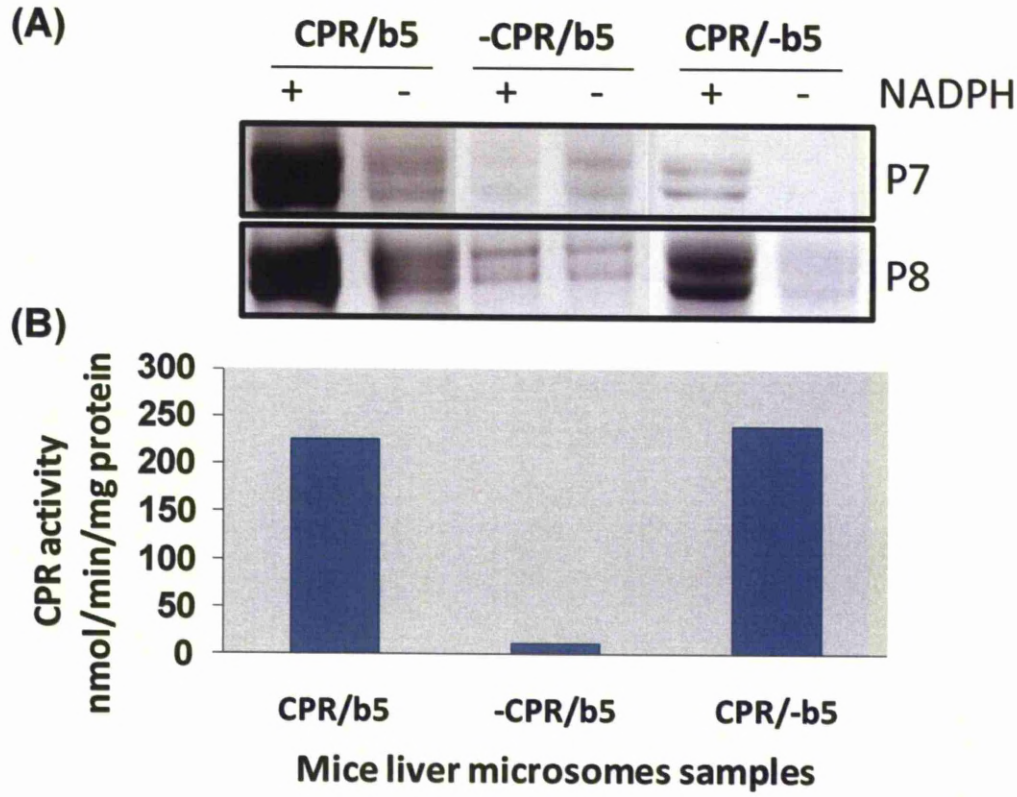

Figure 5.9. The effect of conditional deletion of CPR and *b5* on P450s/ Pyrethroid CC-ABPs reactivity in mouse hepatic microsomes. (A) Liver-specific knockout of the essential electron transfer protein cytochrome P450 reductase (CPR), resulting in essentially complete ablation of hepatic microsomal P450 activity. In CPR-null female mouse, the treatment of liver microsomal proteome (0.2 μM P450s content adjusting using CO assay(Omura and Sato, 1964a)) with 20 μM pyrethroid ABPP probes in the presence or absence of NADPH (1 mM) did not show any NADPH-dependent probe-labelling, where mice conditionally deleted cytochrome *b5* (*b5*) the NADPH dependent probe labelling greatly influenced. [B] Typical CPR activity for mice liver microsomes samples used for pyrethroid ABPP treatment measured by standard cytochrome *c* reduction assay (Pritchard *et al.*, 2006), data are average for 2 replicates.

5.2.7. Identification of P450s that metabolise deltamethrin using deltamethrin like ABPP probe (P7RS)

Probes P3R and P7RS recognise CYP6M2 and CYP6P3, enzymes that metabolise pyrethroids such as permethrin and deltamethrin in *An. gambiae* (Müller *et al.*, 2008; Stevenson *et al.*, 2011). To decide which probes to taken forward to determine P450 targets in hepatic microsomes rats, initial experiments were carried out to compare their reactivity against rat microsomes before and after affinity purification.

Strong NADPH dependent fluorescent signals were observed in the 48-55 kDa regions with both probes, either before or after affinity purification (Figure 5.10). Since P7RS produced the strongest signal and was most similar to deltamethrin, the band was excised, subjected to in-gel trypsin digestion, and the resulting peptides analyzed by multidimensional LC-MS/MS (Wright and Cravatt, 2007) (Figure 5.11).

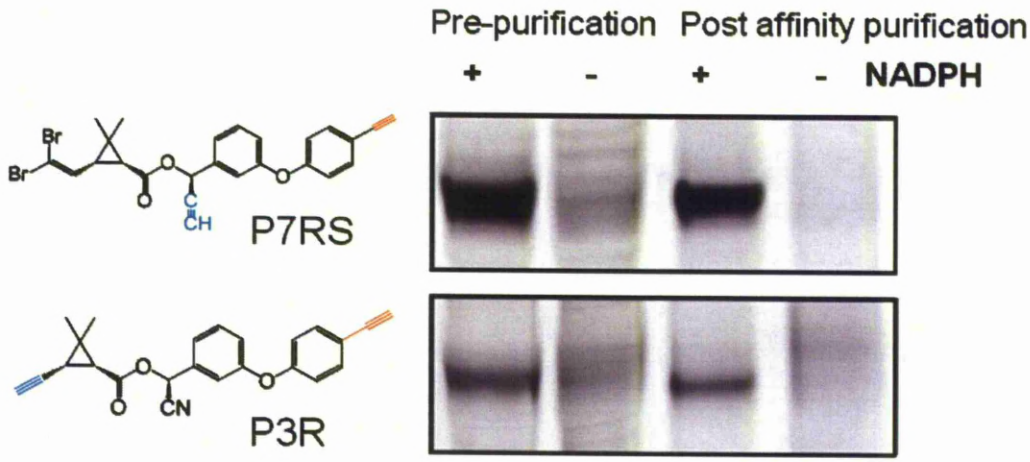

Figure 5.10. Enrichment of NADPH-dependent protein targets of probe 7RS from rat liver proteome. Probe labelling and affinity purification was carried out following the methodology mentioned in material and method section (Chapter 5)

5.2.7.1. Protein identification

Proteins were identified using the Mascot search algorithm and semi quantified by the exponentially modified protein abundance index (emPAI). This value offer approximate, label-free, relative quantitation of proteins in a mixture. This is obtained based on protein coverage by the peptide matches in a database search (Ishihama *et al.*, 2005). Based on these criteria, several specific targets that are involved in metabolism of drugs and pesticides were identified, all of which represented members of the P450 super family, flavin-containing monooxygenase (FMO), aldehyde dehydrogenase, epoxide hydrolase and uridine 5'-diphospho-glucuronosyltransferase (UDP glucuronosyltransferase 2B families) (Table 5.1 and Figure 5.12). Most importantly, P450s were the major constituent of the labelled band with (84% of total) and the most abundant P450 labelled was CYP2C11, a known deltamethrin metaboliser (Anand *et al.*, 2006a; Anand *et al.*, 2006b; Godin *et al.*, 2007; Godin *et al.*, 2006). Furthermore, the second most abundant unknown gene, LOC293989, is an orthlogue of human P450 CYP2C19 another known deltamethrin metaboliser (Godin *et al.*, 2007) (Table 5.1 and Figure 5.12). Although rat P450s CYP2C6 and CYP2C11 were reported earlier to have higher capability to metabolise deltamethrin, with *K*m 21.6, 31.9 μM and *V*max 150.0, 205.8 pmol/min/pmol P450 for CYP2C6 and CYP2C11 respectively (Godin *et al.*, 2007), the CYP2C6 wasn't identified from RLM sample. Interestingly sequence alignment of LOC293989 shows 97% and 74% protein sequence identity with deltamethrin metabolisers CYP2C6 (rat) and CYP2C19 (human) respectively which may suggest the involvement of this protein in pyrethroid metabolism (further investigation to define the function of this protein is required).

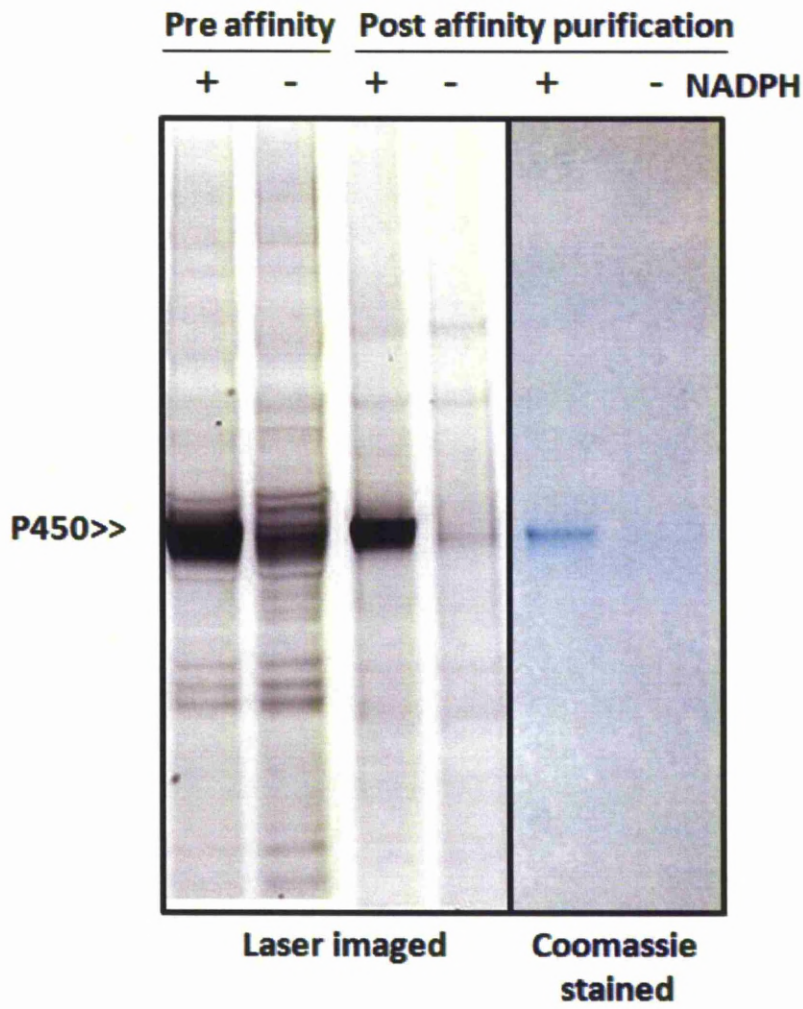

Figure 5.11. Enrichment of NADPH-dependent protein targets of probe 7RS from rat liver proteome.

Table 5.1. Enzymes labelled by P7RS in rat liver microsomes

	Protein	Mass Da	Score [a]	emPAI[b]
1	CYP2C11	57144	1371	9.48
2	LOC293989 (orthlogues to CYP2C19)	56048	878	3.85
3	CYP2C23	56396	346	1.02
4	UDP-g2B5 precursor	49498	225	0.85
5	UDP-g 2B5	60553	231	0.74
6	CYP2C13	49660	220	0.74
7	CYP2C7	56151	336	0.72
8	CYP2D10	57039	382	0.62
9	CYP2D1	57139	339	0.62
10	CYP2D26	56648	283	0.62
11	UDP-g2B3	60485	179	0.58
12	FMO3	59921	267	0.5
13	Epoxide hydrolase	52548	205	0.42
14	UDP-glucuronosyltransferase 2B4	61020	124	0.42
15	CYP2D3	56991	261	0.38
16	Aldh3a2 Fatty aldehyde dehydrogenase	54047	173	0.33
17	CYP2C13 (male-specific)	55824	144	0.31
18	CYP2B3	56348	133	0.31
19	CYP4V3	60541	163	0.29
20	CYP2C7	53254	150	0.26
21	CYP2A2	56309	104	0.24
22	CYP4F4	60011	131	0.23
23	CYP2C70	56120	164	0.18
24	CYP2A1	55959	85	0.18
25	CYP4A2	57932	107	0.17
26	CYP3A2	57694	90	0.17

(a) Ions score is -10*Log (P), where P is the probability that the observed match is a random event. Individual ions scores > 41 indicate identity or extensive homology ($p<0.05$). Protein scores are derived from ions scores as a non-probabilistic basis for ranking protein hits. (b) Exponentially modified protein abundance index.

Although the deltamethrin metabolisers CYP2C6, CYP2C11 and CYP3A2 are known being expressed at high level of expression in RLM (Godin *et al.*, 2007) however, CYP2C11 labbeled and identified as major protein target (46%) from RLM by P7RS where CYP3A2 was the lowest constituent (1%) of labbled proteins (Figure 5.12). This observation may confirm the sutibility of P7RS in detecting the active protein in deltamethrin metabolism in native proteomes. Additionally, other enzymes involved in pyrethroid metabolism like CYP2A1, CYP2C13, CYP2D1, and CYP3A2 (Godin *et al.*, 2007; Scollon *et al.*, 2009) were identified from RLM samples (Table 5.1). These data shows that the deltamethrin like probe (P7RS) is capable of identifying P450's associated with pyrethroid metabolism. However, other enzymes that their role in pyrethroid metabolism are not clearly shown have been identified in RLM sample as target protein which might suggest that these enzymes are linked to pyrethroid metabolism (warrants further investigation).

5.2.7.2. Identification of other genes pulled down by P7RS

From the results it was clear that P7RS did not just target P450s; around 16% of the proteins identified were other drug metabolising enzymes. These included. FMO a membrane binding enzyme which catalyzes the NADPH-dependent oxygenation of various nitrogen-, sulphur-, and phosphorous-containing xenobiotics and ALDH3a2, a polymorphic enzyme responsible for the oxidation of aldehyde to carboxylic acids. Aldehyde dehydrogenase is particularly interesting since it can operate in concert with P450s - following ester hydrolysis by P450s or esterases it can oxidise the 3-phenoxybenzaldehyde released from alpha cyano pyrethroid to 3-phenoxybenzoic acid.

(A)

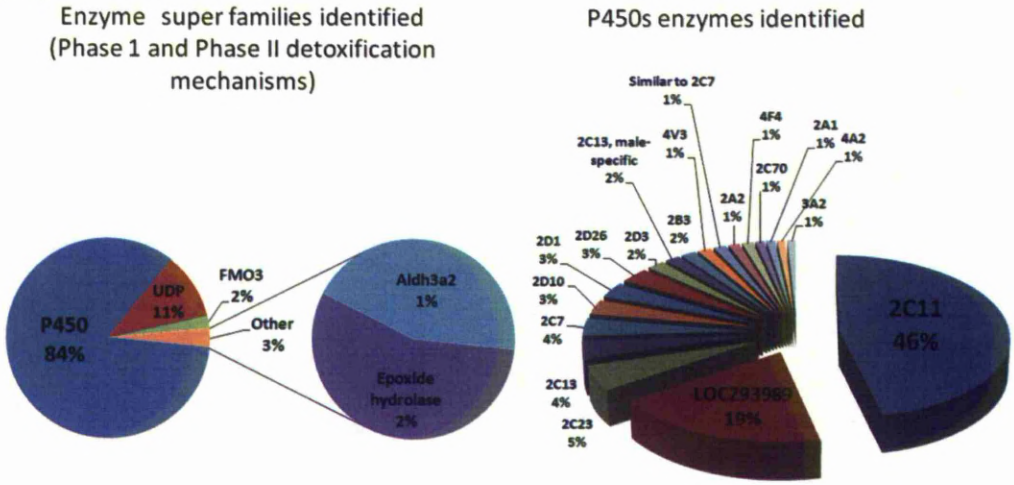

(B)

Cytochrome P450 2C11 (Coverage: 51%, Score: 1371)

```
1    MDPVLVLVLT LSSLLLLSLW RQSFGRGKLP PGPTPLPIIG NTLQIYMKDI
51   GQSIKKFSKV YGPIFTLYLG MKPFVVLHGY EAVKEALVDL GEEFSGRGSF
101  PVSERVNKGL GVIFSNGMQW KEIRRFSIMT LRTFGMGKRT IEDRIQEEAQ
151  CLVEELRKSK GAPFDPTFIL GCAPCNVICS IIFQNRFDYK DPTFLNLMHR
201  FNENFRLFSS PWLQVCNTFP AIIDYFPGSH NQVLKNFFYI KNYVLEKVKE
251  HQESLDKDNP RDFIDCFLNK MEQEKHNPQS EFTLESLVAT VTDMFGAGTE
301  TTSTTLRYGL LLLLKHVDVT AKVQEEIERV IGRNRSPCMK DRSQMPYTDA
351  VVHEIQRYID LVPTNLPHLV TRDIKFRNYF IPKGTNVIVS LSSILHDDKE
401  FPNPEKFDPG HFLDERGNFK KSDYFMPFSA GKRICAGEAL ARTELFLFFT
451  TILQNFNLKS LVDVKDIDTT PAISGFGHLP PFYEACFIPV QRADSLSSHL
501
```

LOC293989 Cytochrome P450-likeorthologus to CYP2C19 (Coverage: 37%, Score: 878)

```
1    MDLVMLLVLT LTCLILLSIW RQSSGRGKLP PGPIPLPIIG NIFQLNVKNI
51   TQSLTSFSKV YGPVFTLYFG MKPTVILHGY EAVKEALIDH GEEFAERGSF
101  PVVEKINKDL GIVFSHGNRW KEIRRFTLTT LRNLGMGKRN IEDHVQEEAR
151  CLVEELRKTN GSPCDPTFIL GCAPCNVICS IIFQNRFDYK DQDFLNLMEK
201  LNENMKILSS PWTQFCSFFP VLIDYCPGSH TTLAKNMYYN RNYLLKKIKE
251  HQESLDVTNP RDFIDYYLIK WKQENHNPNS EFTLENLSIT VTDLFAAGTE
301  TTSTTLRYAL LLLLKCPEVT AKVQEEIDRV VGKHRSPCMQ DRSRMPYTDA
351  MIHEVQRFID LIPTNLPHAV TCDIKFRNYL IPKGTTIITS LSSVLHDSKE
401  FPDPEIFDPG HFLDGNGKFK KSDYFMPFSA GKRMCAGEGL ARMELFLFLT
451  TILQNFKLKS VLHPKDIDTT PVFNGFASLP PFYELCFIPL
```

Figure 5.12. Proteins identified in rat liver microsomes after incubation with the deltamethrin like probe P7RS in the presence of NADPH. (A) Percentage constitution of Phase I and phase II detoxification enzymes activities labelled by P7RS in rat liver microsomes, calculated based on emPAI for each identified Enzyme (Ishihama *et al.*, 2005), relative protein abundant calculated by dividing emPAI value of the protein by the total emPAI total protein time 100 B) Top two P450s enzymes identified, matched peptides shown in Bold Red, Tryptic Peptides Identified by LC-MS/MS Analysis for P7RS-Enriched P450 Enzymes from rat liver proteomes.

This may also support the idea that release of the reactive species can produce labelling to proteins in vicinity of active P450s. Interestingly, the most abundant phase II (conjugative) detoxification protein was UDP-glucuronosyltransferase (11% of protein identified (Figure 5.12). These enzymes catalyze the addition of the glucuronic acid moiety to xenobiotics for elimination from the body (King *et al.*, 2000), including glucuronic conjugation of permethrin ester hydrolysis products in rats (Figure 5.13) (Noort *et al.*, 2008). It is therefore feasible that such compounds could form protein-pyrethroid conjugates upon transacylation mechanism or via Amadori product formation (Noort *et al.*, 2008) (Figure 5.14).

5.3.Conclusions

A set of type I and type II pyrethroid mimic probes , P2, 3R, 4S, 5R 6S, 7RS and 8RS have been developed. In general, the pyrethroid ABPP probes lacking bromine atoms displayed lower probe labelling activity relative to P7RS and P8RS the halogenated deltamethrin-like ABPP, indicating that the halogen atoms may be important in P450 active site recognition. The ABPPS may also help in understanding the function of redox partners such as CPR and *b5* on regulating activity of P450s that metabolise pyrethroid. For instance, the liver-specific knockout of CPR which knocked out P7RS and P8RS labelling in mouse microsomes (Figure 5.9) confirmed the MBI mechanism, while the reduction in labelling intensity in *b5* knockout mice indicates a cooperative role in enhancing activity. Finally, the present study has exploited the ability of pyrethroid ABPPs to label P450 sized molecules in rodent and mosquito microsomes. The deltamethrin ABPP P7RS was the most potent probe and used for this study because of its potency and common use of deltamethrin in vector control.

Affinity purification and enrichment of non induced rat liver P450s, showed that labelled proteins mainly belonged to phase I and II detoxification enzyme super families. 85% of the labelled were P450s, and the major two abundant enzymes detected were CYP2C11 and the orthlogues to CYP2C19 in human; both are confirmed deltamethrin metabolisers (Anand *et al.*, 2006a; Anand *et al.*, 2006b; Godin *et al.*, 2007; Godin *et al.*, 2006). Thus P7RS targets several key members of P450 subfamilies that contribute to pyrethroid metabolism *i.e.*, CYP2C11, CYP3A2.

In summary, a novel set of selective pyrethroid ABPPs have been developed that satisfies the major criteria expected for identification of enzymes associated with pyrethroid metabolism including; (i) NADPH dependent labelling of catalytic P450 enzymes, and (ii), targeting and labelling of several CYP enzymes associated with pyrethroid resistance with minimal cross reactivity with other proteins.

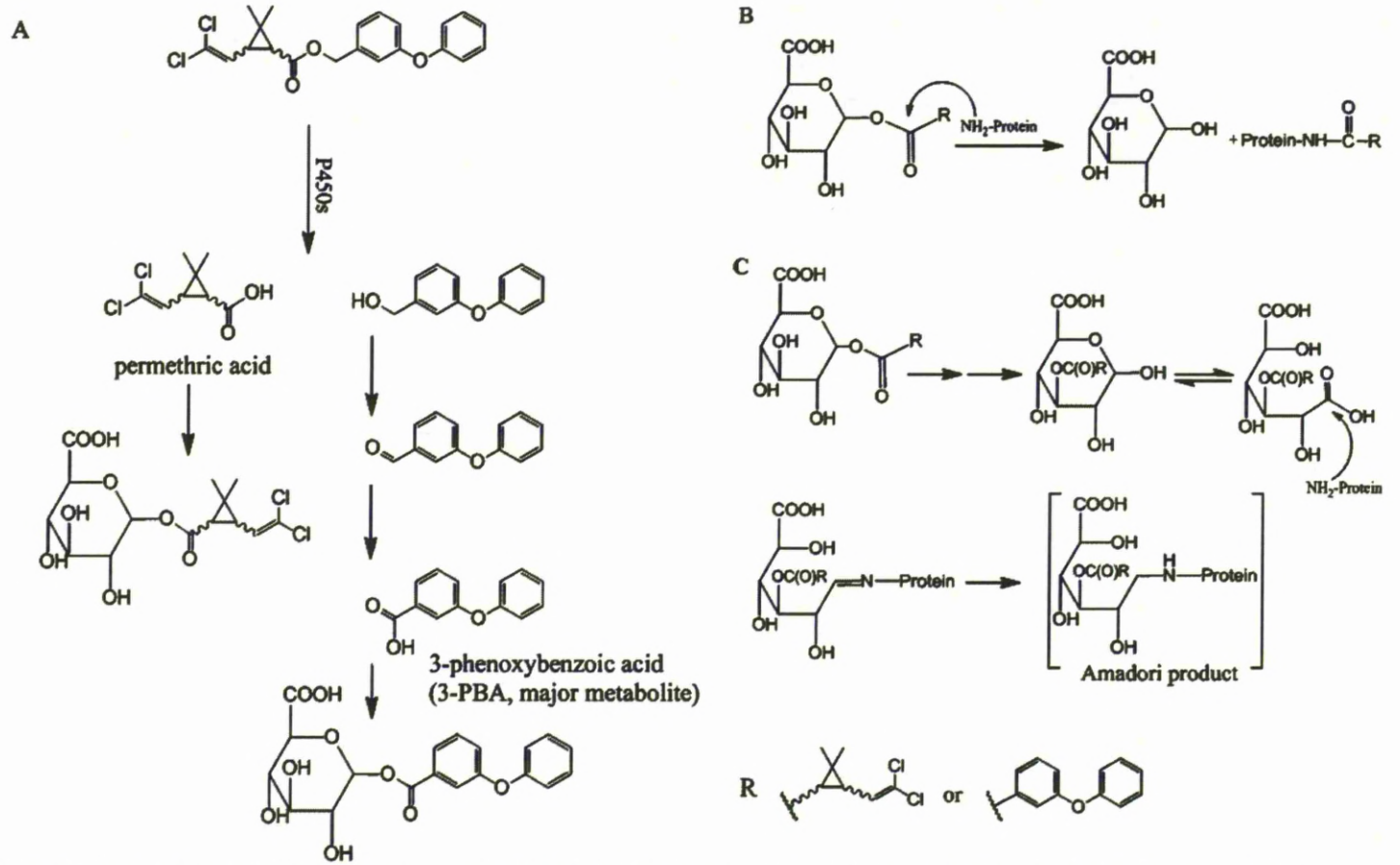

Figure 5.13. Metabolism of permethrin in mammals which leads to protein adducts. (A) metabolism of permethrin in mammals. Adduct formation of acylglucuroindes with proteins by means of the transacylation mechanism (B) (Noort *et al.*, 2008) or Amadori's rearrangement (C).

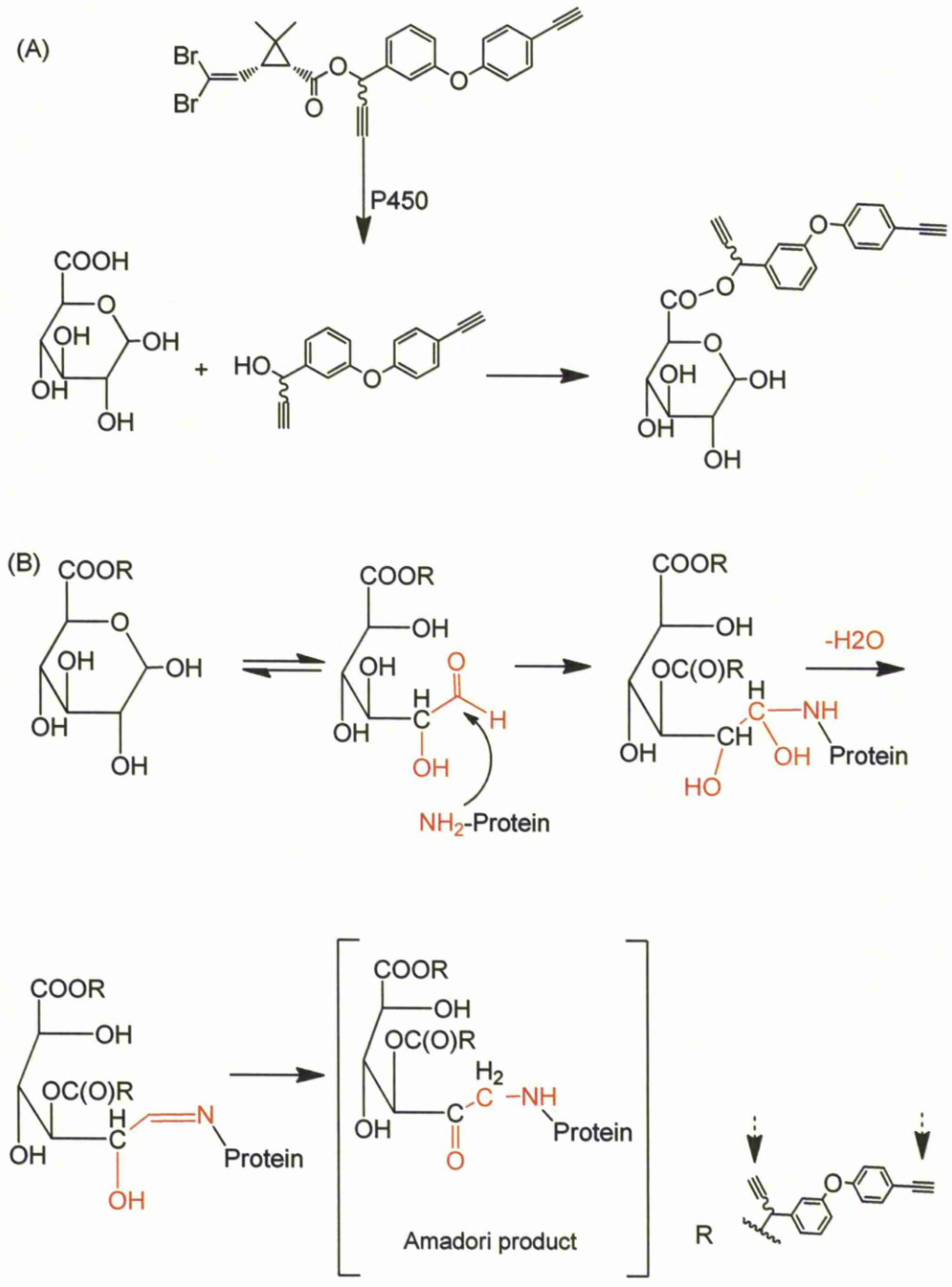

Figure 5.14. Postulated metabolism of probe 7RS in RLM that leads to UDP-glucuronosyltransferase adducts. (A) metabolism of P7RS in mammals. (B) Adduct formation of acylglucuroindes with proteins by means of the Amadori rearrangement, dashed arrows refer to free acetylene for click reaction.

5.4.Materials and methods

5.4.1. Chemicals and reagents

The pyrethroid ABPPs used are shown in Figure 5.15, Probe 1 (P1) a general P450 probe and the rhodamine biotin trifunctional azide were kindly provided by Cravatt's laboratory, Scripps Research Institute, USA. Biotin azide was kindly given by Professor Paul O` M Neill, Liverpool University. ß-Nicotinamide adenine dinucleotide phosphate, reduced form, tetrasodium salt (NADPH) were obtained from Melford, UK.

Luminescent P450 activity assays were performed in white 96-well plates (Thermo Fisher Scientifc, Hudson, NH) using the commercially available P450-Glo's substrate Luciferin-PPXE (Promega, Madison, WI). DMSO solvents were reagent grade Sigma Aldrich. The click chemistry ligand, tris [(1-benzyl-1H-1,2,3-triazol-4-yl)methyl]amine, was purchased from Sigma-Aldrich Chemical Co. (UK). Alexa Fluor® 488 azide was purchased from Invitrogen Company (UK).

5.4.2. Microsomes preparation

Rat liver microsomes: Rat liver microsomes prepared from male Wistar rats which had P450 contents 0.52 nmol/mg proteins measured by CO assay (Omura and Sato, 1964a) was kindly provided by Dr. Alison Shone, Molecular Biochemical Parasitology group, Liverpool School of Tropical Medicine, Liverpool, UK.

Mouse microsomes: Male mouse liver microsomes samples prepared from transgenic animals that have conditional deletions of liver CPR or *b5* along with normal mouse controls were kindly provided by Professor Roland Wolf, Biomedical Research Institute, University of Dundee (UK).

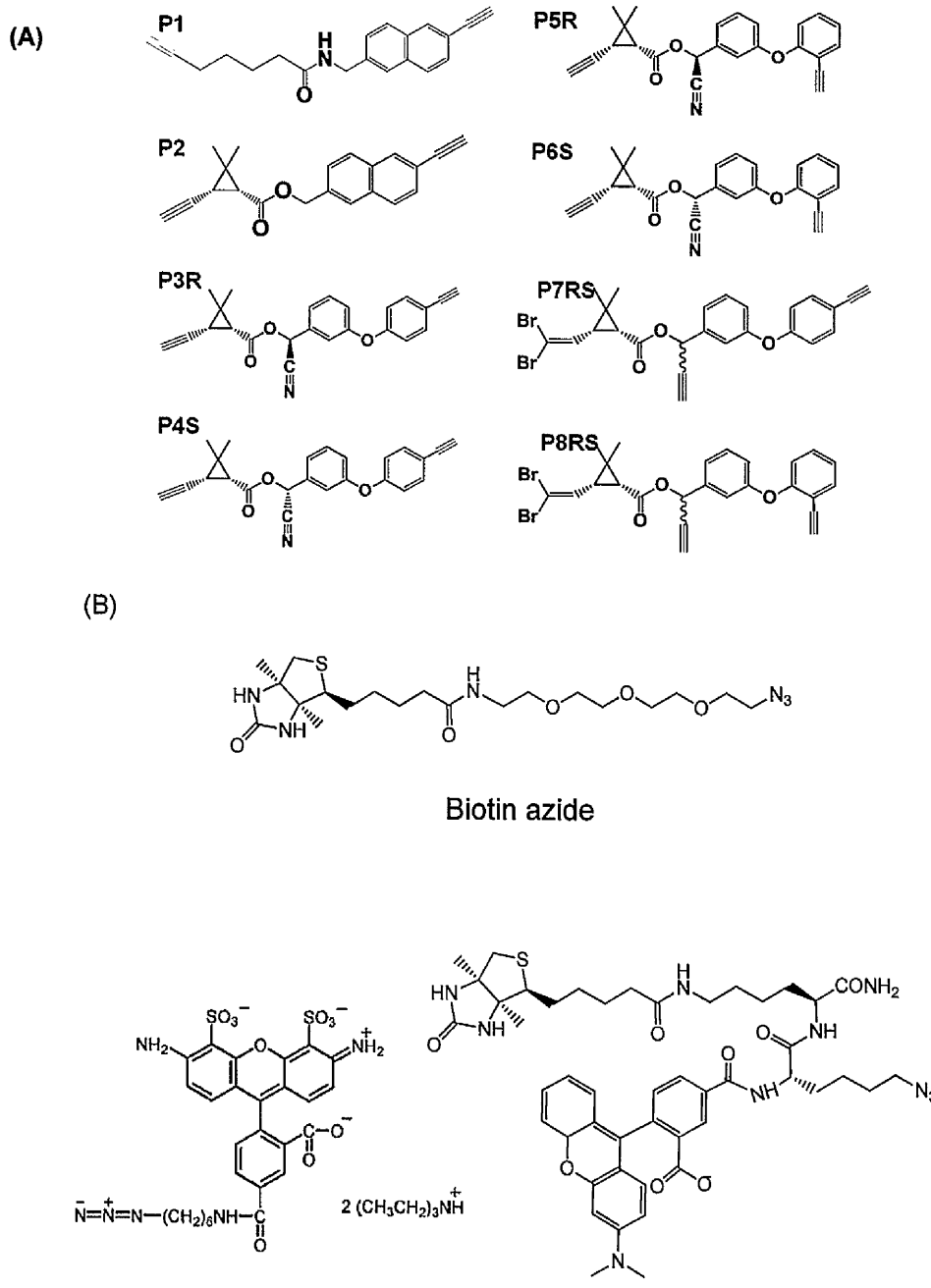

Figure 5.15. Chemical structures of pyrethroid ABPPs and Azide reporters. (A) Pyrethroid ABPPs shown were generated by including a reactive warhead (red acetylene) at a predicted primary site of oxidation, and a latent click handle (blue acetylene group) either in the middle replacing the alpha cyano group or at terminal position replacing bromine atoms. P1 is 2EN-ABPP, a generic positive control probe. R and S refer to pyrethroid enantiomer. (B) Copper based click reaction azide reporter used in detection and ABPP target pull-down.

Mosquito microsmes: Mosquito microsomes were prepared as described by Inceoglu *et al.* (Inceoglu *et al.*, 2009) with some modifications. Briefly: preparation of mosquitoes microsomes from adults (~200 individuals per colony) were done by removal of the heads to avoid enzyme inhibition from xanthommatin eye pigments (Schonbrod and Terriere, 1971).

Mosquitoes were treated with liquid nitrogen in a sieve ~2 mm mesh size. Small steel balls were gently shaken over the mosquitoes to fractionate their bodies and to separate the smaller heads, legs, wings parts from the joint abdominal-thoracic components. The thoracic abdominal complex was then washed with 3 ml of ice-cold homogenization buffer (HB: 0.1 M sodium phosphate (Sigma), pH 7.5, 1 mM phenylmethylsulphonyl fluoride (PMSF, sigma), 0.1 mM dithiothreitol (DTT, Invitrogen), and 1 mM 1-phenyl-2-thiourea (PTU, Sigma). The PMSF and PTU were dissolved in ethanol and added to the HB such that concentration of ethanol never exceeded 1% (vol:vol) of the total buffer volume, filtered and re-suspended in 10 ml of HB. The microsomes were prepared by homogenization of the complex by 40-ml glass Dounce homogenizer with a loose B pestle (Wheaton Science, Millville, NJ). The separation of the homogenate into cytosolic and microsomal extracts was done with centrifugation steps at 4° C. The initial centrifugation was performed at 10,000 *xg* for 15 min to remove insoluble debris. A second centrifugation at 100,000 x*g* for 1 h was performed to pellet the microsomes. The microsomal pellet was resuspended in 500 µl of ice-cold resuspension buffer (HB without PTU but contains 20% glycerol). Protein concentration was measured in triplicate by the Bradford method (Bradford, 1976) with Bio-Rad reagents using bovine serum albumin as a protein standard.

5.4.3. Western blot detection

Stock solutions were made of ABPP probes (P1, P2, P3R, P4S, P5R, P6S, P7RS and P8RS) in DMSO (20 mM), $CuSO_4$ in water (50 mM), Tris(2-carboxyethyl)phosphine hydrochloride (TCEP) in water (50 mM), and Tris-triazolyl ligand (TBTA) (1.7mM in 4:1 *t*-butanol: DMSO). Recombinant CYP6P3 normalised to 0.2 μM in Dulbecco Phosphate Buffer Saline pH 7.4 (D-PBS obtained from Invitrogen) and treated with pyrethroid ABPP probe **2** at 10 μM in presence and absence of 1 mM NADPH (Sigma). Samples were incubated at 37°C for 1 hr, and, 44 μl of sample transferred to a clean eppendorf tube for tag (biotin azide reporter) treatment.

In accordance with click chemistry (CC) conditions optimized by Speers and Cravatt (Speers and Cravatt, 2004b) samples were treated with 1μl of biotin-azide (2.5 mM stock in DMSO) followed by 1 μl of freshly prepared TCEP (50mM stock in water) and 3.3μl of ligand (1.7 mM stock in DMSO:t-butanol 1:4) giving a t-butanol concentration of 5%. Samples were gently vortexed and 1μl of $CuSO_4$ (50mM stock in water) were added. Each sample was gently vortexed and allowed to react at room temperature for 1 hr in the dark with regular vortexing every 15 min. The reaction was quenched by addition of 200 μl of cold methanol. Then samples were briefly centrifuged (5900g, 4 min at 4°C) to pellet the precipitated protein and remove excess reagents. The supernatant was discarded and 50 μl (1 volume) of D-PBS and 50 μl (1 volume) of standard 2x SDS-PAGE loading buffer (reducing) were added to the protein pellet. Samples were sonicated to solubilise the proteins and heated for 8 min at 90° C. Proteins were then separated by SDS-PAGE (~30 μg of protein/gel lane) and

transferred by electro blotting (semi dried) onto nitrocellulose membranes. Membrane was blocked in phosphate buffer saline (TPBS) with 1% Tween and 3% (wt per vol) bovine serum albumin (Sigma) fraction V, either 1 h at 25°C or overnight at 4°C. The blot was washed three times with washing buffer (0.1% TPBS). Then the blot was treated with an avidin-horseradish peroxidase conjugate (1:10000 dilutions) in TPBS with 1% BSA for 1 hr at 25°C. Thereafter the blot was washed with TPBS three times (10 min wash), treated with SuperSignal West Pico chemiluminescent substrate (Pierce, UK), and exposed to film for 0.1 to 15 min before development. The relative amounts of pyrethroid probe-biotin labelling were estimated by film densitometry.

5.4.4. Labelling of P450 enzymes by pyrethroid ABPP probes

Recombinant P450 proteomes CYP6P3, CYP6M2 and CYP6Z2 were normalised to 0.2 μM in D-PBS pH 7.4 and treated with ABPPs at 20 μM in the presence and absence of 1 mM NADPH. Samples were incubated at 37°C for 1 hr. Thereafter, 44 μl of sample was transferred to a clean eppendorf tube for reporter addition (Alexa Fluor® 488 azide reporter 0.5 μl of a 5 mM stock solution in DMSO). Following addition of reporter the click chemistry (CC) reaction was proceeded with conditions optimized by Speers and Cravatt(Speers and Cravatt, 2004b) mentioned above. Following the addition of CC reagents samples were vortexed and left at room temperature in the dark for 1 hr, at which time 2x SDS-PAGE loading buffer (reducing) was added to each reaction. The samples were heated at 90° C for 8 min and then 30 μl per well loaded onto gels NuPAGE® Novex 4-12% Bis-Tris Gel (Invitrogen, UK). After electrophoresis, gels were rinsed in a destain solution (5:4:1 water/methanol/acetic acid) overnight (in the dark), and fluorescence intensities were

measured by using Ettan DIGE Laser imager (GE Healthcare) at CY2 filter. Equal protein loading was confirmed by using Gel code Blue® Coomassie stain (Pierce, UK).

5.4.5. Identification of deltamethrin like ABPP targets in rat liver microsomes.

Liver microsomal proteome samples (1 ml of 2 mg/ml protein in PBS) were treated with either probe 3 or 7RS (10 GM, 2.0 GL of a stock solution in DMSO) in the presence or absence of 1 mM NADPH. The samples were incubated at 37° C for 45 min and then treated with a trifunctional azido biotin-rhodamine reporter group (4.0 µl of a 5 mM stock solution in DMSO) followed by vortexing. Click reaction was preceded by addition of CC's regents as mentioned in previous sections and left at room temperature in the dark for 1 h. Following the click reaction incubation probe labelled proteins was enriched according to Wright and Cravatt (Wright and Cravatt, 2007) using streptavidin agarose beads. Briefly, samples were centrifuged (5,900 xg, 4 min, 4° C) to pellet the protein. The supernatant was discarded and cold methanol (0.40 ml) was added to the pellets and the proteins were resuspended by sonication (3-5 s) and then rotated (10 min, 4°C). The centrifugation step was repeated, the supernatant discarded, and methanol (0.40 ml) was added to the pellets and the proteins were resuspended by sonication (3-5 s) and then rotated (10 min, 4° C) once again. The samples were pelleted by centrifugation once more, and the supernatant discarded. PBS (1.0 ml) containing SDS (1.2%) was added to the pellets and subsequently resuspended by sonication (3-5 sec). The samples were heated at 90° C for 8 min and then cooled to room temperature. Proteins were then enriched by rotating samples (1.5 h) with streptavidin-agarose beads (0.1 ml suspension solution) in a PBS media diluted to 0.2% SDS. The PBS media was removed and the beads were rinsed with 0.2% SDS

in PBS (1.5 ml, 3x), urea (6.0 M, 1.5 ml, 3x), and PBS buffer (1.5 ml, 3x). SDS-PAGE loading buffer (2x, reducing, 50µl) was added to the beads and heated at 90° C for 8 min. The samples (35 µl) were loaded onto SDS-PAGE gels and separated. Gels were imaged onto Ettan DIGE Laser imager (GE Healthcare) at CY3 filter to determine the labelling in presence and absence of NADPH. Following imaging, the gel coomassie stained using Gel code Blue® Coomassie stain (Pierce, UK). The darkly stained bands from 48-55 kDa were excised with a razorblade and diced into small cubes.

The gel pieces were washed with water and sent to finger prints proteomic facilities lab, Dundee University, UK (http://proteomics.lifesci.dundee.ac.uk/rates.html) for trypsin digestion and nLC-MS/MS analysis.

6. Final discussion

Novel tools and research methods that enable the direct and selective identification of the P450s active in insecticide metabolism and therefore linked to resistance at a mechanistic level was the major objectives of this PhD project. To achieve this goal we designed and synthesised pyrethroid mimetic ABPP probes following rational design approach. This approach recently, proved enormous befit towards designing selective and potent inhibitor for Fatty acid amide hydrolase (FAAH) in which can be directed to develop ABPP for FAAH (Ahn *et al.*, 2009; Alexander and Cravatt, 2005).

6.1.Investigating mechanism-based inhibition of P450s by selected arylalkynes

Certain arylalkynes, i.e. 1EPh, 4EBi, 2EMe, 2POX and 4EDF, were selected for their structure similarity with alcohol moieties in deltamethrin, bifenthrin and other pyrethroid recommended for ITNs treatment by WHOPES (Figure 1.4, Chapter 1). Their ability to act as MBI was used as an indication of their ABPP capacity. While the rigid biphenyl structure like 4-EBi proved a MBI for RLM (Foroozesh *et al.*, 1997), flexible arylalkyne like 1EPh has not been examined before for MBI against P450. The most important observation is that flexible structures, i.e. 1EPh, 2POX and 2EMe, showed significant MBI for RLM and NADPH dependent inhibition for CYP6P3. This result draws attention to the size and shape of the molecule being important parameters for inactivation of pyrethroid metaboliser CYP6P3. 1EPh in particular proved interesting because this contains a phenoxybenzene moiety commonly found in pyrethroid and ethynyl group substituted at the primary site of oxidation by P450s (*para* position) (Stevenson *et al.*, 2011).

6.2.Rational design of pyrethroid ABPPs

The rigidity of arylalkyne seemed to play an important role in directing the molecule in CYP6P3 active site for oxidation leading to MBI for P450. Therefore, to further confirm this hypothesis and get an insight into the MBI of pyrethroid molecules bearing an arylalkyne moiety, the MBI inhibition of CYP6P3 was examined using composite deltamethrin and bifenthrin analogues containing 2POX and 4-EBi (Chapter 3). In general deltamethrin and bifenthrin analogues containing 2POX further confirmed NADPH dependent inhibition for CYP6P3 including C3 and C4, against those with a rigid arylalkyne moiety (4EBi) that did not. However, spectroscopic analysis and HPLC metabolism profiles of C3 and C4 showed these compounds to be substrates (rapidly degraded in many metabolites) for CYP6P3 (Figure 3.2 and Fig.3.3 Chapter 3). This paradoxical observation can be explained if NADPH dependent inhibition was due to irreversible binding of metabolites rather than the parent compounds. This is further supported by the fact that P450s can attack multiple sites on the same substrate and therefore produce multiple metabolites (Stevenson *et al.*, 2011). The metabolites observed by HPLC warrants further investigation, although the complexity of CYP6P3 inactivation diminishes the opportunity for further using C3 and C4 compounds as templates for activity based protein profiling probes design.

6.3.In *silico* prediction of pyrethroid inhibitors binding to CYP6P3

In *silico* modelling study has provide a useful approach in predicting drug-P450 interaction (McLaughlin *et al.*, 2005). A homology model of CYP2D6, together with molecular docking techniques has been utilised earlier to perform in *silico* screen for inhibitor binding to CYP2D6 and to inform the possible sites of drug metabolism by P450 (McLaughlin *et al.*, 2005; Yu *et al.*, 2006). Here, the available CYP6P3

homology model (Stevenson *et al.*, 2011) was also used to help predict the key pyrethroid–active site interactions, and indicates on how the molecule might be oriented in the CYP6P3 active site allowing enzyme inactivation and labelling.

Initially, inhibitor docking calculations suggested that the length of the alcohol group in both C3 and C4 is likely to influence binding posture in a more favourable position for the metabolism at ester bond. This representation suggest that using phenoxybenzyl moiety based aryl alkyne such as (IEPh) to design the pyrethroid ABPP may be the most favourable choice to help enhance the probe binding in modes that would allow for metabolism at the alcohol side of the molecule. Therefore, a number of novel pyrethroid ABPP probes were designed based on the 1EPh analogues or propargyl ether (2POX) (Figure 3.5).

These compounds were based on the chemical scaffold of deltamethrin, with modifications on the terminal bromine atom end or the middle alpha cyano group to provide an acetylene group for the click handle. Docking calculations with the CYP6P3 structural model predicted that those probes containing a phenoxybenzyl moiety were most likely to have high affinity binding in a relevant orientation for oxidation leading to irreversible inhibition. Pyrethroid ABPPs that contain bromine atoms were predicted to have higher binding affinity comparable to non halogenated probes. All compounds designed based on phenoxybenzyl moiety were taken forward and synthesised as illustrated and discussed in chapter 4.

6.4.Pyrethroid ABPP probes validation

6.4.1. Identification of P450s metabolise deltamethrin using deltamethrin like ABPP probe (P7RS)

Comparative profiling study of the synthesised pyrethroid ABPP probes was carried out against *An. gambiae* recombinant P450s in association with pyrethroid resistance including CYP6P3, CYP6M2 and CYP6Z2. We pursued this study to confirm that P450s were legitimate targets of the novel pyrethroid ABPPs, and to identify probes that selectively label P450 pyrethroid metabolisers in an activity-based manner. The probe library was reactive against P450s and demonstrated mechanistic labelling of recombinant P450s, albeit with variable selectivity and specificity (Figure 5.5). Cytochrome P450s involved in pyrethroid metabolism, CYP6M2 and CYP6P3, were broadly labelled by the pyrethroid ABPPs, whereas the non pyrethroid metaboliser CYP6Z2 displayed more limited labelling. However, all pyrethroid ABPPs that lacked bromine atoms (P3R, P4S, P5R and P6S) displayed lower or minimal probe labelling in comparison with bromine containing P7RS and P8RS. This suggests the importance of the halogen molecules in P450 active site recognition, consistent with modelling predictions (Chapter 3). Furthermore, probes P3R and P7RS which contains acetylene group at *para* position of phenoxybenzyl moiety (4` position) appeared to favour the labelling of the pyrethroid metabolisers CYP6P3 and CYP6M2. This is consistent with *para* hydroxylation being the major site of metabolism by these P450s (Stevenson *et al.*, 2011), validating the positioning of the acetylene 'warhead'. The deltamethrin like probe P7RS in particular showed selective and strong labelling of CYP6P3 and CYP6M2 consistent with their role in pyrethroid metabolism (Müller *et al.*, 2008; Stevenson *et al.*, 2011).

6.4.2. In vitro labelling of P450s from different species

When tested against rodent and mosquito microsomes, pyrethroid ABPPs demonstrated a broad range of potential applications in the functional characterisation of P450 activities from different biological samples i.e. they labelled P450 sized bands across species.

Cytochrome P450 enzymes requires the transfer of two electrons from cytochrome P450 reductase (Farooq and Roberts, 2010; Meunier *et al.*, 2004; Omura and Sato, 1964b; Paine *et al.*, 2005). These electrons are donated by NADPH; therefore, the catalytic activity of P450s is NADPH and CPR dependent. Thus conditional deletion of CPR in mouse was used as an additional control to further confirm the mechanistic labelling of P450 by P7RS and P8RS. Liver-specific knockout of the essential electron transfer protein (CPR) resulting in essentially complete abolition of hepatic microsomal P450 activity consistent with CPR's role in P450s activity was successfully measured upon using probes P7RS and P8RS. In addition, mouse liver microsomes that has conditional deletion of *b5* was greatly affected labelling intensity obtained with either P7RS or P8RS..

6.4.3. Pyrethroid ABPP labeling of rat liver microsomes

An affinity purification and enrichment of non induced rat liver P450 using probe P7RS, further proved the mechanistic labelling of P7RS for P450s where only NADPH dependent band presented either before or after affinity purification. Additionally, the LC-MS/MS analysis for trypsin digested NADPH dependent band were identified many P450s proteins. However P7RS also shows the capability to label enzymes belonged to phase I and phase II detoxification enzyme super families. The

P450s constituted about 85% of the enzymes identified, while the major two abundant enzymes detected were CYP2C11 and an orthlogues of human CYP2C19. The CYP2C11 and CYP2C19 are both known to mediate pyrethroid metabolism and their role in metabolism of deltamethrin are well characterised and confirmed (Godin *et al.*, 2007; Godin *et al.*, 2006). Thus the major objective of the thesis has been achieved. It is also apparent that P7RS targets many P450s whose role in pyrethroid metabolism is not established, and it will be interesting in future to examine these further. More interesting perhaps was the fact that P7RS did not target only P450s. 16% of the proteins identified included flavin-containing monooxygenases (FMO), ALDH3a2, epoxide hydrolase and UDP-glucuronosyltransferase, which are also associated with detoxification. Of these, the most important enzyme in Phase II (conjugative) detoxification mechanism was UDP-glucuronosyltransferase, which represented 11% of the protein identified in this sample (Figure 5.14). These enzymes are known to catalyze the addition of the glucuronic acid moiety to xenobiotics which turn the molecule in hydrophilic form easy to be eliminated from body (King *et al.*, 2000). In summary the utilisation of probe P7RS has addressed three important points: first, P7RS has selectively identified directly P450s important in deltamethrin metabolism like CYP2C11. Second, this probe targets and identifies proteins with unknown function such LOC293989 where bioinformatics shows great structural similarity with pyrethroid metaboliser CYP2C6 (rat) and CYP2C19 (humane). Third, P7RS successfully identified proteins from other super family that involved in pyrethroid metabolism such as FMO3, Aldehyde dehydrogenase and UDP-glucuronosyltransferase.

6.5. Conclusion and perspectives

We developed a suite of novel pyrethroid ABPP that shows effectiveness in detection and identification of CYP enzymes functional activity in pyrethroid binding and metabolism either in recombinant or in native proteomic samples. These probes not only proved the capability for addressing the functional state of CYP enzymes but also proved its capability to selectively label and identify the essential enzymes in pyrethroid metabolism in hepatic microsomes from rat.

Due to low level of P450 content in mosquito's samples, gel based protein identification failed to identifyP450 bound probes purified from these samples although significant NADPH dependent labelling was observed after affinity purification (Figure 5.8, Chapter 5). New LC-MS/MS with high resolution in tandem with recently developed MudPIT-CC-ABPP (Jessani *et al.*, 2005; Speers and Cravatt, 2009) may provide a significant approach for future work to identify and quantify functional enzyme activity in samples such as mosquitoes with low P450s content. This method is not only quite desirable for identification of low content enzymes but also could be consolidated in single experiment to identify probe-site labelling which extend the application of pyrethroid ABPP beyond identifying essential enzymes to identify the catalytic residue in the active site. Identification of probe site labelling can be consolidated with genetics tools to map active site which may provide useful data to enhance the computational approaches like in *silico* models. For example identification of probe-site labelling could greatly help in identifying important single nucleotide polymorphism (SNP) changes that alters P450 enzyme activity in pyrethroid resistant strains. In other words, pyrethroid ABPP can be linked to computational modelling and site directed mutagenesis to map the P450 active site in order to determine the amino

acid residues have detrimental effect on substrate active site recognition and labelling. For example the comparative profiling study with probe 2 (Figure 5.3, chapter 5) has clearly confirmed the probe selectivity to bind CYP6P3. Therefore, this probe was taken forward in a pilot study in combination with molecular modelling, to systematically map the active site of CYP6 enzymes and to identify the residues involved in molecular recognition of the probe. The structure modelling was used to predict the binding mode of the probe that leads to irreversible binding and to predict the residues that discriminate probe labelling between the CYP6P3 and CYP6M2 enzyme. The predicted binding modes of probe 2 in CYP6P3 and CYP6M2 active site, represented steric differences between the active sites that may determine binding leads to effective metabolism (Figure 6.1). In CYP6M2 the Val_{372} projects into the active site in a position to cause clashes with the substrate, supported by two flanked proline residue Pro_{371} and Pro_{373} in substrate recognition site 5 (SRS5 backbone). Also, the model predicts the nucleophilic residue Thr_{318} in CYP6P3 as the possible target residue to react with the reactive species (ketene intermediate) to form a covalent adduct (Figure 6.1 and Scheme 6.1). Therefore the consideration was given to mutate and replace this residue with inactive threonine analogue 'alanine residue' using site directed mutagenesis to check its function in enzyme catalytic activity and probe labelling. Although the data obtained from gene sequencing of the mutant plasmid has been confirmed successful mutation but the functional expression of the mutant CYP6P3 was not successful. However, the bioinformatics study pointed out that this residue is quite conserved through panel of CYP enzymes including CYP3A4, CYP6M2, CYP6Z2 and CYP6P3, which may justify the importance of Thr_{318} in P450 structure stability.

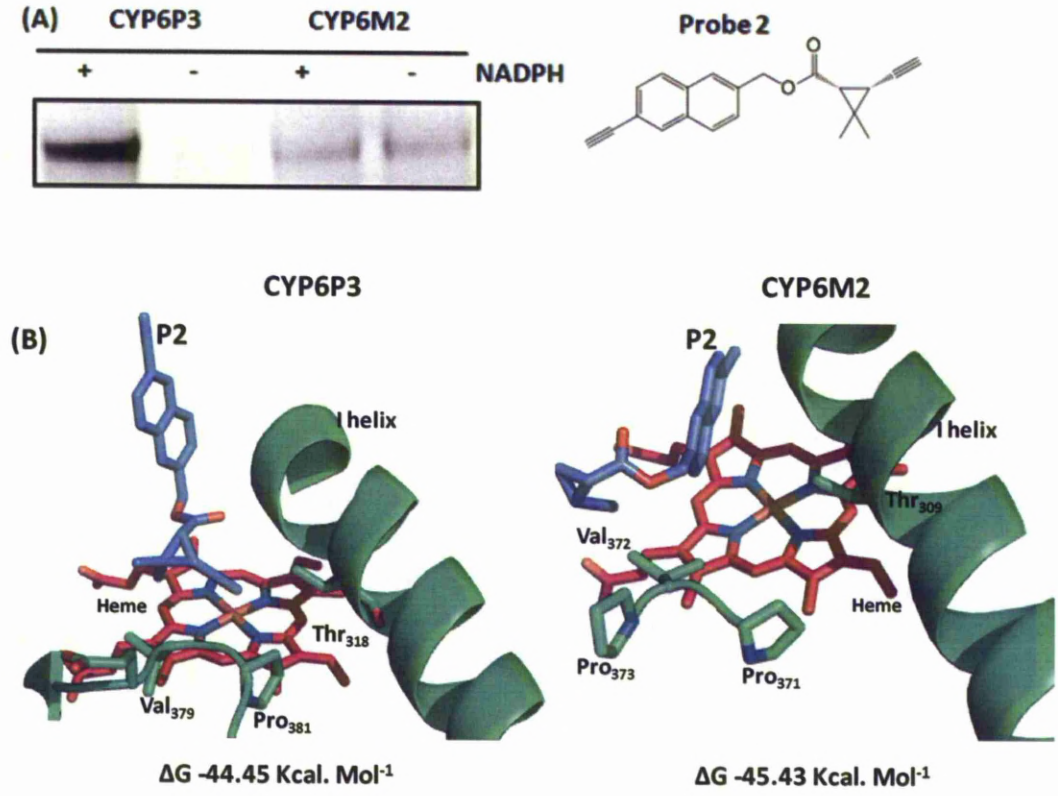

Figure 6.1. Selective labelling of 6P3 by type I pyrethroid mimic probe P2. (A) Labelling of 6P3 and 6M2 by pyrethroid ABPP (P2) (B) Molecular modelling showing the binding of P2 (violate stick) in the active site of CYP6P3 and CYP6M2. Probe 2 was docked into the active site of CYP6P3 and CYP6M2 using GOLD docking software as mentioned in material and method section (chapter 3). I-helix and the heme are shown in green ribbon and red stick for CYP6P3 and CYP6M2, respectively. Amino acid residue proposed to be targeted by ketene generated from oxidation of P2 leads to covalent adduct is shown in CYP6P3 and CYP6M2 models. Steric differences of the active site between CYP6M2 and CYP6P3 are illustrated by showing the binding site domain SRS5 of booth enzymes. In 6M2 the V_{372} projects into the active site in a position to cause clashes with the substrate, supported by to flanked prolines residue.

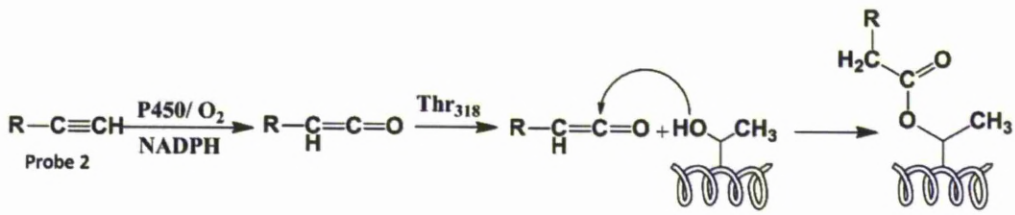

Scheme 6.1. Proposed mechanism for the formation of P2-protein adducts.

Further characterisation of other amino acid residues is being investigated to map the active site for amino acids essential in probe recognition and labelling. However, we believe that probe-site labelling identification using mass spectrometer will have a direct answer in such direction and provide more information for enhancing in *silico* modelling studies. In general the ABPP approach is quite amenable for being applied in different platforms and we envisage that this will encourage the wide use of pyrethroid ABPP in several research themes from structural and functional analysis to developing highly miniaturized protein microarray for measuring P450s activities in pyrethroid resistant and susceptible strains.

For example, since pyrethroid ABPPs are quite close to the structure of synthetic pyrethroids, utilising this approach in competitive inhibition screening of new compounds could afford high throughput tools for screening new synergists, and insecticides at molecular as well as cellular levels. This eventually will help in accelerating the development of selective and exceptionally active insecticides. Furthermore, the availability of high quality antibodies against a panel of mosquitoes P450s essential in pyrethroid metabolism could be devised to develop ABPP-microarray. Protein microarrays provide a novel approach of miniaturized platform of ABPP that can consolidate into single step the isolation, detection, and identification of probe labelled enzymes (Figure 1.15 Chapter 1) (Sieber et al., 2004). This system is expected to exhibit higher sensitivity and resolution than gel technology, sufficient to differentiate CYP enzymes activities between pyrethroid susceptible and resistant insects. In summary, P450-directed ABPs probes will have the potential to serve as

valuable research tools for the functional characterization of this large and diverse enzyme family and help in providing addressing answers to different controversial research themes like protein/protein interaction.

References

Adam, G.C., Burbaum, J., Kozarich, J.W., Patricelli, M.P. and Cravatt, B.F. (2004) Mapping enzyme active sites in complex proteomes. J Am Chem Soc 126, 1363-8.

Adam, G.C., Cravatt, B.F. and Sorensen, E.J. (2001) Profiling the specific reactivity of the proteome with non-directed activity-based probes. Chem Biol 8, 81-95.

Adam, G.C., Sorensen, E.J. and Cravatt, B.F. (2002a) Chemical strategies for functional proteomics. Mol Cell Proteomics 1, 781-90.

Adam, G.C., Sorensen, E.J. and Cravatt, B.F. (2002b) Proteomic profiling of mechanistically distinct enzyme classes using a common chemotype. Nat Biotechnol 20, 805-9.

Adam, G.C., Sorensen, E.J. and Cravatt, B.F. (2002c) Trifunctional chemical probes for the consolidated detection and identification of enzyme activities from complex proteomes. Mol Cell Proteomics 1, 828-35.

Agard, N.J., Prescher, J.A. and Bertozzi, C.R. (2004) A strain-promoted [3 + 2] azide-alkyne cycloaddition for covalent modification of biomolecules in living systems. J Am Chem Soc 126, 15046-7.

Aguiar, M., Masse, R. and Gibbs, B.F. (2005) Regulation of cytochrome P450 by posttranslational modification. Drug Metab Rev 37, 379-404.

Ahn, K., Johnson, D.S., Mileni, M., Beidler, D., Long, J.Z., McKinney, M.K., Weerapana, E., Sadagopan, N., Liimatta, M., Smith, S.E., Lazerwith, S., Stiff, C., Kamtekar, S., Bhattacharya, K., Zhang, Y., Swaney, S., Van Becelaere, K., Stevens, R.C. and Cravatt, B.F. (2009) Discovery and characterization of a highly selective FAAH inhibitor that reduces inflammatory pain. Chem Biol 16, 411-20.

Albericio, F., Kneib-Cordonier, N., Biancalana, S., Gera, L., Masada, R.I., Hudson, D. and Barany, G. (1990) Preparation and application of the 5-(4-(9-fluorenylmethyloxycarbonyl)aminomethyl-3,5-dimethoxyphenoxy)-valeric acid (PAL) handle for the solid-phase synthesis of C-terminal peptide amides under mild conditions. The Journal of Organic Chemistry 55, 3730-3743.

Alexander, J.P. and Cravatt, B.F. (2005) Mechanism of carbamate inactivation of FAAH: implications for the design of covalent inhibitors and in vivo functional probes for enzymes. Chem Biol 12, 1179-87.

Anand, S.S., Bruckner, J.V., Haines, W.T., Muralidhara, S., Fisher, J.W. and Padilla, S. (2006a) Characterization of deltamethrin metabolism by rat plasma and liver microsomes. Toxicol Appl Pharmacol 212, 156-66.

Anand, S.S., Kim, K.B., Padilla, S., Muralidhara, S., Kim, H.J., Fisher, J.W. and Bruckner, J.V. (2006b) Ontogeny of hepatic and plasma metabolism of deltamethrin in vitro: role in age-dependent acute neurotoxicity. Drug Metab Dispos 34, 389-97.

Atieli, F.K., Munga, S.O., Ofulla, A.V. and Vulule, J.M. (2010) The effect of repeated washing of long-lasting insecticide-treated nets (LLINs) on the feeding success and survival rates of Anopheles gambiae. Malar J 9, 304.

Baskin, J.M., Prescher, J.A., Laughlin, S.T., Agard, N.J., Chang, P.V., Miller, I.A., Lo, A., Codelli, J.A. and Bertozzi, C.R. (2007) Copper-free click chemistry for dynamic in vivo imaging. Proc Natl Acad Sci U S A 104, 16793-7.

Bayburt, T.H. and Sligar, S.G. (2002) Single-molecule height measurements on microsomal cytochrome P450 in nanometer-scale phospholipid bilayer disks. Proc Natl Acad Sci U S A 99, 6725-30.

Beier, J.C., Keating, J., Githure, J.I., Macdonald, M.B., Impoinvil, D.E. and Novak, R.J. (2008) Integrated vector management for malaria control. Malar J 7 Suppl 1, S4.

Berge, J.B., Feyereisen, R. and Amichot, M. (1998) Cytochrome P450 monooxygenases and insecticide resistance in insects. Philos Trans R Soc Lond B Biol Sci 353, 1701-5.

Birner-Gruenberger, R. and Hermetter, A. (2007) Activity-based proteomics of lipolytic enzymes. Curr Drug Discov Technol 4, 1-11.

Bock, P.E. (1992a) Active-site-selective labeling of blood coagulation proteinases with fluorescence probes by the use of thioester peptide chloromethyl ketones. I. Specificity of thrombin labeling. J Biol Chem 267, 14963-73.

Bock, P.E. (1992b) Active-site-selective labeling of blood coagulation proteinases with fluorescence probes by the use of thioester peptide chloromethyl ketones. II. Properties of thrombin derivatives as reporters of prothrombin fragment 2 binding and specificity of the labeling approach for other proteinases. J Biol Chem 267, 14974-81.

Bogyo, M., McMaster, J.S., Gaczynska, M., Tortorella, D., Goldberg, A.L. and Ploegh, H. (1997) Covalent modification of the active site threonine of proteasomal beta subunits and the Escherichia coli homolog HslV by a new class of inhibitors. Proc Natl Acad Sci U S A 94, 6629-34.

Bogyo, M., Verhelst, S., Bellingard-Dubouchaud, V., Toba, S. and Greenbaum, D. (2000) Selective targeting of lysosomal cysteine proteases with radiolabeled electrophilic substrate analogs. Chem Biol 7, 27-38.

Boonsuepsakul, S., Luepromchai, E. and Rongnoparut, P. (2008) Characterization of Anopheles minimus CYP6AA3 expressed in a recombinant baculovirus system. Arch Insect Biochem Physiol 69, 13-21.

Bradford, M.M. (1976) A rapid and sensitive method for the quantitation of microgram quantities of protein utilizing the principle of protein-dye binding. Anal Biochem 72, 248-54.

Brandling-Bennett, A.D. and Penheiro, F. (1996) Infectious diseases in Latin America and the Caribbean: are they really emerging and increasing? Emerg Infect Dis 2, 59-61.

Briseno-Garcia, B., Gomez-Dantes, H., Argott-Ramirez, E., Montesano, R., Vazquez-Martinez, A.L., Ibanez-Bernal, S., Madrigal-Ayala, G., Ruiz-Matus, C., Flisser, A. and Tapia-Conyer, R. (1996) Potential risk for dengue hemorrhagic fever: the isolation of serotype dengue-3 in Mexico. Emerg Infect Dis 2, 133-5.

Brooke, B.D., Kloke, G., Hunt, R.H., Koekemoer, L.L., Temu, E.A., Taylor, M.E., Small, G., Hemingway, J. and Coetzee, M. (2001) Bioassay and biochemical analyses of insecticide resistance in southern African Anopheles funestus (Diptera: Culicidae). Bull Entomol Res 91, 265-72.

Brown, T.M., Bryson, P.K. and Payne, G.T. (1996) Synergism by Propynyl Aryl Ethers in Permethrin-Resistant Tobacco Budworm Larvae, Heliothis virescens. Pesticide Science 46, 323-331.

Busvine, J.R. (1951) Mechanism of resistance to insecticide in houseflies. Nature 168, 193-5.

Chandre, F., Darriet, F., Duchon, S., Finot, L., Manguin, S., Carnevale, P. and Guillet, P. (2000) Modifications of pyrethroid effects associated with kdr mutation in Anopheles gambiae. Med Vet Entomol 14, 81-8.

Chen, E.I., Hewel, J., Felding-Habermann, B. and Yates, J.R., 3rd (2006) Large scale protein profiling by combination of protein fractionation and multidimensional protein identification technology (MudPIT). Mol Cell Proteomics 5, 53-6.

Chiu, T.L., Wen, Z., Rupasinghe, S.G. and Schuler, M.A. (2008) Comparative molecular modeling of Anopheles gambiae CYP6Z1, a mosquito P450 capable of metabolizing DDT. Proc Natl Acad Sci U S A 105, 8855-60.

Codelli, J.A., Baskin, J.M., Agard, N.J. and Bertozzi, C.R. (2008) Second-generation difluorinated cyclooctynes for copper-free click chemistry. J Am Chem Soc 130, 11486-93.

Cox-Singh, J., Hiu, J., Lucas, S.B., Divis, P.C., Zulkarnaen, M., Chandran, P., Wong, K.T., Adem, P., Zaki, S.R., Singh, B. and Krishna, S. (2010) Severe malaria - a case of fatal Plasmodium knowlesi infection with post-mortem findings: a case report. Malar J 9, 10.

Cox-Singh, J. and Singh, B. (2008) Knowlesi malaria: newly emergent and of public health importance? Trends Parasitol 24, 406-10.

Cravatt, B.F., Wright, A.T. and Kozarich, J.W. (2008) Activity-based protein profiling: from enzyme chemistry to proteomic chemistry. Annu Rev Biochem 77, 383-414.

Croom, E.L., Wallace, A.D. and Hodgson, E. (2010) Human variation in CYP-specific chlorpyrifos metabolism. Toxicology 276, 184-91.

Das, P.K., Das, L.K., Parida, S.K., Patra, K.P. and Jambulingam, P. (1993) Lambdacyhalothrin treated bed nets as an alternative method of malaria control in tribal villages of Koraput District, Orissa State, India. Southeast Asian J Trop Med Public Health 24, 513-21.

David, J.-P., Strode, C., Vontas, J., Nikou, D., Vaughan, A., Pignatelli, P.M., Louis, C., Hemingway, J. and Ranson, H. (2005a) The Anopheles gambiae detoxification

chip: A highly specific microarray to study metabolic-based insecticide resistance in malaria vectors. Proceedings of the National Academy of Sciences of the United States of America 102, 4080-4084.

David, J.P., Strode, C., Vontas, J., Nikou, D., Vaughan, A., Pignatelli, P.M., Louis, C., Hemingway, J. and Ranson, H. (2005b) The Anopheles gambiae detoxification chip: a highly specific microarray to study metabolic-based insecticide resistance in malaria vectors. Proc Natl Acad Sci U S A 102, 4080-4.

Deigner, H.P., Kinscherf, R., Claus, R., Fyrnys, B., Blencowe, C. and Hermetter, A. (1999) Novel reversible, irreversible and fluorescent inhibitors of platelet-activating factor acetylhydrolase as mechanistic probes. Atherosclerosis 144, 79-90.

Deussen, H.J., Danielsen, S., Breinholt, J. and Borchert, T.V. (2000) Design and synthesis of triglyceride analogue biotinylated suicide inhibitors for directed molecular evolution of lipolytic enzymes. Bioorg Med Chem Lett 10, 2027-31.

Djegbe, I., Cornelie, S., Rossignol, M., Demettre, E., Seveno, M., Remoue, F. and Corbel, V. (2011) Differential Expression of Salivary Proteins between Susceptible and Insecticide-Resistant Mosquitoes of Culex quinquefasciatus. PLoS One 6, e17496.

Djimde, A., Doumbo, O.K., Cortese, J.F., Kayentao, K., Doumbo, S., Diourte, Y., Dicko, A., Su, X.Z., Nomura, T., Fidock, D.A., Wellems, T.E., Plowe, C.V. and Coulibaly, D. (2001) A molecular marker for chloroquine-resistant falciparum malaria. N Engl J Med 344, 257-63.

Djouaka, R.F., Bakare, A.A., Coulibaly, O.N., Akogbeto, M.C., Ranson, H., Hemingway, J. and Strode, C. (2008) Expression of the cytochrome P450s, CYP6P3 and CYP6M2 are significantly elevated in multiple pyrethroid resistant populations of Anopheles gambiae s.s. from Southern Benin and Nigeria. BMC Genomics 9, 538.

Dolan, G., Terkuile, F.O., Jacoutot, V., White, N.J., Luxemburger, C., Malankirii, L., Chongsuphajaisiddhi, T. and Nosten, F. (1993) Bed Nets for the Prevention of Malaria and Anemia in Pregnancy. Transactions of the Royal Society of Tropical Medicine and Hygiene 87, 620-626.

Donato, M.T., Jimenez, N., Castell, J.V. and Gomez-Lechon, M.J. (2004) Fluorescence-based assays for screening nine cytochrome P450 (P450)

activities in intact cells expressing individual human P450 enzymes. Drug Metab Dispos 32, 699-706.

Elangovan, A., Wang, Y.H. and Ho, T.I. (2003) Sonogashira coupling reaction with diminished homocoupling. Org Lett 5, 1841-4.

Elliott, M., Farnham, A.W., Janes, N.F., Needham, P.H., Pulman, D.A. and Stevenson, J.H. (1973) A photostable pyrethroid. Nature 246, 169-70.

Etang, J., Chandre, F., Guillet, P. and Manga, L. (2004) Reduced bio-efficacy of permethrin EC impregnated bednets against an Anopheles gambiae strain with oxidase-based pyrethroid tolerance. Malar J 3, 46.

Evans, D.A., Katz, J.L. and West, T.R. (1998) Synthesis of diaryl ethers through the copper-promoted arylation of phenols with arylboronic acids. An expedient synthesis of thyroxine. Tetrahedron Letters 39, 2937-2940.

Farooq, Y. and Roberts, G.C. (2010) Kinetics of electron transfer between NADPH-cytochrome P450 reductase and cytochrome P450 3A4. Biochem J 432, 485-93.

Fellig, J., Barnes, J.R., Rachlin, A.I., O'Brien, J.P. and Focella, A. (1970) Substituted phenyl 2-propynyl ethers as carbamate synergists. Journal of Agricultural and Food Chemistry 18, 78-80.

Feyereisen, R. (1999) Insect P450 enzymes. Annu Rev Entomol 44, 507-33.

Fine, B.C. (1961) Pattern of pyrethrin-resistance in houseflies. Nature 191, 884-5.

Finn, R.D., McLaughlin, L.A., Ronseaux, S., Rosewell, I., Houston, J.B., Henderson, C.J. and Wolf, C.R. (2008) Defining the in Vivo Role for cytochrome b5 in cytochrome P450 function through the conditional hepatic deletion of microsomal cytochrome b5. J Biol Chem 283, 31385-93.

Florens, L., Washburn, M.P., Raine, J.D., Anthony, R.M., Grainger, M., Haynes, J.D., Moch, J.K., Muster, N., Sacci, J.B., Tabb, D.L., Witney, A.A., Wolters, D., Wu, Y., Gardner, M.J., Holder, A.A., Sinden, R.E., Yates, J.R. and Carucci, D.J. (2002) A proteomic view of the Plasmodium falciparum life cycle. Nature 419, 520-6.

Foroozesh, M., Primrose, G., Guo, Z., Bell, L.C., Alworth, W.L. and Guengerich, F.P. (1997) Aryl acetylenes as mechanism-based inhibitors of cytochrome P450-dependent monooxygenase enzymes. Chem Res Toxicol 10, 91-102.

Garrison, A.W. (2006) Probing the enantioselectivity of chiral pesticides. Environ Sci Technol 40, 16-23.

Gatei, W., Kariuki, S., Hawley, W., ter Kuile, F., Terlouw, D., Phillips-Howard, P., Nahlen, B., Gimnig, J., Lindblade, K., Walker, E., Hamel, M., Crawford, S., Williamson, J., Slutsker, L. and Shi, Y.P. (2010) Effects of transmission reduction by insecticide-treated bed nets (ITNs) on parasite genetics population structure: I. The genetic diversity of Plasmodium falciparum parasites by microsatellite markers in western Kenya. Malar J 9, 353.

Gibtner, T., Hampel, F., Gisselbrecht, J.P. and Hirsch, A. (2002) End-cap stabilized oligoynes: model compounds for the linear sp carbon allotrope carbyne. Chemistry 8, 408-32.

Godin, S.J., Crow, J.A., Scollon, E.J., Hughes, M.F., DeVito, M.J. and Ross, M.K. (2007) Identification of rat and human cytochrome p450 isoforms and a rat serum esterase that metabolize the pyrethroid insecticides deltamethrin and esfenvalerate. Drug Metab Dispos 35, 1664-71.

Godin, S.J., Scollon, E.J., Hughes, M.F., Potter, P.M., DeVito, M.J. and Ross, M.K. (2006) Species differences in the in vitro metabolism of deltamethrin and esfenvalerate: differential oxidative and hydrolytic metabolism by humans and rats. Drug Metab Dispos 34, 1764-71.

Grabarek, J. and Darzynkiewicz, Z. (2002) In situ activation of caspases and serine proteases during apoptosis detected by affinity labeling their enzyme active centers with fluorochrome-tagged inhibitors. Exp Hematol 30, 982-9.

Greenbaum, D.C., Arnold, W.D., Lu, F., Hayrapetian, L., Baruch, A., Krumrine, J., Toba, S., Chehade, K., Bromme, D., Kuntz, I.D. and Bogyo, M. (2002a) Small molecule affinity fingerprinting. A tool for enzyme family subclassification, target identification, and inhibitor design. Chem Biol 9, 1085-94.

Greenbaum, D.C., Baruch, A., Grainger, M., Bozdech, Z., Medzihradszky, K.F., Engel, J., DeRisi, J., Holder, A.A. and Bogyo, M. (2002b) A role for the protease falcipain 1 in host cell invasion by the human malaria parasite. Science 298, 2002-6.

Gubler, D.J. and Clark, G.G. (1995) Dengue/dengue hemorrhagic fever: the emergence of a global health problem. Emerg Infect Dis 1, 55-7.

Gygi, S.P., Rist, B., Gerber, S.A., Turecek, F., Gelb, M.H. and Aebersold, R. (1999) Quantitative analysis of complex protein mixtures using isotope-coded affinity tags. Nat Biotechnol 17, 994-9.

Hammons, G.J., Alworth, W.L., Hopkins, N.E., Guengerich, F.P. and Kadlubar, F.F. (1989) 2-ethynylnaphthalene as a mechanism-based inactivator of the cytochrome P-450 catalyzed N-oxidation of 2-naphthylamine. Chem Res Toxicol 2, 367-74.

He, K., Falick, A.M., Chen, B., Nilsson, F. and Correia, M.A. (1996) Identification of the heme adduct and an active site peptide modified during mechanism-based inactivation of rat liver cytochrome P450 2B1 by secobarbital. Chem Res Toxicol 9, 614-22.

Hemingway, J., Beaty, B.J., Rowland, M., Scott, T.W. and Sharp, B.L. (2006) The Innovative Vector Control Consortium: improved control of mosquito-borne diseases. Trends Parasitol 22, 308-12.

Hemingway, J., Field, L. and Vontas, J. (2002) An overview of insecticide resistance. Science 298, 96-7.

Hemingway, J. and Ranson, H. (2000) Insecticide resistance in insect vectors of human disease. Annu Rev Entomol 45, 371-91.

Hougard, J.M., Duchon, S., Darriet, F., Zaim, M., Rogier, C. and Guillet, P. (2003) Comparative performances, under laboratory conditions, of seven pyrethroid insecticides used for impregnation of mosquito nets. Bull World Health Organ 81, 324-33.

Huang, H., Stok, J.E., Stoutamire, D.W., Gee, S.J. and Hammock, B.D. (2005) Development of optically pure pyrethroid-like fluorescent substrates for carboxylesterases. Chem Res Toxicol 18, 516-27.

Inceoglu, A.B., Waite, T.D., Christiansen, J.A., McAbee, R.D., Kamita, S.G., Hammock, B.D. and Cornel, A.J. (2009) A rapid luminescent assay for measuring cytochrome P450 activity in individual larval Culex pipiens complex mosquitoes (Diptera: Culicidae). J Med Entomol 46, 83-92.

Ishihama, Y., Oda, Y., Tabata, T., Sato, T., Nagasu, T., Rappsilber, J. and Mann, M. (2005) Exponentially modified protein abundance index (emPAI) for estimation of absolute protein amount in proteomics by the number of sequenced peptides per protein. Mol Cell Proteomics 4, 1265-72.

Ishiyama, T., Murata, M. and Miyaura, N. (1995) Palladium(0)-Catalyzed Cross-Coupling Reaction of Alkoxydiboron with Haloarenes: A Direct Procedure for Arylboronic Esters. The Journal of Organic Chemistry 60, 7508-7510.

Jamjoom, G.A., Mahfouz, A.A., Badawi, I.A., Omar, M.S., al-Zoghaibi, O.S., al-Amari, O.M., Ibrahim, M. and Siam, I. (1994) Acceptability and usage of permethrin-impregnated mosquito bed nets in rural southwestern Saudi Arabia. Trop Geogr Med 46, 355-7.

Jan Gerrits, P., Zumbrägel, F. and Marcus, J. (2001) Analyzing the hydrocyanation reaction: chiral HPLC and the synthesis of racemic cyanohydrins. Tetrahedron 57, 8691-8698.

Jeffery, D.A. and Bogyo, M. (2003) Chemical proteomics and its application to drug discovery. Curr Opin Biotechnol 14, 87-95.

Jessani, N., Liu, Y., Humphrey, M. and Cravatt, B.F. (2002) Enzyme activity profiles of the secreted and membrane proteome that depict cancer cell invasiveness. Proc Natl Acad Sci U S A 99, 10335-40.

Jessani, N., Niessen, S., Wei, B.Q., Nicolau, M., Humphrey, M., Ji, Y., Han, W., Noh, D.Y., Yates, J.R., 3rd, Jeffrey, S.S. and Cravatt, B.F. (2005) A streamlined platform for high-content functional proteomics of primary human specimens. Nat Methods 2, 691-7.

Jin, T., Zeng, L., Lu, Y., Xu, Y. and Liang, G. (2010) Identification of resistance-responsive proteins in larvae of Bactrocera dorsalis (Hendel), for pyrethroid toxicity by a proteomic approach. Pesticide Biochemistry and Physiology 96, 1-7.

Jurat-Fuentes, J.L. and Adang, M.J. (2007) A proteomic approach to study Cry1Ac binding proteins and their alterations in resistant Heliothis virescens larvae. Journal of Invertebrate Pathology 95, 187-191.

Kalesh, K.A., Tan, L.P., Lu, K., Gao, L., Wang, J. and Yao, S.Q. (2010) Peptide-based activity-based probes (ABPs) for target-specific profiling of protein tyrosine phosphatases (PTPs). Chem Commun (Camb) 46, 589-91.

Kam, C.M., Abuelyaman, A.S., Li, Z., Hudig, D. and Powers, J.C. (1993) Biotinylated isocoumarins, new inhibitors and reagents for detection, localization, and isolation of serine proteases. Bioconjug Chem 4, 560-7.

Kaneko, H. (2011) Pyrethroids: Mammalian metabolism and toxicity. J Agric Food Chem 59, 2786-91.

Katsuda, Y. (1999) Development of and future prospects for pyrethroid chemistry. Pesticide Science 55, 775-782.

Kent, U.M., Juschyshyn, M.I. and Hollenberg, P.F. (2001) Mechanism-based inactivators as probes of cytochrome P450 structure and function. Curr Drug Metab 2, 215-43.

Kidd, D., Liu, Y. and Cravatt, B.F. (2001) Profiling serine hydrolase activities in complex proteomes. Biochemistry 40, 4005-15.

King, C.D., Rios, G.R., Green, M.D. and Tephly, T.R. (2000) UDP-glucuronosyltransferases. Curr Drug Metab 1, 143-61.

Kitz, R. and Wilson, I.B. (1962) Esters of methanesulfonic acid as irreversible inhibitors of acetylcholinesterase. J Biol Chem 237, 3245-9.

Korytko, P.J. and Scott, J.G. (1998) CYP6D1 protects thoracic ganglia of houseflies from the neurotoxic insecticide cypermethrin. Arch Insect Biochem Physiol 37, 57-63.

Krogstad, D.J. (1996) Malaria as a reemerging disease. Epidemiol Rev 18, 77-89.

Kumar, S., Zhou, B., Liang, F., Wang, W.Q., Huang, Z. and Zhang, Z.Y. (2004) Activity-based probes for protein tyrosine phosphatases. Proc Natl Acad Sci U S A 101, 7943-8.

Leake, D.W., Jr. and Hii, J.L. (1994) Observations of human behavior influencing the use of insecticide-impregnated bednets to control malaria in Sabah, Malaysia. Asia Pac J Public Health 7, 92-7.

Liu, N. and Scott, J.G. (1996) Genetic analysis of factors controlling high-level expression of cytochrome P450, CYP6D1, cytochrome b5, P450 reductase, and

monooxygenase activities in LPR house flies, Musca domestica. Biochem Genet 34, 133-48.

Liu, Y., Patricelli, M.P. and Cravatt, B.F. (1999) Activity-based protein profiling: the serine hydrolases. Proc Natl Acad Sci U S A 96, 14694-9.

Lo, L.C., Pang, T.L., Kuo, C.H., Chiang, Y.L., Wang, H.Y. and Lin, J.J. (2002) Design and synthesis of class-selective activity probes for protein tyrosine phosphatases. J Proteome Res 1, 35-40.

Luxemburger, C., McGready, R., Kham, A., Morison, L., Cho, T., Chongsuphajaisiddhi, T., White, N.J. and Nosten, F. (2001) Effects of malaria during pregnancy on infant mortality in an area of low malaria transmission. Am J Epidemiol 154, 459-65.

Martinez-Torres, D., Chandre, F., Williamson, M.S., Darriet, F., Berge, J.B., Devonshire, A.L., Guillet, P., Pasteur, N. and Pauron, D. (1998) Molecular characterization of pyrethroid knockdown resistance (kdr) in the major malaria vector Anopheles gambiae s.s. Insect Mol Biol 7, 179-84.

McAbee, R.D., Kang, K.D., Stanich, M.A., Christiansen, J.A., Wheelock, C.E., Inman, A.D., Hammock, B.D. and Cornel, A.J. (2004) Pyrethroid tolerance in Culex pipiens pipiens var molestus from Marin County, California. Pest Manag Sci 60, 359-68.

McLaughlin, L.A., Niazi, U., Bibby, J., David, J.P., Vontas, J., Hemingway, J., Ranson, H., Sutcliffe, M.J. and Paine, M.J. (2008) Characterization of inhibitors and substrates of Anopheles gambiae CYP6Z2. Insect Mol Biol 17, 125-35.

McLaughlin, L.A., Paine, M.J., Kemp, C.A., Marechal, J.D., Flanagan, J.U., Ward, C.J., Sutcliffe, M.J., Roberts, G.C. and Wolf, C.R. (2005) Why is quinidine an inhibitor of cytochrome P450 2D6? The role of key active-site residues in quinidine binding. J Biol Chem 280, 38617-24.

Meslin, F.X. (1997) Global aspects of emerging and potential zoonoses: a WHO perspective. Emerg Infect Dis 3, 223-8.

Metcalf, R.L., Fukuto, T.R., Wilkinson, C., Fahmy, M.H., El-Aziz, A.A. and Metcalf, E.R. (1966) Mode of Action of Carbamate Synergists. Journal of Agricultural and Food Chemistry 14, 555-562.

Meunier, B., de Visser, S.P. and Shaik, S. (2004) Mechanism of oxidation reactions catalyzed by cytochrome p450 enzymes. Chem Rev 104, 3947-80.

Morgan, J.C., Irving, H., Okedi, L.M., Steven, A. and Wondji, C.S. (2010) Pyrethroid resistance in an Anopheles funestus population from Uganda. PLoS One 5, e11872.

Morou, E., Dowd, A.J., Rajatileka, S., Steven, A., Hemingway, J., Ranson, H., Paine, M. and Vontas, J. (2010) A simple colorimetric assay for specific detection of glutathione-S transferase activity associated with DDT resistance in mosquitoes. PLoS Negl Trop Dis 4.

Müller, P., Warr, E., Stevenson, B.J., Pignatelli, P.M., Morgan, J.C., Steven, A., Yawson, A.E., Mitchell, S.N., Ranson, H., Hemingway, J., Paine, M.J.I. and Donnelly, M.J. (2008) Field-Caught Permethrin-Resistant *Anopheles gambiae* Overexpress CYP6P3, a P450 That Metabolises Pyrethroids. PLoS Genet 4, e1000286.

Muller, O., Quinones, M., Cham, K., Aikins, M. and Greenwood, B. (1994) Detecting Permethrin on Treated Bed Nets. Lancet 344, 1699-1700.

Muller, P., Donnelly, M.J. and Ranson, H. (2007) Transcription profiling of a recently colonised pyrethroid resistant Anopheles gambiae strain from Ghana. BMC Genomics 8, 36.

Muller, P., Warr, E., Stevenson, B.J., Pignatelli, P.M., Morgan, J.C., Steven, A., Yawson, A.E., Mitchell, S.N., Ranson, H., Hemingway, J., Paine, M.J. and Donnelly, M.J. (2008) Field-caught permethrin-resistant Anopheles gambiae overexpress CYP6P3, a P450 that metabolises pyrethroids. PLoS Genet 4, e1000286.

Murray, M. and Butler, A.M. (2004) Comparative inhibition of inducible and constitutive CYPs in rat hepatic microsomes by parathion. Xenobiotica 34, 723-39.

Nahlen, B.L., Clark, J.P. and Alnwick, D. (2003) Insecticide-treated bed nets. Am J Trop Med Hyg 68, 1-2.

Narahashi, T. (1996) Neuronal ion channels as the target sites of insecticides. Pharmacol Toxicol 79, 1-14.

Narahashi, T., Carter, D.B., Frey, J., Ginsburg, K., Hamilton, B.J., Nagata, K., Roy, M.L., Song, J.H. and Tatebayashi, H. (1995) Sodium channels and GABAA receptor-channel complex as targets of environmental toxicants. Toxicol Lett 82-83, 239-45.

Nauen, R. (2007) Insecticide resistance in disease vectors of public health importance. Pest Manag Sci 63, 628-33.

Nicholson, D.W., Ali, A., Thornberry, N.A., Vaillancourt, J.P., Ding, C.K., Gallant, M., Gareau, Y., Griffin, P.R., Labelle, M., Lazebnik, Y.A. and et al. (1995) Identification and inhibition of the ICE/CED-3 protease necessary for mammalian apoptosis. Nature 376, 37-43.

Nikou, D., Ranson, H. and Hemingway, J. (2003) An adult-specific CYP6 P450 gene is overexpressed in a pyrethroid-resistant strain of the malaria vector, Anopheles gambiae. Gene 318, 91-102.

Nikou D, R.H., Hemingway J ((2003)) An adult-specific *CYP6* P450 gene is overexpressed in a pyrethroid-resistant strain of the malaria vector, *Anopheles gambiae*. Gene 318, 91–102.

Noort, D., van Zuylen, A., Fidder, A., van Ommen, B. and Hulst, A.G. (2008) Protein adduct formation by glucuronide metabolites of permethrin. Chem Res Toxicol 21, 1396-406.

Okerberg, E.S., Wu, J., Zhang, B., Samii, B., Blackford, K., Winn, D.T., Shreder, K.R., Burbaum, J.J. and Patricelli, M.P. (2005) High-resolution functional proteomics by active-site peptide profiling. Proc Natl Acad Sci U S A 102, 4996-5001.

Olayemi, I.K., A. T. Ande, G. Danlami and U. Abdullahi (2011) Influence of Blood Meal Type on Reproductive Performance of the Malaria Vector, *Anopheles gambiae* s.s. (Deptera: Culicidae). Journal of Entomology 1-9.

Omura, T. and Sato, R. (1964a) The Carbon Monoxide-Binding Pigment of Liver Microsomes. I. Evidence for Its Hemoprotein Nature. J Biol Chem 239, 2370-8.

Omura, T. and Sato, R. (1964b) The Carbon Monoxide-Binding Pigment of Liver Microsomes. Ii. Solubilization, Purification, and Properties. J Biol Chem 239, 2379-85.

Paine, M., Scrutton, N., Munro, A., Gutierrez, A., Roberts, G. and Wolf, C. (2005) Electron Transfer Partners of Cytochrome P450. In Ortiz de Montellano, P.R. (ed.), Cytochrome P450, Springer US, pp. 115-148.

Pass, G.J., Carrie, D., Boylan, M., Lorimore, S., Wright, E., Houston, B., Henderson, C.J. and Wolf, C.R. (2005) Role of hepatic cytochrome p450s in the pharmacokinetics and toxicity of cyclophosphamide: studies with the hepatic cytochrome p450 reductase null mouse. Cancer Res 65, 4211-7.

Patricelli, M.P. (2002) Activity-based probes for functional proteomics. Brief Funct Genomic Proteomic 1, 151-8.

Patricelli, M.P., Giang, D.K., Stamp, L.M. and Burbaum, J.J. (2001) Direct visualization of serine hydrolase activities in complex proteomes using fluorescent active site-directed probes. Proteomics 1, 1067-71.

Patricelli, M.P., Szardenings, A.K., Liyanage, M., Nomanbhoy, T.K., Wu, M., Weissig, H., Aban, A., Chun, D., Tanner, S. and Kozarich, J.W. (2007) Functional interrogation of the kinome using nucleotide acyl phosphates. Biochemistry 46, 350-8.

Pedra, J.H., Festucci-Buselli, R.A., Sun, W., Muir, W.M., Scharf, M.E. and Pittendrigh, B.R. (2005) Profiling of abundant proteins associated with dichlorodiphenyltrichloroethane resistance in Drosophila melanogaster. Proteomics 5, 258-69.

Plassmeyer, M.L., Reiter, K., Shimp, R.L., Jr., Kotova, S., Smith, P.D., Hurt, D.E., House, B., Zou, X., Zhang, Y., Hickman, M., Uchime, O., Herrera, R., Nguyen, V., Glen, J., Lebowitz, J., Jin, A.J., Miller, L.H., MacDonald, N.J., Wu, Y. and Narum, D.L. (2009) Structure of the Plasmodium falciparum circumsporozoite protein, a leading malaria vaccine candidate. J Biol Chem 284, 26951-63.

Price, R.N. and Nosten, F. (2001) Drug resistant falciparum malaria: clinical consequences and strategies for prevention. Drug Resist Updat 4, 187-96.

Pritchard, M.P., McLaughlin, L. and Friedberg, T. (2006) Establishment of functional human cytochrome P450 monooxygenase systems in Escherichia coli. Methods Mol Biol 320, 19-29.

Ramphul, U., Boase, T., Bass, C., Okedi, L.M., Donnelly, M.J. and Muller, P. (2009) Insecticide resistance and its association with target-site mutations in natural

populations of Anopheles gambiae from eastern Uganda. Trans R Soc Trop Med Hyg 103, 1121-6.

Ranson, H., Claudianos, C., Ortelli, F., Abgrall, C., Hemingway, J., Sharakhova, M.V., Unger, M.F., Collins, F.H. and Feyereisen, R. (2002) Evolution of supergene families associated with insecticide resistance. Science 298, 179-81.

Ranson, H., Jensen, B., Vulule, J.M., Wang, X., Hemingway, J. and Collins, F.H. (2000) Identification of a point mutation in the voltage-gated sodium channel gene of Kenyan Anopheles gambiae associated with resistance to DDT and pyrethroids. Insect Mol Biol 9, 491-7.

Roberts, D.R., Laughlin, L.L., Hsheih, P. and Legters, L.J. (1997a) DDT, global strategies, and a malaria control crisis in South America. Emerg Infect Dis 3, 295-302.

Roberts, E.S., Hopkins, N.E., Foroozesh, M., Alworth, W.L., Halpert, J.R. and Hollenberg, P.F. (1997b) Inactivation of cytochrome P450s 2B1, 2B4, 2B6, and 2B11 by arylalkynes. Drug Metab Dispos 25, 1242-8.

Rostovtsev, V.V., Green, L.G., Fokin, V.V. and Sharpless, K.B. (2002) A stepwise huisgen cycloaddition process: copper(I)-catalyzed regioselective "ligation" of azides and terminal alkynes. Angew Chem Int Ed Engl 41, 2596-9.

Rowland, M., Bouma, M., Ducornez, D., Durrani, N., Rozendaal, J., Schapira, A. and Sondorp, E. (1996) Pyrethroid-impregnated bed nets for personal protection against malaria for Afghan refugees. Trans R Soc Trop Med Hyg 90, 357-61.

Sacher, R.M., Metcalf, R.L. and Fukuto, T.R. (1968) Propynyl naphthyl ethers as selective carbamate synergists. Journal of Agricultural and Food Chemistry 16, 779-786.

Saghatelian, A. and Cravatt, B.F. (2005) Assignment of protein function in the postgenomic era. Nat Chem Biol 1, 130-42.

Saghatelian, A., Jessani, N., Joseph, A., Humphrey, M. and Cravatt, B.F. (2004) Activity-based probes for the proteomic profiling of metalloproteases. Proc Natl Acad Sci U S A 101, 10000-5.

Sanders, E.J., Borus, P., Ademba, G., Kuria, G., Tukei, P.M. and LeDuc, J.W. (1996) Sentinel surveillance for yellow fever in Kenya, 1993 to 1995. Emerg Infect Dis 2, 236-8.

Scharf, M.E., Neal, J.J., Marcus, C.B. and Bennett, G.W. (1998) Cytochrome P450 purification and immunological detection in an insecticide resistant strain of German cockroach (Blattella germanica, L.). Insect Biochem Mol Biol 28, 1-9.

Schmidinger, H., Birner-Gruenberger, R., Riesenhuber, G., Saf, R., Susani-Etzerodt, H. and Hermetter, A. (2005) Novel fluorescent phosphonic acid esters for discrimination of lipases and esterases. Chembiochem 6, 1776-81.

Schonbrod, R.D. and Terriere, L.C. (1971) Inhibition of housefly microsomal epoxidase by the eye pigment, xanthommatin. Pesticide Biochemistry and Physiology 1, 409-417.

Scollon, E.J., Starr, J.M., Godin, S.J., DeVito, M.J. and Hughes, M.F. (2009) In vitro metabolism of pyrethroid pesticides by rat and human hepatic microsomes and cytochrome p450 isoforms. Drug Metab Dispos 37, 221-8.

Scott, J.G. (1999) Cytochromes P450 and insecticide resistance. Insect Biochem Mol Biol 29, 757-77.

Scott, J.G., Foroozesh, M., Hopkins, N.E., Alefantis, T.G. and Alworth, W.L. (2000) Inhibition of Cytochrome P450 6D1 by Alkynylarenes, Methylenedioxyarenes, and Other Substituted Aromatics. Pesticide Biochemistry and Physiology 67, 63-71.

Scott, J.G., Liu, N. and Wen, Z. (1998) Insect cytochromes P450: diversity, insecticide resistance and tolerance to plant toxins. Comp Biochem Physiol C Pharmacol Toxicol Endocrinol 121, 147-55.

Shan, G., Hammer, R.P. and Ottea, J.A. (1997) Biological Activity of Pyrethroid Analogs in Pyrethroid-Susceptible and -Resistant Tobacco Budworms, Heliothis virescens (F.)†. Journal of Agricultural and Food Chemistry 45, 4466-4473.

Shan, G. and Hammock, B.D. (2001) Development of sensitive esterase assays based on alpha-cyano-containing esters. Anal Biochem 299, 54-62.

Sieber, S.A., Mondala, T.S., Head, S.R. and Cravatt, B.F. (2004) Microarray platform for profiling enzyme activities in complex proteomes. J Am Chem Soc 126, 15640-1.

Silverman, R.B. (1995) Mechanism-based enzyme inactivators. Methods Enzymol 249, 240-83.

Speers, A.E., Adam, G.C. and Cravatt, B.F. (2003) Activity-based protein profiling in vivo using a copper(i)-catalyzed azide-alkyne [3 + 2] cycloaddition. J Am Chem Soc 125, 4686-7.

Speers, A.E. and Cravatt, B.F. (2004a) Chemical strategies for activity-based proteomics. Chembiochem 5, 41-7.

Speers, A.E. and Cravatt, B.F. (2004b) Profiling enzyme activities in vivo using click chemistry methods. Chem Biol 11, 535-46.

Speers, A.E. and Cravatt, B.F. (2009) Activity-Based Protein Profiling (ABPP) and Click Chemistry (CC)–ABPP by MudPIT Mass Spectrometry. John Wiley & Sons, Inc., Current Protocols in Chemical Biology.

Stevenson, B.J., Bibby, J., Pignatelli, P., Muangnoicharoen, S., O'Neill, P.M., Lian, L.-Y., Müller, P., Nikou, D., Steven, A., Hemingway, J., Sutcliffe, M.J. and Paine, M.J.I. Cytochrome P450 6M2 from the malaria vector Anopheles gambiae metabolizes pyrethroids: Sequential metabolism of deltamethrin revealed. Insect Biochemistry and Molecular Biology In Press, Corrected Proof.

Stevenson, B.J., Bibby, J., Pignatelli, P., Muangnoicharoen, S., O'Neill, P.M., Lian, L.Y., Muller, P., Nikou, D., Steven, A., Hemingway, J., Sutcliffe, M.J. and Paine, M.J. (2011) Cytochrome P450 6M2 from the malaria vector Anopheles gambiae metabolizes pyrethroids: Sequential metabolism of deltamethrin revealed. Insect Biochem Mol Biol.

Still, W.C., Kahn, M. and Mitra, A. (1978) Rapid chromatographic technique for preparative separations with moderate resolution. The Journal of Organic Chemistry 43, 2923-2925.

Syafruddin, D., Hidayati, A.P., Asih, P.B., Hawley, W.A., Sukowati, S. and Lobo, N.F. (2010) Detection of 1014F kdr mutation in four major Anopheline malaria vectors in Indonesia. Malar J 9, 315.

Tanaka, K., Mori, A. and Inoue, S. (1990) The cyclic dipeptide cyclo[(S)-phenylalanyl-(S)-histidyl] as a catalyst for asymmetric addition of hydrogen cyanide to aldehydes. The Journal of Organic Chemistry 55, 181-185.

Thompson, D.F., Malone, J.B., Harb, M., Faris, R., Huh, O.K., Buck, A.A. and Cline, B.L. (1996) Bancroftian filariasis distribution and diurnal temperature differences in the southern Nile delta. Emerg Infect Dis 2, 234-5.

Thornberry, N.A., Peterson, E.P., Zhao, J.J., Howard, A.D., Griffin, P.R. and Chapman, K.T. (1994) Inactivation of interleukin-1 beta converting enzyme by peptide (acyloxy)methyl ketones. Biochemistry 33, 3934-40.

Torres, E.P., Salazar, N.P., Belizario, V.Y. and Saul, A. (1997) Vector abundance and behaviour in an area of low malaria endemicity in Bataan, the Philippines. Acta Trop 63, 209-20.

Tsai, C.S., Li, Y.K. and Lo, L.C. (2002) Design and synthesis of activity probes for glycosidases. Org Lett 4, 3607-10.

UNICEF (2004) MALARIA
A MAJOR CAUSE OF CHILD DEATH
AND POVERTY IN AFRICA. The United Nations Children's Fund, http://www.rollbackmalaria.org/docs/rps_publications/unicef_malaria_en.pdf.

Uttamchandani, M., Li, J., Sun, H. and Yao, S.Q. (2008) Activity-based protein profiling: new developments and directions in functional proteomics. Chembiochem 9, 667-75.

Vocadlo, D.J. and Bertozzi, C.R. (2004) A strategy for functional proteomic analysis of glycosidase activity from cell lysates. Angew Chem Int Ed Engl 43, 5338-42.

Vulule, J.M., Beach, R.F., Atieli, F.K., McAllister, J.C., Brogdon, W.G., Roberts, J.M., Mwangi, R.W. and Hawley, W.A. (1999) Elevated oxidase and esterase levels associated with permethrin tolerance in Anopheles gambiae from Kenyan villages using permethrin-impregnated nets. Med Vet Entomol 13, 239-44.

Wang, C.C., Bozdech, Z., Liu, C.L., Shipway, A., Backes, B.J., Harris, J.L. and Bogyo, M. (2003) Biochemical analysis of the 20 S proteasome of Trypanosoma brucei. J Biol Chem 278, 15800-8.

Wellems, T.E. and Plowe, C.V. (2001) Chloroquine-resistant malaria. J Infect Dis 184, 770-6.

WHO (1995) World Health Organization, Vector control for malaria and other mosquito-borne diseases : report of a WHO study group. World Health Organization. .

WHO (2004) WHO Regional Office for the Eastern Mediterranean, Integrated vector management: strategic framework for the Eastern Mediterranean Region 2004-2010 World Health Organization. .

WHO (2005) "Roll Back Malaria, World Health Organization, UNICEF, WORLD MALARIA REPORT " World Health Organization.

WHO (2006) Global Malaria Programme, Indoor residual spraying, Use of indoor residual spraying for scaling up global malaria control and elimination. World Health Organization. .

WHO (2010) WHO Global Malaria Programme,WORLD MALARIA REPORT World Health Organization. .

Williams, E.B., Krishnaswamy, S. and Mann, K.G. (1989) Zymogen/enzyme discrimination using peptide chloromethyl ketones. J Biol Chem 264, 7536-45.

Wondji, C.S., Irving, H., Morgan, J., Lobo, N.F., Collins, F.H., Hunt, R.H., Coetzee, M., Hemingway, J. and Ranson, H. (2009) Two duplicated P450 genes are associated with pyrethroid resistance in Anopheles funestus, a major malaria vector. Genome Res 19, 452-9.

Wright, A.T. and Cravatt, B.F. (2007) Chemical proteomic probes for profiling cytochrome p450 activities and drug interactions in vivo. Chem Biol 14, 1043-51.

Wright, A.T., Song, J.D. and Cravatt, B.F. (2009) A suite of activity-based probes for human cytochrome P450 enzymes. J Am Chem Soc 131, 10692-700.

Yadouleton, A.W., Padonou, G., Asidi, A., Moiroux, N., Bio-Banganna, S., Corbel, V., N'Guessan, R., Gbenou, D., Yacoubou, I., Gazard, K. and Akogbeto, M.C. (2010) Insecticide resistance status in Anopheles gambiae in southern Benin. Malar J 9, 83.

Yamamoto, I., Elliott, M. and Casida, J.E. (1971) The metabolic fate of pyrethrin I, pyrethrin II, and allethrin. Bull World Health Organ 44, 347-8.

Yu, J., Paine, M.J., Marechal, J.D., Kemp, C.A., Ward, C.J., Brown, S., Sutcliffe, M.J., Roberts, G.C., Rankin, E.M. and Wolf, C.R. (2006) In silico prediction of drug binding to CYP2D6: identification of a new metabolite of metoclopramide. Drug Metab Dispos 34, 1386-92.

Zhang, M. and Scott, J.G. (1996) Cytochrome b5 Is Essential for Cytochrome P450 6D1-Mediated Cypermethrin Resistance in LPR House Flies. Pestic Biochem Physiol 55, 150-6.

Zhou, X., Scharf, M.E., Meinke, L.J., Chandler, L.D. and Siegfried, B.D. (2005) Immunological assessment of an insecticide resistance-associated esterase in the Western corn rootworm. Arch Insect Biochem Physiol 58, 157-65.

Appendix I

Cytochrome P450 destruction assay

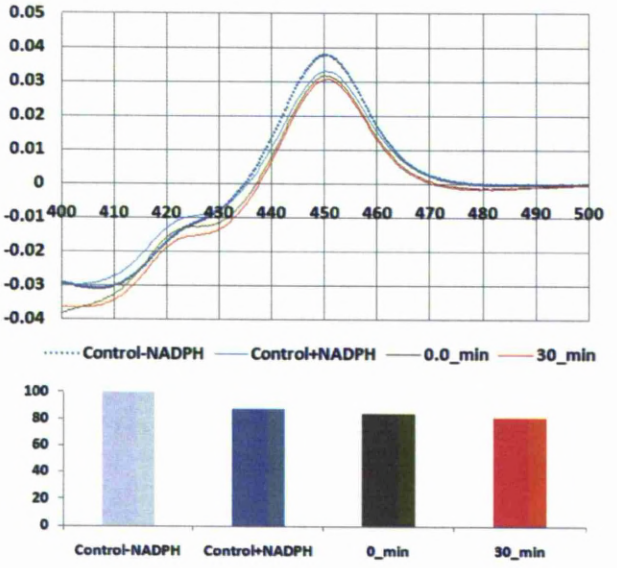

Figure A.I.1. Carbon monoxide spectroscopic analysis (CO Spec) of Rat Liver Microsomes (0.4 uM) before and after incubation at 37°C with 10 uM of 2-ethynyl-6-methoxynaphthalene (2EMe) in presence and absence of NADPH. P450 content was measured by addition of reducing agent $Na_2S_2O_4$ (~1 mg) to each cuvette and a reference spectrum from 400 to 500 nm recorded. CO was gently bubbled into the solution in the cuvette for 1 min, the cuvette was immediately capped, and the spectrum between 400 and 500 nm was measured.

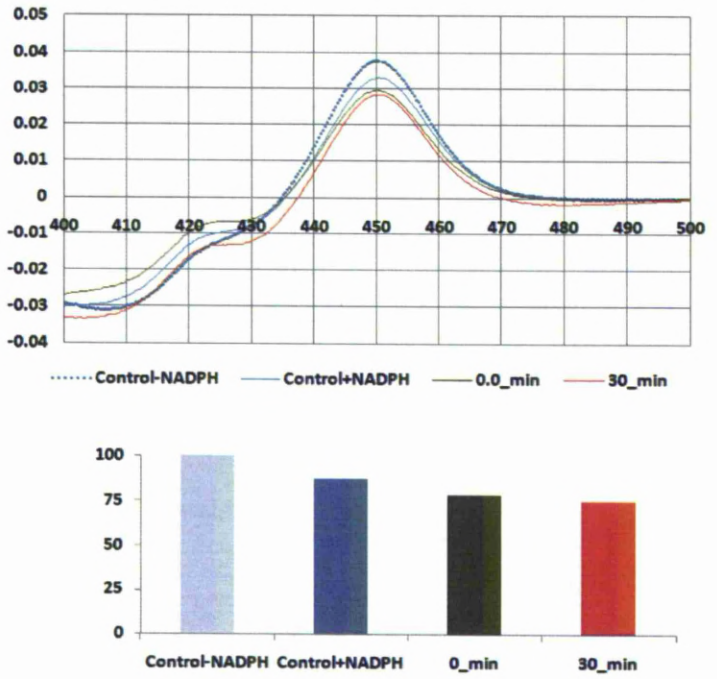

Figure A.I.2 Carbon monoxide spectroscopic analysis (CO Spec) of Rat Liver Microsomes (0.4 uM) before and after incubation at 37°C with 10 uM of 1-ethynyl-4-phenoxybenzene (1EPh) in presence and absence of NADPH, P450 content was measured by addition of reducing agent $Na_2S_2O_4$ (~1 mg) to each cuvette and a reference spectrum from 400 to 500 nm recorded. CO was gently bubbled into the solution in the cuvette for 1 min, the cuvette was immediately capped, and the spectrum between 400 and 500 nm was measured.

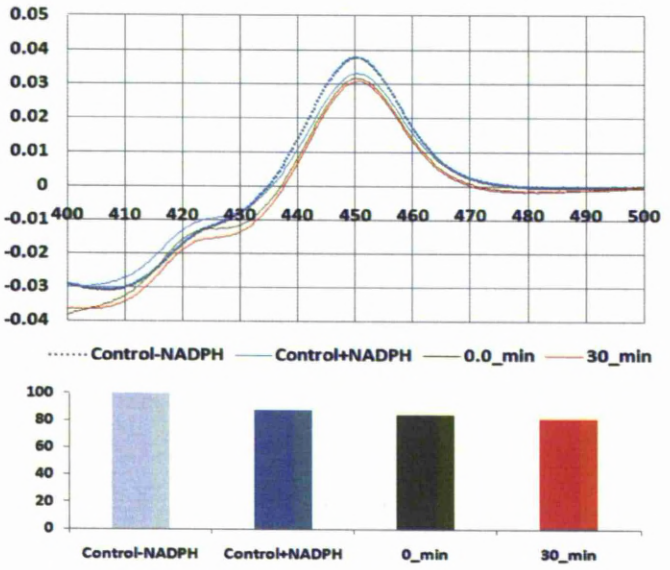

Figure A.I.3. Carbon monoxide spectroscopic analysis (CO Spec) of Rat Liver Microsomes (0.4 uM) before and after incubation at 37°C with 10 uM of 4-ethynyl-1, 2-difluorobenzene (4EDF) in presence and absence of NADPH, P450 content was measured by addition of reducing agent $Na_2S_2O_4$ (~1 mg) to each cuvette and a reference spectrum from 400 to 500 nm recorded. CO was gently bubbled into the solution in the cuvette for 1 min, the cuvette was immediately capped, and the spectrum between 400 and 500 nm was measured.

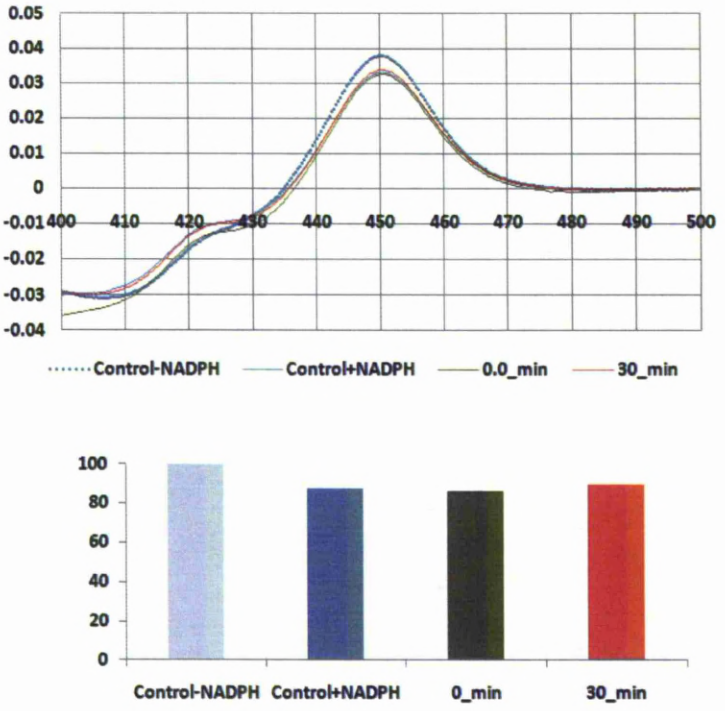

Figure A.I.4. Carbon monoxide spectroscopic analysis (CO Spec) of Rat Liver Microsomes (0.4 uM) before and after incubation at 37°C with 10 uM of 4-ethynyl-1, 1'-biphenyl (4EBi) in presence and absence of NADPH, P450 content was measured by addition of reducing agent $Na_2S_2O_4$ (~1 mg) to each cuvette and a reference spectrum from 400 to 500 nm recorded. CO was gently bubbled into the solution in the cuvette for 1 min, the cuvette was immediately capped, and the spectrum between 400 and 500 nm was measured.

Appendix II

^{1}HNMR and ^{13}C spectrum of synthesised pyrethroid ABPP probes

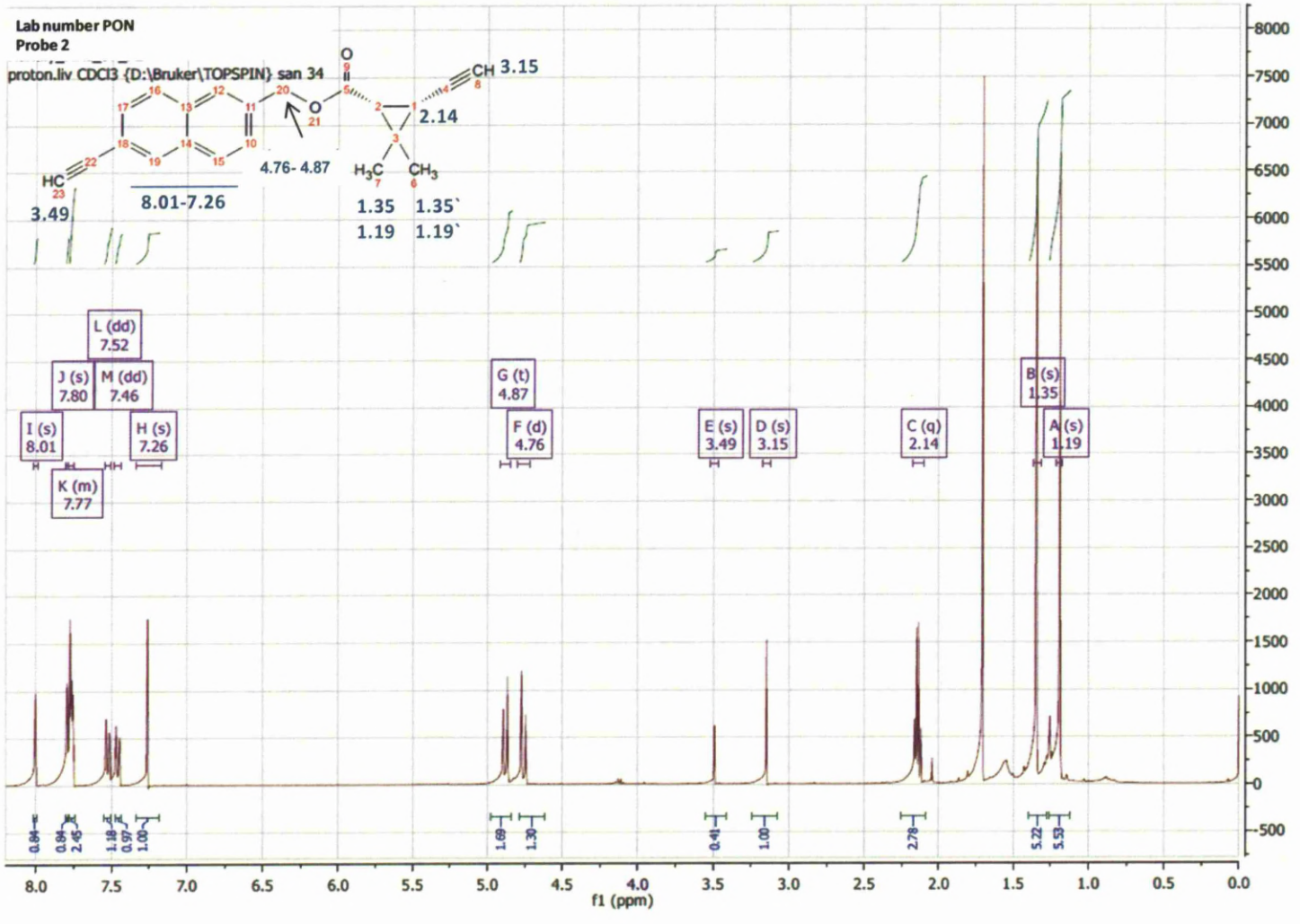
Lab number PON
Probe 2
proton.liv CDCl3 {D:\Bruker\TOPSPIN} san 34
3.15
2.14
4.76- 4.87
8.01-7.26
3.49
1.35 1.35`
1.19 1.19`
L (dd) 7.52
J (s) 7.80
M (dd) 7.46
I (s) 8.01
H (s) 7.26
K (m) 7.77
G (t) 4.87
F (d) 4.76
E (s) 3.49
D (s) 3.15
C (q) 2.14
B (s) 1.35
A (s) 1.19
f1 (ppm)

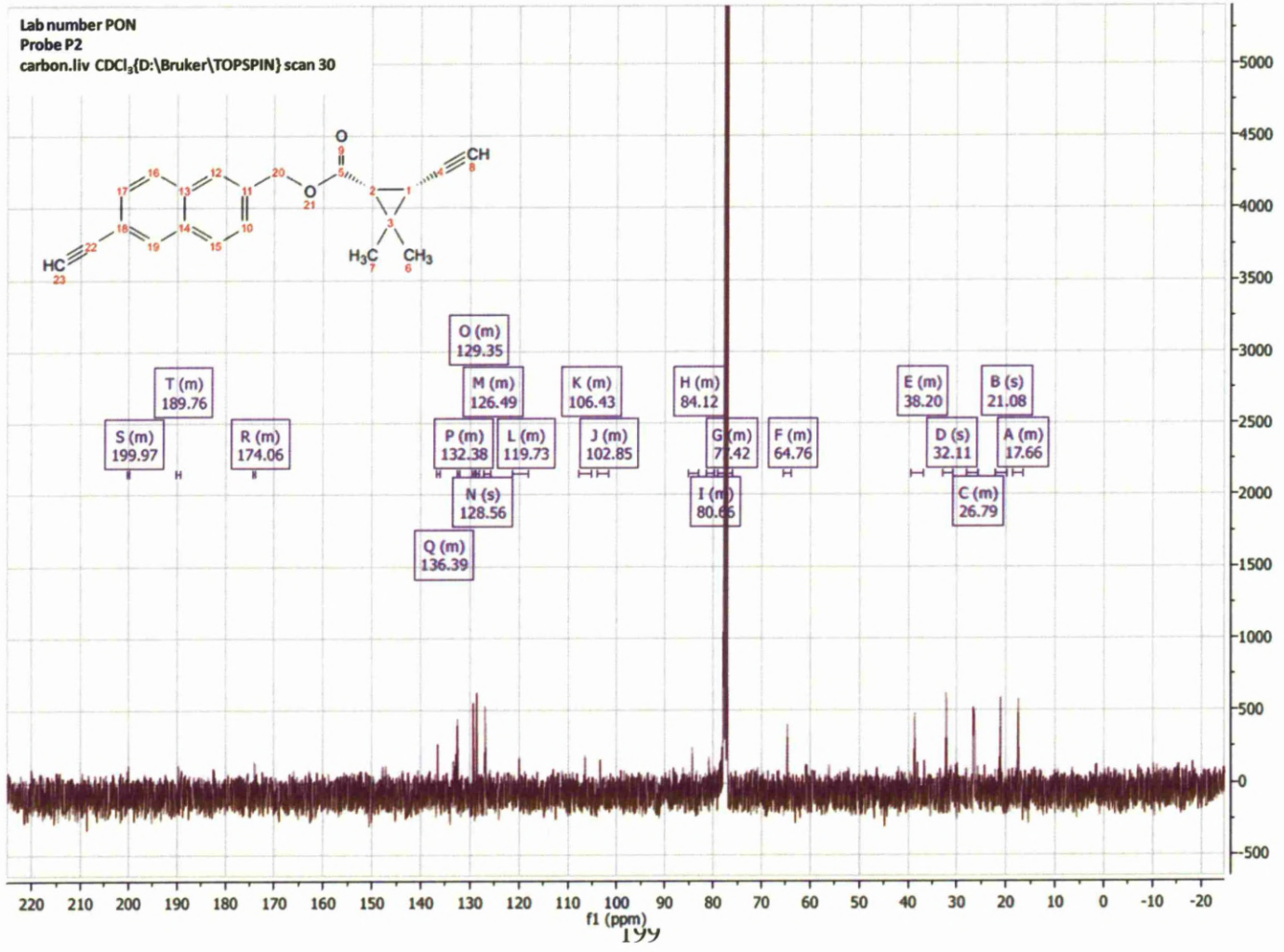
Lab number PON
Probe P2
carbon.liv CDCl3{D:\Bruker\TOPSPIN} scan 30
O (m) 129.35
M (m) 126.49
K (m) 106.43
H (m) 84.12
E (m) 38.20
B (s) 21.08
T (m) 189.76
S (m) 199.97
R (m) 174.06
P (m) 132.38
L (m) 119.73
J (m) 102.85
G (m) 77.42
F (m) 64.76
D (s) 32.11
A (m) 17.66
N (s) 128.56
I (m) 80.65
C (m) 26.79
Q (m) 136.39
f1 (ppm)

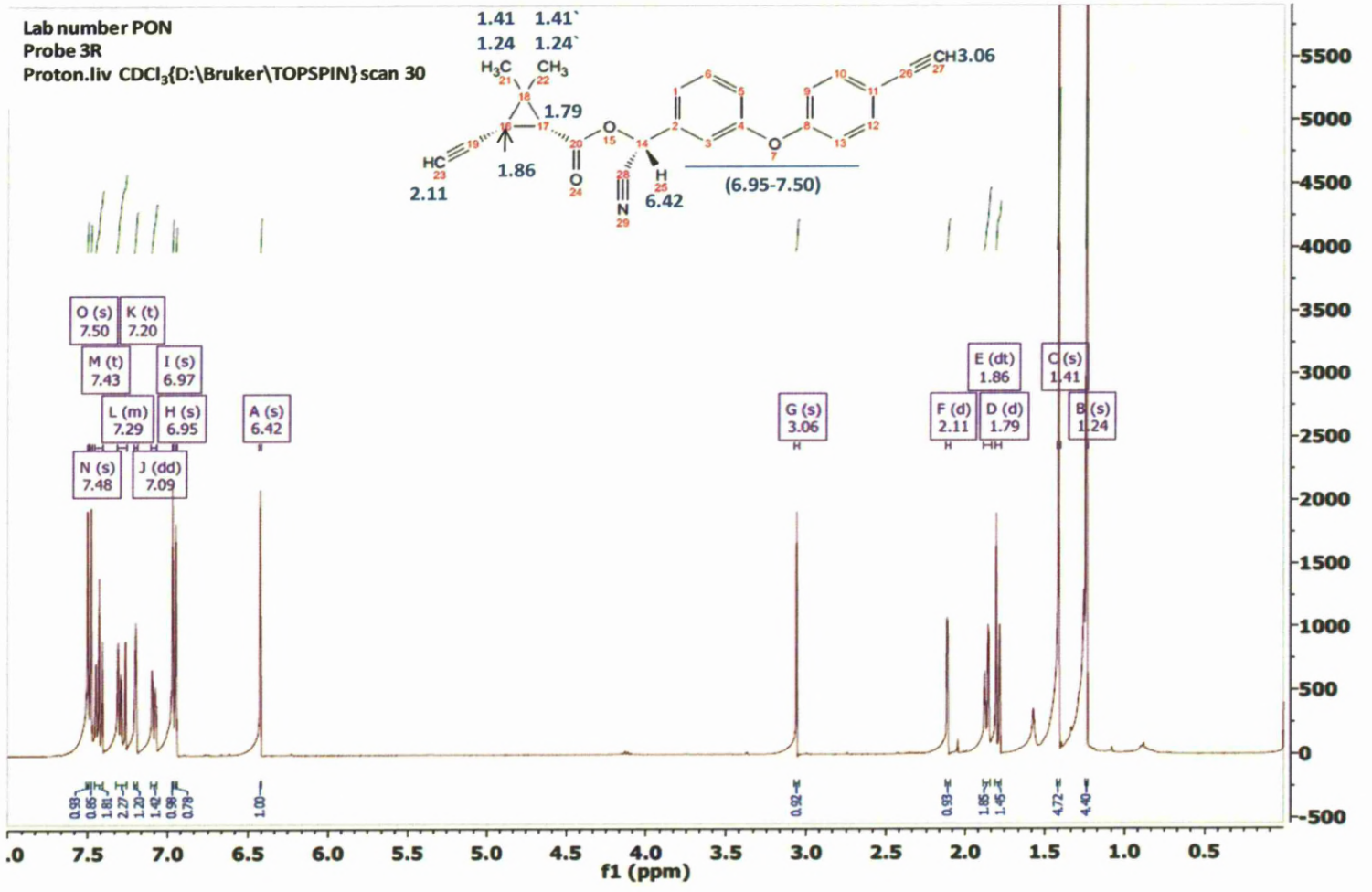
Lab number PON
Probe 3R
Proton.liv CDCl3{D:\Bruker\TOPSPIN} scan 30
1.41 1.41`
1.24 1.24`
1.79
1.86
2.11
6.42
(6.95-7.50)
3.06
O (s) 7.50
K (t) 7.20
M (t) 7.43
I (s) 6.97
L (m) 7.29
H (s) 6.95
A (s) 6.42
N (s) 7.48
J (dd) 7.09
G (s) 3.06
E (dt) 1.86
F (d) 2.11
D (d) 1.79
C (s) 1.41
B (s) 1.24
f1 (ppm)

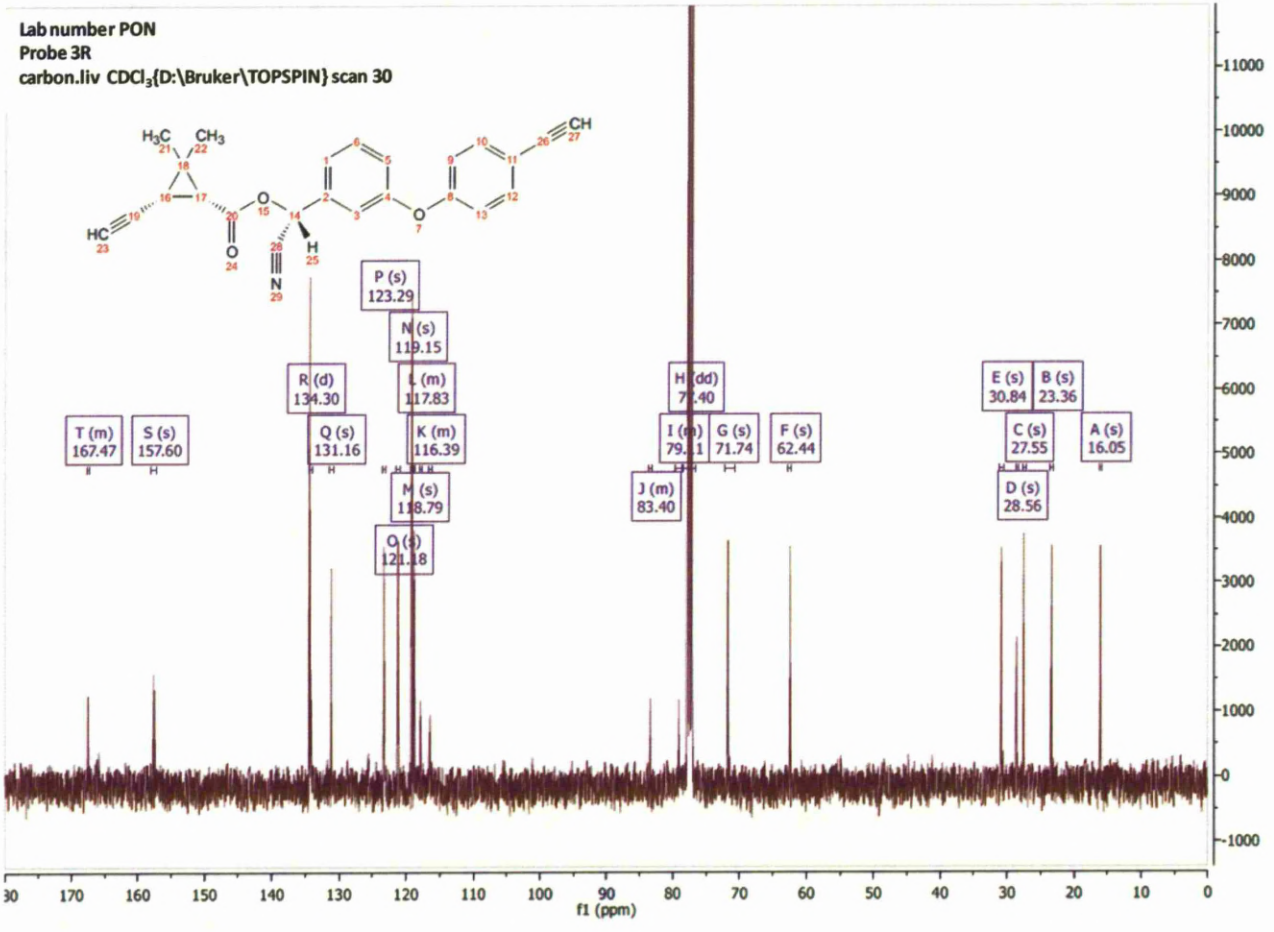
Lab number PON
Probe 3R
carbon.liv CDCl3{D:\Bruker\TOPSPIN} scan 30
T (m) 167.47
S (s) 157.60
R (d) 134.30
Q (s) 131.16
P (s) 123.29
N (s) 119.15
L (m) 117.83
K (m) 116.39
M (s) 118.79
O (s) 121.18
H (dd) 77.40
I (m) 79.11
G (s) 71.74
F (s) 62.44
J (m) 83.40
E (s) 30.84
B (s) 23.36
C (s) 27.55
A (s) 16.05
D (s) 28.56
f1 (ppm)

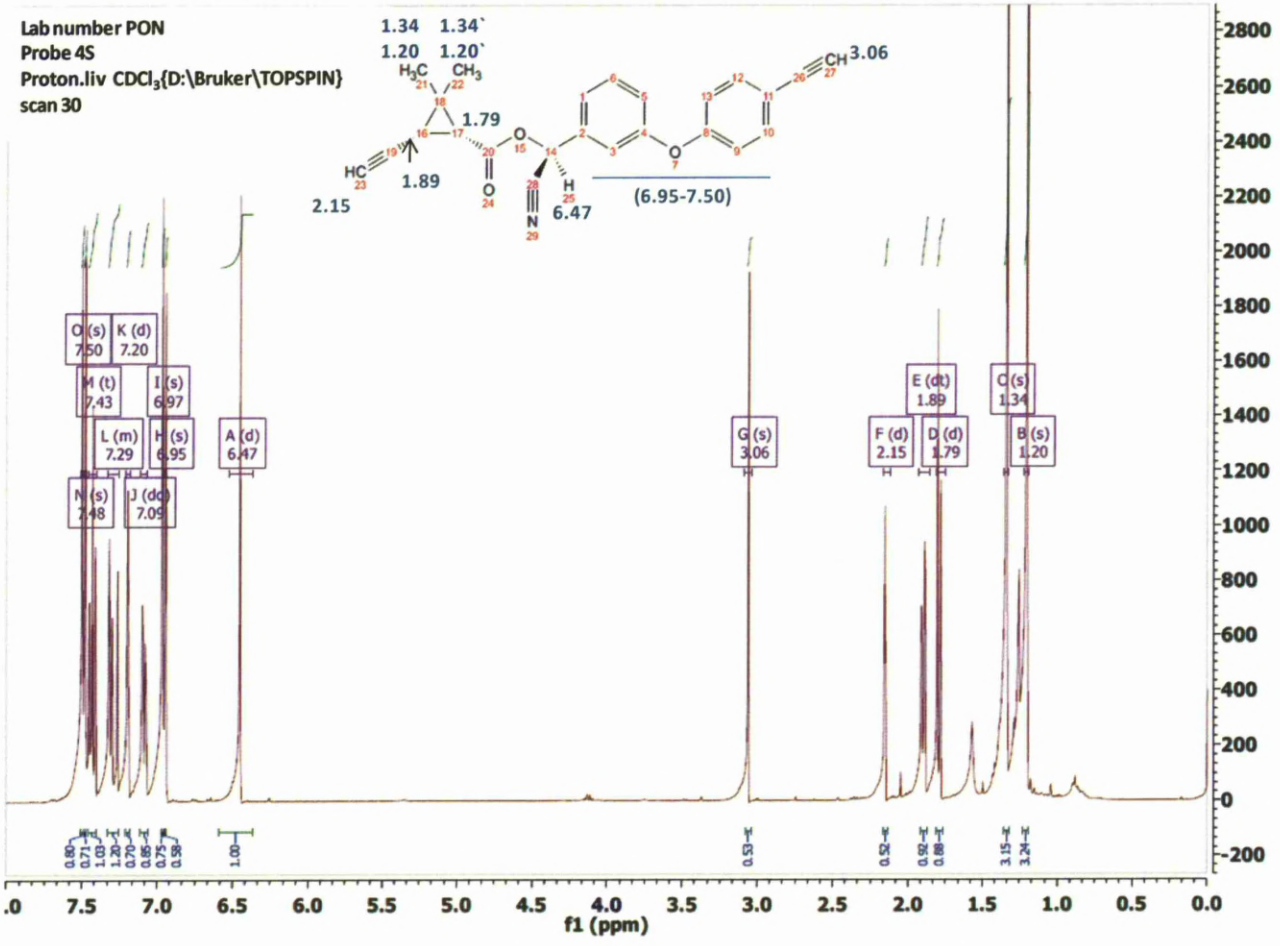
Lab number PON
Probe 4S
Proton.liv CDCl3{D:\Bruker\TOPSPIN}
scan 30
1.34 1.34`
1.20 1.20`
3.06
1.79
1.89
2.15
6.47
(6.95-7.50)
O (s) 7.50
K (d) 7.20
M (t) 7.43
I (s) 6.97
L (m) 7.29
H (s) 6.95
A (d) 6.47
N (s) 7.48
J (dd) 7.09
G (s) 3.06
E (dt) 1.89
F (d) 2.15
D (d) 1.79
C (s) 1.34
B (s) 1.20
f1 (ppm)

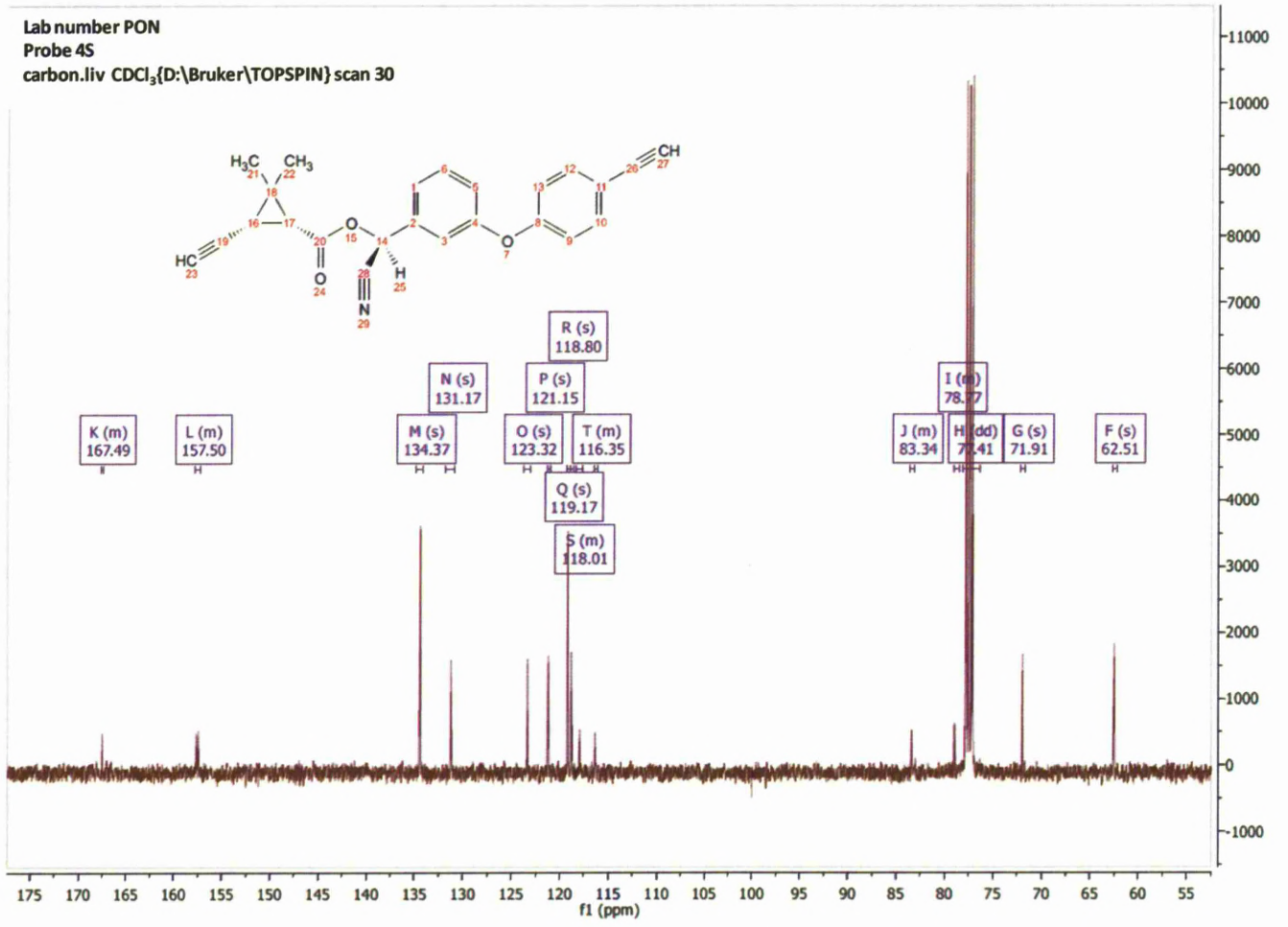
Lab number PON
Probe 4S
carbon.liv CDCl3{D:\Bruker\TOPSPIN} scan 30
K (m) 167.49
L (m) 157.50
M (s) 134.37
N (s) 131.17
O (s) 123.32
P (s) 121.15
Q (s) 119.17
R (s) 118.80
S (m) 118.01
T (m) 116.35
J (m) 83.34
H (dd) 77.41
G (s) 71.91
F (s) 62.51
f1 (ppm)

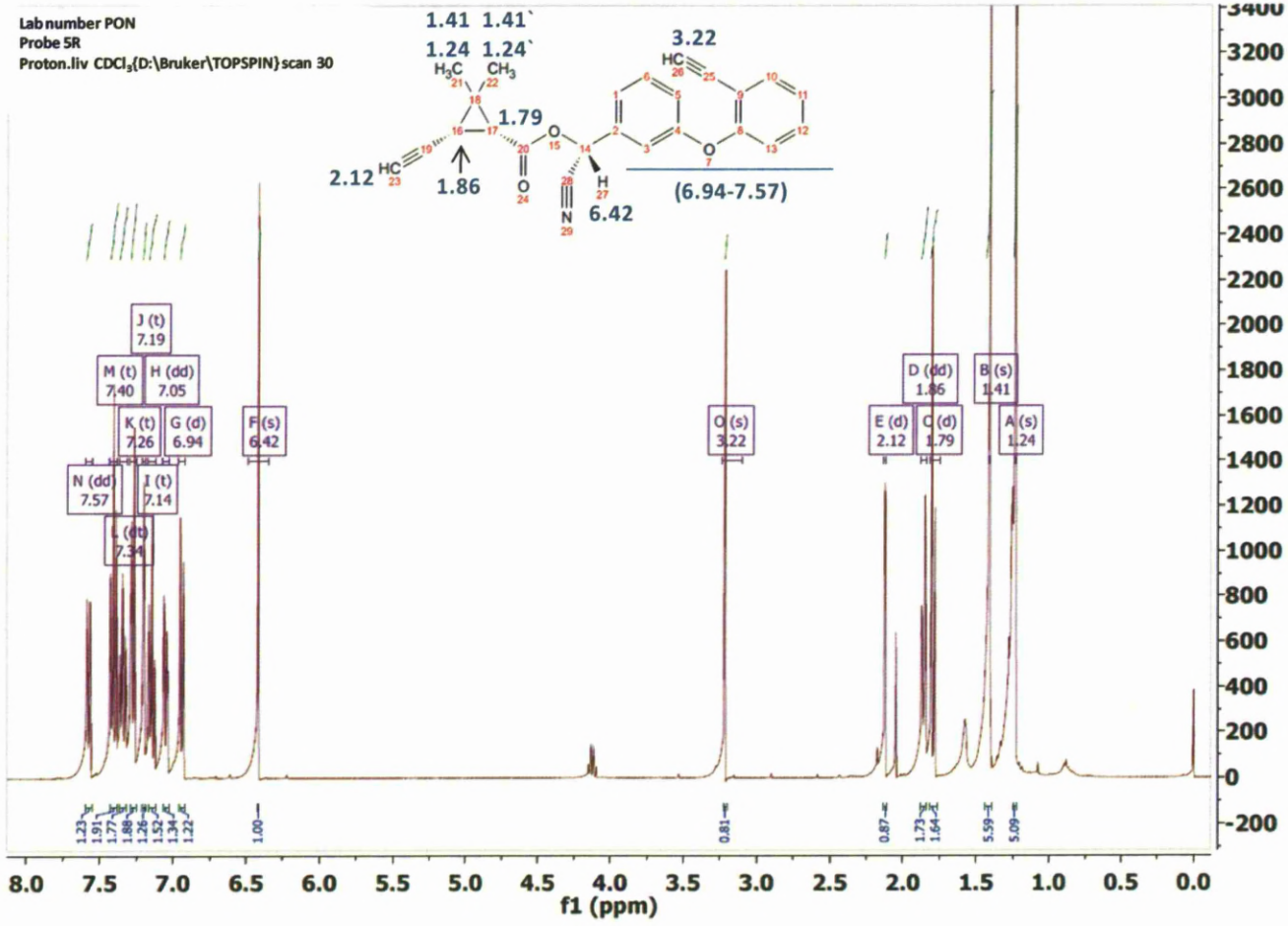
Lab number PON
Probe 5R
Proton.liv CDCl3(D:\Bruker\TOPSPIN) scan 30
1.41 1.41`
1.24 1.24`
3.22
1.79
2.12
1.86
6.42
(6.94-7.57)
J (t) 7.19
M (t) 7.40
H (dd) 7.05
K (t) 7.26
G (d) 6.94
F (s) 6.42
N (dd) 7.57
I (t) 7.14
L (dt) 7.34
O (s) 3.22
D (dd) 1.86
E (d) 2.12
C (d) 1.79
B (s) 1.41
A (s) 1.24
f1 (ppm)

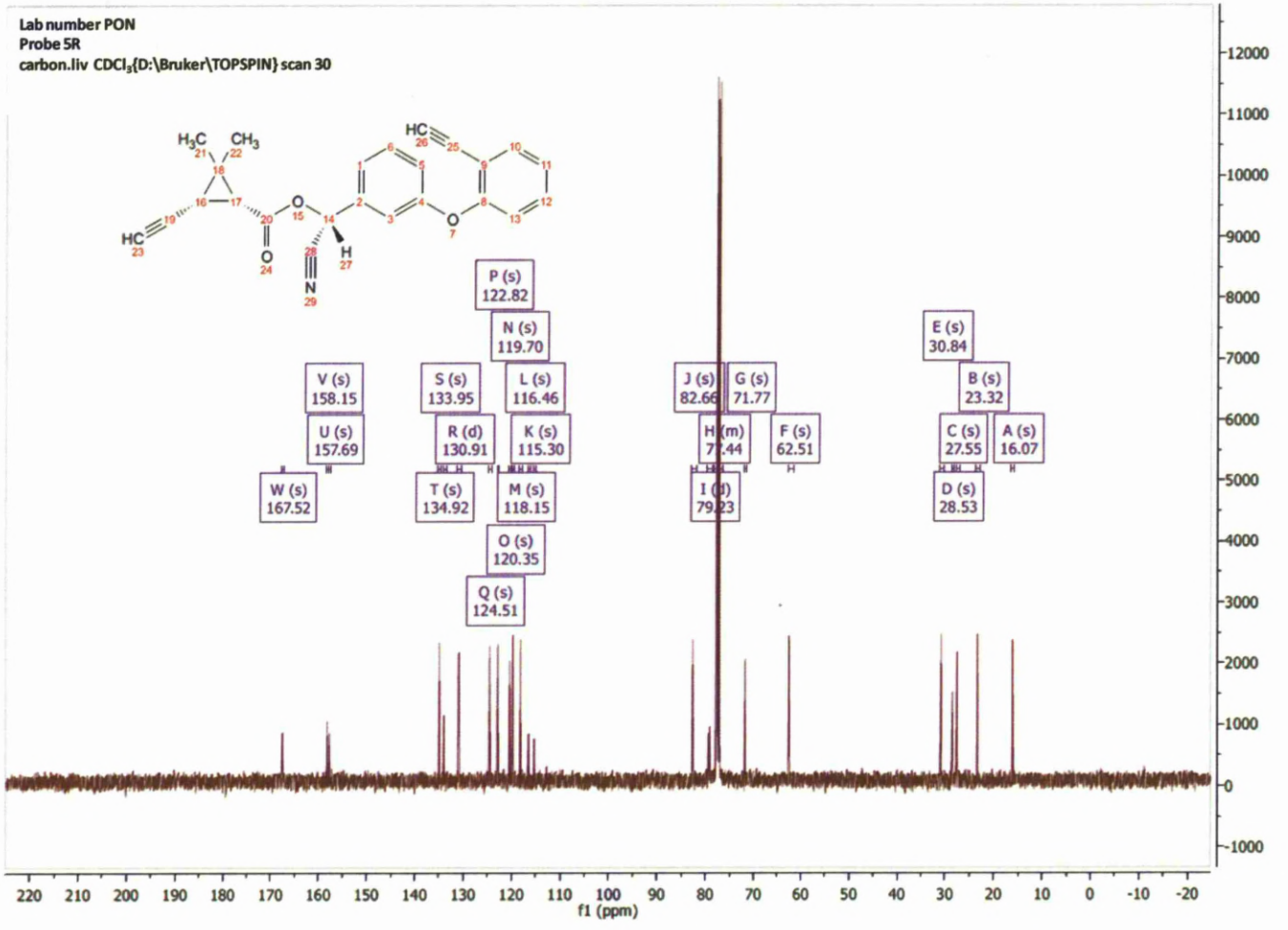
Lab number PON
Probe 5R
carbon.liv CDCl3{D:\Bruker\TOPSPIN} scan 30
P (s) 122.82
N (s) 119.70
V (s) 158.15
S (s) 133.95
L (s) 116.46
J (s) 82.66
G (s) 71.77
E (s) 30.84
B (s) 23.32
U (s) 157.69
R (d) 130.91
K (s) 115.30
H (m) 77.44
F (s) 62.51
C (s) 27.55
A (s) 16.07
W (s) 167.52
T (s) 134.92
M (s) 118.15
I (t) 79.23
D (s) 28.53
O (s) 120.35
Q (s) 124.51
f1 (ppm)

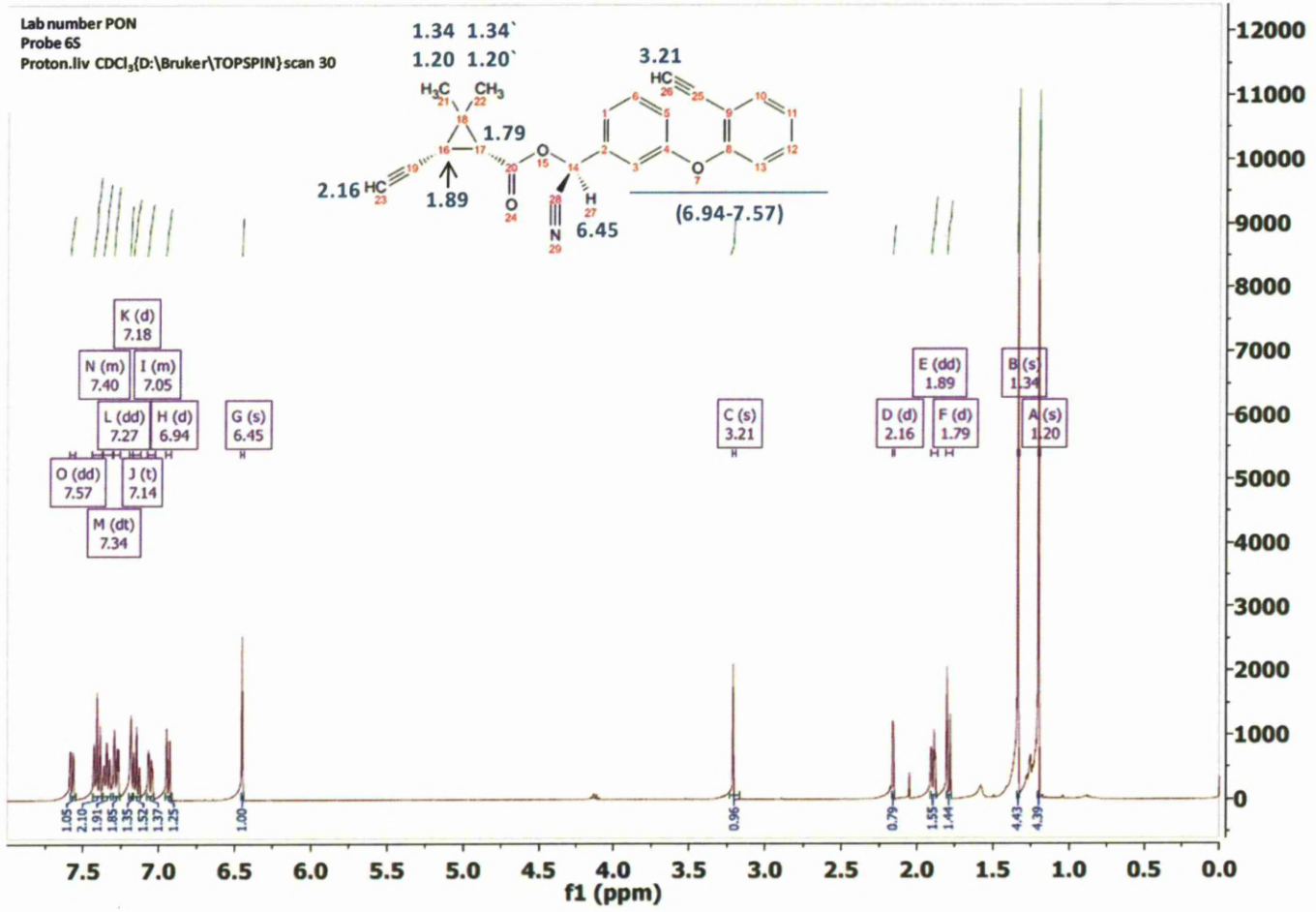
Lab number PON
Probe 6S
Proton.liv CDCl3{D:\Bruker\TOPSPIN}scan 30
1.34 1.34`
1.20 1.20`
3.21
1.79
2.16
1.89
6.45
(6.94-7.57)
K (d) 7.18
N (m) 7.40
I (m) 7.05
L (dd) 7.27
H (d) 6.94
G (s) 6.45
O (dd) 7.57
J (t) 7.14
M (dt) 7.34
C (s) 3.21
E (dd) 1.89
D (d) 2.16
F (d) 1.79
B (s) 1.34
A (s) 1.20
f1 (ppm)

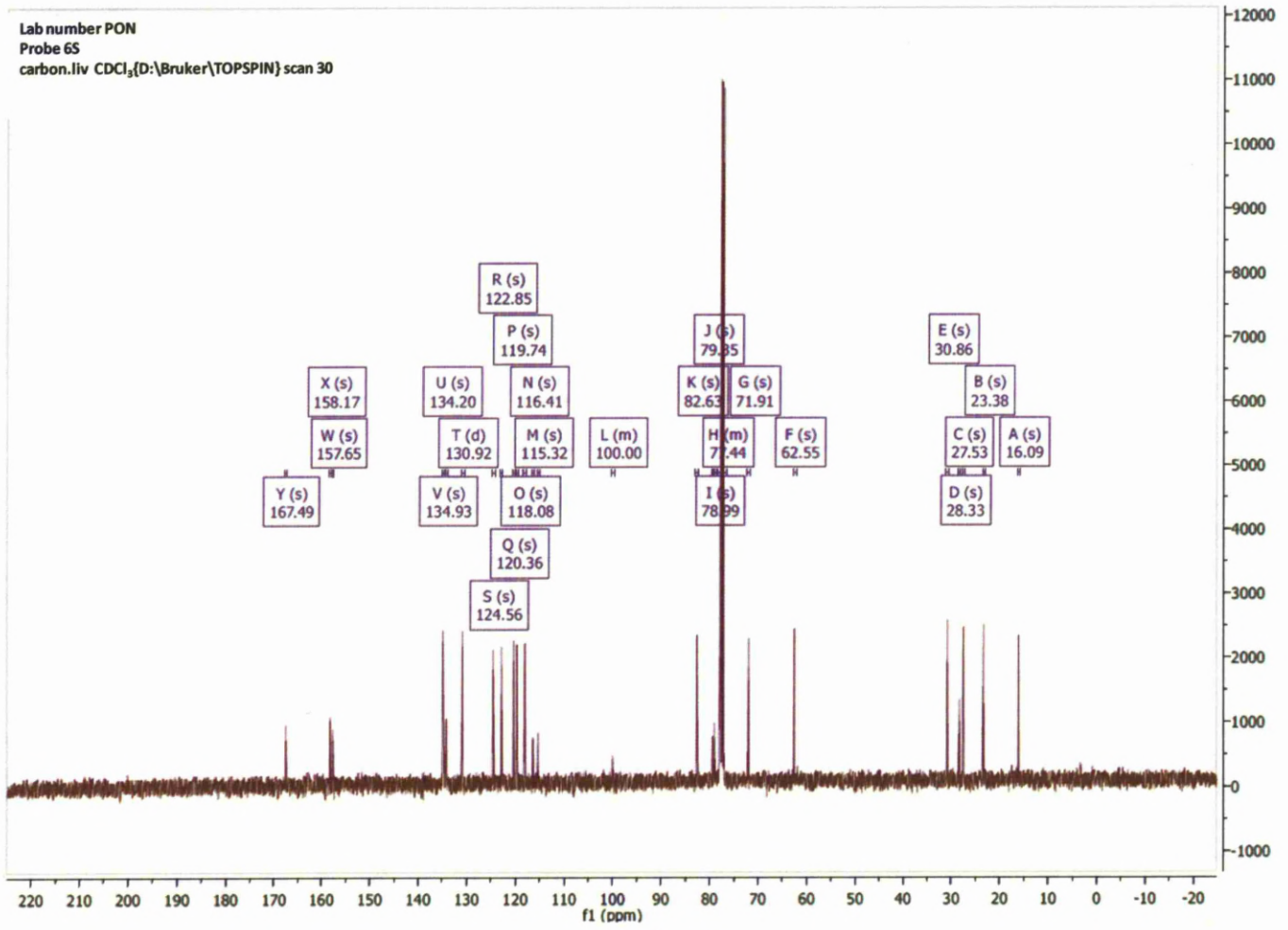
Lab number PON
Probe 6S
carbon.liv CDCl3{D:\Bruker\TOPSPIN} scan 30
R (s) 122.85
P (s) 119.74
J (s) 79.35
E (s) 30.86
X (s) 158.17
U (s) 134.20
N (s) 116.41
K (s) 82.63
G (s) 71.91
B (s) 23.38
W (s) 157.65
T (d) 130.92
M (s) 115.32
L (m) 100.00
H (m) 77.44
F (s) 62.55
C (s) 27.53
A (s) 16.09
Y (s) 167.49
V (s) 134.93
O (s) 118.08
I (s) 78.99
D (s) 28.33
Q (s) 120.36
S (s) 124.56
f1 (ppm)

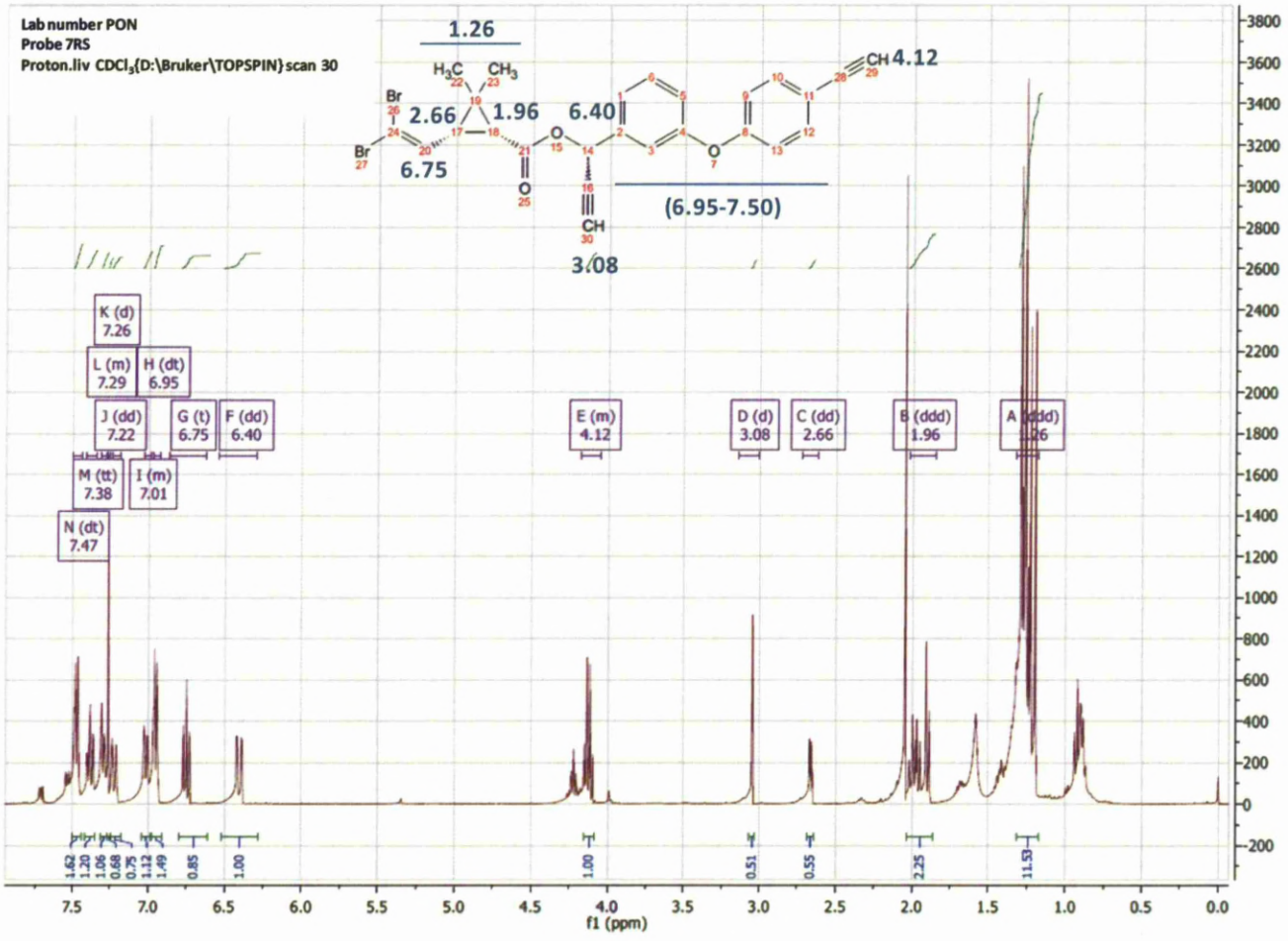
Lab number PON
Probe 7RS
Proton.liv CDCl3{D:\Bruker\TOPSPIN}scan 30
1.26
2.66
1.96
6.40
6.75
4.12
(6.95-7.50)
3.08
K (d) 7.26
L (m) 7.29
H (dt) 6.95
J (dd) 7.22
G (t) 6.75
F (dd) 6.40
M (tt) 7.38
I (m) 7.01
N (dt) 7.47
E (m) 4.12
D (d) 3.08
C (dd) 2.66
B (ddd) 1.96
A (ddd) 1.26
f1 (ppm)

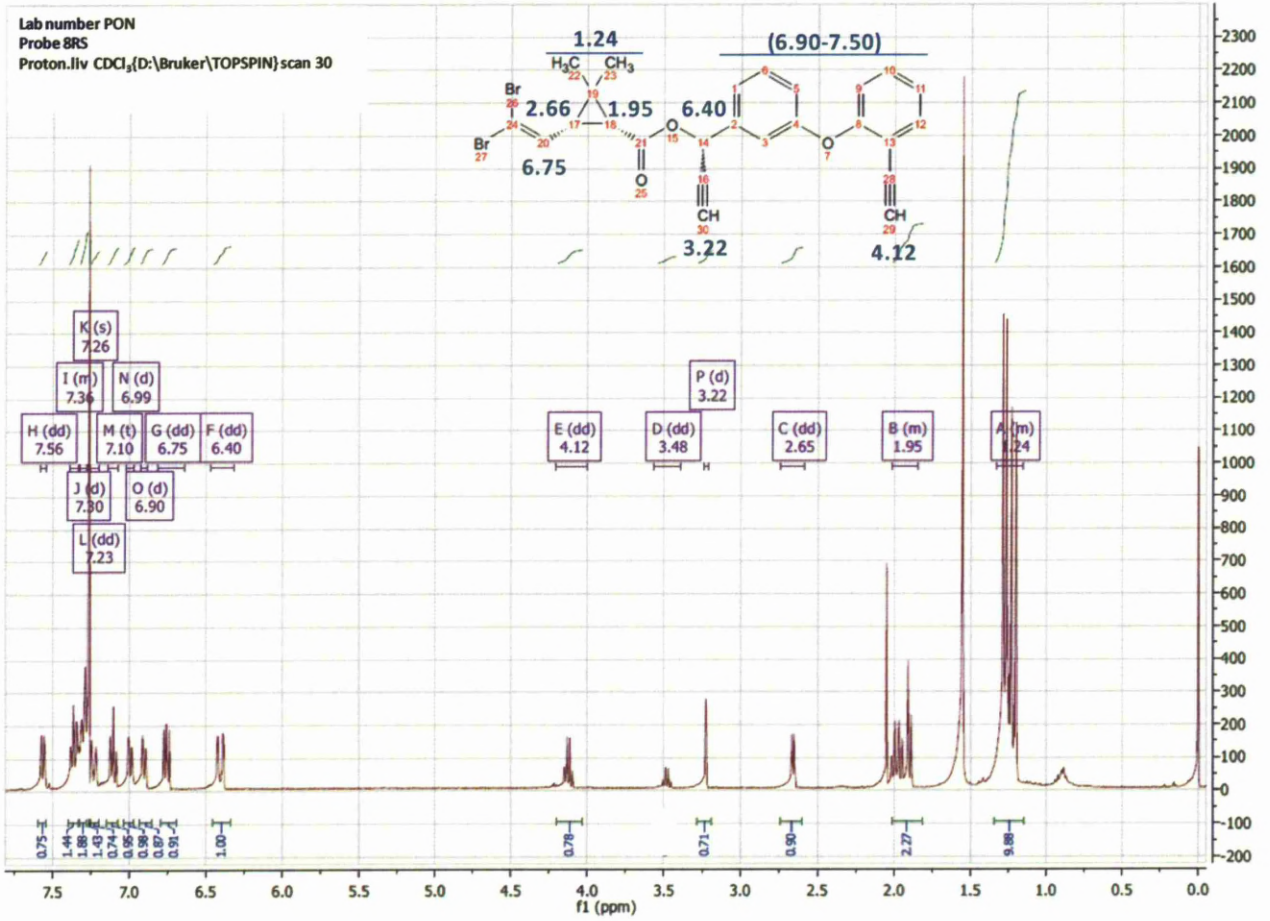
Lab number PON
Probe 8RS
Proton.liv CDCl3{D:\Bruker\TOPSPIN} scan 30
1.24
(6.90-7.50)
2.66
1.95
6.40
6.75
3.22
4.12
K (s) 7.26
I (m) 7.36
N (d) 6.99
H (dd) 7.56
M (t) 7.10
G (dd) 6.75
F (dd) 6.40
J (d) 7.30
O (d) 6.90
L (dd) 7.23
P (d) 3.22
E (dd) 4.12
D (dd) 3.48
C (dd) 2.65
B (m) 1.95
A (m) 1.24
f1 (ppm)

Appendix III

Chemical Structure of the compounds used

1. Aryl alkynes

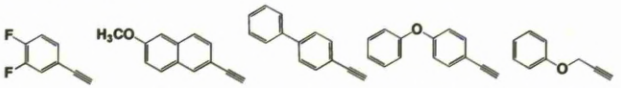

4EDF 2EMe 4EBi 1EPh 2POX

2. Deltamethrin and bifenthrin analogues

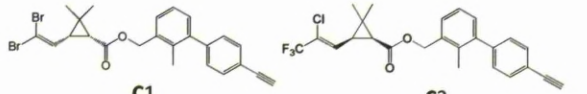

C1 C2

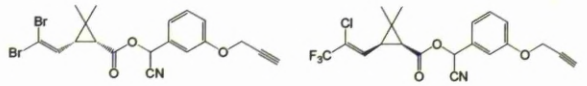

C3 C4

3. Probes designed for CYP6P3 docking calculations

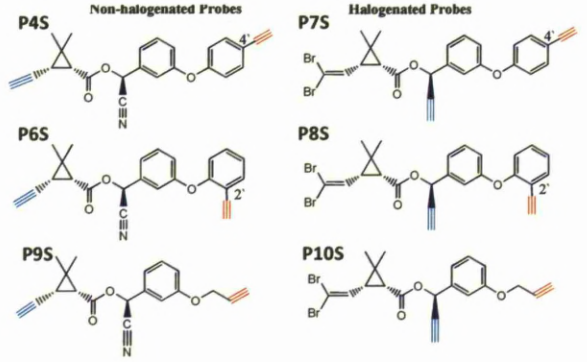

4. Chemical structure of pyrethroid ABPPs and azide reporter

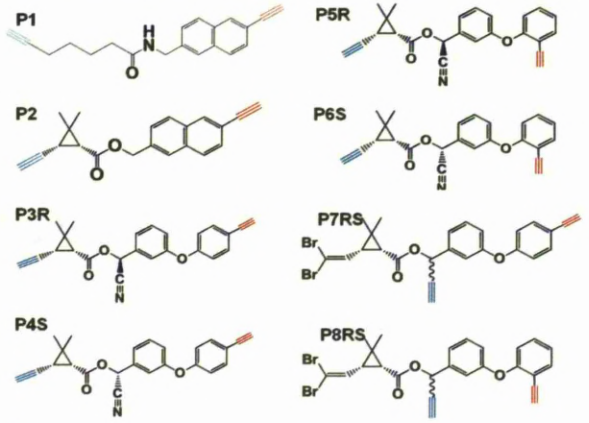

(B)

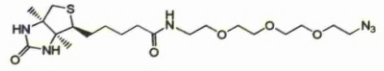

Biotin azide

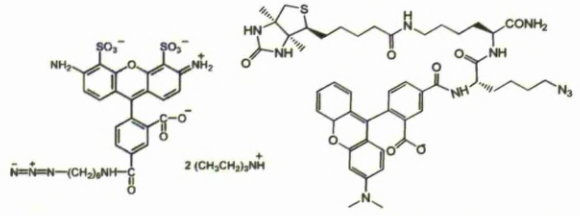

Alexa Fluor 488 Azide Rhodamine-Biotin Trifunctional Azide